

POLITECNICO DI TORINO

Master's degree in Civil Engineering

Master's Degree Thesis

# Robust optimization of MTMD systems for the control of vibrations

A robust optimal design based on genetic algorithms of MTMD systems excited  
by random vibrations



## **Supervisors**

prof. Giuseppe Carlo Marano

prof. Alessandro Palmeri

prof. Rita Greco

## **Candidate**

Fabio Pellizzari

March 2020



POLITECNICO DI TORINO

Corso di Laurea Magistrale in Ingegneria Civile

Tesi di Laurea Magistrale

# Ottimizzazione robusta di sistemi a MTMD per il controllo delle vibrazioni

Un design robusto ottimale basato su algoritmi genetici di sistemi a MTMD  
eccitati da vibrazioni random



## **Relatori**

prof. Giuseppe Carlo Marano

prof. Alessandro Palmeri

prof. Rita Greco

## **Candidato**

Fabio Pellizzari

Marzo 2020



## Abstract

The introduction of external devices to control the vibrations of a structure is an effective method to protect vulnerable systems without the necessity of expensive stiffening. Between the different technologies developed, the Multiple Tuned Mass Dampers(MTMD) is one of the simplest and most reliable; if properly designed, the MTMD systems aim to deal with a wide distribution of structural natural frequencies and damp them. The main advantages are to be inherently stable and to be guaranteed to work either in exercise conditions than during major events. In addition, MTMD is attractive as it dissipates a substantial amount of vibration energy of main structure without requiring any connection to ground. The applications concern structural issues as seismic vibrations, wind effects, traffic loads on bridges and many others.

Nevertheless, uncertainties in the behaviour of structures under random dynamic excitations have important implications on the MTMD effectiveness, causing detuning from the main system or undesired amplifications due to an in-phase tuning. A robust optimization aims to better control deviations from the design target and suits sensitive devices as MTMD. To quantify these deviations, a study in the field of random vibrations has to be performed in order to describe the response in terms of probabilistic indicators. Uncertainties must be considered also on the mechanical parameters that characterize the system to perform a proper sensitivity analysis.

In this thesis, a robust optimum design of the MTMD is proposed, considering uncertainty both in parameters of the structure than in the model of external earthquake action. At this aim, a random vibration analysis of the response is adopted together with a direct linear perturbation method applied on the uncertain parameters. The input excitation is modelled as Gaussian, white noise, mean-zero signal, passing through the Tajimi-Kanai filter, used to model the base acceleration applied to the system. Robustness is then performed, maximizing both efficiency in vibration control and sensitivity to the uncertain of the parameters of the system, while the design vector is a collection of MTMD parameters. A genetic algorithm is used to perform a multi-objective optimization and define a Pareto front to then apply an a posteriori choice of the best design for different frequencies, damping ratios and number of dampers, considering both acceleration and displacement reduction.



## Abstract

L'introduzione di dispositivi esterni per il controllo delle vibrazioni di una struttura è un efficace metodo di protezione di sistemi vulnerabili che evita di ricorrere a costosi irrigidimenti. Tra le possibili soluzioni sviluppate, la tecnologia dei Multiple Tuned Mass Dampers (MTMD, o smorzatori a massa accordata) è una delle più semplici e affidabili; se propriamente progettati, i MTMD sono capaci di smorzare un ampio intervallo di frequenze del sistema principale. I principali vantaggi sono nell'intrinseca stabilità e nella capacità di lavorare sia in condizioni di servizio che durante gli eventi più forti. Inoltre, i MTMD sono particolarmente interessanti per la capacità di dissipare una cospicua quantità di energia senza richiedere collegamenti col terreno. Le applicazioni nel campo dell'ingegneria strutturale riguardano eccitazioni sismiche, effetti del vento, del traffico e molte altre.

Tuttavia, le incertezze sul comportamento del sistema soggetto a eccitazioni dinamiche di natura random hanno importanti implicazioni sull'efficacia dei MTMD, causando una perdita dell'attonimento o indesiderati effetti di amplificazione in fase col sistema principale. Per quantificare queste deviazioni, uno studio nel campo delle vibrazioni random è necessario in modo da descrivere la risposta tramite indicatori probabilistici. Inoltre, anche l'incertezza sui parametri meccanici del sistema deve essere propriamente descritta per poter effettuare un'analisi di sensitività appropriata.

In questa tesi, è proposto un approccio robusto alla ricerca dell'optimum di design dei parametri meccanici del MTMD, considerando le incertezze sia sui parametri della struttura che sul modello adottato per descrivere l'azione sismica. A questo scopo, un'analisi della risposta nel campo delle vibrazioni random e il metodo della perturbazione diretta sono stati adottati. L'eccitazione in ingresso è assunta come un rumore bianco a media nulla con distribuzione gaussiana, passante attraverso il filtro di Tajimi-Kanai, usato per modellare l'accelerazione alla base del sistema. La robustezza è ottenuta massimizzando sia l'efficienza nel controllo delle vibrazioni che la sensitività alle incertezze dei parametri del sistema, mentre le caratteristiche del MTMD sono raccolte nel vettore dei parametri di progetto. Un approccio multi-obiettivo di ottimizzazione è applicato, ricorrendo ad algoritmi genetici per costruire il fronte di Pareto che permetta di scegliere a posteriori il migliore design tra le diverse soluzioni possibili in termini di frequenza, rapporto di smorzamento e numero di smorzatori, considerando sia la riduzione di accelerazione che di spostamento.



# Contents

<b>List of Figures</b>	5
<b>1 Random vibrations</b>	11
1.1 Vibrations . . . . .	11
1.2 Deterministic vibrations . . . . .	12
1.2.1 Harmonic vibration . . . . .	12
1.2.2 The unit step function and the unit pulse function . . . . .	17
1.2.3 Series of impulse induced vibrations . . . . .	17
1.3 Historical develop of random vibration . . . . .	18
1.4 Stochastic processes characteristics . . . . .	19
1.4.1 Classification of random processes . . . . .	20
1.4.2 Stationary and ergodic processes . . . . .	21
1.4.3 Operations on random processes . . . . .	22
1.5 Statistic and probability parameters . . . . .	22
1.5.1 Mono dimensional probability distribution . . . . .	22
1.5.2 Higher order distributions . . . . .	23
1.5.3 Independent and conditioned distributions . . . . .	24
1.5.4 Mono-dimensional stochastic parameters . . . . .	25
1.5.5 N-dimensional stochastic parameters . . . . .	26
1.5.6 Gaussian (or Normal) distribution . . . . .	27
1.5.7 Exponential distribution . . . . .	28
1.5.8 Poisson distribution . . . . .	28
1.6 Stochastic process probabilistic characterization . . . . .	29
1.6.1 Time averages . . . . .	29
1.6.2 Stationarity . . . . .	30
1.6.3 Fourier's transform . . . . .	30
1.6.4 Frequency domain . . . . .	31
1.6.5 Energetic interpretation of the PSD . . . . .	32
1.6.6 Spectral moments . . . . .	34
1.6.7 Analytical description of different type of processes . . . . .	36
1.7 Failure analysis in random vibration . . . . .	40
1.7.1 Rate of up-crossing . . . . .	40
1.7.2 Distribution of peaks . . . . .	42
1.7.3 Extreme values distribution and first-passage relationship . . . . .	43
1.7.4 First passage failure possible distributions and approximations . . . . .	44
1.7.5 Improved maximum values distributions . . . . .	46

<b>2</b>	<b>Dynamic response to random vibrations</b>	<b>51</b>
2.1	Single degree of freedom random vibration analysis . . . . .	51
2.1.1	Indirect time stochastic dynamic analysis . . . . .	52
2.1.2	Frequency analysis domain . . . . .	54
2.1.3	Stochastic parameters in frequency domain . . . . .	55
2.1.4	Frequency analysis of a SDF system . . . . .	56
2.2	Multiple degrees of freedom random vibration analysis . . . . .	57
2.2.1	Modal decomposition . . . . .	60
2.2.2	Time domain analysis of the uncoupled MDF system . . . . .	61
2.2.3	Frequency analysis of the uncoupled equation of motion . . . . .	63
2.2.4	State-space formulation of equation of motion . . . . .	64
2.2.5	Stochastic analysis of the state space equations . . . . .	66
2.2.6	Direct stochastic analysis of linear systems . . . . .	67
2.3	Theory of filters . . . . .	73
2.4	Physical modelling of earthquakes . . . . .	76
2.4.1	Response and design spectrum . . . . .	77
2.4.2	Spectrum consistent with the design spectrum . . . . .	80
2.4.3	Seismic acceleration as stationary, Gaussian, white, filtered random process . . . . .	81
2.4.4	Non-stationary models of the seismic action . . . . .	84
<b>3</b>	<b>Optimization process</b>	<b>86</b>
3.1	Uncertain in structural analysis . . . . .	87
3.2	Performance and limit state . . . . .	88
3.2.1	Structural resistance and demand as independent normal variables . . . . .	88
3.2.2	First and Second Order Reliability Method (FORM and SORM) . . . . .	90
3.2.3	Response Surface Method (RSM) . . . . .	92
3.2.4	The Monte Carlo Simulation (MCS) . . . . .	92
3.3	Optimization . . . . .	95
3.4	Single Objective Optimization . . . . .	96
3.4.1	Convex and not-convex problems . . . . .	97
3.5	Single Objective optimization Problem (SOP) . . . . .	97
3.6	Mathematical Programming (MP) . . . . .	98
3.6.1	Sequential Mathematical Programming . . . . .	98
3.7	Evolving Algorithms methods (EA) . . . . .	100
3.8	Genetic algorithms (GA) . . . . .	101
3.8.1	Encoding . . . . .	102
3.8.2	Fitness function . . . . .	102
3.8.3	Selection . . . . .	102
3.8.4	Genetic Operators . . . . .	103
3.9	Evolution Strategies (ES) . . . . .	103
3.9.1	Continuous problems . . . . .	103
3.9.2	Discrete optimization problems . . . . .	105
3.9.3	Techniques to handle the constraints . . . . .	105
3.10	Multi-Objective optimization (MOP) . . . . .	107
3.10.1	Pareto distribution of the optimal solutions . . . . .	108
3.10.2	Selection criteria . . . . .	110
3.10.3	Standard methods to solve the MOP . . . . .	111
3.10.4	Evolutionary Algorithms for solving multi-objective optimization problems . . . . .	113
3.11	Probabilistic based design optimization . . . . .	114
3.11.1	Reliability Based Design Optimization (RBDO) . . . . .	114
3.11.2	Robust Design Optimization (RDO) . . . . .	116

<b>4 Tuned Mass Dampers</b>	119
4.1 Control of vibrations	119
4.2 Historical development of TMD	121
4.3 Recent developments in TMDs analysis	122
4.4 Dynamic principles of MTMD	125
4.5 Applications in the structural field	129
4.5.1 Some applications for TMDs	130
4.6 Optimization of MTMD systems	135
4.6.1 Parameters uncertain in random vibrations	137
4.6.2 Perturbational methods	138
4.6.3 Direct perturbation method	139
4.6.4 Optimization approach for MTMD systems	142
<b>5 Robust optimization of MTMD systems</b>	144
5.1 Dynamic random vibrations analysis of the system	145
5.1.1 Proposed approaches to determine the failure probability	149
5.2 Direct perturbation method and uncertain	151
5.3 Optimization algorithm	152
5.3.1 Adopted algorithm	152
5.4 Obtained results	154
5.4.1 Deterministic analysis	154
5.4.2 Robust optimization	157
5.4.3 Concluding remarks	159
5.5 Conclusions	159
5.6 Future develops	160
<b>Appendix A-System matrices and their derivatives</b>	182
Protected case	182
Unprotected case	184
<b>Appendix B-Tabulated results</b>	186
Deterministic results for different frequency ratio	186
Deterministic optimization	187
Robust optimization	188
<b>Bibliography</b>	191
<b>Index</b>	195

# List of Figures

1.1	Damped and forced SDF system. . . . .	12
1.2	Free vibrations of a SDF not forced system for: (a) $c < c_{crit}$ (solid line), (b) $c = c_{crit}$ (dotted line), (c) $c > c_{crit}$ (dashed line)[46]. . . . .	14
1.3	Transient and steady state part of the response[46]. . . . .	15
1.4	a) Magnification factor for different $\beta$ and $\xi_0$ , and b) phase angle associated[46]. . . . .	16
1.5	Unit step function and related Dirac's delta function[46]. . . . .	17
1.6	Schematic representation of a general linear system[40]. . . . .	18
1.7	Duhamel integral analysis of an impulsive signal[40]. . . . .	19
1.8	Time history of a random signal[15]. . . . .	20
1.9	Ensemble of random time series that constitute the stochastic process[15]. . . . .	21
1.10	Probability density function (PDF). . . . .	23
1.11	Joint PDF function[46]. . . . .	24
1.12	Standard normal distribution: (a) PDF, (b) CDF[60]. . . . .	28
1.13	Periodic function $x(t)$ : a) time history, b) power spectrum[46]. . . . .	33
1.14	Harmonic process: a) Time series, b) Autocorrelation function, c) Spectral density function[46]. . . . .	36
1.15	Narrow band process: a) Time series, b) Autocorrelation function, c) Spectral density function[46]. . . . .	37
1.16	Broad band process: a) Time series, b) Autocorrelation function, c) Spectral density function[46]. . . . .	38
1.17	White noise process: a) Time series, b) Autocorrelation function, c) Spectral density function[46]. . . . .	39
1.18	Crossings of threshold $u$ by the process $X(t)$ [40]. . . . .	40
1.19	Phase diagram of the crossing event[40]. . . . .	41
1.20	Division of the stationary time between up-crossings. . . . .	46
1.21	Schematization of a broad band mean zero process ( $\mu_X(t) = 0$ ). . . . .	47
2.1	Transfer function $ H_x(\omega) $ for $\xi_0 = 0.05, 0.1, \text{ and } 0.20$ [40]. . . . .	57
2.2	Schematic representation of the filtering[46]: a) input signal, filter, b) output signal. . . . .	74
2.3	Schematic representation of the filtering operation[46]: a) Narrow band filter, b) Broad band filter. . . . .	74
2.4	Filtering process for mono correlated, mono varied signal[46] . . . . .	76
2.5	Comparison between $S_a-S_{pa}$ and $S_v-S_{pv}$ for damping ratio $\xi_0 = 0.05$ and acceleration histories: a) N-S El Centro (1940), b) S-E Taft (1952)[46]. . . . .	79
2.6	Average elastic response spectrum for different acceleration histories and different local conditions[57]. . . . .	79
2.7	Acceleration histories in different sites with indication of the absolute peaks[46]. . . . .	82
2.8	Acceleration histories and Husid function fo the components: a) N-S of El Centro's earthquake (1940), b) S-E of the Talft's earthquake (1952)[46]. . . . .	82

2.9	Tajimi-Kanai filter schematic representation[46]. . . . .	84
3.1	Gaussian joint PDF for capacity and demand cut by the limit state surface (corresponding to the plane $r=s$ )[60]. . . . .	89
3.2	Graphical interpretation of the FORM principle[60]. . . . .	90
3.3	Graphical interpretation of the SORM principle[60]. . . . .	91
3.4	MC sampling for the normal distribution with 8 samples[60]. . . . .	94
3.5	Latin Hypercube sampling for the normal distribution with 8 samples[60]. . . . .	94
3.6	a) a convex one-variable function with a global minimum, b) a non-convex one-variable function with a global and a local minimum[60]. . . . .	97
3.7	A multiple linear segment penalty function[60]. . . . .	106
3.8	Dominated, dominating and incomparable regions with respect to point A in the objective space[60]. . . . .	108
3.9	Dominated, feasible region and corresponding Pareto Front in the objective space for a bidimensional problem[60]. . . . .	110
3.10	Approaches to the design: a) deterministic design approach (dashed line), b) robust design approach (solid line). . . . .	117
4.1	Model of the Frahm absorber system. . . . .	121
4.2	Magnification factor of displacement $D = X_f/X_{st}$ for different damping ratio $\xi = C/C_c$ and frequency ratio $\beta = \omega/\Omega_n$ [17]. The mass ratio is fixed at $\mu = 1/20 = 5\%$ and the TMD is perfectly tuned, $f = \omega_{tmd}/\Omega_n = 1$ . . . . .	122
4.3	Dynamic scheme of MTMD system for a SDF structure . . . . .	125
4.4	Response spectre of the system: a) with a single TMD and b) with MTMD. . . . .	127
4.5	Most common typologies of TMD[53]. . . . .	130
4.6	Plan and sectional view of the five-storeys pagoda structure of the Horyu-Ji temple in Japan[47]. . . . .	131
4.7	Vibration control mechanisms of the pagoda[47]. . . . .	132
4.8	The pendulum of the main TMD system of the Taipei 101[54]. . . . .	133
4.9	Plan and elevation of the bridge showing the arrangement of dampers[16]. . . . .	134
4.10	Plan view of a typical 16 m length of deck showing viscous dampers and tuned mass dampers[16]. . . . .	135
4.11	Viscous dampers in plane between cables and deck at piers[16]. . . . .	136
5.1	Dynamic scheme of MTMD system for a SDF structure. . . . .	145
5.2	Optimal parameters and $OF_{displ}$ for varying frequency ratio $\psi$ and number of TMDs	161
5.3	Optimal parameters and $OF_{acc}$ for varying frequency ratio $\psi$ and number of TMDs	162
5.4	Tajimi-Kanai PSD for $\omega_K = 18.64 \text{ rad/s}$ , $\xi_K = 0.4$ and $S_0 = 1000 \text{ cm}^2/\text{s}^3$ . . . . .	163
5.5	PSD of acc. $S_{\ddot{X}\ddot{X}}$ , for the Tajimi-Kanai spectrum in fig.5.4, $\omega_s = 13.96 \text{ rad/s}$ and $\xi_s = 0.05$ . . . . .	163
5.6	Clough-Penzien PSD for $\omega_K = 18.64 \text{ rad/s}$ , $\xi_K = 0.4$ , $\omega_P = 2.0 \text{ rad/s}$ , $\xi_P = 0.6$ and $S_0 = 1000 \text{ cm}^2/\text{s}^3$ . . . . .	164
5.7	PSD of displ., $S_{XX}$ , for the Clough-Penzien spectrum in fig.5.6, $\omega_s = 13.96 \text{ rad/s}$ and $\xi_s = 0.05$ . . . . .	164
5.8	Deterministic optimal tuning ratios for uniform damping ratio (displ.). . . . .	165
5.9	Deterministic optimal damping ratios for uniform tuning ratio (displ.). . . . .	165
5.10	Deterministic optimal combinations of tuning and damping ratio (displ.). . . . .	166
5.11	$OF_{displ}$ deterministic analysis comparison between fixed damping ratio, fixed tuning ratio and free parameters. . . . .	166
5.12	Deterministic optimal tuning ratios for uniform damping ratio (acc.). . . . .	167
5.13	Deterministic optimal damping ratios for uniform tuning ratio (acc.). . . . .	167

5.14	Deterministic optimal combinations of tuning and damping ratio (acc.) . . . . .	168
5.15	$OF_{acc}$ deterministic analysis comparison between fixed damping ratio, fixed tuning ratio and free parameters. . . . .	168
5.16	$OF_{displ}$ (empty points) and $OF_{acc}$ (solid points) deterministic analysis comparison between fixed damping ratio, fixed tuning ratio and free parameters. . . . .	169
5.17	Robust optimal frequencies for uniform damping ratio (displ.) . . . . .	169
5.18	Robust optimal damping ratios for uniform frequency (displ.) . . . . .	170
5.19	Robust optimal combinations of parameters (displ.) . . . . .	170
5.20	Pareto front for uniform damping ratio (displ.) . . . . .	171
5.21	Pareto front for uniform frequency (displ.) . . . . .	171
5.22	Pareto front for free parameters (displ.) . . . . .	172
5.23	Reduced robust optimal frequencies for uniform damping ratio (displ.) . . . . .	172
5.24	Reduced Pareto front for uniform damping ratio (displ.) . . . . .	173
5.25	Reduced robust optimal damping ratio for uniform frequencies (displ.) . . . . .	173
5.26	Reduced Pareto front for uniform frequency (displ.) . . . . .	174
5.27	Reduced robust optimal combinations of parameters (displ.) . . . . .	174
5.28	Reduced Pareto front for free parameters (displ.) . . . . .	175
5.29	Robust optimal frequencies for uniform damping ratio (acc.) . . . . .	175
5.30	Robust optimal damping ratios for uniform frequency (acc.) . . . . .	176
5.31	Robust optimal combinations of parameters (acc.) . . . . .	176
5.32	Pareto front for uniform damping ratio (acc.) . . . . .	177
5.33	Pareto front for uniform frequency (acc.) . . . . .	177
5.34	Pareto front for free parameters (acc.) . . . . .	178
5.35	Reduced robust optimal frequencies for uniform damping ratio (acc.) . . . . .	178
5.36	Reduced Pareto front for uniform damping ratio (acc.) . . . . .	179
5.37	Reduced optimal damping ratio for uniform frequencies (acc.) . . . . .	179
5.38	Reduced Pareto front for uniform frequency (acc.) . . . . .	180
5.39	Reduced robust optimal combinations of parameters (acc.) . . . . .	180
5.40	Reduced Pareto front for free parameters (acc.) . . . . .	181



## Introduction

The *Multiple Tuned Mass Dampers* technology (MTMD) is a simple and reliable method between the possible external control technologies used for dynamic excitations. The MTMD does not require to act on the basement of the structure and can perform several times also for small swings in exercise conditions. It is ideal for many dynamic problems, especially for the control of recurrent vibrations in slender structures as towers, long span bridges and skyscrapers.

The technology is an extension of the *Single Tuned Mass Damper* (STMD) of which the first design was defined by Frahm in the 1909 that received a US patent for it[20]. During the years many improvements have been proposed considering systems with different mechanical properties, non-linear behaviour or under different design conditions. The single TMD consists in an added element with designed dynamic characteristics that mitigates the existing vibrations of the system if properly tuned to the latter. Energetic studies[23] has showed that the TMD reduces the energy input by changing the dynamic characteristics of the system and increasing the dissipative capacity. If the TMD is properly designed, the dissipation is focused around the frequencies of the main system with the biggest energy amount (i.e., around the resonance). Unfortunately, the single TMD is particularly sensible to small changes in the main system parameters with associated risks of detuning or even undesired in-phase amplifications.

In the 50's Welbourn and Bishop performed several analysis on TMD and, between other important results, introduced also the use of several tuned masses, defining the first form of MTMD[5]. The MTMD technology is overall more robust than the single TMD thanks to the wider range of damped frequencies, nevertheless, it is sensible as well to uncertain shifts from the design frequencies. These aspects make the TMD and MTMD particularly suitable for a robust design optimization in order to minimize both effectiveness and the sensitivity of the system to the deviations from the design target. To do that, both the stochastic nature of the excitation and of the design parameters have to be studied.

The studies performed in the field of probability during the last two centuries, together with the awareness about the random nature of actions applied to structures, led to the development of the studies in the field of random vibrations. In the theory of random vibrations all the dynamic actions and responses are described in terms of stochastic indicators as correlations, power spectral density and so on. The final aim is to have a dynamic description that takes in account the random nature of the excitation. A typical approach to characterize the dynamic actions in the random vibrations field is to take a white noise Gaussian input, for which simple solutions are available, and filter it with an appropriate intermediate system that describes the final action (i.e., a filter). For seismic actions, the Tajimi-Kanai filter is a popular solution due to its simplicity and to the capability to describe properly the resonance effects. Before performing a robust analysis, some results concerning the deterministic behavior of the MTMD for different characteristics of system and filter are given in order to have a reference for the robust analysis.

The perturbational methods are a popular branch of the approaches to the study of uncertainties used to evaluate the sensitivity to deviations of design parameters. They introduce a small change in the parameters from the design point and investigate the effect on the response. Among the others, the direct perturbation has the main advantage, compared to other solutions, of not requiring a full description of the distributions of random variables but only their moments. This approach reduces significantly the effort required for the analysis and avoids a full probabilistic description that is not always possible and, moreover, sensible to small errors in the probability distributions of the uncertain parameters.

Once the system response and its sensitivity are determined, a bidimensional objective function vector, containing the design point and its sensitivity, is used to perform a robust optimization. In this thesis, a genetic algorithm (GA) is used to manage the non convexity of the design dominion. Based on a simplified imitation of the evolution theory stated by Darwin, the GAs have been used in many optimization applications during the years to deal with high complexity problems thanks to their heuristic nature. They use fixed-sized bit strings mapped to the values of the design variables, while recombination and mutation operators allow to keep the diversity of the population that pass through to a fitness functions to evaluate the performance at each step of the optimization. The not adapt characteristic are eliminated while the best ones remain toward the best fit for the problem. The idea of GAs is that it is possible to reach the best solution by building together the blocks that characterize the nature of the population.

The final aim is to investigate the optimal number, frequency and damping ratio of the tuned masses for a fixed mass ratio (depending on technological limits) and different parameters of the system, while the structure is excited by a seismic input. The different configurations are investigated and results compared without a priori choices that would influence them.

In the first chapter, some basis about vibrations, probability and the theory of random processes are given. After that, the failure analysis in random vibration is explained. The second chapter is dedicated to the analysis of the response of systems excited by random vibrations, either single and multiple degrees of freedom ones. Then, the theory of filters and the modelling of seismic actions is presented. The third chapter introduces the optimization problem in the single and multi objective case, the typologies adopted and their limits are explained. The fourth chapter focuses on the TMD technology, describing the dynamic model, the design assumptions and some applications. After that, the direct perturbation method and the robust optimization approach for the TMD and MTMD in the random vibrations framework are presented. The fifth chapter focus on the proposed method for the robust optimization of MTMD systems excited by a stationary seismic random input. A deterministic analysis for varying design parameters is performed as reference and then a numerical sample analyzed to do comparisons on the results.

# Chapter 1

## Random vibrations

The description of dynamic actions applied on structures is one of the biggest deal in the structural design. The dynamic effects are difficulty to predict, influenced by the properties of the system and more demanding for the structures. In a simple manner, an action is said to be dynamic if the frequency of occurrence of its peaks is comparable to the natural frequency of the structure itself. From this simple definition, it is immediate how the system itself plays an important role in the dynamic response and influences the final behaviour.

The deterministic study of vibrations fails in giving a real description of the expected actions due to the randomness that characterizes them. The studies performed to overcomes this problem have brought to light the *random vibrations*, a class of time signals which cannot be easily described by a predictable analytic function and require a probabilistic analysis for their characterization. In this chapter, a summary about deterministic vibrations is presented to then introduce the main aspects concerning the properties and classification of random vibrations. After that, the analysis of peaks is explained in order to determine the failure probability associated to a process.

### 1.1 Vibrations

The state of excitation induced on a system by external dynamical forces takes the name of vibration. The vibrations can be divided according to different criteria, in first instance there are:

- *Free vibrations*: the system is left free to move after an initial excitation immediately removed at the beginning of motion. If the system has a Single Degree of Freedom (SDF), it moves with a single frequency associated to it called *natural frequency*. If instead the system has Multiple Degrees of Freedom (MDF), the motion is a linear combination of the main modes of vibration obtained by a modal decomposition.
- *Forced vibrations*: the forcing excitation remains applied on the system all along the motion and influences the response of the system. Particularly dangerous is the case in which the natural and exciting frequency coincide, causing a "resonance" effect with big amplifications of vibrations.
- *Undamped vibrations*: when frictions and energy dissipations are negligible in the analysis.
- *Damped vibrations*: when frictions and energy dissipations are not negligible in the analysis.
- *Linear vibrations*: the equation of motion is solvable in linear field by known solutions, the superposition principle is applicable.

- *Non-linear vibrations*: the equation of motion is not solvable by linear equations and a closed form is not always possible. This case includes the increasing damage (or fatigue) of the structure. Many methods have been developed, generally a linearisation is used.
- *Deterministic vibrations*: defined along time by a deterministic function.
- *Random vibrations*: defined along time by a stochastic function.

The typical nature of vibrations on real structure is forced, slightly damped, non-linear and random, however, for design purposes simplifications are often assumed.

## 1.2 Deterministic vibrations

Before defining the random vibrations, the response of a single degree of freedom system under a deterministic excitation is briefly introduced. First the harmonic case is analysed to give some remarks about the nature of the dynamic excitation. After that, a description of the response to a series of impulses is given to consider actions that do not have a specific analytical law. The references adopted for this section have been Muscolino[46] and Lutes & Sarkani[40] where further informations can be found.

### 1.2.1 Harmonic vibration

The most general case of deterministic vibration for a SDF system is the damped forced case, schematized in fig.1.1:

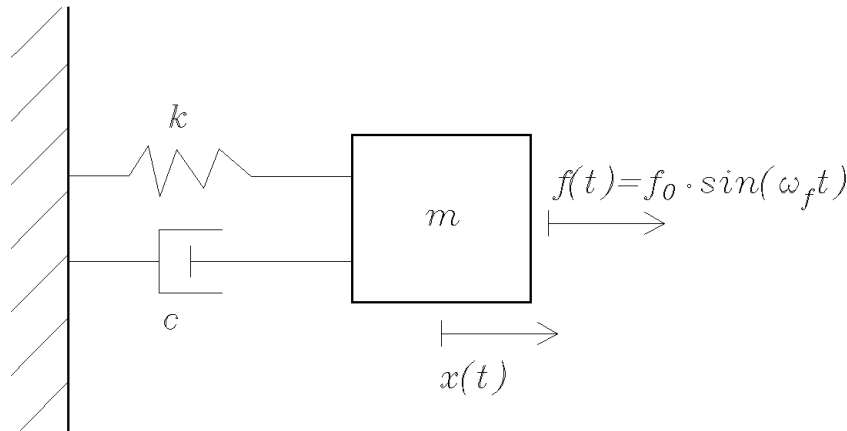


Figure 1.1: Damped and forced SDF system.

The term  $k$  gathers all the contributes to the stiffness of the system,  $m$  is the total mass,  $c$  is a viscous term containing the frictions and dissipations converted in a linear term <sup>1</sup>,  $f(t)$  is the external force, assumed as sinusoidal, and  $x(t)$  the deterministic displacement of the element, while  $t$  indicates the time.

<sup>1</sup>This is a typical approximation in the modelling due to the difficulties of giving a precise description of the damping effects. Therefore, it is generally considered in a form convenient for the analysis and coherent with the expected final response.

By applying the D'Alembert principle, the dynamic equilibrium is expressed as an equivalent static one at every instant of time under the force  $f(t) = f_0 \cdot \sin(\omega_f t)$ , where  $f_0$  is a constant and  $\omega_f$  is the external force frequency:

$$m \cdot \ddot{x}(t) + c \cdot \dot{x}(t) + k \cdot x(t) = f_0 \cdot \sin(\omega_f t) \quad (1.1)$$

where the symbol  $\dot{[\bullet]}$  indicates the time derivative of  $[\bullet]$ . The canonic form of the equation is given by dividing every member for the mass  $m$ :

$$\ddot{x}(t) + 2\xi_0\omega_0 \cdot \dot{x}(t) + \omega_0^2 \cdot x(t) = \frac{f_0}{m} \cdot \sin(\omega_f t) \quad (1.2)$$

where  $\omega_0^2 = k/m$  is the natural frequency of the oscillator and  $\xi_0 = c/(2\sqrt{mk}) = c/(2m\omega_0)$  is the damping ratio respect to the critical damping  $c_{crit} = 2m\omega_0$ . The name derives from the fact that, considering a damped free vibration, for  $c > c_{crit}$ , the motion decays with an exponential law, while for  $c < c_{crit}$ , it decays with an harmonic damped law. The natural period of the system is defined as:

$$T_0 = 2\pi\sqrt{\frac{m}{k}} \quad (1.3)$$

and is connected to the natural frequency by the following relation:

$$\omega_0 = \frac{2\pi}{T_0} = \sqrt{\frac{k}{m}} \quad (1.4)$$

The solution to the equation of motion can be expressed as sum of the homogeneous solution  $x_{om}(t)$ , with external force  $f(t) = 0$ , and a particular one  $x_p(t)$ :

$$x(t) = x_{om}(t) + x_p(t) \quad (1.5)$$

The homogenous solution in the damped case has the following form:

$$x_{om}(t) = e^{-\xi_0\bar{\omega}_0 t} [C_1 \cdot \cos(\bar{\omega}_0 t) + C_2 \cdot \sin(\bar{\omega}_0 t)] \quad (1.6)$$

where  $\bar{\omega}_0 = \omega_0\sqrt{1 - \xi_0^2}$  is the reduced frequency of the system due to damping. The two constants are obtained by fixing the initial conditions  $x(0) = x_0$  and  $\dot{x}(0) = \dot{x}_0$ :

$$C_1 = x_0, \quad C_2 = \frac{\dot{x}_0 + \xi_0\omega_0 \cdot x_0}{\bar{\omega}_0} \quad (1.7)$$

Introducing the following relations:

$$\bar{\rho}_0 = \left[ x_0^2 + \left( \frac{\dot{x}_0 + \xi_0\omega_0 \cdot x_0}{\bar{\omega}_0} \right)^2 \right]^{\frac{1}{2}}, \quad \tan \bar{\varphi}_0 = \frac{\dot{x}_0 + \xi_0\omega_0 \cdot x_0}{\bar{\omega}_0 \cdot x_0} \quad (1.8)$$

where  $\bar{\varphi}_0$  takes the name of phase angle and  $\rho_0$  is a function that interpolates the maximum of response, the solution is expressed as:

$$x(t) = \rho_0 \cdot e^{-\xi_0\omega_0 t} \cdot \cos(\bar{\omega}_0 t - \bar{\varphi}_0) \quad (1.9)$$

The general behave of the free vibrating system is shown in fig.1.2. The period, defined as  $\bar{T} = \bar{\omega}_0/2\pi$ , is increased by the damping as the frequency  $\bar{\omega}_0$  is reduced by it.

The particular solution has to satisfy identically eq.(1.2), its form is chosen to be similar to the exciting force:

$$x_p(t) = \rho_p \cdot \sin(\omega_f t - \varphi_p) \quad (1.10)$$

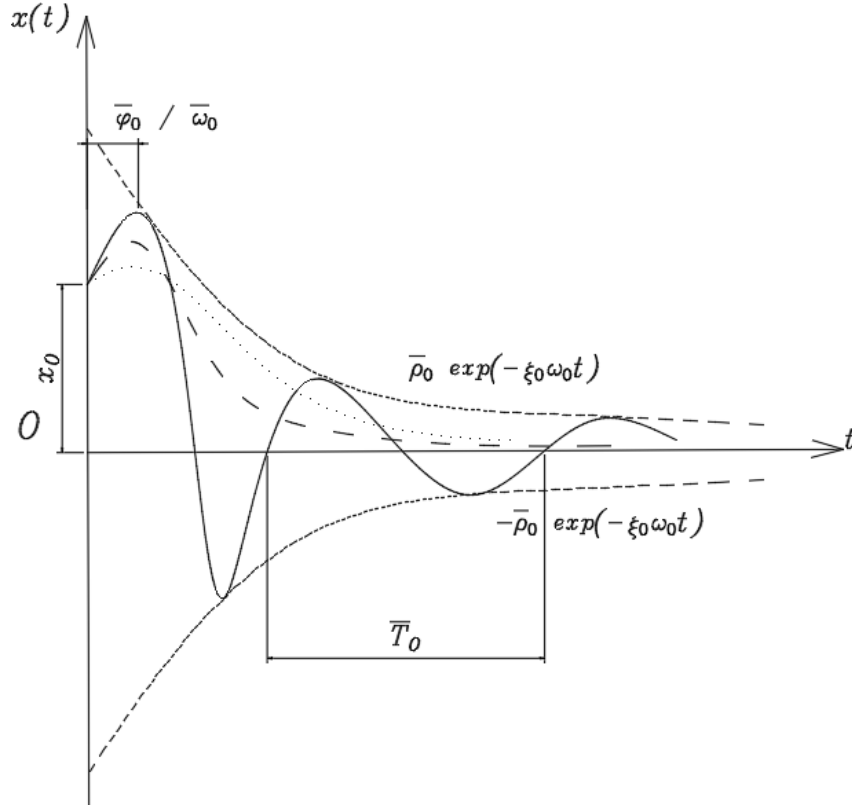


Figure 1.2: Free vibrations of a SDF not forced system for: (a)  $c < c_{crit}$  (solid line), (b)  $c = c_{crit}$  (dotted line), (c)  $c > c_{crit}$  (dashed line)[46].

Substituting it in eq.(1.2) gives:

$$\rho_p = \frac{f_0}{k} \frac{1}{\sqrt{[1 - (\omega_f/\omega_0)^2] + [2\xi_0(\omega_f/\omega_0)]^2}} \quad (1.11)$$

$$\tan(\varphi_p) = \frac{2\xi_0(\omega_f/\omega_0)}{1 - (\omega_f/\omega_0)^2} \quad (1.12)$$

In the case of  $c < c_{crit}$ , typical of the ordinary structures, the homogeneous contribute decays exponentially with the time, while the particular solution contribute persists until the external force is applied. The response is divided in two parts: the transitory and the steady state. The first depends significantly from the homogeneous solutions (that is, the initial conditions), the second is enough far from the beginning of motion to be independent from them.

The constants that appear in the homogeneous solutions are fixed by imposing the initial conditions on the global response:

$$x(0) = x_{om}(0) + x_p(0) = x_0, \quad \dot{x}(0) = \dot{x}_{om}(0) + \dot{x}_p(0) = \dot{x}_0 \quad (1.13)$$

The decay of the homogenous part depends significantly from the damping ratio of the system: the higher the damping, the shorter the transitory and the response will enter in the steady state before. Referring to fig.1.3, during the steady state the response does not depend from the passed time but simply from the  $\Delta t$  passed since the beginning of the last period of the sinusoid.

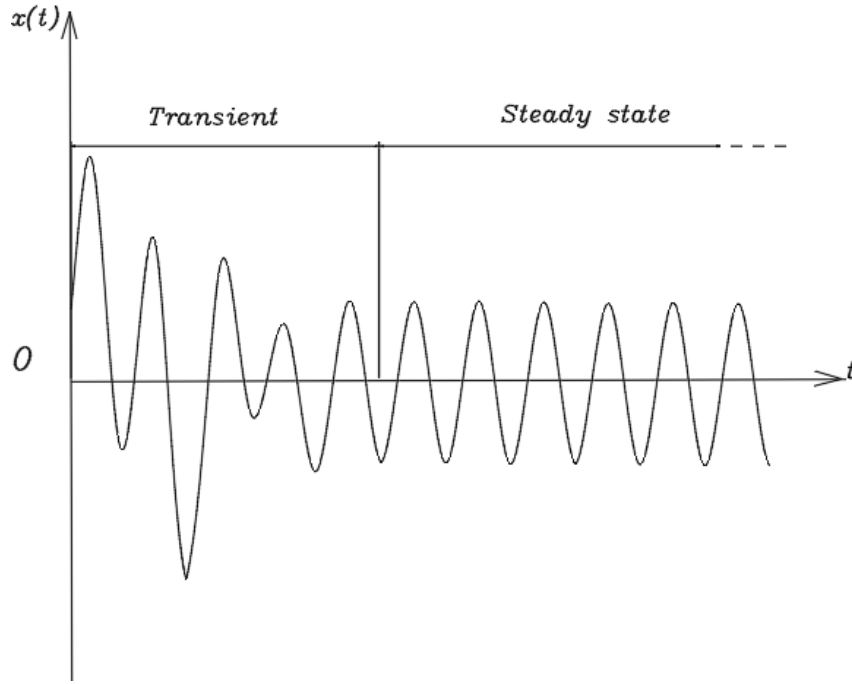


Figure 1.3: Transient and steady state part of the response[46].

From eq.(1.10) useful informations about the response can be obtained. Setting as nil the argument of the harmonic function, it is possible to get the delay time  $t_d$  between the first maximum of the exciting force and the particular response:

$$t_d = \frac{\varphi_p}{\omega_f} = \frac{\varphi_p}{2\pi} T_f \quad (1.14)$$

where  $T_f = 2\pi/\omega_f$  is the exciting force period. The static response is obtained by setting the inertial and damping forces as nil in eq.(1.1), getting  $x_{st} = f_0/k$ . By comparison with the dynamic solution, the *dynamic amplification factor*  $D$  is introduced:

$$D = \frac{x_p(t)|_{max}}{x_{st}} = \frac{1}{\sqrt{[1 - (\omega_f/\omega_0)^2]^2 + [2\xi_0(\omega_f/\omega_0)]^2}} \quad (1.15)$$

$D$  expresses the magnification of the external action due to dynamic effects. The particular solution in eq.(1.10) can be rewritten as:

$$x_p(t) = D \cdot x_{st} \cdot \sin(\omega_f t - \varphi_p) \quad (1.16)$$

By parametric studies, the *dynamic amplification factor*, also called *magnification factor*, has been plotted in a graph over the frequency ratio between external force and system  $\beta = \omega_f/\omega_0$ . Comparing the phase angle  $\varphi_p$  over  $\beta$  with  $D$  gives some useful information, both graphs are reported in fig.1.4.

At the variation of  $\beta$  different response of the system occurs:

1.  $\beta \cong 0$  corresponds to the static case ( $D \cong 1$ ): the force varies so slowly respect to the period of the system that it can be approximated as static. The phase angle  $\varphi_p = 0$ , no delay between external force and response.

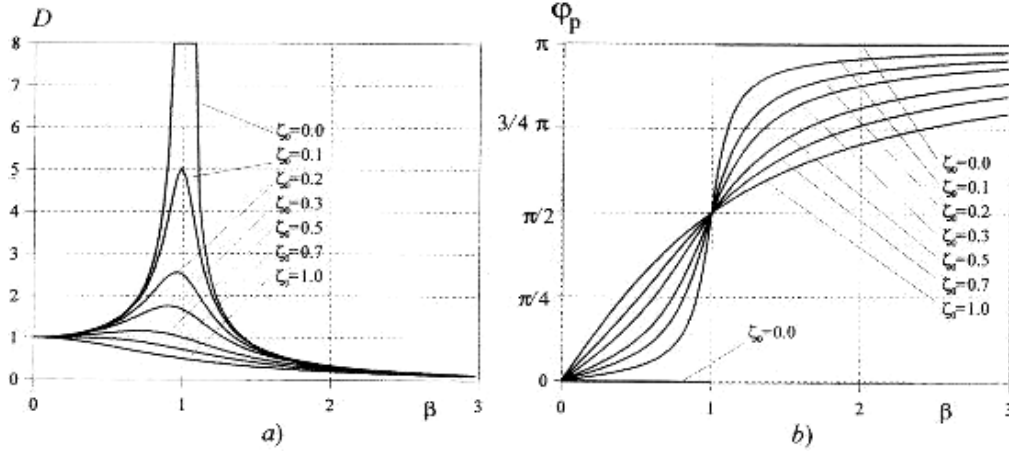


Figure 1.4: a) Magnification factor for different  $\beta$  and  $\xi_0$ , and b) phase angle associated[46].

2.  $\beta \cong 1$  corresponds to the *resonance* frequency: the magnification factor increases significantly and the phase angle  $\varphi_p$  tends to an asymptote where the sign of the tangent changes. There are different cases:
  - if the damping ratio  $\xi_0 = 0$ ,  $D$  has an asymptote for  $\beta \rightarrow 1$  and the response diverges; the phase angle  $\varphi_p = 0$  until  $\beta < 1$  and becomes  $\varphi_p = \pi$  for  $\beta > 1$ . This property is also used in the dynamic monitoring to find the resonance frequency of existing structures by measurements of the phase angle.
  - For  $0 < \xi_0 < 0.5$ , the dynamic factor  $D > 1$ , this is the typical case of civil structures where  $\xi_0 < 0.10$ .
3. For  $\beta > 1.41$ ,  $D < 1$  and the static response is higher than the dynamic one.
4. For  $\beta \rightarrow \infty$ , the dynamic coefficient  $D \rightarrow 0$ : the external force varies so quickly respect to the period of the system that the latter remains at rest.

For any value of  $\xi_0$ , the phase angle at the resonance ( $\omega_f = \omega_0$ ) passes through  $\varphi_p = \pi/2$ , that means  $t_d = T_f/4$ . For  $\beta \geq 1$  if  $\xi_0 \neq 0$ , or for  $\beta > 1$  if  $\xi_0 = 0$ , the phase angle is  $\varphi \cong \pi$  and the delay time is equal to  $t_d = T_f/2$ . The external force is said to be in *phase opposition*,  $f(t)$  is max while  $x(t)$  is min and vice versa.

The maximum of the magnification factor is at  $\beta = 1$  only if  $\xi_0 = 0$ , in fact, the damping reduces the frequency of the system:

$$\beta_{max} = \sqrt{1 - \xi_0^2}, \quad D_{max} = D(\beta_{max}) = \frac{\omega_0}{2\xi_0\bar{\omega}_0} = \frac{1}{2\xi_0\sqrt{1 - \xi_0^2}} \quad (1.17)$$

The abscissa of the change of sign of the phase angle varies as well:

$$\varphi_p(\beta_{max}) = \tan^{-1} \left[ \frac{\sqrt{1 - \xi_0^2}}{\xi_0} \right] \quad (1.18)$$

However, considering the small damping of the typical civil structures, the resonance frequency can be approximated as  $\beta_{max} \cong 1$  and  $\bar{\omega}_0 \cong \omega_0$ , therefore:

$$D_{max} \cong \frac{1}{2\xi_0}, \quad \varphi_p(\beta_{max}) \cong \tan^{-1} \left( \frac{1}{\xi_0} \right) \quad (1.19)$$

From the previous analysis it is evident how the response depends on the exciting force and the system properties. Thus, every system has a different behaviour under the same external excitation, amplifying or reducing it depending on the cases

### 1.2.2 The unit step function and the unit pulse function

The harmonic case is an idealization of the real nature of vibrations that generally are irregular and variable. The dynamic description of forces not definable by specific analytical functions can be done as superposition of impulses. Let introduce the following functions: the *unit step function*  $U(\bullet)$  and the *unit pulse function*  $\delta(\bullet)$ , of which the *Dirac's delta function* is a particular case.

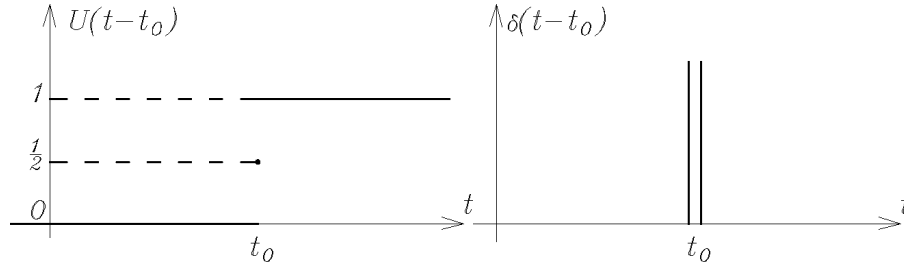


Figure 1.5: Unit step function and related Dirac's delta function[46].

Referring to figure 1.5, given a fixed time  $t_0$  of the step, the *unit step function*  $U(t-t_0)$  is[46]:

$$U(t-t_0) = \begin{cases} 0, & \text{for } (t-t_0) < 0 \\ 1/2, & \text{for } (t-t_0) = 0 \\ 1, & \text{for } (t-t_0) > 0 \end{cases} \quad (1.20)$$

The main use of this function is basically the description of an abrupt change. The corresponding *Dirac's delta function*  $\delta(t-t_0)$  is defined as:

$$\delta(t-t_0) = \begin{cases} 0, & \text{for } (t \neq t_0) \\ \infty, & \text{for } (t = t_0) \end{cases} \quad (1.21)$$

The unit step is connected to the unit pulse by a differential relation:

$$\delta(t-t_0) = \frac{d}{dt}U(t-t_0) \quad (1.22)$$

$$U(t-t_0) = \int_{-\infty}^t \delta(t-t_0) d\tau \quad (1.23)$$

These functions have many specific properties, in this thesis the useful ones will be cited when necessary, a detailed description is given by Muscolino[46].

### 1.2.3 Series of impulse induced vibrations

The impulse function is used for the description of not immediately analytically definable excitation and is the basis for vibrations analysis. Considering the SDF system excited by a generic force  $f(t)$  in fig.1.6, the system can be studied as superposition of impulses.

Fig.1.7 shows how to describe the response  $h_x(t)$  to a series of *impulsive signal*  $\delta(t)$  introduced at a time  $s$  defined as:

$$f(t) = \int_{-\infty}^{+\infty} f(s) \cdot \delta(t-s) ds = \int_{-\infty}^{+\infty} f(t-r) \cdot \delta(r) ds \quad (1.24)$$

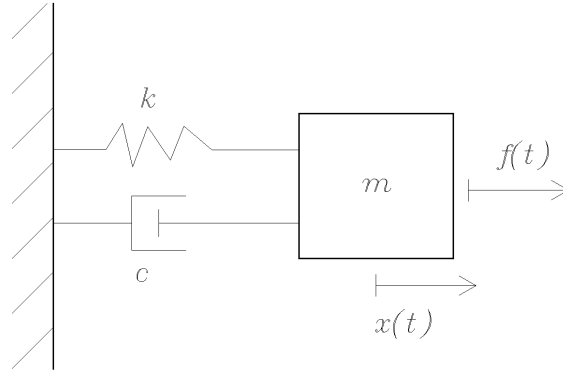


Figure 1.6: Schematic representation of a general linear system[40].

where  $r = t - s$ . Multiplying the unit pulse response for its amplitude and superposing gives the global response:

$$x(t) = \int_{-\infty}^{+\infty} f(s) \cdot h_x(t - s) ds = \int_{-\infty}^{+\infty} f(t - r) \cdot h_x(r) dr \quad (1.25)$$

This operation is called *convolution*, eq.(1.25) takes the name of *Duhamel convolution integral* and  $h_x(t)$  of *impulse response function* of the system for a pulse introduced at time  $s$ . Assigning the initial conditions, the equation becomes:

$$x(t) = \int_s^{+\infty} f(s) \cdot h_x(t - s) ds + h_x(s) \cdot f(s) \quad (1.26)$$

Eq.(1.26) is valid for time unvarying impulse response function but it is also possible to obtain a similar equation for a time varying impulse response function[40].

To resolve eq.(1.25) it is necessary to define the *impulse response function*  $h_x(t)$  for the dynamic system in study. In the most general case, for the SDF system represented in figure 1.6, the equation of motion is:

$$m \cdot \ddot{x}(t) + c \cdot \dot{x}(t) + k \cdot x(t) = f(t) \quad (1.27)$$

The corresponding *impulse response function*  $h_x(t)$  takes the form:

$$h_x(t) = \frac{e^{-\xi\omega_0 t}}{m \cdot \omega_d} \sin(\omega_d t) \cdot U(t) \quad (1.28)$$

where  $\omega_d = \omega_0(1 - \xi^2)^{1/2}$  is the damped frequency and  $U(t)$  the unit step function.

### 1.3 Historical develop of random vibration

An history of the random vibrations theory and of its harbingers is given by Paez[50], from which a short brief is presented here to contextualize the presented theory.

Although random vibrations have been observed for millennia for the effects on structures of earthquakes, wind, ocean waves, and other natural environments, they have been studied in a mathematical framework since only about the turn of the previous century. The first mathematical analysis that could be considered a random vibration one was performed by Einstein when he considered the Brownian movement of particles suspended in a liquid medium.

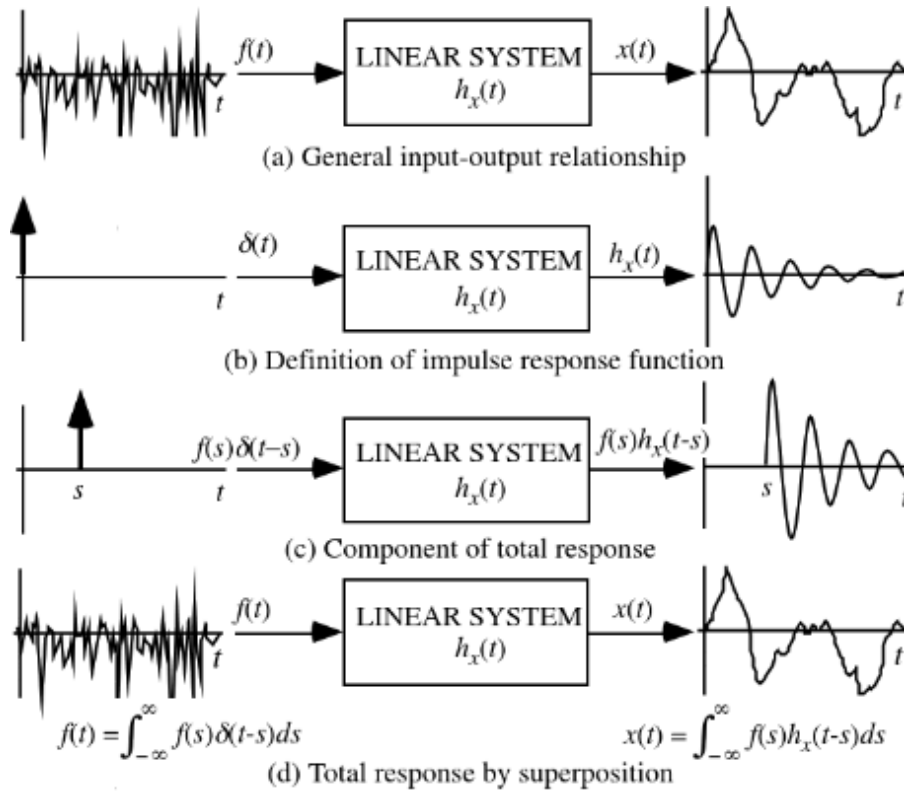


Figure 1.7: Duhamel integral analysis of an impulsive signal[40].

Numerous studies were carried out in the followed decades and in 1930 Norbert Wiener formally defined the spectral density of a stationary random process. However, only in the 1950s the subject of random vibrations of mechanical systems was addressed directly because needed to accurately predict structural response to jet engine noise and missile launch-induced environments. In 1958, Crandall organised a special summer programme at the Massachusetts Institute of Technology to address problems in the various areas of random vibrations of mechanical systems. From this first canonization of the theory, it has developed until today in many fields, including civil engineering, where significant results have been reached in the modelling of induced vibrations.

## 1.4 Stochastic processes characteristics

A description of the concept of random process was given by Crandall & Mark[15]: taking the displacements of an excited system  $x(t)$ , for definition, the vibration is a state of motion introduced by external actions which variate along time  $t$ . During an experiment with fixed initial conditions it is possible to study the time history of this motion (figure 1.8). If the experiment is performed many times and the results are always alike (either regular or irregular), the process is said to be *deterministic*. If instead, with the same fixed conditions, every time a different result is obtained, then the process is said to be *stochastic*. The randomness of the process depends on the variables not under the the experimenter's control and it is possible to define a grade of randomness depending on them. In other words, in random vibration theory the stochastic nature of a time series is directly addressed in order to control better the outcomes of an experiment.

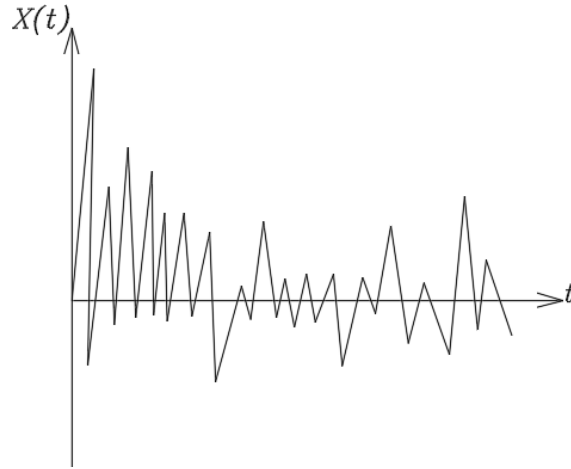


Figure 1.8: Time history of a random signal[15].

Therefore, in the study of a random process it is necessary to distinguish between[40]:

- *random variable*: a possible aleatory variable at a fixed instant of time  $t^*$  along the time history  $t$ ;
- *Time series*(or sample function): a sample time history  $X(t)$  characterizing the stochastic process  $\{X(t)\}$ ;
- *stochastic (or random) process*: the uncertain history of the response over a range of time values  $\{X(t)\}$ ;

A hierarchy of the random parameters can be defined: if the probability of occurrence  $P(A)$ , of a generic event  $A$ , requires just one value, the description of a random variable implies the construction of a distribution function at a fixed time, while a stochastic process requires the description of the behave of this distribution along the time  $t$ . Referring to picture 1.9, the ensemble constituting the process has  $n$  discrete sample functions corresponding to each repetition of the experiment that, due to its randomness, has no equal results. The stochastic process may be discrete or continuous on the time axis and is generally discrete on the samples axis, though a continuous idealization is possible if justified.

### 1.4.1 Classification of random processes

There are three criteria for the classification of random processes:

- *upon regularity*, consider the frequencies on which is spread the process. It is possible to state four classes:
  - *harmonic process*: maximum of the regularity, concentrated on a single frequency;
  - *narrow band process*: quite regular process, spread on a limited range of frequencies;
  - *broad band process*: more irregular process, spread on a wide range of frequencies;
  - *white noise (or delta-correlated process)*: maximum of the irregularity, the signal is ideally spread over infinite frequencies;
- *upon memory*, consider how the process is influenced by the previous values assumed along its time history;

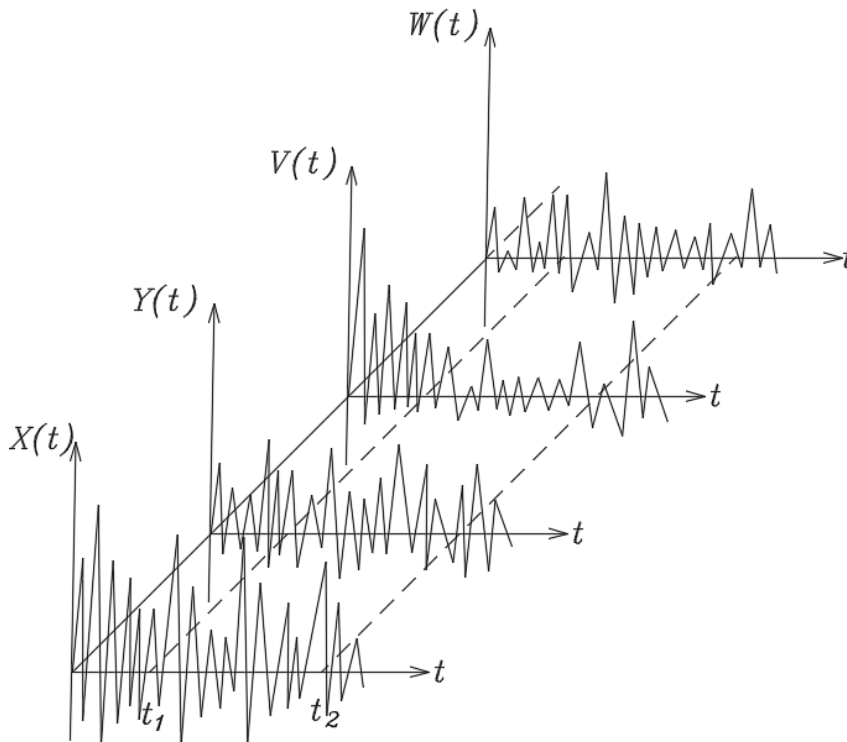


Figure 1.9: Ensemble of random time series that constitute the stochastic process[15].

- *upon distribution type*, depending on the probability density function assumed, generally a Gaussian approximation is used.

Only memoryless processes with different grade of regularity are investigated in this thesis, for a description of the different type of processes the text of Soong and Grigoriu[58] is advised.

### 1.4.2 Stationary and ergodic processes

A process is said to be *stationary* if its probability distribution does not change by a shift along the time axis[15]. In a simpler manner, at time  $t_i$  and at another time  $t_i + \tau$  the distributions of the random variables are the same. Crandall and Mark[15] proposed the example of a truck travelling along a constant roughness road at constant speed to explain this concept: there are no reasons to assume that the distribution may change along time assumed these hypothesis. This condition is ideal, in fact, a stationary process must have no beginning and no end as the border conditions perturb the behave. However, for a long period of measurement and enough far from the extremes the assumption may be appropriate. There are different type of stationarity connected to different probabilistic indicators, the most important are of distribution and probabilistic moments. It is logic that a stationarity in distribution implies a stationarity in the moments obtained from it, while the reverse is not necessary true.

A stochastic process is said to be *ergodic* if it is possible to assume the behave along time of a single sample function  $X(t)$  as representative of the entire random processes  $\{X(t)\}$ . An ergodic process is also stationary but the opposite is not necessary true. For instance[15], if there are  $n$  trucks travelling with the same speed along the same road, the assumption of ergodicity

may be justified. Ergodicity is very useful in the study of a registered process because aims to use a single sample function to describe it all. However, it is generally difficult to demonstrate ergodicity because it requires to take a significant group of samples, an operation that eliminates itself the advantages of the assumption. For these reasons, ergodicity is generally assumed from the beginning when seems justified.

### 1.4.3 Operations on random processes

A detailed exposition of how to approach continuity, differentiability, integration and other operations applied to random processes is explained by Lutes and Sarkani[40]. In a simplified manner, by remanding to the reference for some delicate mathematical aspects, the operations are applied as for any other temporal series with some particularities:

- a stochastic process converges to a random variables in a point;
- the derivative of a stochastic process is stationary but its integral is not generally so.

Basically, the random processes are treatable as every temporal series but with the complication of being stochastic and, therefore, to be treated with the instruments of probability.

## 1.5 Statistic and probability parameters

Once the ensemble of sample functions that describes the random process is defined, it can be characterized with the tools of probability. In this paragraph, the main formulations for the probabilistic description of an ensemble are presented and then extended to the random processes. The capital letters,  $X, Y, \dots$ , indicate the random variables and the small letters,  $x, y, \dots$ , a possible extraction of them.

### 1.5.1 Mono dimensional probability distribution

Given an ensemble of  $n$  possible outcomes of an experiment, for definition, the occurrence probability  $P(X^{(j)})$  of an event  $X^{(j)}$  is equal to:

$$P(X^{(j)}) = \frac{1}{n} \sum_{k=1}^m x_{fav} \tag{1.29}$$

where  $m$  is the number of favourable outcomes between the  $n$  possible ones. This variable takes the name of *probability mass function* and is concentrated on discrete values, the sum of the probability of all the elements is equal for definition to one. This concept can be extended to a continue ideal variable, introducing the *Probability Density Function* (PDF)  $p_X(x)$ . For definition,  $p_X(x) \cdot dx$  is the probability that the continue variable  $X$  lies between the value  $x$  and  $x + dx$ :

$$P(x \leq X \leq x + dx) = \int_x^{x+dx} p_X(x) dx = p_X(x) \cdot dx \tag{1.30}$$

The PDF is additive and the probability that  $X$  lies between  $a$  and  $b$ , illustrated in fig.1.10, is:

$$P(a \leq X \leq b) = \int_a^b p_X(x) dx \tag{1.31}$$

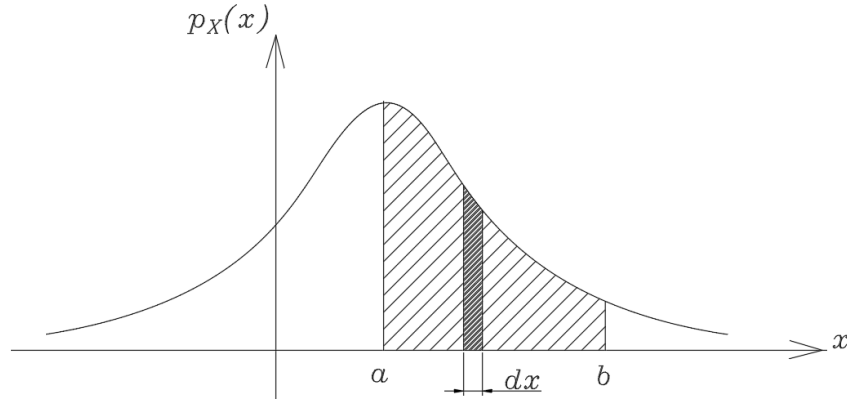


Figure 1.10: Probability density function (PDF).

To the PDF is directly connected the *Cumulative Density Function* (CDF)  $F(X)$ , that gives the total probability that the variable  $X$  has passed a fixed value  $x_p$ . The CDF may range between 0 and 1 and is defined as:

$$p_X(x) = \frac{d}{dx}F_X(x), \quad P(X \leq x_p) = F_X(x_p) = \int_{-\infty}^{x_p} p_X(x) dx \quad (1.32)$$

From the reverse relation it is possible to extract the fractile  $x_p$  of the distribution:

$$x_p = F^{-1}(P) \quad (1.33)$$

Substituting eq.(1.31) in eq.(1.32) gives:

$$P(a \leq X \leq b) = \int_a^b p_X(x) dx = F_X(b) - F_X(a) \quad (1.34)$$

## 1.5.2 Higher order distributions

The concepts expressed in the previous section are extendable to  $n$ -dimensional joint distributions by coupling more random variables. The coupled distributions are widely used in the description of stochastic processes because it is necessary to define the relations between ensembles at different instants of time. The following definitions are expressed in a 2D space for sake of simplicity but they can be easily extended to the  $n$ -dimensional case by increasing the number of random variables investigated[46].

Referring to fig.1.9, the distributions for two ensemble,  $X = X(t_1)$  and  $Y = Y(t_1)$ , at the same instant of time  $t_1$ , are extracted and eq.(1.30) extended in the 2D case (fig.1.11).

$$P(x \leq X \leq x + dx; y \leq Y \leq y + dy) = \int_x^{x+dx} \int_y^{y+dy} p_{XY}(x, y) dx dy \quad (1.35)$$

Eq.(1.35) represents an integration over an infinitesimal area of favourable conditions. Thus, the defined 3D volume corresponding to the probability of the event is the extension in 2D of (1.31):

$$P(a_1 \leq X \leq b_1; a_2 \leq Y \leq b_2) = \int_{a_2}^{b_2} \int_{a_1}^{b_1} p_{XY}(x, y) dx dy \quad (1.36)$$

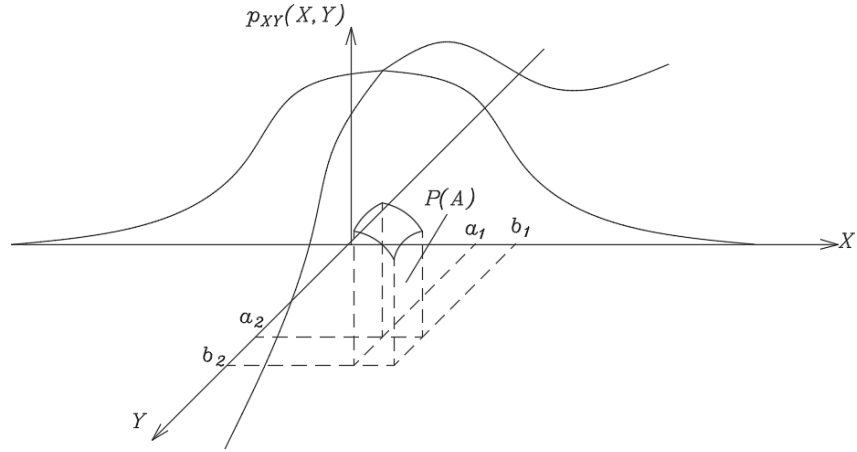


Figure 1.11: Joint PDF function[46].

The joint PDF is normalized at the one:

$$\int_{-\infty}^{+\infty} \int_{-\infty}^{+\infty} p_{XY}(x, y) dx dy = 1 \quad (1.37)$$

From the joint PDF it is possible to extract the corresponding marginal PDF for each distribution:

$$p_X = \int_{-\infty}^{+\infty} p_{XY}(x, y) dy \cdot p_Y = \int_{-\infty}^{+\infty} p_{XY}(x, y) dx \quad (1.38)$$

and the corresponding CDF:

$$P(X \leq x_p; Y \leq y_p) = F_{XY}(x_p, y_p) = \int_{-\infty}^{x_p} \int_{-\infty}^{y_p} p_{XY}(x, y) dx dy \quad (1.39)$$

The reverse relation gives:

$$p_{XY}(x, y) = \frac{\partial^2 F_{XY}(x, y)}{\partial x \partial y} \quad (1.40)$$

### 1.5.3 Independent and conditioned distributions

In the study of random processes the concepts of independent and conditioned event are often used to describe properly some elements, as the initial conditions, in the probabilistic field.

An event  $A$  is said to be conditioned by another event  $B$  if the outcome of the latter influences the outcome of  $A$ . In the ensembles theory this is expressed as:

$$P(A | B) = \frac{P(A \cap B)}{P(B)} = \frac{P(A \cdot B)}{P(B)} \quad (1.41)$$

the study of the related PDF shows that:

$$p_X(X = x | Y = y) = \frac{p_{XY}(x, y)}{p_Y(y)} \quad (1.42)$$

From eq.(1.32) the corresponding conditioned CDF is:

$$F_X(x_p | Y = y) = \int_{-\infty}^{x_p} p_X(X = x | Y = y) dx \quad (1.43)$$

In the random processes theory the use of conditioned CDF is quite common to express the initial conditions effects or the up-crossing of a threshold.

Two events  $A$  and  $B$  are said to be independent if the probability of their intersection is equal to the intersection of their probabilities. Strictly speaking, this means that the event  $A$  and  $B$  are not influenced by each other:

$$P(A \cap B) = P(A) \cdot P(B) \quad (1.44)$$

Substituting eq.(1.44) into eq.(1.41) shows that two independent events are also unconditioned:

$$P(A | B) = P(A) \quad (1.45)$$

The study of the related PDF leads to:

$$p_{XY} = p_X \cdot p_Y, \quad p_X(X = x | Y = y) = \frac{p_{XY}(x, y)}{p_Y(y)} = p_X \quad (1.46)$$

From eq.(1.32), the corresponding conditioned CDF is:

$$F_{XY} = F_X \cdot F_Y, \quad F_X(x_p | Y = y) = \int_{-\infty}^{x_p} p_X(X = x | Y = y) dx = F_X \quad (1.47)$$

The same relations can be applied for  $X$  conditioning  $Y$  by swapping the index in the previous equations. The assumption of independence implies many simplifications on the probabilistic characterization of a process but is not always justified and should be adopted with caution.

### 1.5.4 Mono-dimensional stochastic parameters

Starting from the previous distributions, some descriptors of the behave of the ensemble can be introduced. The discrete moment of  $k^{th}$  order,  $m_k$ , and its continuous extension are respectively:

$$m_k = \frac{1}{n} \sum_{k=1}^m x_j^k, \quad m_k = \int_{-\infty}^{+\infty} x^k \cdot p_X(x) dx \quad (1.48)$$

The  $1^{st}$  order moment, the *mean value*, indicates the average value of the distribution:

$$m_1 = \frac{1}{N} \sum_{k=1}^m x_j, \quad \mu = \int_{-\infty}^{+\infty} x \cdot p_X(x) dx \quad (1.49)$$

The  $2^{nd}$  order moment, the *mean square*, indicates the dispersion of the values from the origin:

$$m_2 = \frac{1}{N} \sum_{k=1}^m x_j^2, \quad \mu^2 = \int_{-\infty}^{+\infty} x^2 \cdot p_X(x) dx \quad (1.50)$$

The higher order moments are generally less used. For instance, the  $3^{rd}$  and the  $4^{th}$  (respective the skewness and Kurthosis moments) give informations about the shape of the distribution. Given the mean square, it is possible to calculate the *variance* that indicates the dispersion of the values from the mean and is defined as  $S^2$  for the discrete case and  $\sigma^2$  for the continuous idealization:

$$S^2 = \frac{1}{n} \sum_{k=1}^m (x_j - m_1)^2, \quad \sigma^2 = \int_{-\infty}^{+\infty} (x - \mu)^2 \cdot p_X(x) dx \quad (1.51)$$

The square root of the *variance* corresponds to the *standard deviation* from the mean value:

$$S = \sqrt{S^2} = \sqrt{\frac{1}{n} \sum_{k=1}^m (x_j - m_1)^2}, \quad \sigma = \sqrt{\sigma^2} = \sqrt{\int_{-\infty}^{+\infty} (x - \mu)^2 \cdot p_X(x) dx} \quad (1.52)$$

To work with normalized values is introduced the *deviation coefficient*, defined as  $\eta = \sigma_X/\mu_X$ . The deviation coefficient gives the value of deviation normalized over the the mean in order to compare quantities of different dimensions.

The moments can be defined alternatively by the use of the *linear operator mean*  $E[\bullet]$ . Taking a continuous function  $g(x)$ , its mean is:

$$E[g(x)] = \int_{-\infty}^{+\infty} g(x) \cdot p_X(x) dx \quad (1.53)$$

### 1.5.5 N-dimensional stochastic parameters

Taking an  $n$ -order joint PDF, the  $n$ -dimensional moments are introduced as extension of equation (1.48). The theory is here explained for the 2D distribution but can be easily extended to  $n$ -dimensional ones. The moment of  $k = r + s$  order of a 2D joint PDF is defined as

$$E[X^r, Y^s] = \int_{-\infty}^{+\infty} \int_{-\infty}^{+\infty} x^r \cdot y^s \cdot p_{XY}(x, y) dx dy, \quad k = r + s \quad (1.54)$$

The marginal and mixed values corresponding to the  $n$ -order moment are:

$$\text{Mean:} \quad \mu_X = E[X], \quad \mu_Y = E[Y] \quad (1.55)$$

$$\text{Mean square:} \quad E[X^2], \quad E[XY], \quad E[Y^2] \quad (1.56)$$

The bidimensional mean square has matrix form:

$$\Phi_{XY} = \begin{bmatrix} E[X^2] & E[XY] \\ E[YX] & E[Y^2] \end{bmatrix} \quad (1.57)$$

The same is valid for the bidimensional covariance matrix

$$\mathbf{K}_{XY} = \begin{bmatrix} \sigma_X^2 & \sigma_{XY} \\ \sigma_{YX} & \sigma_Y^2 \end{bmatrix} = \begin{bmatrix} E[X^2] - \mu_X^2 & E[(x - \mu_X)(y - \mu_Y)] \\ E[(y - \mu_Y)(x - \mu_X)] & E[Y^2] - \mu_Y^2 \end{bmatrix} \quad (1.58)$$

In the bidimensional case, the *linear correlation coefficient*  $\rho_{XY}$  can be introduced:

$$\rho_{XY} = \frac{\sigma_{XY}}{\sigma_X \cdot \sigma_Y} \quad (1.59)$$

The correlation coefficient expresses the linear correlation between two random variables and may range between 1 (max linear correlation) and 0 (no linear correlation), this limit is due to the Schwartz inequality[46]. However, the absence of a linear correlation does not exclude the presence of non-linear dependence. In general, two independent variables are always uncorrelated while the reverse is not necessarily true.

### 1.5.6 Gaussian (or Normal) distribution

The *Gaussian (or Normal) distribution* is a widely used PDF for the description of many physical phenomena. Its importance derives from the easy characterization once that the first and second order moments are given and from the suitability to describe the behavior of many ensembles. Despite this, there are limits to its uses and many problems require to adopt different distributions. Moreover, the Gaussian distribution may assume negative values and this is often problematic when working with physical quantities.

The Gaussian distribution (PDF) of a random variable  $X$  is defined as:

$$p_X(x) = \varphi(x) = \frac{1}{\sqrt{2\pi} \cdot \sigma_X} \cdot \exp\left[-\frac{(x - \mu_X)^2}{2\sigma_X^2}\right], \quad -\infty < x < \infty \quad (1.60)$$

The corresponding CDF cannot be obtained in closed form and a numerical integration of eq.(1.60) is necessary:

$$F_X(x) = \Phi(x) = \frac{1}{\sqrt{2\pi} \cdot \sigma_X} \int_{-\infty}^x \exp\left[-\frac{(x - \mu_X)^2}{2\sigma_X^2}\right] dx, \quad -\infty < x < \infty \quad (1.61)$$

It is possible to define a normalized Gaussian distribution by applying a transformation to the random variable  $X$  and setting  $Z = (X - \mu_X)/\sigma_X$ . In this way, the obtained PDF has mean  $\mu_Z = 0$ , variance  $\sigma_Z^2 = 1$  and can be written in the form:

$$p_Z(z) = \varphi(z) = \frac{1}{\sqrt{2\pi}} \cdot \exp\left(-\frac{z^2}{2}\right) \quad (1.62)$$

The corresponding CDF is:

$$F_Z(z) = \Phi(z) = \int_{-\infty}^z p_Z(z) dz = \frac{1}{\sqrt{2\pi}} \int_{-\infty}^z \exp\left(-\frac{z^2}{2}\right) dz \quad (1.63)$$

The reason for this transformation is the simplification in numerical calculations of eq.(1.61). In fact, the results obtained for the standard form have been tabulated for  $z \in [0,1]$  and every Gaussian distribution can be transformed in the normalized form (and then back) to get the desired results without performing again the numerical integration. The standard normal distribution is plotted in fig.1.12; from statistical calculations, for a value of  $\pm 3\sigma$ , the 99.7% of the set of random variables is covered and the evaluation can be considered enough affordable.

The normal distribution is completely defined from its first two moments (mean and variance), a property that implies a big reduction of the informations required to characterize it. Moreover, according to the *central limit theorem*, a sequence of mutually independent and identically distributed random variables converges, for a high number of outcomes, to a *normal distribution*. For these reasons, many physical ensembles are modelled as Gaussian.

In the case of a *bivariate normal distribution*, with two independent random variables  $X$  and  $Y$ , the joint PDF is:

$$p_{XY}(x, y) = \frac{1}{2\pi\sigma_X\sigma_Y\sqrt{1-\rho^2}} \exp\left[-\frac{v}{2(1-\rho^2)}\right] \quad (1.64)$$

where  $\rho$  is the correlation coefficient defined in (1.59) and  $v$  is equal to:

$$v = \frac{(x - \mu_X)^2}{\sigma_X^2} - \frac{2\rho(x - \mu_X)(y - \mu_Y)}{\sigma_X\sigma_Y} + \frac{(y - \mu_Y)^2}{\sigma_Y^2} \quad (1.65)$$

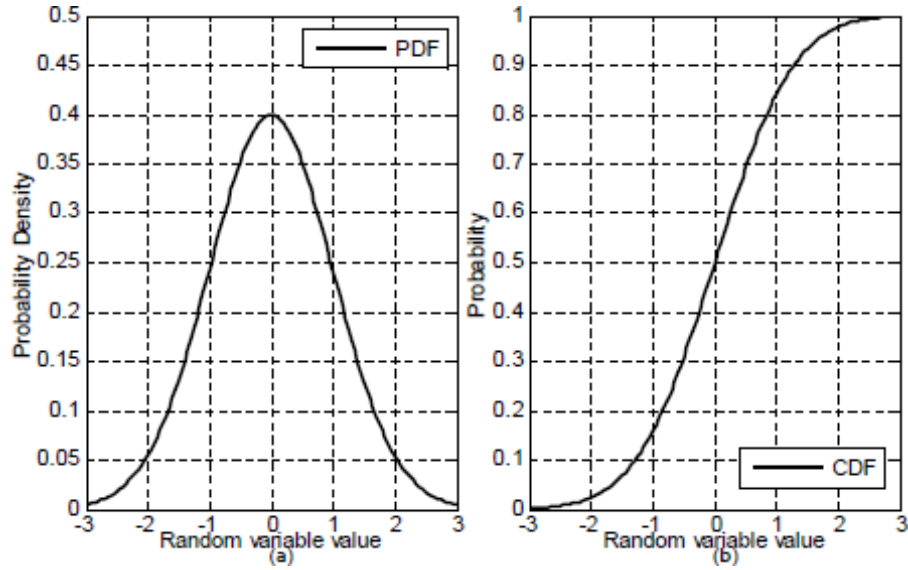


Figure 1.12: Standard normal distribution: (a) PDF, (b) CDF[60].

### 1.5.7 Exponential distribution

The exponential distribution is widely used in the analysis of first time occurrence of rare events. The exponential PDF is defined as:

$$f(x, \lambda) = \begin{cases} 0, & \text{for } x < 0 \\ \lambda e^{-\lambda x}, & \text{for } x \geq 0 \end{cases} \quad (1.66)$$

The corresponding CDF is:

$$F(x, \lambda) = \begin{cases} 0, & \text{for } x < 0 \\ 1 - e^{-\lambda x}, & \text{for } x \geq 0 \end{cases} \quad (1.67)$$

It is possible to demonstrate that the mean of the exponential distribution is  $\mu_X = 1/\lambda$  and the variance is  $\sigma_X^2 = 1/\lambda^2$ .

### 1.5.8 Poisson distribution

The Poisson distribution is used in the description of rare events sequential occurrence: it is quite simple to describe and, moreover, generally conservative in the assumption of independent events. The Poisson PDF is defined as:

$$f(k, \lambda) = \frac{\lambda^k e^{-\lambda}}{k!}, \quad \lambda \in \mathbb{R}^+, k \in \mathbb{N}_0 \quad (1.68)$$

where  $k$  is the events counting indicator. The corresponding CDF is:

$$F(k, \lambda) = e^{-\lambda} \sum_{i=0}^{\lfloor k \rfloor} \frac{\lambda^i}{i!} \quad (1.69)$$

where  $\lfloor a \rfloor$  indicates the floor function, that takes as input a real number  $a$  and gives as output the greatest integer less than or equal to  $a$ . The mean is  $\mu_X = \lambda$  and the variance too is  $\sigma^2 = \lambda$ . The Poisson distribution for  $k = 1$  corresponds to the exponential one. This should not surprise: the probability of occurrence between the events of the Poisson process is exponentially distributed.

## 1.6 Stochastic process probabilistic characterization

The concepts expressed in section 1.5 are applicable to the study of random processes along time domain by using the linear operator mean, defined in eq.(1.53), to the variables  $X_1 = X(t_1)$ ,  $X_2 = X(t_2), \dots, X_n = X(t_n)$ . That is, the same probabilistic parameters defined in the samples ensemble at a fixed time  $t_i$  can be applied between one or more random variables at different instants of time, defining a *time average*. To avoid confusion between the two cases, the following notation will be used:

- $X, Y, \dots$  indicate the different random variables along the ensemble either at a fixed time  $t_i$  or between different instants of time;
- $X_1, X_2, \dots, X_n$  indicate the same random variable at different instants of time;

The respective variables in small letters indicate one of their realization, either in time domain or along the random variables ensemble.

### 1.6.1 Time averages

The time average at a fixed instant of time  $t$  is defined as[40]:

$$\mu_X(t) = E[X(t)] = \int_{-\infty}^{+\infty} x \cdot p_x[x(t)] dt \quad (1.70)$$

Referring to figure 1.9, the mean between a random variable  $X_1$  at time  $t_1$  and  $X_2$  at time  $t_2$  can be calculated. This function is called *auto-correlation*  $\Phi_{XX}(t_1, t_2)$  and expresses the link between the same random variable at two different instants of time.

$$\Phi_{XX}(t_1, t_2) = E[X_1 X_2] = \int_{-\infty}^{+\infty} \int_{-\infty}^{+\infty} x_1 \cdot x_2 \cdot p_{X_1 X_2}(x_1, x_2) dx_1 dx_2 \quad (1.71)$$

In the same way as for the mean square of a joint PDF, the marginal distributions can also be extracted. The same parameter defined between two random variables  $X_1$  and  $Y_2$  at different time instants  $t_1$  and  $t_2$  is defined *cross-correlation* function  $\Phi_{XY}(t_1, t_2)$ :

$$\Phi_{XY}(t_1, t_2) = E[X_1 Y_2] = \int_{-\infty}^{+\infty} \int_{-\infty}^{+\infty} x_1 \cdot y_2 \cdot p_{X_1 X_2}(x_1, x_2) dx_1 dx_2 \quad (1.72)$$

The *auto-covariance* between the same variables along time is:

$$K_{XX}(t_1, t_2) = \int_{-\infty}^{+\infty} \int_{-\infty}^{+\infty} (x_1 - \mu_{x_1}) \cdot (x_2 - \mu_{x_2}) \cdot p_{X_1 X_2}(x_1, x_2) dx_1 dx_2 \quad (1.73)$$

The *cross-covariance* is:

$$K_{XY}(t_1, t_2) = \int_{-\infty}^{+\infty} \int_{-\infty}^{+\infty} (x_1 - \mu_{x_1}) \cdot (y_2 - \mu_{y_2}) \cdot p_{X_1 Y_2}(x_1, y_2) dx_1 dy_2 \quad (1.74)$$

The auto-correlation is always a positive even function of time  $t$  and expresses the similarity of the random variables at different instants of time. The cross-correlation instead may variate in the shape depending on the analyzed variables.

### 1.6.2 Stationarity

If the process is stationary, useful simplifications can be done in the definition of the previous parameters. In fact, if the distributions depend only from the time shift  $\tau = t_2 - t_1$ , then the mean does not change along time, i.e., it is constant. The correlation and covariance functions instead become dependent only from the time shift  $\tau$  between the distributions of the two variables of interest. Thus, the *stationary mean* is  $\mu_X = \text{cost}$ , the *stationary correlation*  $R_{XX}(\tau = t_2 - t_1)$ , and *stationary covariance*  $C_{XX}(\tau = t_2 - t_1)$ , take respectively the form:

$$\Phi_{XX}(t_1, t_2) = R_{XX}(\tau = t_2 - t_1) = \int_{-\infty}^{+\infty} x(t) \cdot x(t + \tau) \cdot p_{X, X+\tau}(x, x + \tau) d\tau \quad (1.75)$$

and

$$\begin{aligned} K_{XX}(t_1, t_2) &= C_{XX}(\tau = t_2 - t_1) = \\ &= \int_{-\infty}^{+\infty} [x(t) - \mu_X] \cdot [x(t + \tau) - \mu_X] \cdot p_{X, X+\tau}(x, x + \tau) d\tau \end{aligned} \quad (1.76)$$

Substituting the value  $\tau = 0$ , that means  $t_1 = t_2$ , the correlation converges to the mean square and the covariance to the variance of the random variable ensemble. This involves an important observation, for the Schwartz inequality[40], the average of a variable with itself is always higher than the cross-average with another, in fact:

$$E^2[X_1 X_2] \leq E[X_1^2] \cdot E[X_2^2] \quad (1.77)$$

This means that the auto-correlation between an instant,  $t_1$ , and a second one,  $t_2$ , is less than the variance at a fixed instant of time or at most equal to it if  $t_1 \equiv t_2$ . The same is true if the time instants are swapped, that is:

$$\Phi_{XX}(t_1, t_2) \leq \sigma_X^2(t_1), \quad \Phi_{XX}(t_2, t_1) \leq \sigma_X^2(t_2), \quad \forall t_1, t_2 \quad (1.78)$$

### 1.6.3 Fourier's transform

An analysis in the frequency domain aims to describe important aspects of a random process that otherwise would be not immediate to see in time domain. To do a shift from time to frequency it is necessary to introduce the *Fourier's transform*  $\bar{f}(\omega)$  of a function  $f(t)$  as:

$$\bar{f}(\omega) = \frac{1}{2\pi} \int_{-\infty}^{+\infty} f(t) \cdot e^{-i\omega t} dt \quad (1.79)$$

The *reverse Fourier's transform* of the function aims to return back to time domain from the frequency one and is:

$$f(t) = \int_{-\infty}^{+\infty} \bar{f}(\omega) \cdot e^{i\omega t} d\omega \quad (1.80)$$

To apply the Fourier's transform, the condition that the transformed function has to be limited on an infinite integration domain must be fulfilled, otherwise, the function would diverge:

$$\int_{-\infty}^{+\infty} |f(t)| dt < \infty \quad (1.81)$$

Not all functions respect this condition and to avoid problems in unbounded cases sometimes a limited domain of integration is considered. Generally, a cut-off frequency is chosen depending on the analysis performed and how the higher (and lower) frequencies weight on the response.

### 1.6.4 Frequency domain

To extend the concept of the Fourier analysis in the random vibration field, the deterministic variable  $x(t)$  has to be substituted with the random correspondent one,  $X(t)$ :

$$\bar{X}(\omega) = \frac{1}{2\pi} \int_{-\infty}^{+\infty} X(t) \cdot e^{-i\omega t} dt \quad (1.82)$$

In this way, a new stochastic process  $\{\bar{X}(\omega)\}$  in the frequency domain is defined[40]. From this process, the main stochastic parameters in frequency domain are obtainable. The mean is:

$$\mu_{\bar{X}}(\omega) = \frac{1}{2\pi} \int_{-\infty}^{+\infty} \mu_X(t) \cdot e^{-i\omega t} dt = \bar{\mu}_X(\omega) \quad (1.83)$$

The Fourier's transform is a linear operator and, therefore, the mean of the Fourier transform of a process  $\{X(\omega)\}$  is equal to the Fourier transform of the mean of the process itself.

For what concerns the second order moments, the fact that  $\{X(\omega)\}$  is not a real process requires to define them in a slightly different way. The complex conjugate (defined as  $w^*$  for a generic complex variable  $w$ ) is used. The autocorrelation becomes:

$$\Phi_{\bar{X}\bar{X}}(\omega_1, \omega_2) = E[\bar{X}(\omega_1) \cdot \bar{X}^*(\omega_2)] \quad (1.84)$$

In this way, the frequency auto-correlation takes real value for  $\omega_1 = \omega_2 = \omega$  as it should be:

$$\Phi_{\bar{X}\bar{X}}(\omega, \omega) = E[\bar{X}^2(\omega)] \quad (1.85)$$

From the auto-correlation, the auto-covariance is calculated:

$$K_{\bar{X}\bar{X}}(\omega, \omega) = E\left[ [\bar{X}(\omega_1) - \mu_{\bar{X}}(\omega_1)] \cdot [\bar{X}(\omega_2) - \mu_{\bar{X}}(\omega_2)]^* \right] \quad (1.86)$$

In explicit form this means:

$$K_{\bar{X}\bar{X}}(\omega, \omega) = \frac{1}{4\pi^2} \int_{-\infty}^{+\infty} \int_{-\infty}^{+\infty} K_{XX}(t_1, t_2) \cdot \exp[-i(\omega_1 t_1 - \omega_2 t_2)] dt_1 dt_2 \quad (1.87)$$

The biggest problem in the application of the analysis in frequency domain is that the previous expressions do not exist for many case of interest. In particular, if  $\{X(t)\}$  is a stationary process, it is easy to verify that its stochastic parameters (mean, correlation and variance) do not tend to zero as  $t \rightarrow \infty$ . A solution to this problem is using a truncated Fourier transform[40], but this approach implies a loss of information about the process. Moreover, if the response is not well known, it is not easy to determine a cut-off frequency.

The Fourier transform of the correlation function, calculated in eq.(1.84), is an important parameter for the description of the random process and takes the name of *Power Spectral Density* (PSD)  $S_{XX}$  or, for mixed terms, of *cross-power spectral density*  $S_{XY}$ :

$$S_{XX}(\omega_1, \omega_2) = \int_{-\infty}^{+\infty} \Phi_{XX}(t_1, t_2) \cdot e^{-i\omega t} dt \quad (1.88)$$

$$S_{XY}(\omega_1, \omega_2) = \int_{-\infty}^{+\infty} \Phi_{XY}(t_1, t_2) \cdot e^{-i\omega t} dt \quad (1.89)$$

In opposite way, applying the reverse Fourier transform, the correlation function from the power spectral density is obtainable:

$$\Phi_{XX}(t) = \int_{-\infty}^{+\infty} S_{XX}(\omega_1, \omega_2) \cdot e^{i\omega t} d\omega \quad (1.90)$$

$$\Phi_{XY}(t) = \int_{-\infty}^{+\infty} S_{XY}(\omega_1, \omega_2) \cdot e^{i\omega t} d\omega \quad (1.91)$$

The *power spectral density* is an even function of the frequency  $\omega$  as the *correlation function* is an even function of time  $t$ . The PSD is a descriptor of the behave of a process that gives the frequencies that characterize it in an immediate representation. For the same reasons stated for the auto-correlation, the auto PSD is always maximum between a frequency and itself ( $\omega_1 \equiv \omega_2$ ) and decreases for different values of  $\omega_1$  and  $\omega_2$ .

Physically, it is not possible to define negative frequencies and in practical applications it is preferred to define a *unilateral power spectral density*, containing only the positive frequencies of the process. To have the same energy content subtended by the spectral density function, the values have to be multiplied for 2. If instead of the circular frequency  $\omega$ , the normal one  $f$  (measured experimentally) is used, it is necessary to multiply the values for  $2\pi$ :

$$G_{XX}(\omega) = 2 \cdot S_{XX}(\omega) \quad G_{XX}(f) = 4\pi \cdot S_{XX}(\omega) \quad (1.92)$$

### 1.6.5 Energetic interpretation of the PSD

Given a deterministic registration of a function  $x(t)$  with duration  $t_f$  (for example an acceleration history), the *energy*  $\varepsilon_x(t_f)$  of the function  $x(t)$  in the time interval  $t_f$  is defined as[46]:

$$\varepsilon_x(t_f) = \alpha \int_0^{t_f} x^2(t) dt \quad (1.93)$$

where  $\alpha$  is a constant used to give the dimension of an energy to the second member. For instance, if  $x(t)$  is a displacement,  $\alpha$  is the ratio between stiffness and registration time, with the result that  $\varepsilon_x$  is a potential energy. If  $x(t)$  is a velocity,  $\alpha$  is the ratio between mass and registration time, with the result that  $\varepsilon_x$  is a kinetic energy.

A periodic function of period  $T_p$  can be expressed by a Fourier series as:

$$x(t) = \frac{1}{2}a_0 + \sum_{k=1}^{+\infty} [a_k \cos(k \cdot \omega_p t) + b_k \sin(k \cdot \omega_p t)] \quad (1.94)$$

where  $a_k$  and  $b_k$  are determined by the following expressions:

$$a_k = \frac{2}{T_p} \int_{-T_p/2}^{T_p/2} x(t) \cdot \cos(k \cdot \omega_p t) dt, \quad b_k = \frac{2}{T_p} \int_{-T_p/2}^{T_p/2} x(t) \cdot \sin(k \cdot \omega_p t) dt \quad (1.95)$$

where  $\omega_p = 2\pi/T_p$  is the *fundamental circular frequency* of the periodic function  $x(t)$ . The other frequencies, multiples of the fundamental one, are called the *harmonics of the periodic function*. The term  $a_0$  is called *continue component*. By substituting (1.94) in (1.93), the energy of an harmonic process in the period  $T_p$  (except for the  $\alpha$  constant) is obtained:

$$\varepsilon_x(T_p) = T_p \left[ \frac{a_0^2}{4} + \sum_{k=1}^{+\infty} \frac{a_k^2 + b_k^2}{2} \right] \quad (1.96)$$

For eq.(1.96), the total energy of the process, in the range  $[n \cdot T_p, (n + 1) \cdot T_p]$ , is given by the sum of more contributes:

- the energy of the continue component  $T_p \cdot a_0^2/4$ ;
- the energy of the fundamental frequency  $T_p \cdot (a_1^2 + b_1^2)/2$ ;
- the energy of the main harmonics  $T_p \cdot (a_k^2 + b_k^2)/2$ , for  $k \geq 2$ .

Therefore, the amount of energy of an harmonic process is constant along a period but infinite in  $(-\infty, +\infty)$ . In analogy with the optics, it is possible to represent the energy associated to the different frequencies by an *energy spectrum of the periodic function*. The spectrum shows the energy associated to every frequency in the period  $T_p$ . Usually, instead of determining the energy content in the period, it is preferred to determinate the energy in the unit of time, i.e., the power of the process:

$$S_x(T_p) = \frac{\varepsilon_x(T_p)}{T_p} = \frac{a_0^2}{4} + \sum_{k=1}^{+\infty} \frac{a_k^2 + b_k^2}{2} \quad (1.97)$$

The obtained function takes the name of *power spectrum* of the periodic function  $x(t)$ . An example is given in fig.1.13: as expected, the main energy content (given by multiplying the values of the power spectre for the period  $T_p$ ) is concentrated at the fundamental frequency.

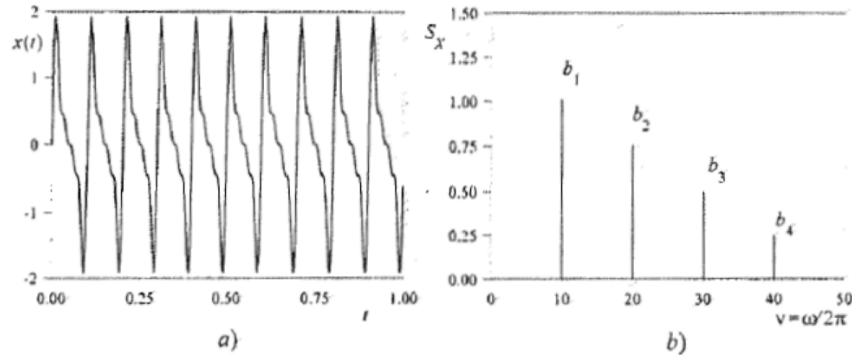


Figure 1.13: Periodic function  $x(t)$ : a) time history, b) power spectrum[46].

If a function  $x(t)$  is not periodic but satisfies the condition in eq.(1.81), it is still possible to determine the spectrum by calculating its Fourier transform:

$$\bar{x}(\omega) = \int_{-\infty}^{+\infty} x(t) \cdot e^{-i\omega t} dt = \int_{-\infty}^{+\infty} x(t) \cdot [\cos(\omega t) - i \sin(\omega t)] dt \quad (1.98)$$

The real and imaginary part can be separated:

$$\text{Re}[\bar{x}(\omega)] = \int_{-\infty}^{+\infty} x(t) \cdot [\cos(\omega t)] dt, \quad \text{Im}[\bar{x}(\omega)] = \int_{-\infty}^{+\infty} x(t) \cdot [\sin(\omega t)] dt \quad (1.99)$$

and the modulus of the function is:

$$C_x(\omega) = |x(\omega)| = \sqrt{x(\omega) \cdot x^*(\omega)} = \sqrt{(\text{Re}[\bar{x}(\omega)])^2 + (\text{Im}[\bar{x}(\omega)])^2} \quad (1.100)$$

For the *Parseval equality*[40], it is possible to demonstrate that the energy of the function, in the range  $(-\infty, +\infty)$ , is:

$$\varepsilon_x = \frac{\alpha}{2\pi} \int_{-\infty}^{+\infty} C_x^2(\omega) d\omega \quad (1.101)$$

This means that a non-periodic function has finite energy content. The terms inside the integral of (1.101),  $C_x^2(\omega) d\omega$ , is, except for  $\alpha/2\pi$ , the contribute given to the total energy by the harmonics of the Fourier's transform in an infinitesimal circular frequency interval between  $\omega$  and  $\omega + d\omega$ . Therefore,  $C_x^2(\omega)$  is the spectre of the *specific energy* or *power spectral density* of the function  $x(t)$ . The diagram of the square roots of  $|x(\omega)| \equiv C_x(\omega)$  characterizes the *Fourier's spectrum* of the the function. In conclusion, it is evident that the Fourier's spectrum of a continue function at a certain frequency is bounded to the energy contained by the function at that frequency.

Briefly, there are three main differences between the spectral representation of a deterministic periodic and not periodic functions defined in the dominion  $(-\infty, +\infty)$ [46]:

- the periodic functions show, differently from the not periodic ones, a discontinuous spectrum. The energy is concentrated only on the fundamental frequency and on its multiples.
- For periodic functions, the energy is finite in the interval  $T_p$  but is infinite in the range  $(-\infty, +\infty)$ ; consequently, they are better represented by the power spectrum defined in eq.(1.97) than from an energy spectrum.
- For the non periodic continuous functions, that have a Fourier transform, the total energy is finite and it is possible to represent the spectral properties by the power spectral density  $C_x^2(\omega)$  or the Fourier's spectrum  $|x(\omega)| \equiv C_x(\omega)$ .

Considering a stationary, mean zero, process  $X(t)$ , it can be seen as an ensemble of infinite samples with constant mean value and stationary mean square (i.e. independent from  $t$ ). From the Parceval equality, the energy of the process, equals to the mean of the random energy of each sample, can be evaluate as:

$$\varepsilon_x = \alpha \cdot E \left[ \int_{-\infty}^{+\infty} X^2(t) dt \right] = \alpha \int_{-\infty}^{+\infty} \Phi_X^2(t) dt = \frac{\alpha}{2\pi} \cdot E \left[ \int_{-\infty}^{+\infty} |X^2(\omega)| d\omega \right] = +\infty \quad (1.102)$$

Therefore, the mean square of a stationary process has infinite energy. For this reason, the energy content of stationary processes is often described by a power spectral density. The finite Fourier transform of  $X(t)$  in the interval  $(-T, T)$  is:

$$X(\omega, T) = \int_{-T}^T X(t) \cdot e^{-i\omega t} dt \quad (1.103)$$

and the correspondent power spectral density is:

$$S_{XX}(\omega) = \lim_{T \rightarrow \infty} \frac{1}{2T} \left\{ \frac{\alpha}{2\pi} \cdot E[|X(\omega, T)|^2] \right\} \equiv \frac{\alpha}{2\pi} \lim_{T \rightarrow \infty} \frac{1}{2T} \cdot E[|X(\omega, T)|^2] \quad (1.104)$$

where  $2T$  is the time interval in which the samples of the random stationary processes  $X(t)$  is defined. The so defined power spectral density  $S_{XX}(\omega)$  is always positive and coincides with the Fourier transform of the autocorrelation function calculated in (1.88).

### 1.6.6 Spectral moments

In a similar way to the ordinary probabilistic moments in time domain, it is possible to define the  $j^{th}$  order *spectral moment* associated to the *unilateral spectral density function* respect to  $\omega = 0$ [40]:

$$\lambda_{j,X} = \int_0^{+\infty} \omega^j \cdot G_X(\omega) d\omega \quad (1.105)$$

The moment of order zero is:

$$\lambda_{X,0} = \int_0^{+\infty} G_X(\omega) d\omega = \sigma_X^2 \quad (1.106)$$

This means that the total energy subtended by the spectral density function corresponds to the variance of the ensemble of random variables. According to this expression and to eq.1.104, a stationary process has finite energy content at a fixed time only if it has finite variance and vice-versa. In a similar way, the moments of even order correspond to the variance of the time derivatives of  $X$ :

$$\lambda_{X,2} = \int_0^{+\infty} \omega^2 \cdot G_X(\omega) d\omega = \sigma_{\dot{X}}^2 \quad (1.107)$$

$$\lambda_{X,4} = \int_0^{+\infty} \omega^4 \cdot G_X(\omega) d\omega = \sigma_{\ddot{X}}^2 \quad (1.108)$$

and so on. The odd spectral moments have no particular physical meaning but are important as well because involved in the description of the general behave of the process. The moments calculated according to this formulations take the name of *geometric spectral moments*.

In analogy with the static moments, the ratio between the moments of  $n^{th}$  and  $0^{th}$  order gives useful indicators. In particular:

$$\omega_{1,X} = \frac{\int_0^{+\infty} \omega \cdot G_X(\omega) d\omega}{\int_0^{+\infty} G_X(\omega) d\omega} = \frac{\lambda_{X,1}}{\lambda_{X,0}} \quad (1.109)$$

corresponds to the *central frequency of the process* in analogy to the centroid. The same can be done for the *second order central moment* in analogy with the radius of gyration:

$$\omega_{2,X} = \left( \frac{\int_0^{+\infty} \omega^2 G_X(\omega) d\omega}{\int_0^{+\infty} G_X(\omega) d\omega} \right)^{1/2} = \sqrt{\frac{\lambda_{X,2}}{\lambda_{X,0}}} \quad (1.110)$$

Manipulating a bit the previous expression leads to:

$$\omega_{2,X} = \sqrt{\frac{1}{\lambda_{X,0}} \left( \lambda_{X,2} - \frac{\lambda_{X,1}^2}{\lambda_{X,0}} \right)} = q_X \cdot \omega_{2,X} \quad (1.111)$$

where  $q_X$  is the *bandwidth* of the process defined as:

$$q_X = \sqrt{1 - \frac{\lambda_{X,1}^2}{\lambda_{X,0} \cdot \lambda_{X,2}}}, \quad 0 \leq q_X \leq 1 \quad (1.112)$$

A value of  $q_X$  near to 1 indicates a broad band process, while  $q_X$  near to 0 indicates a narrow band process. The bandwidth is a very important parameter because gives information on the general behaviour of the response process itself. It is also possible to give higher order forms for the bandwidth as:

$$\alpha_j = \frac{\lambda_j}{(\lambda_0 \cdot \lambda_{2,j})^{1/2}} \quad (1.113)$$

By substituting eq.(1.105) in (1.113) some probabilistic relations of interest can be found; for instance, the variance of the time derivative of the process[40].

### 1.6.7 Analytical description of different type of processes

In this paragraph, with reference to Muscolino[46], are showed the analytic descriptions of different grade of regularity zero mean processes, introduced in sec.1.4.1.

#### Harmonic (sinusoidal) process

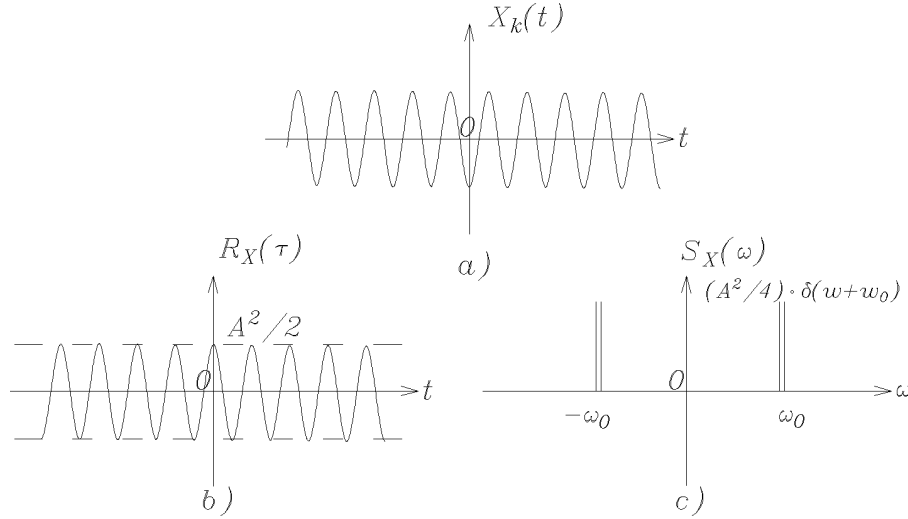


Figure 1.14: Harmonic process: a)Time series, b)Autocorrelation function, c) Spectral density function[46].

A sample  $X^{(k)}$  of a process is said to be harmonic (in this case sinusoidal) if it has the form:

$$X^{(k)}(t) = A \cdot \sin(\omega_0 t + \theta^{(k)}) \quad (1.114)$$

where  $\theta$  is an aleatory variable with uniform PDF in the range  $[0, 2\pi]$ :

$$p_\theta(\theta) = \frac{1}{2\pi}, \quad 0 \leq \theta \leq 2\pi \quad (1.115)$$

By applying eq.(1.75) to the expression of  $X^{(k)}$  given in eq.(1.114), and assuming the distribution in eq.(1.115), the auto-correlation function assumes the form:

$$R_{XX}(\tau) = A^2 \int_0^{2\pi} \sin(\omega_0 t + \theta) \cdot \sin[\omega_0(t + \tau) + \theta] \cdot p_\theta(\theta) d\theta = \frac{A^2}{2} \cos(\omega_0 \cdot \tau) \quad (1.116)$$

The corresponding unilateral spectral density and  $i^{th}$  moment are:

$$G_{XX}(\omega) = A^2 \cdot \delta(\omega - \omega_0) \quad (1.117)$$

$$\lambda_{i,X} = \omega_0^i \cdot \lambda_{0,x}, \quad \forall i \quad (1.118)$$

The harmonic process has its energy concentrated on only two symmetric frequencies and correlation function that fluctuates between two maximums corresponding to the beginning and end of the period (fig.1.14). The bandwidth  $q_X = 0$  is nil due to the presence of only one frequency (in absolute value) characterizing the process.

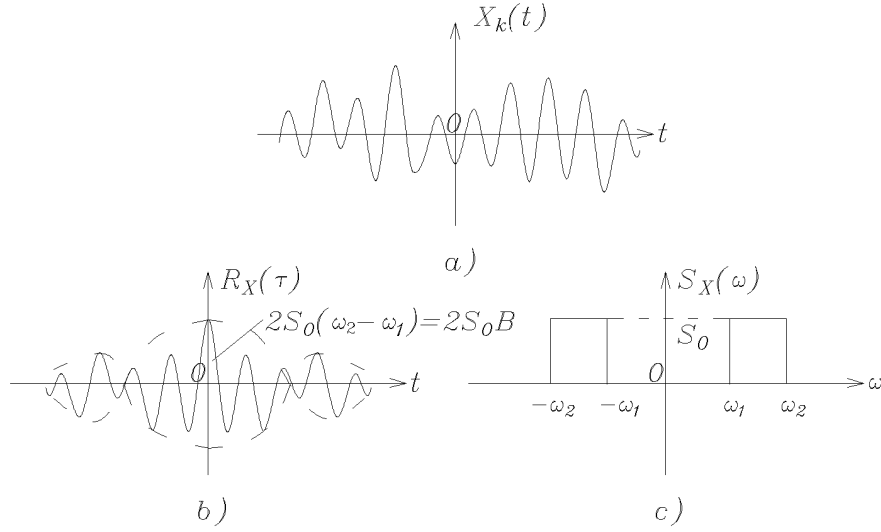


Figure 1.15: Narrow band process: a) Time series, b) Autocorrelation function, c) Spectral density function[46].

### Narrow band process

A *narrow band process* has its energy concentrated on a limited range of frequencies of width  $B = |\omega_2 - \omega_1|$  (fig.1.15). The *central frequency* corresponds to  $\omega_c = \pm(\omega_2 + \omega_1)/2$ , the spectral power density assumes value:

$$\begin{aligned} S_x(\omega) &= S_0, & \omega_1 < |\omega| < \omega_2 \\ S_x &= 0, & \text{elsewhere} \end{aligned} \quad (1.119)$$

The narrowband process can be enveloped between its peaks to define an harmonic approximation of its behave. Assuming a co-sinusoidal envelope of the process, and using eq.(1.90), the relative correlation function is:

$$R_{XX}(\tau) = 2 \int_{\omega_1}^{\omega_2} S_0 \cdot \cos(\omega\tau) d\omega = 2S_0B \left( \frac{\sin(B/2 \tau)}{B/2 \tau} \right) \cdot \cos(\omega_c\tau) \quad (1.120)$$

The variance is obtained by a limit analysis:

$$\sigma_{XX}^2 = \lim_{\tau \rightarrow 0} R_{XX}(\tau) = 2S_0 \cdot B = 2S_0 \cdot (\omega_2 - \omega_1) \quad (1.121)$$

that corresponds to the area subtended by the spectral density function. The *narrow band process* has a main frequency concentrated around a central value  $\omega_c$ ; considering the case  $B \rightarrow 0$ , the process collapses to the harmonic one. The spectral moments of the lower orders are:

$$\lambda_{0,X} = 2S_0 \cdot B, \quad (1.122)$$

$$\lambda_{1,X} = 2S_0 \cdot B \cdot \omega_c, \quad (1.123)$$

$$\lambda_{2,X} = 2S_0 \cdot B \cdot (\omega_c^2 + B^2/12), \quad (1.124)$$

The *bandwidth*, for values of  $B \ll \omega_c$ , is:

$$q_X = \frac{B}{\sqrt{12\omega_c^2 + B^2}} \simeq \frac{B}{\omega_c\sqrt{12}} \quad (1.125)$$

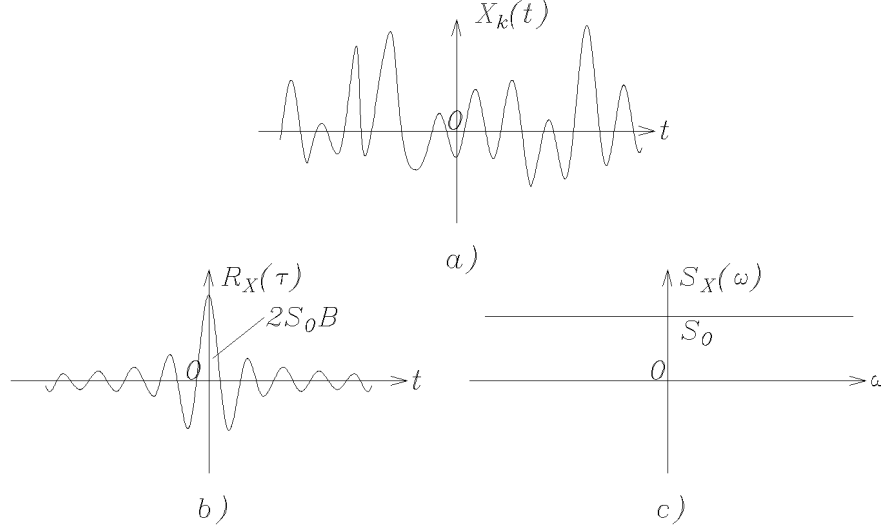
**Broad band process**


Figure 1.16: Broad band process: a) Time series, b) Autocorrelation function, c) Spectral density function[46].

A *broadband process* has spectral density function not nil on a wide range of frequencies; in other words, it means that  $B = |\omega_2 - \omega_1|$  is big. Between the broadband processes, a wide used class is the one of the *ideal broadband stochastic process* (fig.1.16). Analytically, their power spectral density assumes value:

$$\begin{aligned} S_{XX}(\omega) &= S_0, & |\omega| \leq B \\ S_{XX} &= 0, & |\omega| > B \end{aligned} \quad (1.126)$$

By using eq.(1.90) the auto-correlation function is:

$$R_{XX}(\tau) = 2 \int_{\omega_1}^{\omega_2} S_0 \cdot \cos(\omega\tau) d\omega \simeq 2 \int_0^B S_0 B \left( \frac{\sin(B/2 \cdot \tau)}{B/2 \cdot \tau} \right) \cdot \cos(\omega_c \tau) \quad (1.127)$$

The lower orders spectral moments are:

$$\lambda_{0,X} = 2S_0 \cdot B, \quad (1.128)$$

$$\lambda_{1,X} = S_0 \cdot B^2, \quad (1.129)$$

$$\lambda_{2,X} = 2S_0 \cdot B^3/3, \quad (1.130)$$

and the bandwidth is  $q_X = 0.5$ .

**White noise**

A *white noise* has spectral density function constant over an infinity range of frequencies; in other words, it means that  $B \rightarrow \infty$ . Between the white processes, a wide used class is the one of the *ideal white noise process* (fig.1.17). Analytically:

$$S_x(\omega) = S_W, \quad \forall \omega \quad (1.131)$$

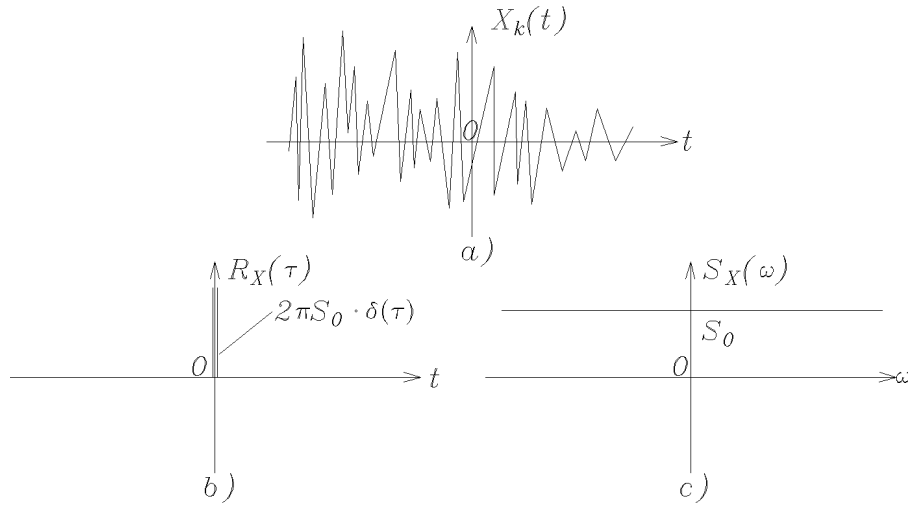


Figure 1.17: White noise process: a) Time series, b) Autocorrelation function, c) Spectral density function[46].

By using eq.(1.90), assuming  $S_W = S_0 = \text{const}$ , the relative correlation function is a Dirac's delta-function:

$$R_{XX}(\tau) = R_W(\tau) = \int_{-\infty}^{+\infty} S_0 \cdot \exp[i\omega \cdot t] d\omega = S_0 \int_{-\infty}^{+\infty} \exp[i\omega \cdot t] d\omega = 2\pi S_W \cdot \delta(\tau) \quad (1.132)$$

The  $i^{\text{th}}$  spectral moment is  $\lambda_{i,X} = \infty$ , for  $i = 0,1,2$  and the bandwidth is  $q_X = 1$

### White noise and delta-correlated process

The concept of *delta-correlated process* is really important in the theory of random vibrations, in fact, many physical processes  $F(t)$  can be assumed to be so erratic that two generic distributions  $F(t_1)$  and  $F(t_2)$  are independent unless  $t_1$  and  $t_2$  are almost equal, i.e., delta-correlated. As the two time instants are nearer and as a sort of correlation appears, but it decays rapidly with the increasing of distance.

Generally, it is assumed a delta of time  $T_c$  in which  $F(t_1)$  and  $F(t_2)$  are significantly dependent; considering a difference of time  $|t_2 - t_1| > T_c$ , then  $F(t_1)$  and  $F(t_2)$  are not dependent any more over that delta of time. If  $T_c$  is small compared to the other characteristic time values, then it is possible to say, by limiting the process, that  $F(t_1)$  and  $F(t_2)$  are independent for  $t_1 \neq t_2$ . The motivations for this approach are strictly of convenience: modelling a delta-correlated process is much easier than a nearly delta-correlated one.

Comparing these observations with the results of sec.1.6.7, it is easy to see that the ideal delta-correlated process corresponds to the white noise. In most applications, the white noise is assumed as input for a filter to have both simple formulations that the capability to describe properly the physical phenomena; for this reason, it is widely used in random vibration studies.

## 1.7 Failure analysis in random vibration

Once that the response process is properly described, a criteria to define a safety margin for the system has to be fixed. The failure analysis in the field of random vibrations is based on the study of the peaks of the process for two possible collapse modes:

- *first passage collapse*: considers a design threshold that corresponds to an unacceptable damage for the structure. The study considers the *global peaks* of the process along a time interval  $T$  to create a distribution of extreme values;
- *fatigue collapse*: this problem is connected to cyclic load-unload states and depends only on the *local peaks* (that correspond to an inversion of trend);

The dynamic analysis can be uncoupled from the failure one, in fact, once the response process  $\{X(t)\}$  is obtained, it can be analysed independently from the previous develops. In this thesis, only the first passage failure, in the hypothesis of linear behave, is considered. Both the cases are widely explained on Muscolino[46], Krandall & Mark[15], Lutes & Sarkani[40] and on Lin[38].

To get the first passage failure probability a well defined procedure has to be followed:

1. determine the *rate of up-crossing*  $\nu_X^+$  of the fixed design threshold  $u$  by the process  $\{X(t)\}$ ;
2. find a PDF and CDF of peaks for the process  $\{X(t)\}$ ;
3. determine a process  $\{Y(t)\}$  of the peaks of  $\{X(t)\}$ ;
4. define a first passage distribution and relates it to the peaks over the assigned threshold;
5. determine the probability of failure for the assigned threshold (or get the threshold corresponding to a fixed probability of failure).

### 1.7.1 Rate of up-crossing

The rate of up-crossings of an assigned threshold is not the most intuitive way to determine the occurrence of peaks. In fact, the peaks are connected to the maxima of the process and formally should be determined, referring to fig.1.18, by searching the values of  $X(t) > u$  with  $\dot{X}(t) \geq 0$  and  $\ddot{X}(t) \leq 0$ . Being the process stochastic, the description of the maxima requires to know the joint PDF function of  $p_{X\dot{X}\ddot{X}}$  and to perform a probabilistic analysis on it. On Lin[38], a description of this procedure is reported but the final solution, also for the simplest stationary Gaussian case, is difficult to handle numerically.

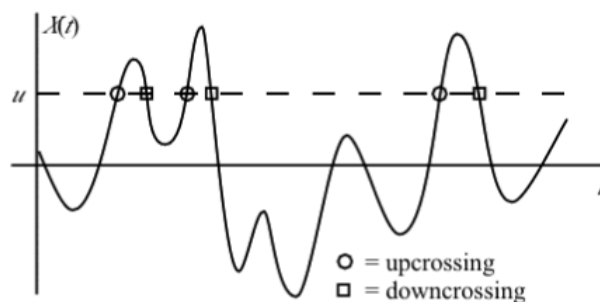


Figure 1.18: Crossings of threshold  $u$  by the process  $X(t)$ [40].

The typical approach is to relate the peaks occurrence of maxima to the up-crossings, introducing the hypothesis that, supposed an enough high threshold, the number of maxima over it is equal to the up-crossings. The justification for this assumption is that for higher value of  $u$  it is less likeable to have troughs over it. This hypothesis is exact for narrow band processes, where the behave tends to an harmonic one, and is conservative for the others because it estimates always an higher number of peaks than the real ones. Therefore, the analysis of peaks is possible with only the joint PDF  $p_{X\dot{X}}$ , searching  $X(t) > u$  with  $\dot{X}(t) \geq 0$ .

Denoting with  $\nu_X^+(u, t)$  the expected rate of occurrence of the event  $X(t) > u$  with  $\dot{X}(t) \geq 0$ , the number of up-crossing is determined by the integration along time of this value. Reversing this relation leads to write the rate of up-crossing as the limits:

$$\nu_X^+(u, t) = \lim_{\Delta t \rightarrow 0} \frac{P(\text{one up-crossing of } u \text{ in } [t, t + \Delta t])}{\Delta t} \quad (1.133)$$

that corresponds to a derivation operation. Using the phase diagram in figure 1.19, the probability of eq.(1.133) can be found geometrically. Assumed an enough small  $\Delta t$ , the value  $\dot{X}(t)$  can be considered as constant. Thus, an up-crossing will occur only if:

$$0 < u - X(t) < \dot{X}(t) \cdot \Delta t \quad (1.134)$$

which can be rewritten as:

$$u - \dot{X}(t) \cdot \Delta t < X(t) < u \quad (1.135)$$

This probability can be calculated by applying an integration over this area (shaded in fig.1.19) of the joint PDF  $p_{X\dot{X}}$ :

$$P(\text{one up-crossing of } u \text{ in } [t, t + \Delta t]) \approx \int_0^{+\infty} \int_{u-v\Delta t}^u p_{X(t)\dot{X}(t)}(w, v) dw dv \quad (1.136)$$

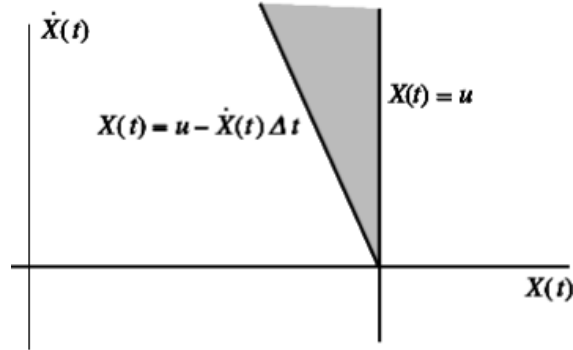


Figure 1.19: Phase diagram of the crossing event[40].

Considering that  $\Delta t$  is infinitesimal,  $w \approx u$  and  $p_{X(t)\dot{X}(t)}(w, v) \approx p_{X(t)\dot{X}(t)}(u, v)$ . The expression becomes:

$$P(\text{one up-crossing of } u \text{ in } [t, t + \Delta t]) \approx \int_0^{+\infty} (v \cdot \Delta t) \cdot p_{X(t)\dot{X}(t)}(u, v) dv \quad (1.137)$$

The expected rate of up-crossing, substituting in (1.133), is:

$$\nu_X^+(u, t) = \int_0^{+\infty} v \cdot p_{X(t)\dot{X}(t)}(u, v) dv \quad (1.138)$$

It is also possible to obtain the same result by a different approach based on algebra rather than on geometry[40]. Eq.(1.138) can be rewritten in terms of conditioned PDF as:

$$\nu_X^+(u, t) = p_{X(t)}(u) \int_0^{+\infty} v \cdot p_{\dot{X}(t)} [v | X(t) = u] dv \quad (1.139)$$

The rate of down-crossing of a negative threshold is equal to  $\nu_X^+(u, t)$  for signs elision:

$$\nu_X^-( -u, t) = - \int_0^{+\infty} v \cdot p_{X(t)\dot{X}(t)}(-u, v) dv = -p_{X(t)}(-u) \int_0^{+\infty} v \cdot p_{\dot{X}(t)} [v | X(t) = -u] dv \quad (1.140)$$

For a double barrier problem, this leads to:

$$\nu_{|X|}(u, t) = \nu_X^+(u, t) + \nu_X^-( -u, t) = 2 \nu_X^+(u, t) \quad (1.141)$$

### Stationary Gaussian processes

For the case of Stationary Gaussian process the expressions of sec.1.7.1 has a simplified solution; in particular, once given the mean and variance, the joint PDF can be easily obtained as done in sec.1.5.6. The expression of eq.(1.138) becomes:

$$\nu_x^+ = \frac{1}{2\pi} \frac{\sigma_{\dot{X}}}{\sigma_X} \exp\left(-\frac{u^2}{2\sigma_X^2}\right) \quad (1.142)$$

Similar formulations can be written also for the non-stationary case[40].

### 1.7.2 Distribution of peaks

The probability distribution of the peaks of the process  $\{X(t)\}$  is determined similarly to the rate of up-crossing in sec.1.7.1. Defined  $\nu_p[t; X(t) \leq u]$  as the rate of occurrence of peaks not exceeding the level  $u$ , assuming that for an infinitesimal  $\Delta t$  no more than one peak can occur, means that:

$$\nu_p[t; X(t) \leq u] \cdot \Delta t = P(\text{one peak} \leq u \text{ in } [t, t + \Delta t]) \quad (1.143)$$

is equal to  $\nu_p(t)$ : the total expected rate of peaks, which is the limit as  $u$  goes to infinity of  $\nu_p[t; X(t) \leq u]$ . The latter can be written as:

$$\nu_p(t) \cdot \Delta t = P(\text{one peak in } [t, t + \Delta t]) \quad (1.144)$$

Moreover, it applies also the following relation:

$$P(\text{one peak} \leq u \text{ in } [t, t + \Delta t]) = P(\text{one peak in } [t, t + \Delta t]) \cdot P(\text{one peak} \leq u | \text{peak in } [t, t + \Delta t]) \quad (1.145)$$

In which the last term corresponds to the cumulative distribution function of peaks after a passed time  $t$ :

$$F_P(t)(u) = P(\text{one peak} \leq u | \text{peak during } [t, t + \Delta t]) \quad (1.146)$$

Putting together eq.(1.146) with (1.144) gives:

$$F_P(t)(u) = \frac{\nu_p[t; X(t) \leq u]}{\nu_p(t)} \quad (1.147)$$

The rate of occurrence of peaks below  $u$  can be determined as follow. A unit step process  $U[-\dot{X}(t)]$  is considered such that gives a positive step for each peak of  $X(t)$  and a negative step

for each valley. Its derivative is the Dirac's delta function  $-\ddot{X}(t) \cdot \delta[-\dot{X}(t)]$ . Multiplying for  $U[-\ddot{X}(t)]$  eliminates the Dirac's delta function and gives a peaks counting function. In a similar way, multiplying for  $U[u - X(t)]$ , only the peaks above the level  $u$  are obtained. Finally:

$$\nu_p[t; X(t) \leq u] = E(-\ddot{X}(t) \cdot \delta[-\dot{X}(t)] \cdot U[-\ddot{X}(t)] \cdot U[u - X(t)]) \quad (1.148)$$

That put in eq.(1.147) gives:

$$F_P(t)(u) = \frac{E(-\ddot{X}(t) \cdot \delta[-\dot{X}(t)] \cdot U[-\ddot{X}(t)] \cdot U[u - X(t)])}{E(-\ddot{X}(t) \cdot \delta[-\dot{X}(t)] \cdot U[-\ddot{X}(t)])} \quad (1.149)$$

that can be written as joint PDF:

$$F_P(t)(u) = \frac{\int_{-\infty}^{+\infty} \int_{-\infty}^{+\infty} \int_{-\infty}^{+\infty} (-z) \cdot \delta(-v) \cdot U(-z) \cdot U(u - w) \cdot p_{[X(t)\dot{X}(t)\ddot{X}(t)]}(w, v, z) \, dw \, dv \, dz}{\int_{-\infty}^{+\infty} \int_{-\infty}^{+\infty} (-z) \cdot \delta(-v) \cdot U(-z) \cdot p_{[\dot{X}(t)\ddot{X}(t)]}(v, z) \, dv \, dz} \quad (1.150)$$

or in the simpler form:

$$F_P(t)(u) = \frac{\int_{-\infty}^0 \int_{-\infty}^u |z| \cdot p_{[X(t)\dot{X}(t)\ddot{X}(t)]}(u, 0, z) \, dw \, dz}{\int_{-\infty}^0 |z| \cdot p_{[\dot{X}(t)\ddot{X}(t)]}(0, z) \, dz} \quad (1.151)$$

Taking the derivative of the latter, the corresponding PDF is:

$$p_P(t)(u) = \frac{\int_{-\infty}^0 |z| \cdot p_{[X(t)\dot{X}(t)\ddot{X}(t)]}(u, 0, z) \, dz}{\int_{-\infty}^0 |z| \cdot p_{[\dot{X}(t)\ddot{X}(t)]}(0, z) \, dz} \quad (1.152)$$

From these distributions the probabilistic parameters of interest can be obtained. Unfortunately, the determination of peaks is quite complex and requires higher order distributions of the original process  $\{X(t)\}$ . As stated before, the procedure typically used is to relate it to the up-crossing distribution that is then connected to the first passage occurrence.

### 1.7.3 Extreme values distribution and first-passage relationship

The first passage to study the extreme values distribution is to define a stochastic process  $\{Y(t)\}$  of the extreme values extracted from the process  $\{X(t)\}$ :

$$Y(t) = \max[X(s)], \quad 0 \leq s \leq t \quad (1.153)$$

Therefore, the distribution of the extreme values of  $\{X(t)\}$  corresponds to the distribution of the random variable  $Y(t)$ . This process is not stationary independently from the nature of  $\{X(t)\}$ ; indeed, a longer observation time implies a larger amount of peaks of  $\{X(t)\}$ . The cumulative distribution  $L_X(u, t)$  of  $Y(t)$  is:

$$L_X(u, t) = F_{Y(t)}(u) = P[Y(t) \leq u] = P[X(s) \leq u : 0 \leq s \leq t] \quad (1.154)$$

If  $u$  is a critical value for the failure of the system, this CDF takes the name of *probability of survival*. By derivation, the corresponding PDF is:

$$p_{Y(t)} = \frac{\partial}{\partial u} L_X(u, t) \quad (1.155)$$

Let introduce the first time of up-crossing  $T_X(u)$  of a threshold  $u$  as:

$$X[T_X(u) = u], \quad \dot{X}[T_X(u)] > 0 \quad (1.156)$$

$T_X(u)$  is a random variable and the ensemble  $\{T_X(u)\}$  is a stochastic process that depends on the critical value  $u$ . There is a relationship between the first-passage time and the extreme values of the distribution. Indeed, the event  $\{X(s) \leq u : 0 \leq s \leq t\}$  of eq.(1.154) can be also written as  $\{X(0) \leq u, T_X(u) \geq t\}$ , because  $X(s)$  can be less than  $u$  throughout the time interval only if it starts below it and does not have an up-crossing during that interval. Thus, the CDF of the peaks over  $u$  can be written in function of the first up-crossing of the threshold  $u$ :

$$L_X(u, t) = P[X(0) \leq u] \cdot P[T_X(u) \geq t | X(0) \leq u] = L_X(u, 0) \cdot P[T_X(u) \geq t | X(0) \leq u] \quad (1.157)$$

If the system is initially at rest or the deterministic initial condition  $X(t) \leq u$  is given, then  $P[X(0) \leq u] = 1$  and the expression can be simplified. By taking the derivative respect to  $t$  of eq.(1.157) the corresponding PDF is:

$$p_{T_X}[t | X(0) \leq u] = -\frac{1}{L_X(u, 0)} \cdot \frac{\partial}{\partial t} L_X(u, t) \quad (1.158)$$

This relation is very important because it transforms the peaks analysis, quite onerous for the probabilistic description of the response, in a first up-crossing problem that is easier to be handled.

#### 1.7.4 First passage failure possible distributions and approximations

The most properly form to express the probability of survival is an exponential function of time:

$$L_X(u, t) = L_X(u, 0) \cdot \exp\left[-\int_0^t \eta_X(u, s) ds\right] \quad (1.159)$$

In fact, the distributions adopted for the occurrence of extreme events is generally exponential. With some manipulations,  $\eta_X(u, t)$  can be written as function of  $L_X(u, t)$ [40]:

$$\eta_X(u, t) = \lim_{\Delta t \rightarrow 0} \frac{1}{\Delta t} E(\text{up-crossing in } [t, t + \Delta t] | X(0) \leq u, \text{ no up-crossing prior to } t) \quad (1.160)$$

$\eta_X(u, t)$  is a sort of conditioned occurrence rate of up-crossing of  $u$ , given the initial conditions and the fact that no up-crossing has been before. It takes the name of *hazard function* and, similarly to the up-crossing rate, it is written as:

$$\eta_X(u, t) = \int_0^{+\infty} v \cdot p_{X(t)\dot{X}(t)}(u, v | X(0) \leq u, \text{ no up-crossing in } [0, t]) dv \quad (1.161)$$

This form is not really useful because the conditioned PDF is generally unknown. However, it gives informations about the analytical principles behind the problem and allows to do some important considerations. Most physical processes have a finite memory, i.e.,  $X(t)$  and  $X(t - \tau)$  can be generally considered as independent for  $\tau > T$ , given  $T$  quite large, therefore, for  $t > T$ :

$$\begin{aligned} p_{[X(t)\dot{X}(t)]}(u, v | X(0) \leq u, \text{ no up-crossing in } [0, t]) &\approx \\ \approx p_{[X(t)\dot{X}(t)]}(u, v | X(0) \leq u, \text{ no up-crossing in } [t - T, t]) &\end{aligned} \quad (1.162)$$

If  $\{X(t)\}$  is stationary, then also its conditioned PDF is stationary too because independent from the origin of the time axis. That means, the conditioned probability and the hazard function tend asymptotically to a stationary behave as  $t$  increases. Considering this, the survival function can be expressed as:

$$L_X(u, t) = L_0 \cdot \exp[-\eta_X(u) \cdot t], \quad \text{for large } t \quad (1.163)$$

the value of  $L_0$  is instead connected to the behaviour of  $\eta_X(u, t)$  for small values of  $t$  and attention must be paid in that case[40]. Unfortunately, it is not easy to calculate  $\eta_X(u, t)$  and different approximations have been developed to find a proper value.

### Poisson approximation

A possible approximation for  $\eta_X(u, t)$  is to fix it equal to the unconditional up-crossing rate,  $\nu_X^+(u, t)$ , neglecting the effects of initial conditions:

$$L_X(u, t) \approx L_X(u, 0) \cdot \exp\left[-\int_0^t \nu_X(u, s) ds\right] \quad (1.164)$$

If  $\{X(t)\}$  is a stationary process, the expression becomes:

$$L_X(u, t) \approx L_X(u, 0) \cdot \exp\left[-\nu_X(u) \cdot t\right] \quad (1.165)$$

the corresponding PDF for the stationary case obtained from (1.158) and (1.165) is:

$$p_{T_X}(t) \approx \nu_X^+(u) \cdot \exp[-\nu_X^+(u) \cdot t] \quad (1.166)$$

From eq.(1.166) the different probabilistic characteristics can be obtained. The Poisson process gives exponential distribution between different occurrences and, therefore, the first passage occurrence follows an exponential distribution in the stationary case.

The Poisson approximation fails in the description of the very narrow band processes. Indeed, in a narrow band process, an up-crossing of the level  $u$  at time  $t$  is very likely to be associated with another up-crossing a period later thanks to the slowly varying amplitude of  $\{X(t)\}$ . If instead  $u$  is very large, the assumption of independent up-crossing seems legit because generally the crossings are far from each other.

However, eq.(1.164) gives a conservative overestimation of  $\eta_X(u, t)$  because it implies an underestimation of  $L_X(u, t)$  and, therefore, a higher failure probability. Nevertheless, the term  $L_X(u, 0)$  may become important in some situations: when  $u$  is so small that  $P[X(t) < u]$  is very small but the conditions  $X(0) < u$  is fixed, it is easy that an up-crossing occurs very quickly.

Mathematically,  $L_X(u, t)$  should approach zero as  $u \rightarrow -\infty$  for any finite  $t$  value in proximity of zero, this for every  $L_X(u, 0)$  assumed. This unbounded behavior violates the previous hypothesis of  $\eta_X(u, t) \leq \nu_X^+(u, t)$  and must be carefully kept in mind.

In case of *double-barrier problem*, with symmetric threshold, eq.(1.159) may be rewritten as:

$$L_{|X|}(u, t) = L_{|X|}(u, 0) \cdot \exp\left(-\int_0^t \eta_{|X|}(u, s) ds\right) \quad (1.167)$$

In case of symmetry,  $\eta_X(u, v; t) = \nu_{|X|}^+(u, s) = \nu_X^+(u, s) + \nu_X^-(-u, s)$ , or, in a simpler manner, considering that they are equals,  $\nu_{|X|}^+(u, s) = 2 \nu_X^+(u, s)$ .

It is also possible to considerate a not symmetric threshold and simply adding the two contributes opposite in sign. The Poisson approximation for the first passage failure of a stationary process coincides with an exponential distribution of the following form:

$$p_{T_X} = \nu_X^+(u) \cdot \exp[-\nu_X^+(u) \cdot t] \quad (1.168)$$

The mean, that corresponds to the *crossing rate*, is:

$$E[T_X(u)] = [\nu_X^+(u)]^{-1} \quad (1.169)$$

### 1.7.5 Improved maximum values distributions

The Poisson approximation main limit is the assumption of independent up-crossings which results in excessively conservative approximations in many cases (and not conservative ones in the special case of low threshold). Many authors have found improved formulations considering solutions valid for both narrow and broad band case. This mainly because it is hard to quantify how being far from the ideal narrow or broad band process influences the quality of results; therefore, a general solution is the best to be adopted.

The first improvements that can be done is to correct the Poisson approximation for  $X(0) \leq 0$  to improve the estimation of  $\eta_X(u, t)$  for small values of  $u$ . Recalling that the time of first passage  $T_X(u)$  for the Poisson approximation is a stationary random variable, it can be considered as equivalent to  $T_{CR}$ , the time between two up-crossing (see fig.1.20). The latter can be divided in two parts:

- the time  $T_1$  between the up-crossing and following down-crossing;
- the time  $T_2$  from the down-crossing to the following up-crossing.

Of the two, only the segment  $T_2$  is spent under the threshold and a possible conservative assumption is to approximate  $T_{CR}$  with  $T_2$ .

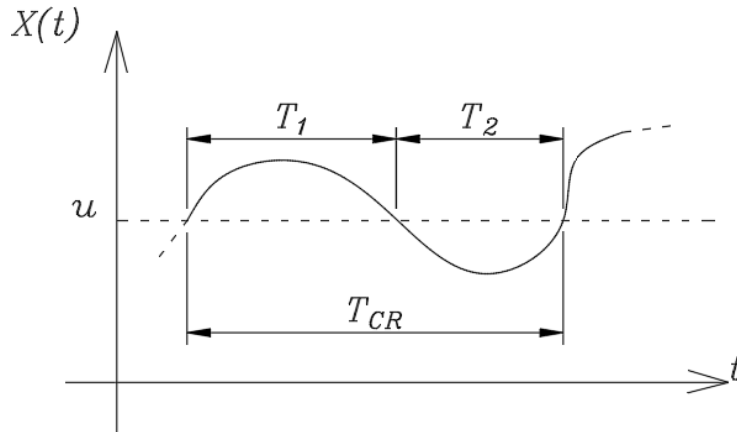


Figure 1.20: Division of the stationary time between up-crossings.

As stated before, the arrival rate (i.e. the mean of the Poisson distribution) is, for eq.(1.169), the inverse of  $E[T_2]$ . Since  $T_2$  is the time spent under  $u$ , it derives that  $E(T_2) = E[T_{CR}] \cdot P(X < u)$ . Unfortunately, there is no exact solution for  $E[T_{CR}]$ , the hypothesis that  $T_2$  is governed by a Poisson process excludes that also  $T_{CR}$  is characterized by the same distribution.

Nevertheless, it could be a reasonable approximation to assume a Poisson distribution for it, therefore,  $E(T_2) = [\nu_X^+(u)]^{-1}$ . Considering this, the survival function for the non-stationary and stationary case becomes:

$$\eta_X(u, t) \approx \frac{\nu_X^+(u, t)}{F_{X(t)}(u)}, \quad \eta_X(u, t) \approx \frac{\nu_X^+(u)}{F_X(u)} \quad (1.170)$$

This approximation corrects the error in proximity of low values of the threshold  $u$ .

In case of narrow band process, the Poisson approximation of independent up-crossing shows to be not adapt to describe the process of peaks. For a narrow band process with slowly varying

amplitude  $\{A(t)\}$  around the mean value  $\mu_X(t)$ , a single up-crossing of the level  $u$  by  $[\mu_X(t) + A(t)]$  is likely to be associated with several others. Starting from this assumption, a narrow band approximation may be written. In the case of a stationary process, the problem can be transformed in a mean zero equivalent one<sup>2</sup>; Fig.1.21 shows the schematization of this process.

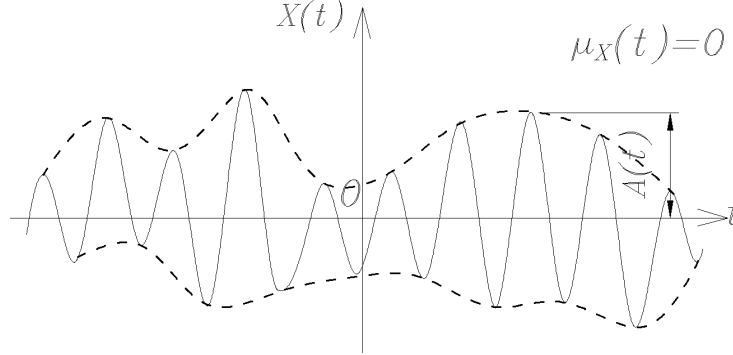


Figure 1.21: Schematization of a broad band mean zero process ( $\mu_X(t) = 0$ ).

The simplest form of survival function approximation is assuming the extreme values of the processes  $\{X(t)\}$  as coincident with the ones of the envelope of amplitude  $\{A(t)\}$ :

$$L_X(u, t) \approx L_A(u, t) = L_A(u, 0) \cdot \exp\left(-\int_0^t \eta_A(u, s) ds\right) \quad (1.171)$$

Being  $A(t) \geq X(t)$  an envelope of the peaks of  $X(t)$ , then  $L_A(u, t) \leq L_X(u, t)$  for all  $u$  and  $t$  and eq.(1.171) is always conservative. To determine  $\eta_A(u, t)$  the Poisson approximation is assumed:

$$\eta_A(u, t) = \nu_A^+(u, t) \quad (1.172)$$

That in the stationary case is:

$$L_X(u, t) \approx L_A(u, t) = L_A(u, 0) \cdot \exp[-\nu_A^+(u, s) \cdot t] \quad (1.173)$$

Similarly to the Poisson approximation,  $\eta_A(u, t)$  can be corrected for a very small threshold  $u$ . Both for stationary case than the non-stationary one:

$$\eta_A(u, t) \approx \frac{\nu_A^+(u)}{F_A(u)}, \quad \eta_A(u, t) \approx \frac{\nu_A^+(u, t)}{F_{A(t)}(u)} \quad (1.174)$$

Using  $F_{A(t)}(u)$  is slightly different from using  $F_{X(t)}(u)$ . In fact, the process  $X(t)$  is likely to pass the threshold much easier than  $A(t)$  during the first cycle (i.e.,  $t \leq 2\pi/\omega_c$ , where  $\omega_c$  is the envelope frequency). Nevertheless, this difference shows to be significant only during the first cycle and the approximation is good for a passed time  $t \geq 2\pi/\omega_c$ [40].

The narrow band approximation however fails in the case of big threshold because many of the  $A(t)$  up-crossings are not accompanied by  $X(t)$ . On the other hand, as  $u$  becomes large  $\eta_X(u, t) \rightarrow \nu_X^+(u, t)$ . Therefore, the real response is something in the middle of the two cases; to

<sup>2</sup>The non stationary case is more complicated because the varying mean implies a variable threshold, this problem will not be addressed here.

find it, it is necessary to estimate the fraction of  $A(t)$  up-crossings that are accompanied by  $X(t)$ . Significant results in this calculation come from the work of Vanmarcke.

Let consider the time  $T_1$  between an up-crossing and down-crossing of the function  $A(t)$  in a scheme similar to the one in fig.1.20; the time  $T_1$  corresponds to the interval in which  $A(t) > u$ . It is likely that as longer is  $T_1$  as the probability of up-crossing of  $X(t)$  is higher and vice versa. According to Vanmarcke this can be expressed as:

$$P[\text{no up-crossing by } X(t) \mid T_1 = \tau] \approx [1 - \nu_X^+(0, t) \cdot \tau] \cdot U[1 - \nu_X^+(0, t) \cdot \tau] \quad (1.175)$$

considering the period of an average cycle of  $\{X(t)\}$  as  $[\nu_X^+(0, t)]^{-1}$ , the up-crossing of  $X(t)$  is sure if  $T_1$  exceeds the period, and its probability grows linearly for  $T_1$  smaller than the period. Of course, this is a crude approximation but is better than considering the up-crossings of  $\{X(t)\}$  and  $\{A(t)\}$  always accompanied. A form for the distribution of  $T_1$  has to be assumed, the exponential one is a reasonable option considering that the real behave is in the middle between Poisson and a narrow band case:

$$P_{T_1}(\tau) = \frac{\exp[-\tau/E(T_1)]}{E(T_1)} \quad (1.176)$$

assuming that  $E(T_1) = E(T_{CR}) \cdot P[A(t) > u] \approx P[A(t) > u] / \nu_A^+(u, t)$  gives:

$$P[\text{up-cross. by } X(t) \text{ in } T_1] \approx \frac{P[A(t) > u] \cdot \nu_X^+(0, t)}{\nu_A^+(u, t)} \approx \left[ 1 - \exp\left(\frac{-\nu_A^+(u, t)}{P[A(t) > u] \cdot \nu_X^+(0, t)}\right) \right] \quad (1.177)$$

Considering the survival function as a conditioned probability applied to the rate of up-crossing envelope (i.e  $\eta_X(u, t) \approx \nu_A^+(u, t) \cdot P[\text{up-crossing by } X(t) \text{ during } T_1]$ ), gives:

$$\eta_X(u, t) \approx P[A(t) > u] \cdot \nu_X^+(0, t) \cdot \left[ 1 - \exp\left(\frac{-\nu_A^+(u, t)}{P[A(t) > u] \cdot \nu_X^+(0, t)}\right) \right] \quad (1.178)$$

This approximation shows to be equivalent, for the limit case of  $u \rightarrow 0$ , with eq.(1.172). Moreover, in the special case of Gaussian process, eq.(1.178) is identical to the Poisson approximation,  $\eta_X(u, t) \equiv \nu_X^+(u, t)$ . Including the effects of the initial conditions gives:

$$\eta_X(u, t) \approx \frac{P[A(t) > u] \cdot \nu_X^+(0, t)}{P[A(t) < u]} \cdot \left[ 1 - \exp\left(\frac{-\nu_A^+(u, t)}{P[A(t) > u] \cdot \nu_X^+(0, t)}\right) \right] \quad (1.179)$$

This is not exactly the approximation proposed by Vanmarcke that uses a more sophisticated assumption on the behaviour of  $\{X(t)\}$ . However, the expression of Vanmarcke can be found from eq.(1.178), in the Gaussian case, by setting  $P[A(t) > u] \cdot \nu_X^+(0, t) = \nu_X^+(u, t)$ ; similar results can be found for the other distributions. The Vanmarcke form is:

$$\eta_X(u, t) \approx \nu_X^+(u, t) \cdot \left[ 1 - \exp\left(\frac{-\nu_A^+(u, t)}{\nu_X^+(u, t)}\right) \right] \left( 1 - \frac{\nu_X^+(u, t)}{\nu_X^+(0, t)} \right)^{-1} \quad (1.180)$$

To consider a double barrier it is not possible to simply replace  $X(t)$  with  $|X(t)|$  because the approximation is based on the envelope cross rate described by an amplitude  $|A(t)|$ . Considering that, the obtained formulation seems to suit better a double barrier problem with  $A(t)$  as approximation for the  $|X(t)|$  process.

The approximation for double threshold is given by imposing an up-crossing if  $T_1$  exceeds, instead of the period  $[\nu_X^+(0, t)]^{-1}$ , an half of it. By replacing  $\nu_X^+(0, t)$  with  $2 \nu_X^+(0, t)$  in (1.175), developing respectively for the uncorrected and corrected case, eq.(1.178) and eq.(1.179) are:

$$\eta_X(u, t) \approx 2P[A(t) > u] \cdot \nu_X^+(0, t) \cdot \left[ 1 - \exp\left(\frac{-\nu_A^+(u, t)}{2P[A(t) > u] \cdot \nu_X^+(0, t)}\right) \right] \quad (1.181)$$

and

$$\eta_X(u, t) \approx \frac{2P[A(t) > u] \cdot \nu_X^+(0, t)}{P[A(t) < u]} \cdot \left[ 1 - \exp\left(\frac{-\nu_A^+(u, t)}{2P[A(t) > u] \cdot \nu_X^+(0, t)}\right) \right] \quad (1.182)$$

Eq.(1.180) becomes:

$$\eta_X(u, t) \approx \nu_{|X|}^+(u, t) \cdot \left[ 1 - \exp\left(\frac{-\nu_A^+(u, t)}{\nu_{|X|}^+(u, t)}\right) \right] \left( 1 - \frac{\nu_X^+(u, t)}{\nu_X^+(0, t)} \right)^{-1} \quad (1.183)$$

For the problems connected to the initial conditions, in the double barrier case the correction can be expressed as:

$$\eta_{|X|}(u, t) = \frac{\nu_{|X|}(u, t)}{P[|X(t)| \leq u]} \quad (1.184)$$

Vanmarcke developed an empirical correction for the stationary, mean zero, Gaussian case. The value  $\nu_A^+(u, t)/\nu_X^+(u, t)$  becomes:

$$\frac{\nu_A^+(u, t)}{\nu_X^+(u, t)} = (2\pi - q_X^2)^{1/2} \cdot \frac{u}{\sigma_X} \quad (1.185)$$

where the bandwidth  $q_X$ , defined in eq.(1.112), is introduced. In the same way, the ratio  $\nu_A^+(u, t)/\nu_{|X|}^+(u, t)$  is an half of this amount. Finally, Vanmarcke suggested, from empiric experiments, to use the value  $[2\pi - q_X^2]^{1.2}$  instead of  $[2\pi - q_X^2]$ . The final equation is:

$$\frac{\eta_X(u)}{\nu_X^+} \approx \left[ 1 - \exp\left(- (1 - q_X^2)^{0.6} (2\pi)^{0.5} \frac{u}{\sigma_X}\right) \right] \cdot \left[ 1 - \exp\left(\frac{-u^2}{2\sigma_X^2}\right) \right]^{-1} \quad (1.186)$$

and for the double threshold

$$\frac{\eta_X(u)}{\nu_{|X|}^+} \approx \left[ 1 - \exp\left(- (1 - q_X^2)^{0.6} (\pi/2)^{0.5} \frac{u}{\sigma_X}\right) \right] \cdot \left[ 1 - \exp\left(\frac{-u^2}{2\sigma_X^2}\right) \right]^{-1} \quad (1.187)$$

To consider the non-stationarity, the correlation coefficient  $\rho_{X\dot{X}}$  has to be adopted and, in both equations,  $(2\pi - q_X^2)^{1.2}$  has to be substituted with  $[(2\pi - q_X^2)^{1.2} - \rho_{X\dot{X}}^2]$ .

Unfortunately, the Vanmarcke approximation requires the knowledge of the bandwidth  $q_X$  and, consequently, the first order spectral moment  $\lambda_1$ . The determination of the spectral moments of odd order is quite complex and has been the focus of many studies about random processes in the last years. An univocal form has still not be found and simplifications have to be assumed.

### Failure probability determination

Once the survival function is determined, the failure CDF is simply the complement to one of it:

$$P_f(t) = 1 - L_X(u, 0) \cdot \exp\left(- \int_0^t \eta_X(u, s) ds\right) \quad (1.188)$$

An acceptable probability of failure  $p$  is set, the fractile of the distribution corresponding to it is extracted, as show in eq.(1.33), and the corresponding failure probability obtained (e.g., the characteristic value,  $p = 0.05$ , or the median value,  $p = 0.50$ ). In the same way, once fixed an acceptable threshold  $u$ , the probability of exceeding corresponding to it can be determined. A value of time  $T$  has to be decided for the analysis, generally the exciting event duration. The obtained results are the reference for a reliability or robustness analysis and, therefore, the final goal of the random vibrations analysis.

### Peak factors for mean zero, Gaussian process

In the analysis of the PDF of the process of maximum of the response  $\{Y(T)\}$  in the time interval  $T$ , it is possible to evaluate the lower fractile  $Y_{T,p}$  that defines the probability  $p$  that the maximum  $Y \leq Y_{T,p}$  in the interval  $[0, T]$ . Putting it in eq.(1.188), once assumed the threshold  $u \equiv Y_{T,p}$  and failure probability coincident with the survival function  $P_f(X_{T,p}, T) \equiv L_X(X_{T,p}, T) = p$ , the unknown  $X_{T,p}$  can be found from a non-linear analysis:

$$L_X(Y_{T,p}, T) = P_f(Y_{T,p}, T) = p \quad (1.189)$$

Therefore, assigned a fractile of interest of the peaks, the threshold up-crossed is found. Let introduce the non dimensional quantity  $\zeta(T, p) = Y_{T,p}/\sigma_X$  to represent the lower fractile of probability  $p$  of the a dimensional process  $\{\hat{Y}(T)\} = \{Y(T)/\sigma_X\}$ . This quantity takes the name of *peak factor* and aims to determine  $Y_{T,p}$  as:

$$Y_{T,p} = \zeta(T, p) \cdot \sigma_X \quad (1.190)$$

Having supposed the process stationary, the standard deviation is constant. The peak factor amplifies the values of standard deviation of  $X(t)$  so that, assigned a fractile of interest  $p$ , the maximum of the process  $|X(t)|$  is determined in  $[0, T]$ . The peak factor of eq.(1.189) can be rewritten in the equivalent form:

$$L_X[\zeta(T, p) \cdot \sigma_X, T] = P_f\left[\frac{\zeta(T, p)}{\sigma_X} \leq \eta_X(T, p)\right] = p \quad (1.191)$$

Muscolino[46] reports the peak factors calculated for the different hypothesis of independent and grouped up-crossings in the stationary case. Formulations for the non stationary case have still not found and the stationary ones are adopted as approximations also for the latter.

## Chapter 2

# Dynamic response to random vibrations

the previously stated formulations, it is possible to characterize properly a generic external action like random process to then apply it to the studied system. Being the excitation applied a random process, consequently, the response will be a random process too. That is, every evaluation of the parameters of response has to be done by stochastic indicators and the safety itself has to be quantified in probabilistic terms. The dynamic principles of the deterministic analysis can be used with some attentions and the solutions in random vibrations field are treatable as extension of deterministic formulations.

In this chapter, the response of SDF and MDF systems to a random vibration input is treated according to the different methods in literature, showing their advantages and disadvantages. In fact, there is not an univocal way to describe the random process of response and the best choice depends on the specific problem. After that, the theory of filters and the modelling of seismic action is presented. The two main references for this chapter have been Muscolino[46] and Lutes & Sarkani[40] that have adopted a similar approach with specific attentions for some particular aspects of the problem.

### 2.1 Single degree of freedom random vibration analysis

There are two ways to treat the problem of stochastic analysis of response to a random process input in either *single-degree of freedom* or *multi-degrees of freedom* systems[40]:

- *Indirect analysis*: finds the deterministic solution of the *equation of motion* to then apply the probabilistic theory to it. It can be further divided in:
  - *Time analysis*: based on the *Duhamel convolution integral*;
  - *Frequency analysis*: by applying the *Fourier's transform* to the response function;
- *Direct stochastic analysis*: it defines a differential equation of the stochastic parameters. It could be applied, in order of complexity, to: *moments*, *cumulants* or even to the PDF (*Fokker-Plank equation*)[40].

Every method has its advantages and disadvantages and no approach is better than the others, the choice depends from the problem analysed and they can be combined if necessary.

### 2.1.1 Indirect time stochastic dynamic analysis

To study the stochastic dynamic in time domain, the random variables,  $X(t)$  and  $F(s)$ , have to be substituted to the determinist ones,  $x(t)$  and  $f(t)$ , in the Duhamel integral in eq.(1.25). The obtained time varying stochastic properties are[40]:

$$X(t) = \int_{-\infty}^{+\infty} F(s) \cdot h_x(t-s) ds = \int_{-\infty}^{+\infty} F(t-r) \cdot h_x(r) dr \quad (2.1)$$

The mean of response is:

$$\mu_X(t) = E[X(t)] = \int_{-\infty}^{+\infty} \mu_F(s) \cdot h_x(t-s) ds = \int_{-\infty}^{+\infty} \mu_F(t-r) \cdot h_x(r) dr \quad (2.2)$$

The auto-correlation of response is:

$$\Phi_{XX}(t_1, t_2) = E[X(t_1)X(t_2)] = \int_{-\infty}^{+\infty} \Phi_{FF}(s_1, s_2) \cdot h_x(t_1-s_1) \cdot h_x(t_2-s_2) ds_1 ds_2 \quad (2.3)$$

or, by a change of variable:

$$\Phi_{XX}(t_1, t_2) = E[X(t_1)X(t_2)] = \int_{-\infty}^{+\infty} \Phi_{FF}(t_1-r_1, t_2-r_2) \cdot h_x(r_1) \cdot h_x(r_2) dr_1 dr_2 \quad (2.4)$$

Defined another process  $Y(t)$  as:

$$Y(t) = \int_{-\infty}^{+\infty} f(s) \cdot h_y(t-s) ds = \int_{-\infty}^{+\infty} F(t-r) \cdot h_y(r) dr \quad (2.5)$$

the cross-correlation of the two responses is:

$$\Phi_{XY}(t_1, t_2) = E[X(t_1)Y(t_2)] = \int_{-\infty}^{+\infty} \Phi_{FF}(s_1, s_2) \cdot h_x(t_1-s_1) \cdot h_y(t_2-s_2) ds_1 ds_2 \quad (2.6)$$

For the study of the velocity and acceleration the derivatives of the response have to be calculated. To do that, the derivative of the impulse response function is introduced as  $h'_x = h_{\dot{x}}$  and  $h''_x = h_{\ddot{x}}$ . The correspondent equation for the cross-correlation is:

$$\Phi_{X\dot{X}}(t_1, t_2) = \frac{\partial}{\partial t_2} \Phi_{XX}(t_1, t_2) = \int_{-\infty}^{+\infty} \Phi_{FF}(s_1, s_2) \cdot h_x(t_1-s_1) \cdot h'_x(t_2-s_2) ds_1 ds_2 \quad (2.7)$$

For the auto-correlation instead is:

$$\Phi_{\dot{X}\dot{X}}(t_1, t_2) = \frac{\partial^2 \Phi_{XX}(t_1, t_2)}{\partial t_1 \partial t_2} = \int_{-\infty}^{+\infty} \Phi_{FF}(s_1, s_2) \cdot h'_x(t_1-s_1) \cdot h'_x(t_2-s_2) ds_1 ds_2 \quad (2.8)$$

Similarly, the acceleration can be obtained. These formulations can be extended to  $n$ -dimensional distributions[40]. The covariance  $K_{XX}(t_1, t_2) = \Phi_{XX}(t_1, t_2) - \mu_x(t_1) \cdot \mu_x(t_2)$  is given by:

$$\begin{aligned} K_{XX}(t_1, t_2) &= \int_{-\infty}^{+\infty} \Phi_{FF}(s_1, s_2) \cdot h_x(t_1-s_1) \cdot h_x(t_2-s_2) ds_1 ds_2 + \\ &- \int_{-\infty}^{+\infty} \mu_F(s_1) \cdot h_x(t_1-s_1) ds_1 \cdot \int_{-\infty}^{+\infty} \mu_F(s_2) \cdot h_x(t_2-s_2) ds_2 \end{aligned} \quad (2.9)$$

Every order moment is uncoupled from the other ones. This means that it is necessary to know just the  $j^{th}$  moment of the input to get the corresponding  $j^{th}$  moment of the output, without the necessity to characterize all the others.

If a complete set of initial conditions is given, it is convenient to modify the convolution integral of eq.(2.1) to implement the initial conditions at time  $t_0$ :

$$X(t) = \sum_j X_{0,j} \cdot g_j(t - t_0) + \int_{t_0}^{+\infty} F(s) \cdot h_X(t - s) ds \quad (2.10)$$

Where  $X_{0,j}$  represents the  $j^{th}$  initial condition value and  $g_j(t - t_0)$  the response due to an unit value of that initial condition at time  $t = t_0$ . The correspondent mean value is:

$$\mu_X(t) = \sum_j X_{0,j} \cdot g_j(t - t_0) + \int_{t_0}^{+\infty} \mu_F(s) \cdot h_x(t - s) ds \quad (2.11)$$

while the auto-covariance of response has a more complex form that takes in account the effect of initial conditions on the process at time  $t_1$  and at time  $t_2$ :

$$\begin{aligned} K_{XX}(t_1, t_2) = & \sum_{j_1} \sum_{j_2} K_{X_{0,j_1} X_{0,j_2}} \cdot g_{j_1}(t_1 - t_0) \cdot g_{j_2}(t_2 - t_0) \\ & + \sum_j \int_{t_0}^{+\infty} K_{X_{0,j} F(s)} \cdot g_j(t_1 - t_0) \cdot [h_x(t_1 - s) + h_x(t_2 - s)] ds + \\ & + \int_{-\infty}^{+\infty} K_{FF}(s_1, s_2) \cdot h_x(t_1 - s_1) \cdot h_x(t_2 - s_2) ds_1 ds_2 \end{aligned} \quad (2.12)$$

A similar equation can be written for the autocorrelation function. Eq.(2.12) gets a simpler form in the case of independence from the initial conditions: the term  $K_{X_{0,j} F(s)}$  would be nil and, consequently, all the second term. Another possible case is that only the initial conditions are random and the stochastic response depends only on them. Alternatively, the initial conditions can be assumed as deterministic: in this case all the initial conditions stochastic parameters as mean, variance or autocorrelation are nil, but the results are still influenced by them.

It is frequent the case of response conditioned by another event  $A$  that includes a complete set of initial conditions at time  $t_0$ , for instance, the behave of the system after a damaging. The stochastic set of initial conditions  $X_{0,j}$  in eq.(2.11) and (2.12) is replaced by a determinist one,  $x_{0,j}$ , whose value is known given  $A$ . The obtained mean is:

$$E[X(t) | A] = \sum_j x_{0,j} \cdot g_j(t - t_0) + \int_{t_0}^{+\infty} E[F(s) | A] \cdot h_x(t - s) ds \quad (2.13)$$

The variance is:

$$\text{Cov}[X(t_1), X(t_2) | A] = \int_{t_0}^{+\infty} \int_{t_0}^{+\infty} \text{Cov}[F(s_1), F(s_2) | A] \cdot h_x(t_1 - s_1) \cdot h_x(t_2 - s_2) ds_1 ds_2 \quad (2.14)$$

All the previous expressions can be particularized for specific situations: the stationary case (where the stochastic parameters are substituted with their stationary equivalents), modulated processes, or delta-correlated processes. A description of the stationary case will be given, the others can be found on Lutes & Sarkani[40].

To be stationary, the excitation process  $F(t)$  must have existed since time  $t = -\infty$  to be not influenced by the initial conditions; by this hypothesis, every transient influence can be considered as decayed. Depending only from the difference of time between two instants, the stationary mean value of excitation can only be constant,  $\mu_F(t-r) = \mu_F = \text{const}$ . Substituting in eq.(2.11) and considering the initial conditions as irrelevant (because given at an infinite negative time) the final equation is:

$$\mu_X(t) = E[X(t)] = \mu_F \cdot \int_{-\infty}^{+\infty} h_x(t-s) ds = \mu_F \cdot h_{X,static} \quad (2.15)$$

There are two possibilities: either  $h_{X,static}$  is infinite and  $\mu_X(t)$  does not exist, or  $\mu_X(t) = \mu_X = \text{const}$ . In particular, if the system has finite static response and the excitation is mean value stationary, then, also the stochastic response is mean stationary. If instead the response of the system is infinite and  $\mu_F \neq 0$ , the mean value of the stochastic response is infinite too.

If the excitation is second moment stationary  $\Phi_{XX}(t_1 - r_1, t_2 - r_2) = R_{FF}(t_1 - r_1 - t_2 - r_2)$  and the initial conditions are irrelevant; substituting in eq.(2.12), the final covariance becomes:

$$\Phi_{XX}(t_1, t_2) = E[X(t_1)X(t_2)] = \int_{-\infty}^{+\infty} \int_{-\infty}^{+\infty} R_{FF}(t_1 - t_2 - r_1 + r_2) \cdot h_x(r_1) \cdot h_x(r_2) dr_1 dr_2 \quad (2.16)$$

If the second moment response  $\Phi_{XX}(t_1, t_2)$  is finite, then it is a function only of the difference  $\tau = t_1 - t_2$  and it becomes a stationary auto-correlation function:

$$R_{XX}(\tau) = \int_{-\infty}^{+\infty} \int_{-\infty}^{+\infty} R_{FF}(\tau - r_1 - r_2) \cdot h_x(r_1) \cdot h_x(r_2) dr_1 dr_2 \quad (2.17)$$

There is a similar form for the cross-correlation:

$$R_{XY}(\tau) = \int_{-\infty}^{+\infty} \int_{-\infty}^{+\infty} R_{FF}(\tau - r_1 - r_2) \cdot h_x(r_1) \cdot h_y(r_2) dr_1 dr_2 \quad (2.18)$$

In the special case of the cross-correlation of a process and its time derivative is:

$$R_{X\dot{X}}(\tau) = \int_{-\infty}^{+\infty} \int_{-\infty}^{+\infty} R_{FF}(\tau - r_1 - r_2) \cdot h_x(r_1) \cdot h'_x(r_2) dr_1 dr_2 \quad (2.19)$$

From which it is easy to get the corresponding stationary covariance  $C_{XX}(\tau)$ .

For the Schwarz inequality  $|R_{XX}(\tau)| \leq E(X^2)$  and  $|C_{XX}(\tau)| \leq \sigma_X^2$ . In other words, the maximum correlation or covariance are between a fixed time distribution and itself. From this relation derives that the stationary mean square cannot be finite if the mean is not finite, because  $E[X^2] = \mu_X^2 + \sigma_X^2$ . It is possible to demonstrate that the variance and covariance of the excitation must be finite so that the corresponding parameters of the response would be finite too[40].

### 2.1.2 Frequency analysis domain

To perform a frequency analysis, the Fourier's transform  $\bar{f}(\omega)$  has to be applied to the time dependent excitation  $f(t)$  and then do the same for  $x(t)$ . Let define the *harmonic transfer function*  $H(\omega)$  as the ratio  $x(t)/f(t)$ , when  $f(t)$  is the pure harmonic function  $e^{i\omega t}$ . In this way, if  $f(t) = e^{i\omega t}$ , then  $x(t) = H_x(\omega) \cdot e^{i\omega t}$ . Proceeding in this way, it is possible to obtain the response to a unitary input in the frequency domain. In fact, considering the time history input:

$$f(t) = \int_{-\infty}^{+\infty} \bar{f}(\omega) \cdot e^{i\omega t} d\omega \quad (2.20)$$

The corresponding output is:

$$x(t) = \int_{-\infty}^{+\infty} \bar{H}_x(\omega) \cdot \bar{f}(\omega) \cdot e^{i\omega t} d\omega \quad (2.21)$$

Comparing this result with the reverse Fourier's transform in eq.(1.80) gives:

$$\bar{x}(\omega) = H_x(\omega) \cdot \bar{f}(\omega) \quad (2.22)$$

To find the relation between the *impulse response function*  $h_x(t)$  and the *transfer function*  $H_x(\omega)$ , the time domain response in eq.(1.25), with the function  $f(t) = e^{i\omega t}$  as input, is calculated:

$$x(t) = \int_{-\infty}^{+\infty} f(t-r) \cdot h_x(r) dr = \int_{-\infty}^{+\infty} e^{i\omega(t-r)} \cdot h_x(r) dr = e^{i\omega t} \int_{-\infty}^{+\infty} e^{-i\omega r} \cdot h_x(r) dr \quad (2.23)$$

For definition of Harmonic transfer function, this response must be  $x(t) = H_x(\omega) \cdot e^{i\omega t}$ , showing that  $H_x(\omega)$  is exactly  $2\pi$  times the Fourier's transform of  $h_x(t)$ :

$$H_x(\omega) = 2\pi \cdot h_x(\omega) = \int_{-\infty}^{+\infty} e^{-i\omega r} \cdot h_x(r) dr \quad (2.24)$$

For some specific real processes, the assumption of stationary frequency is not always acceptable. For instance, the seismic action shows a behavior that changes significantly between the different waves that characterize it. To model this, an evolutionary spectral density, varying along time, can be used ([40] and [46]):

$$x(t) = \int_{-\infty}^{+\infty} H_{xf}(t, \omega) \cdot \bar{f}(\omega) \cdot e^{i\omega t} d\omega \quad (2.25)$$

### 2.1.3 Stochastic parameters in frequency domain

To get the main stochastic parameters in frequency domain it is necessary to substitute the stochastic functions,  $X(t)$  and  $F(s)$ , to the deterministic ones,  $x(t)$  and  $f(t)$ , in eq.(2.22):

$$\bar{X}(\omega) = H_X(\omega) \cdot \bar{F}(\omega) \quad (2.26)$$

By this relation, the mean value is:

$$\bar{\mu}_X(\omega) = H_X(\omega) \cdot \bar{\mu}_F(\omega) \quad (2.27)$$

For the  $2^{nd}$  order moments, in analogy with the double integration requested in the time domain, it is necessary to multiply two times for the *transfer function* with opposite sign in the argument:

$$S_{XX}(\omega) = H_X(\omega) \cdot H_X(-\omega) \cdot S_{FF}(\omega) = |H_X(\omega)|^2 \cdot S_{FF}(\omega) \quad (2.28)$$

The second passage is due to the symmetry of the Spectral Density function, this relation can be seen as an equivalent of (2.3) in the frequency domain. For the cross-spectral density function it is necessary to slightly modify (2.28) in:

$$S_{XY}(\omega) = H_X(\omega) \cdot H_Y(-\omega) \cdot S_{FF}(\omega) = H_X(\omega) \cdot H_Y^*(\omega) \cdot S_{FF}(\omega) \quad (2.29)$$

where the symbol  $m^*$  indicates the complex conjugate of a generic variable  $m$ . For the cross spectral density between response and excitation, the (2.29) becomes:

$$S_{XF}(\omega) = H_X(\omega) \cdot S_{FF}(\omega) \quad (2.30)$$

The correspondents of the relations involving the derivatives in eq.(2.7) are also applicable. It is sufficient to notice that  $x(t) = H_x(\omega) \cdot e^{i\omega t}$  has derivative  $\dot{x}(t) = i\omega \cdot H_x(\omega) \cdot e^{i\omega t}$ , that means  $H_{\dot{x}}(\omega) = i\omega \cdot H_x(\omega)$ . Whatever is the case, once the spectral density function is given, it is always possible to obtain the covariance function by applying the reverse Fourier relation in eq.(1.80).

### 2.1.4 Frequency analysis of a SDF system

To give a better idea of the complementarity of frequency and time analysis, the solution for a SDF oscillator taken from Lutes & Sarkani[40] is proposed to compare it with the results of sec.1.2.1. A generic  $n$ -order differential system can be written in the following form:

$$\sum_{j=0}^n a_j \frac{d^j x(t)}{dt^j} = f(t) \quad (2.31)$$

the corresponding harmonic transfer function is given by the substitution of  $f(t) = e^{i\omega t}$  once set  $x(t) = H_x(\omega) \cdot e^{i\omega t}$  in eq.(2.31):

$$H_x(\omega) = \left[ \sum_{j=0}^n a_j (i\omega)^j \right]^{-1} \quad (2.32)$$

Considering a SDF oscillator, the equation of motion can be written as:

$$m \cdot \ddot{X}(t) + c \cdot \dot{X}(t) + k \cdot X(t) = F(t) \quad (2.33)$$

or, in canonic form, as:

$$\ddot{X}(t) + 2\xi_0\omega_0 \cdot \dot{X}(t) + \omega_0^2 \cdot X(t) = \frac{F(t)}{m} \quad (2.34)$$

where  $\omega_0$  and  $\xi_0$  are respectively the natural frequency and the damping ratio of the main system. The harmonic transfer function for the process  $\{X(t)\}$  can be found by substituting eq.(2.32) to  $X(t)$  in eq.(2.34) and gives:

$$H_x(\omega) = \frac{1}{(k + i\omega c - \omega^2 m)} = \frac{1}{m(\omega_0^2 + 2i\xi_0\omega - \omega^2)} \quad (2.35)$$

where  $\omega$  indicates the external force frequency. Notice that the same expression could be found by calculating the Fourier's transform of eq.(1.28).

eq.(2.35) in eq.(2.28) allows to obtain the power spectral density of a SDF oscillator:

$$S_{XX}(\omega) = |H_X(\omega)|^2 \cdot S_{FF}(\omega) = \frac{S_{FF}}{m^2[(\omega_0^2 - \omega^2)^2 + (2\xi_0\omega)^2]} \quad (2.36)$$

Some considerations similar to the ones stated in sec.1.2.1 can be done starting from this equation.

In fig.2.1, a correspondent in frequency domain of the graph in fig.1.4 is drawn. The value  $m^2\omega_0^4 \cdot |H_x(\omega)|^2 \equiv k^2 \cdot |H_x(\omega)|^2$  (that is equivalent to the response PSD for an unitary input) is plotted over the normalized frequency  $\omega/\omega_0$  for different values of  $\xi_0$ . Considering the intervals of the graph and analysing eq.(2.36):

- for  $\omega \approx 0$ , the response PSD  $S_{XX}(\omega)$  is similar to  $S_{FF}(\omega)$  divided for  $m^2\omega_0^4 \equiv k^2$ . The case is almost static; in fact, the frequency of the exciting force is  $|\omega| \ll \omega_0$ . The response is governed by the stiffness of the system:  $k \cdot X(t) = F(t)$ .
- For  $|\omega| \gg \omega_0$  the PSD value is approximately  $S_{XX} \approx S_{FF}(\omega)/m^4$  and, by time derivation,  $S_{\dot{X}\dot{X}} \approx S_{FF}(\omega)/m^2$ . The system depends primarily on the inertial mass:  $m \cdot \ddot{X}(t) = F(t)$ .
- At the resonance frequency ( $|\omega| \approx \pm\omega_0$ ) the response is greatly amplified and the PSD becomes  $S_{XX}(\omega) \approx S_{FF}(\omega)/(2m\xi_0\omega)^2 = S_{FF}(\omega)/(c^2\omega^2)$  and, by time derivation, the PSD of velocity is  $S_{\dot{X}\dot{X}}(\omega) = S_{FF}(\omega) \cdot c^2$ . The behave of the response is primarily governed by the damping of the system:  $c \cdot \dot{X}(t) = F(t)$ .

Every term plays a role in the differential equation governing the system. The stiffness  $k \cdot X(t)$  dominates the low frequency response, the acceleration  $m \cdot \ddot{X}(t)$  dominates the high frequencies response and the damping  $c \cdot \dot{X}(t) = F(t)$  the resonant frequency response. Considering the low damping ratio of ordinary structures, it is necessary to introduce additional damping contributes to control effectively the resonant response when occurs.

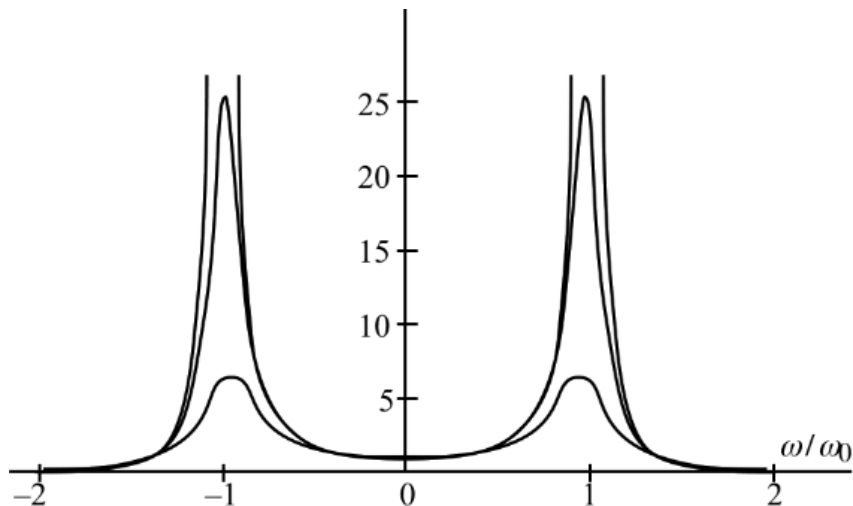


Figure 2.1: Transfer function  $|H_x(\omega)|$  for  $\xi_0 = 0.05, 0.1,$  and  $0.20$ [40].

In conclusion, the choice of the approach to study the response of the system depends primarily on the encountered problem. In the domain of frequency, some important informations about the system can be found by the interpretation of the power spectral density function. Moreover, if the time domain analysis requires the resolution of double convolution integrals, for the frequency analysis instead simple algebraic equations are enough. However, the shape of the spectral density function maybe not so simple and in particular cases a residual complex calculus has to be performed. The choice between the two forms depends on the situations and they can also be combined to have a more comprehensive description of the process.

## 2.2 Multiple degrees of freedom random vibration analysis

The formulations stated for the stochastic analysis of SDF systems are applicable to MDF systems too with some cautions in their extension. The behave of the system is described by a vector  $\vec{X}(t)$  of  $j = 1, \dots, n_X$  elements, where  $n_X$  represents the total number of nodal degrees of freedom, and a vector  $\vec{F}(t)$  of  $l = 1, \dots, n_F$  elements, where  $n_F$  represents the total number of external forces applied. Both these vectors are considered random. The generic response of the  $j^{th}$  degree of freedom (a node) to the total  $n_F$  applied to the body as Dirac's delta pulse is given by[40]:

$$X_j(t) = \sum_{l=1}^{n_F} \int_{-\infty}^{+\infty} h_{jl}(t-s) \cdot F_l(s) ds \quad (2.37)$$

where the term  $h_{jl}(t)$  is the response component  $X_j(t)$  due to a Dirac delta function excitation with  $F_l(t) = \delta_t$  for  $r = l$  and  $F_r(t) = 0$  for  $r \neq l$ . This equation corresponds to the  $j^{th}$  row of the

following matrix equation:

$$\vec{X}(t) = \int_{-\infty}^{+\infty} \mathbf{h}(t-s) \cdot \vec{F}(s) ds \quad (2.38)$$

where  $\mathbf{h}(t)$  is a matrix of dimension  $(n_X \times n_F)$  that gives the response for each degree of freedom to every term of the excitation. Equation (2.38) can be reorganized so that an entire column of  $\mathbf{h}(t)$  matrix is defined by one equation of the form:

$$\vec{X}(t) = [h_{1l}(t), \dots, h_{n_X l}(t)]^T \quad (2.39)$$

where  $\vec{X}(t)$  indicates the response to:

$$\vec{F}(t) = [0, \dots, 0, \delta(t), 0, \dots, 0]^T \quad (2.40)$$

and the nil terms before and after the first impulse are the  $(l-1)$  and  $(n_F-l)$  other excitations on the different nodes (assumed nil for that row).

In the same way, the frequency response of the  $j^{\text{th}}$  degree of freedom to the total  $n_F$  is:

$$X_j(t) = \sum_{l=1}^{n_F} H_{jl}(\omega) \cdot F_l(\omega) \quad (2.41)$$

That corresponds to the  $j^{\text{th}}$  row of the matrix equation:

$$\vec{X}(t) = \mathbf{H}(\omega) \cdot \vec{F}(\omega) \quad (2.42)$$

The relation between the *impulse response function* and the *transmission function* remains valid also in the MDF system as extension in  $n$ -dimension of eq.(2.24):

$$\mathbf{H}_x(\omega) = \int_{-\infty}^{+\infty} \mathbf{h}_x \cdot e^{-i\omega t} dt \quad (2.43)$$

Consequently, the extension of the formulations for the time analysis of section 2.1.1 and the frequency analysis of sec.2.1.2 to MDF systems are immediate. For the mean value are:

$$\vec{\mu}_X(t) = E[\vec{X}(t)] = \int_{-\infty}^{+\infty} \mathbf{h}(t-s) \cdot \vec{\mu}_F(s) ds \quad (2.44)$$

$$\vec{\mu}_X(\omega) = \mathbf{H}(\omega) \cdot \vec{\mu}_F(\omega) \quad (2.45)$$

For the auto-correlation function, that exists only in time domain, is:

$$\begin{aligned} \Phi_{XX}(t, s) &= E[\vec{X}(t)\vec{X}^T(s)] = \\ &= \int_{-\infty}^{+\infty} \int_{-\infty}^{+\infty} \mathbf{h}^T(t-u) \cdot \Phi_{FF}(u, v) \cdot \mathbf{h}^T(s-v) du dv \end{aligned} \quad (2.46)$$

For the auto-covariance similarly is:

$$\begin{aligned} \mathbf{K}_{XX}(t, s) &= \Phi_{XX}(t, s) - \vec{\mu}_X(t) \cdot \vec{\mu}_X^T(s) = \\ &= \int_{-\infty}^{+\infty} \int_{-\infty}^{+\infty} \mathbf{h}^T(t-u) \cdot \mathbf{K}_{FF}(u, v) \cdot \mathbf{h}^T(s-v) du dv \end{aligned} \quad (2.47)$$

In the special case of stationarity, the mean is a constant while the auto-correlation and auto-covariance are:

$$\mathbf{R}_{XX}(\tau) = \int_{-\infty}^{+\infty} \int_{-\infty}^{+\infty} \mathbf{h}^T(u) \cdot \mathbf{R}_{FF}(\tau - u + v) \cdot \mathbf{h}^T(v) \, du \, dv \quad (2.48)$$

$$\mathbf{C}_{XX}(\tau) = \int_{-\infty}^{+\infty} \int_{-\infty}^{+\infty} \mathbf{h}^T(u) \cdot \mathbf{C}_{FF}(\tau - u + v) \cdot \mathbf{h}^T(v) \, du \, dv \quad (2.49)$$

The auto-spectral density is given instead by:

$$\mathbf{S}_{XX}(\omega) = \mathbf{H}(\omega) \cdot \mathbf{S}_{FF}(\omega) \cdot \mathbf{H}^{*T}(\omega) \quad (2.50)$$

The previous relations between the  $j^{\text{th}}$  diagonal element of the response and the matrix form of the solution are still valid.

If the value  $\vec{X}(t_0) = \vec{X}_0$  of the response at time  $t_0$  is known, the expression of the generic response in time domain becomes:

$$\vec{X}(t) = \mathbf{g}(t - t_0) \cdot \vec{X}_0 + \int_{t_0}^t \mathbf{h}(t - s) \cdot \vec{F}(s) \, ds \quad (2.51)$$

where  $\vec{X}_0$  contains a complete set of initial conditions at time  $t_0$  and  $\mathbf{g}(t)$  is a matrix that gives the time histories of the unforced vibration (the homogeneous solution) for unitary values of the initial conditions.

The generic MDF equation of motion with a set of assigned initial conditions is:

$$\mathbf{m} \cdot \ddot{\vec{X}}(t) + \mathbf{c} \cdot \dot{\vec{X}}(t) + \mathbf{k} \cdot \vec{X}(t) = \vec{F}(t), \quad P([\vec{U}(t_0) = \vec{u}_0] \cap [\dot{\vec{U}}(t_0) = \dot{\vec{u}}_0]) = 1 \quad (2.52)$$

where  $\mathbf{m}$  is the mass matrix,  $\mathbf{c}$  is the damping matrix and  $\mathbf{k}$  is the stiffness matrix of the system, all positive definite for physical reasons.  $\vec{X}(t)$  is the random vector of displacements and  $\vec{F}(t)$  is the random excitation applied to the system (the initial conditions are assumed as deterministic in this case). The form of these matrices depends on the characteristics of the system and this equilibrium equation derives from the *energy conservation principle*, where every term plays a role in the total energy balance of the system and how the input energy is distributed between kinetics, elastic and dissipated.

There are different approaches for the study of the MDF equilibrium:

- a time or frequency *integration of the entire set of uncoupled equations*: this approach is really computationally onerous and generally not convenient;
- a *modal space* study of the uncoupled equations of motion: an eigenvector analysis is performed and the modal shapes contributing most to the motion studied. The approach requires some initial hypothesis about the form of the damping matrix that are not always acceptable;
- a *state space* study of the entire system: by transforming the  $n_{\text{dof}}$  equations of  $m^{\text{th}}$  order in  $(m \times n_{\text{dof}})$  equations of  $1^{\text{st}}$  order. This approach is more general than a modal decomposition and does not require particular initial hypothesis, however, if the number of degree of freedom is high, its resolution may become cumbersome.

Moreover, the approaches can be combined. For instance, a state space analysis of the modal shapes is often used.

## 2.2.1 Modal decomposition

Considering the system of eq.(2.52), it is possible to define the *modal matrix*  $\boldsymbol{\theta}$ , of dimension  $(n_{dof} \times n_{dof})$ , with columns the eigenvectors of  $\mathbf{m}^{-1}\mathbf{k}$ . This means that[40]:

$$\mathbf{m}^{-1}\mathbf{k} \cdot \boldsymbol{\theta} = \boldsymbol{\theta} \cdot \boldsymbol{\lambda} \quad (2.53)$$

where  $\boldsymbol{\lambda}$  is the eigenvalues diagonal matrix of dimension  $(n_{dof} \times n_{dof})$  and the  $j^{th}$  element of the diagonal is the eigenvalue corresponding to the eigenvector located in the  $j^{th}$  column of  $\boldsymbol{\theta}$ . Once that the modal matrix is defined, it is used to diagonalize the matrices of the mechanical characteristics of the system:

$$\hat{\mathbf{m}} = \boldsymbol{\theta}^T \mathbf{m} \boldsymbol{\theta} \quad (2.54)$$

$$\hat{\mathbf{k}} = \boldsymbol{\theta}^T \mathbf{k} \boldsymbol{\theta} \quad (2.55)$$

Multiplying both members of eq.(2.53) for  $\mathbf{m}$  gives the equation  $\mathbf{k} \cdot \boldsymbol{\theta} = \mathbf{m} \cdot \boldsymbol{\theta} \boldsymbol{\lambda}$ . Another multiplication for  $\boldsymbol{\theta}^T$  on the left is applied to get  $\hat{\mathbf{k}} = \hat{\mathbf{m}} \cdot \boldsymbol{\lambda}$ . Due to the fact that  $\hat{\mathbf{m}}$ ,  $\hat{\mathbf{k}}$  and  $\boldsymbol{\lambda}$  are symmetric, the transpose of both terms of the previous equation is  $\hat{\mathbf{k}} = \boldsymbol{\lambda} \cdot \hat{\mathbf{m}}$ ; thus, the matrices  $\hat{\mathbf{m}}$  and  $\boldsymbol{\lambda}$  commute. It is necessary to provide the condition  $\hat{\mathbf{m}} \neq \mathbf{0}$ , satisfied only if the eigenvalues do not repeat in  $\boldsymbol{\lambda}$ , and this happens only if  $\hat{\mathbf{m}}$  is diagonal. For the relation  $\hat{\mathbf{k}} = \hat{\mathbf{m}} \cdot \boldsymbol{\lambda}$ ,  $\hat{\mathbf{k}}$  is diagonal too.

Assumed the previous hypothesis, the displacements vector  $\vec{X}(t)$  can be written as a linear expansion of the eigenvectors of  $\mathbf{m}^{-1}\mathbf{k}$ :

$$\vec{X}(t) = \boldsymbol{\theta} \cdot \vec{Z}(t) \quad (2.56)$$

where the  $j^{th}$  component of  $\vec{Z}(t)$  is the projection of  $\vec{X}(t)$  on the  $j^{th}$  eigenvector. In other words,  $\theta_{jl}$  gives the magnitude of the  $X_j(t)$  response due to a unit magnitude of  $Z_l(t)$ , that is, the contribute of each modal shape to the nodal displacements. Usually, the  $l^{th}$  eigenvector (column of  $\boldsymbol{\theta}$ ) is called the *mode shape* and  $Z_l(t)$  is called the *modal amplitude*.  $\vec{X}(t)$  is the *nodal coordinate* of motion and  $\vec{Z}(t)$  the *modal coordinate* of motion. The obtained equation is:

$$\boldsymbol{\theta}^T \mathbf{m} \boldsymbol{\theta} \cdot \vec{\ddot{Z}}(t) + \boldsymbol{\theta}^T \mathbf{c} \boldsymbol{\theta} \cdot \vec{\dot{Z}}(t) + \boldsymbol{\theta}^T \mathbf{k} \boldsymbol{\theta} \cdot \vec{Z}(t) = \boldsymbol{\theta}^T \cdot \vec{F}(t) \quad (2.57)$$

The equation can be rewritten by using the diagonalized matrices:

$$\vec{\ddot{Z}}(t) + \boldsymbol{\beta}^T \cdot \vec{\dot{Z}}(t) + \boldsymbol{\lambda} \vec{Z}(t) = \hat{\mathbf{m}}^{-1} \boldsymbol{\theta}^T \cdot \vec{F}(t) \quad (2.58)$$

where the matrix  $\boldsymbol{\beta}$  is defined as:

$$\hat{\mathbf{c}} = \boldsymbol{\theta}^T \mathbf{c} \boldsymbol{\theta} = \hat{\mathbf{m}} \boldsymbol{\beta} \quad (2.59)$$

It is always possible to write in this form the equations of motion although this formulation is particularly useful for the case in which  $\boldsymbol{\beta}$  is diagonal. In this case, the  $j^{th}$  row can be written as:

$$\ddot{Z}_j(t) + \beta_{jj} \cdot \dot{Z}_j(t) + \lambda_{jj} \cdot Z_j(t) = \frac{1}{\hat{m}_{jj}} \sum_{l=1}^n \theta_{lj} \cdot F_l(t) \quad (2.60)$$

That means, every modal equation is uncoupled from each other and can be solved as an independent SDF oscillator. The assumption of  $\boldsymbol{\beta}$  diagonal is not always justified and many authors wrote about how to model a system under different damping conditions; a wide description of the not ordinary damping models is reported by Muscolino[46]. Typically, is assumed a *classical damping* and *uncoupled modes*; the condition for this assumption is that the matrix  $\mathbf{c}$  is a

linear combination of  $\mathbf{m}$  and  $\mathbf{k}$ . This hypothesis is not always acceptable, for example when a concentrate dissipative element is inserted in the system.

Assumed a classical damping, the equations can be uncoupled and superposed to give the solution of the equations of motion. Fixing  $\omega_j = (\lambda_{jj})^{1/2}$  and  $\beta_{jj} = 2\xi_j\omega_j$ , eq.(2.60) becomes:

$$\ddot{Z}_j(t) + 2\xi_j\omega_j \cdot \dot{Z}_j(t) + \omega_j^2 \cdot Z_j(t) = \frac{1}{\hat{m}_{jj}} \sum_{l=1}^n \theta_{lj} \cdot F_l(t) \quad (2.61)$$

It is possible to demonstrate that the conditions under which the uncoupled hypothesis is verified can be written as:  $\mathbf{k} \mathbf{m}^{-1} \cdot \mathbf{c} = \mathbf{c} \cdot \mathbf{m}^{-1} \mathbf{k}$ . A much simpler condition, sufficient but not necessary, is the *Rayleigh condition*, that requires  $\mathbf{c} = a_1 \cdot \mathbf{m} + a_2 \cdot \mathbf{k}$  for some scalar constants  $a_1$  and  $a_2$ . It is demonstrable that the Rayleigh condition is a special case of the previous one. A more generalized possible Rayleigh condition is the following:

$$\mathbf{c} = \mathbf{m} \sum_{j=0}^J a_j \cdot (\mathbf{m}^{-1} \mathbf{k})^j \quad (2.62)$$

The value of  $J$  is generally set with upper limit  $(n_{dof} - 1)$ , thus, this condition is more restrictive than  $\mathbf{k} \mathbf{m}^{-1} \cdot \mathbf{c} = \mathbf{c} \cdot \mathbf{m}^{-1} \mathbf{k}$  for any value of  $j$  smaller than  $J$ .

The analysis of the uncoupled modes is generally adopted because the damping matrix  $\mathbf{c}$  is not easily determined: it contains frictions, local yielding and other dissipative mechanisms that are difficult to be modelled. The  $\mathbf{m}$  and  $\mathbf{k}$  matrices instead are quite well approximated by the calculations of mass and stiffness. Considering this, the form given to  $\mathbf{c}$  is generally assumed to be the most practical to have a correspondence with the experimental data. One of the most common way to proceed is to fix already a damping ratio  $\xi$  and, knowing  $\boldsymbol{\lambda}$  from the eigenvector analysis, calculate each element of  $\boldsymbol{\beta}$  as  $\beta_j = 2\xi\omega_j$ . In the case of added dissipative systems, the hypothesis of uncoupled modes is not valid any more and methods to perform the modal analysis for not classical damping have to be used, involving a significant increase in complexity[46].

## 2.2.2 Time domain analysis of the uncoupled MDF system

There are two approaches to the time analysis of MDF systems. The first uses the modal decomposition in a deterministic analysis to get the impulse response function  $\mathbf{h}(t)$  and then perform the stochastic analysis presented in section 2.1.1. The second, instead, considers the equations of modal decomposition already as stochastic and gets the mean and covariance of the nodal coordinate  $\vec{X}(t)$  through them[40]. Of course, the two approaches lead to the same result.

As stated in sec.2.2, the  $l^{th}$  column of the response can be written by using the vector of impulse response function  $\mathbf{h}(t) = [h_{1l}(t), \dots, h_{nl}(t)]$  that gives the response  $\vec{X}(t)$  to the  $l^{th}$  excitation  $F_l(t) = \delta(t)$ , where  $l$  is the generic external excitation of the  $n_F$  actions applied to the system. By using eq.(2.60), the excitation of the  $j^{th}$  modal equation is obtainable as  $\theta_{lj} \cdot \delta(t)/m_{jj}$ . The modal responses to the Dirac delta function excitation at node  $l$  are  $Z_j(t) = \theta_{lj} \cdot \hat{h}_{jj}(t)$ , where  $\hat{h}_{jj}(t)$  is the impulse response to the  $j^{th}$  modal equation, already calculated for the SDF system in eq.(1.28) and modified here in:

$$\hat{h}_{jj}(t) = \frac{\exp(-\xi_j\omega_j t)}{\hat{m}_{jj} \cdot \omega_{dj}} \sin(\omega_{dj} t) \cdot U(t) \quad (2.63)$$

where  $\omega_{dj} = \omega_j[1 - \xi_j^2]^{1/2}$  is the damped frequency and  $\hat{m}_{jj}$  is the *modal mass*. Combining eq.(2.56) and eq.(2.63) gives the relation between nodal and modal impulse response function:

$$h_{rl}(t) = X_r(t) = \sum_{j=1}^{n_{dof}} \theta_{rj} \theta_{lj} \cdot \hat{h}_{jj}(t) \quad (2.64)$$

It is possible to extend this relation to the entire impulse response and get:

$$\mathbf{h}(t) = \boldsymbol{\theta} \cdot \hat{\mathbf{h}}(t) \cdot \boldsymbol{\theta}^T \quad (2.65)$$

where  $\hat{\mathbf{h}}(t)$  is the diagonal matrix of the modal impulse response function given in (2.63). This first approach is quite direct and leaves the stochastic analysis described in section 2.1.1 once the impulse response function is calculated. For computation economy, the number of modal shapes analysed are typically limited to a value  $r < j$  sufficient to cover a significant portion of the excited mass.

The second approach applies directly the modal decomposition to the stochastic parameters found in 2.1.1 instead of calculating the matrix  $\mathbf{h}(t)$ . By using eq.(2.56) the corresponding moments of the process are obtained:

$$\vec{\mu}_X(t) = \boldsymbol{\theta} \cdot \vec{\mu}_Z(t) \quad (2.66)$$

$$\boldsymbol{\Phi}_{XX}(t) = \boldsymbol{\theta} \cdot \boldsymbol{\Phi}_{ZZ}(t) \cdot \boldsymbol{\theta}^T \quad (2.67)$$

$$\mathbf{K}_{XX}(t) = \boldsymbol{\theta} \cdot \mathbf{K}_{ZZ}(t) \cdot \boldsymbol{\theta}^T \quad (2.68)$$

The time histories of the components of the stochastic  $\vec{Z}(t)$  vector of modal response are obtained from eq.(2.60) as:

$$Z_j(t) = \sum_{k=1}^n \theta_{kj} \int_{-\infty}^{+\infty} \hat{h}_{jj}(t-s) \cdot F_k(s) ds \quad (2.69)$$

That in matrix form is:

$$\vec{Z}(t) = \int_{-\infty}^{+\infty} \hat{\mathbf{h}}(t-u) \cdot \boldsymbol{\theta}^T \cdot \vec{F}(u) du \quad (2.70)$$

Proceeding in this way, the mean is:

$$\vec{\mu}_X(t) = \boldsymbol{\theta} \cdot \vec{\mu}_Z(t) = \int_{-\infty}^{+\infty} \hat{\mathbf{h}}(t-u) \cdot \boldsymbol{\theta}^T \cdot \vec{\mu}_F(u) du \quad (2.71)$$

The autocorrelation is:

$$\boldsymbol{\Phi}_{ZZ}(t, s) = \int_{-\infty}^{+\infty} \int_{-\infty}^{+\infty} \hat{\mathbf{h}}(t-u) \cdot \boldsymbol{\theta}^T \boldsymbol{\Phi}_{FF}(u, v) \boldsymbol{\theta} \cdot \hat{\mathbf{h}}(t-u) du dv \quad (2.72)$$

which gives the corresponding result in nodal coordinates  $\vec{X}(t)$ :

$$\boldsymbol{\Phi}_{XX}(t, s) = \boldsymbol{\theta} \boldsymbol{\Phi}_{ZZ}(t, s) \boldsymbol{\theta}^T = \boldsymbol{\theta} \int_{-\infty}^{+\infty} \int_{-\infty}^{+\infty} \hat{\mathbf{h}}(t-u) \cdot \boldsymbol{\theta}^T \boldsymbol{\Phi}_{FF}(u, v) \boldsymbol{\theta} \cdot \hat{\mathbf{h}}^T(t-u) du dv \boldsymbol{\theta}^T \quad (2.73)$$

Similarly, for the auto covariance matrix is:

$$\mathbf{K}_{ZZ}(t, s) = \int_{-\infty}^{+\infty} \int_{-\infty}^{+\infty} \hat{\mathbf{h}}(t-u) \cdot \boldsymbol{\theta}^T \mathbf{K}_{FF}(u, v) \boldsymbol{\theta} \cdot \hat{\mathbf{h}}^T(t-u) du dv \quad (2.74)$$

which gives the corresponding result in nodal coordinates  $\vec{X}(t)$ :

$$K_{XX}(t, s) = \boldsymbol{\theta} \mathbf{K}_{ZZ}(t, s) \boldsymbol{\theta}^T = \boldsymbol{\theta} \int_{-\infty}^{+\infty} \int_{-\infty}^{+\infty} \hat{\mathbf{h}}(t-u) \cdot \boldsymbol{\theta}^T \mathbf{K}_{FF}(u, v) \boldsymbol{\theta} \cdot \hat{\mathbf{h}}^T(t-u) du dv \boldsymbol{\theta}^T \quad (2.75)$$

The terms of these products are matrices that contain on the diagonal the auto-correlation and auto-variance, and out of it the cross-correlation and cross-variance terms of the scalar components of the response vector.

The study of the cross-correlation leads to the consideration that, if the damping is small and the frequencies are well separated (as it is typical in ordinary structures), the contribute of the cross-modal forms to the response is limited for non-white broad band excitations. Numerical investigations showed that, the today widely used, *Complete-Quadratic-Combination (CQC)* can better fit the behave of real structures by considering the contribute of the cross terms on the global response[40].

### 2.2.3 Frequency analysis of the uncoupled equation of motion

The same concepts expressed for the time analysis of the uncoupled equations are applied to the frequency analysis[40]. It is possible to calculate the transfer function,  $\mathbf{H}(\omega)$ , and then perform the stochastic analysis presented in section 2.1.2, or consider the equations of modal decomposition already as stochastic and get the mean and covariance of the nodal coordinate  $\vec{X}(t)$  trough them.

If the system has uncoupled modes, by eq.(2.60), the modal harmonic transfer function  $\hat{\mathbf{H}}(\omega)$  is calculated to describe the modal response  $\vec{Z}(t)$ . Then, the nodal transfer matrix  $\mathbf{H}(\omega)$  and the nodal response  $\vec{X}(t)$  are obtained. Considering an input excitation consisting of only one harmonic function  $F_l(t) = e^{i\omega t}$  and replacing it in eq.(2.60) gives:

$$\ddot{Z}_j(t) + 2\xi_j\omega_j \cdot \dot{Z}_j(t) + \omega_j^2 \cdot Z_j(t) = \frac{1}{\hat{m}_{jj}} \sum_{l=1}^n \theta_{lj} \cdot e^{i\omega t} \quad (2.76)$$

The modal response is defined as  $Z_j(t) = \hat{H}_{jl}(\omega) \cdot e^{i\omega t}$ , therefore, the  $(j, l)$  element of the harmonic transfer matrix is:

$$\hat{H}_{jl}(\omega) = \frac{\theta_{lj}}{\hat{m}_{jj}(\omega_j^2 - \omega^2 + 2i \cdot \xi_j\omega_j\omega)} \quad (2.77)$$

In matrix form, the equation becomes:

$$\hat{\mathbf{H}}(\omega) = \hat{\mathbf{m}}^{-1}[\boldsymbol{\lambda} - \omega^2 \mathbf{I} + i\omega \boldsymbol{\beta}]^{-1} \quad (2.78)$$

Using eq.(2.56), the nodal coordinates response,  $\vec{X}(t)$ , to the single harmonic excitation component is given, and the nodal transfer matrix  $\mathbf{H}(\omega)$  obtained:

$$\mathbf{H}(\omega) = \boldsymbol{\theta} \hat{\mathbf{m}}^{-1}[\boldsymbol{\lambda} - \omega^2 \mathbf{I} + i\omega \boldsymbol{\beta}]^{-1} \boldsymbol{\theta}^T \quad (2.79)$$

Alternately,  $\mathbf{H}(\omega)$  can be derived by the modal equations, taking the Fourier's transform of the equations of motion (2.52):

$$[\mathbf{k} - \omega^2 \mathbf{m} + i\omega \mathbf{c}] \cdot \vec{X}(\omega) = \vec{F}(\omega) \quad (2.80)$$

and solving respect to  $\vec{X}$ :

$$\vec{X}(\omega) = [\mathbf{k} - \omega^2 \mathbf{m} + i\omega \mathbf{c}]^{-1} \vec{F}(\omega) \quad (2.81)$$

Comparing it with eq.(2.42) shows that:

$$\mathbf{H}(\omega) = [\mathbf{k} - \omega^2 \mathbf{m} + i\omega \mathbf{c}]^{-1} \quad (2.82)$$

With a bit of matrix manipulation it is possible to demonstrate that the two forms in eq.(2.79) and (2.82) are identical. In fact, eq.(2.79) is the simplified way to get by an eigenvalues analysis the same results of eq.(2.82). Eq.(2.79) requires the calculations of  $\boldsymbol{\theta}$  and  $\boldsymbol{\lambda}$  for the eigenvalues analysis but aims to easily get the harmonic transfer function  $\mathbf{H}(\omega)$  for each frequency. The solution of eq.(2.82) is convenient for a small amount of degrees of freedom and is also applicable for not uncoupled modes. However, the relation between  $H_{XX}(\omega)$  and  $H_{\ddot{X}\ddot{X}}(\omega)$  is valid only once the uncoupled modes, and their correspondent frequencies, are found.

Once the harmonic transfer function from either eq.(2.79) or (2.82) is given, the impulse response function is calculated by applying the inverse Fourier's transform to it:

$$\mathbf{h}(t) = \frac{1}{2\pi} \int_{-\infty}^{+\infty} [\mathbf{k} - \omega^2 \mathbf{m} + i\omega \mathbf{c}]^{-1} e^{i\omega t} d\omega \quad (2.83)$$

By the analysis of the cross-spectral density, similar results to the ones obtained from the analysis of cross-covariance can be done to evidence that for small damping and well separated frequencies the contribute of cross-modal forms to the system is small.

## 2.2.4 State-space formulation of equation of motion

The analysis in the *state space* transforms the  $n_{dof}$  equations of  $m^{th}$  order in  $m \times n_{dof}$  equations of  $1^{st}$  order. The advantage of this approach is that a system of first-order differential equations is easier to be solved requiring only linear operators. Considering the differential equation (2.52), a *state vector*  $\vec{Y}(t) = [\vec{X} \ \dot{\vec{X}}]^T$  is defined. The state vector contains  $2 \times n_{dof}$  *state variables*, called in this way because they indicate all the informations necessary to describe the state of the system at a generic instant of time. The *state equations of the system* have the following form[40]:

$$\mathbf{A} \cdot \vec{Y}(t) + \mathbf{B} \cdot \vec{Y}(t) = \vec{Q}(t) \quad (2.84)$$

In which  $\mathbf{A}$  and  $\mathbf{B}$  are matrices determined from the mechanical parameters of the system and  $\vec{Q}(t)$  contains the excitation terms, all obtained from the original equation of motion.

The knowledge of  $\vec{Y}(t_0)$  at time  $t_0$  gives a complete set of initial conditions that aims to calculate an unique solution to  $\vec{Y}(t)$  for  $t > t_0$ .

The final dimension  $n_Y$  of the state space array that involves  $J$  variables  $X_1(t), \dots, X_J(t)$ , with derivatives up to order  $n_j$  in the variable  $X_j(t)$ , is:

$$n_Y = \sum_{j=1}^J n_j \quad (2.85)$$

The vector  $\vec{Y}(t)$  contains  $X_j(t)$  and its first  $(n_j - 1)$  derivatives for  $j = 1, \dots, J$ . A possible way to define the matrices of the system is to write the (2.52) as:

$$\ddot{\vec{X}}(t) + \mathbf{m}^{-1} \mathbf{c} \cdot \dot{\vec{X}}(t) + \mathbf{m}^{-1} \mathbf{k} \cdot \vec{X}(t) = \mathbf{m}^{-1} \vec{F}(t) \quad (2.86)$$

Then associate a second trivial equation,  $\dot{\vec{X}}(t) - \vec{X}(t) = \vec{0}$ , to have the necessary number of equations. The obtained state system matrices are:

$$\mathbf{A} = \mathbf{I}_{2n} = \begin{bmatrix} \mathbf{I}_n & \mathbf{0} \\ \mathbf{0} & \mathbf{I}_n \end{bmatrix}, \quad \mathbf{B} = \begin{bmatrix} \mathbf{0} & -\mathbf{I}_n \\ \mathbf{m}^{-1} \mathbf{k} & \mathbf{m}^{-1} \mathbf{c} \end{bmatrix}, \quad \vec{Q}(t) = \begin{bmatrix} \vec{0} \\ \mathbf{m}^{-1} \vec{F}(t) \end{bmatrix} \quad (2.87)$$

This form is not unique and there are some advantages in the alternative one:

$$\mathbf{A} = \begin{bmatrix} -\mathbf{k} & \mathbf{0} \\ \mathbf{0} & \mathbf{m} \end{bmatrix}, \quad \mathbf{B} = \begin{bmatrix} \mathbf{0} & \mathbf{k} \\ \mathbf{k} & \mathbf{c} \end{bmatrix}, \quad \vec{Q}(t) = \begin{bmatrix} \vec{0} \\ \mathbf{m}^{-1} \vec{F}(t) \end{bmatrix} \quad (2.88)$$

That gives both  $\mathbf{A}$  and  $\mathbf{B}$  symmetric. The product  $\mathbf{D} = \mathbf{A}^{-1}\mathbf{B}$  takes the name of *system matrix* and has the function to describe in the state space the properties of the system.

By the state space approach, eq.(2.84) is solvable as a set of first-order differential equations of which the homogeneous solution is  $\vec{X}(t) = \exp[-\mathbf{D} \cdot t]$ , with the matrix exponential defined as:

$$\exp(\mathbf{A}) = \sum_{j=0}^{+\infty} \frac{1}{j!} \mathbf{A}^j \quad (2.89)$$

for any square matrix  $\mathbf{A}$ , with  $\mathbf{A}^0$  defined as identity matrix with the dimension of  $\mathbf{A}$  and the generic power of  $i^{th}$  order  $\mathbf{A}^j = \mathbf{A} \cdot \mathbf{A}^{j-1}$  for  $j \geq 1$ . This relation gives the derivate of the solution,  $\vec{Y}(t) = \exp[-\mathbf{D} \cdot t]$ , respect to  $t$ , as  $\dot{\vec{Y}}(t) = -\mathbf{D} \cdot \exp[-\mathbf{D} \cdot t]$ . The non-homogeneous solution is obtained with a convolution integral:

$$\vec{Y}(t) = \int_{-\infty}^t \exp[-\mathbf{D} \cdot (t-s)] \cdot \mathbf{A}^{-1} \vec{Q}(s) ds \quad (2.90)$$

that for a delta-correlated process becomes:

$$\vec{Y}(t) = \int_{-\infty}^t \exp[-\mathbf{D} \cdot (t-s)] \cdot \mathbf{A}^{-1} \cdot \vec{v} \cdot W(s) ds \quad (2.91)$$

where  $\vec{v} = [\mathbf{0} \quad \mathbf{m}^{-1}]^T$  and  $W(s)$  is a generic time varying delta-correlated input. Introducing the *transition matrix*,  $\Theta_Y(t) = \exp[-\mathbf{D} \cdot (t-s)]$ , eq.(2.90) becomes:

$$\vec{Y}(t) = \int_{-\infty}^t \Theta_Y(t) \cdot \mathbf{A}^{-1} \cdot \vec{Q}(s) ds \quad (2.92)$$

while eq.(2.91) becomes:

$$\vec{Y}(t) = \int_{-\infty}^t \Theta_Y(t) \cdot \mathbf{A}^{-1} \cdot \vec{v} \cdot W(s) ds \quad (2.93)$$

These solutions are correct but have the problem of being computationally difficult to be solved if the degrees of freedom become high (frequent case in real structures). The typical approach is to perform an eigenvalue analysis of the state space equations and diagonalize the system matrix  $\mathbf{D}$ . The associated eigenvalues and eigenvectors matrices are indicated as  $\boldsymbol{\lambda}$  and  $\boldsymbol{\theta}$  (in analogy with what done for  $\mathbf{m}^{-1}\mathbf{k}$ ). The equation is  $\mathbf{A}^{-1}\mathbf{B} \cdot \boldsymbol{\theta} = \boldsymbol{\theta} \boldsymbol{\lambda}$  or, in general,  $\mathbf{A}^{-1}\mathbf{B}^j = \boldsymbol{\theta} \boldsymbol{\lambda}^j \boldsymbol{\theta}^{-1}$  for any value of  $j$ . From this condition, the eigenvectors of the system are:  $\exp[-\mathbf{D} \cdot t] = \boldsymbol{\theta} \exp[-\boldsymbol{\lambda} \cdot t] \boldsymbol{\theta}^{-1}$ . The general solution, passing through the modal space, is:

$$\vec{Y}(t) = \int_{-\infty}^t \boldsymbol{\theta} \exp[-\boldsymbol{\lambda} \cdot (t-s)] \boldsymbol{\theta}^{-1} \cdot \mathbf{A}^{-1} \vec{Q}(s) ds \quad (2.94)$$

where  $\exp[-\boldsymbol{\lambda} \cdot (t-s)]$  is a diagonal matrix that contains the scalar exponential function, each term  $\exp[-\lambda_{jj} \cdot (t-s)]$  is the  $j^{th}$  element of the diagonal. Generally, the eigenvectors of  $\mathbf{D}$  are not real and require a complex analysis; this involves a big computational effort to calculate the inverse of  $\boldsymbol{\theta}$ . There are different approaches to face this problem, however, a big simplification is

possible if  $\mathbf{A}$  and  $\mathbf{B}$  are symmetric as defined in eq.(2.88). In the same way as for the eigenvalue analysis of  $\mathbf{m}^{-1}\mathbf{k}$ , it is possible to show that  $\hat{\mathbf{A}} = \boldsymbol{\theta}^T \mathbf{A} \boldsymbol{\theta}$  is diagonal. Calculating the inverse of  $\hat{\mathbf{A}}$ , the result is  $\boldsymbol{\theta}^{-1} = \hat{\mathbf{A}}^{-1} \boldsymbol{\theta}^T \mathbf{A}$ . The final form of the equation is:

$$\vec{Y}(t) = \int_{-\infty}^t \boldsymbol{\theta} \exp[-\boldsymbol{\lambda} \cdot (t-s)] \mathbf{A}^{-1} \boldsymbol{\theta}^T \cdot \vec{Q}(s) ds \quad (2.95)$$

The terms multiplied for  $\vec{Q}(t)$  are nothing but the transition matrix in the modal space:

$$\boldsymbol{\Theta}_Z(t) = \boldsymbol{\theta} \exp[-\boldsymbol{\lambda} \cdot (t-s)] \boldsymbol{\theta}^T = \boldsymbol{\theta} \boldsymbol{\Theta}_Y(t) \boldsymbol{\theta}^T \quad (2.96)$$

Thus, eq.(2.95) becomes:

$$\vec{Y}(t) = \int_{-\infty}^t \boldsymbol{\Theta}_Z(t) \mathbf{A}^{-1} \cdot \vec{Q}(s) ds \quad (2.97)$$

### 2.2.5 Stochastic analysis of the state space equations

There are different approaches to perform the stochastic state space analysis. The first considers to find the  $\mathbf{h}(t)$  and  $\mathbf{H}(\omega)$  matrices as done in 2.1.1 and 2.1.2 for each 1<sup>st</sup> grade equation of the state space. For instance, it is possible to get  $\vec{Y}(t) = [h_{1l}(t), \dots, h_{nl}(t)]^T$  due to a single Dirac delta function pulse as  $Q_l(t)$ . From eq.(2.97) the impulse response function is:

$$\mathbf{h}(t) = \boldsymbol{\Theta}_Y(t) \cdot \mathbf{A}^{-1} \cdot U(t) = \boldsymbol{\theta} \boldsymbol{\Theta}_Z(t) \boldsymbol{\theta}^{-1} \mathbf{A}^{-1} \cdot U(t) \quad (2.98)$$

where  $U(t)$  is the unit step function. In a similar way,  $\vec{Y}(t) = [H_{1l}(\omega), \dots, H_{nl}(\omega)]^T e^{i\omega t}$  is obtained by considering a single harmonic term as  $Q_l(t)$ . From eq.(2.84) results that:

$$[i\omega \mathbf{A} + \mathbf{B}] \cdot \mathbf{H}(\omega) = \mathbf{I}_{nY} \quad (2.99)$$

and from it:

$$\mathbf{H}(\omega) = [i\omega \mathbf{A} + \mathbf{B}]^{-1} = [i\omega \mathbf{I} + \mathbf{D}]^{-1} \mathbf{A}^{-1} = \boldsymbol{\theta} [i\omega \mathbf{I} + \boldsymbol{\lambda}]^{-1} \boldsymbol{\theta}^{-1} \mathbf{A}^{-1} \quad (2.100)$$

The second way is applying the solution of eq.(2.97) to the stochastic parameters after that the eigenvectors analysis is performed. The obtained mean is:

$$\vec{\mu}_Y(t) = \int_{-\infty}^t \boldsymbol{\theta} \boldsymbol{\Theta}_Z(t-s) \boldsymbol{\theta}^{-1} \mathbf{A}^{-1} \cdot \vec{\mu}_Q(s) ds \quad (2.101)$$

The auto-correlation matrix is:

$$\boldsymbol{\Phi}_{YY}(t, s) = \int_{-\infty}^t \int_{-\infty}^t \boldsymbol{\theta} \boldsymbol{\Theta}_Z(t-u) \boldsymbol{\theta}^{-1} \mathbf{A}^{-1} \cdot \boldsymbol{\Phi}_{QQ}(u, v) \cdot (\mathbf{A}^{-1})^T (\boldsymbol{\theta}^{-1})^T \boldsymbol{\Theta}_Z(s-v) \boldsymbol{\theta}^T du dv \quad (2.102)$$

Similarly the auto-covariance is:

$$\mathbf{K}_{YY}(t, s) = \int_{-\infty}^t \int_{-\infty}^t \boldsymbol{\theta} \boldsymbol{\Theta}_Z(t-u) \boldsymbol{\theta}^{-1} \mathbf{A}^{-1} \cdot \mathbf{K}_{QQ}(u, v) \cdot (\mathbf{A}^{-1})^T (\boldsymbol{\theta}^{-1})^T \boldsymbol{\Theta}_Z(s-v) \boldsymbol{\theta}^T du dv \quad (2.103)$$

The auto-spectral density matrix instead is obtained by eq.(2.50):

$$\mathbf{S}_{YY}(\omega) = \boldsymbol{\theta} [i\omega \mathbf{I} + \boldsymbol{\lambda}]^{-1} \boldsymbol{\theta}^{-1} \cdot \mathbf{S}_{QQ}(\omega) \cdot (\mathbf{A}^T)^{-1} (\boldsymbol{\theta}^{T*})^{-1} [i\omega \mathbf{A}^T + \mathbf{B}^T]^{-1} \cdot [-i\omega \mathbf{I} + \boldsymbol{\lambda}^*]^{-1} \boldsymbol{\theta}^{*T} \quad (2.104)$$

where the symbol  $\theta^*$  indicates the complex conjugated. Similar expressions can be written for the non-diagonalized equations. Once assigned a set of initial conditions  $\vec{Y}(t_0)$  to the system, the time history of the response is determined by using eq.(2.98) and (2.51):

$$\vec{Y}(t) = \Theta_Y(t - t_0) \cdot \vec{Y}(t_0) + \int_{t_0}^t \Theta_Y(t - s) \mathbf{A}^{-1} \cdot \vec{Q}(s) ds \quad (2.105)$$

The mean and covariance matrix is given by the substitution of them in (2.105):

$$\vec{Y}(t) = \Theta_Y(t - t_0) \cdot \vec{Y}(t_0) + \int_{t_0}^t \Theta_Y(t - s) \mathbf{A}^{-1} \cdot \vec{\mu}_Q(s) ds \quad (2.106)$$

$$\begin{aligned} \mathbf{K}_{YY}(t, s) &= \Theta_Y(t - t_0) \cdot \mathbf{K}_{YY}(t_0, t_0) \cdot \Theta_Y(s - t_0) + \\ &+ \int_{t_0}^t \int_{t_0}^t \Theta_Y(t - u) \mathbf{A}^{-1} \cdot \mathbf{K}_{QQ}(u, v) \cdot (\mathbf{A}^{-1})^T \Theta_Y(s - v) du dv \end{aligned} \quad (2.107)$$

and also a conditioned mean and covariance as in eq.(2.13) and (2.14) can be obtained:

$$\begin{aligned} E[Y(t) | Y(t_0) = \vec{w}] &= \Theta_Y(t - t_0) \cdot \vec{w} + \\ &+ \int_{t_0}^t \Theta_Y(t - s) \mathbf{A}^{-1} \cdot E[Q(s) | Y(t_0) = \vec{w}] ds \end{aligned} \quad (2.108)$$

and

$$\begin{aligned} \mathbf{K}[\vec{Y}(t) \vec{Y}(t_0) | Y(t_0) = \vec{w}] &= \\ = \int_{t_0}^t \int_{t_0}^t \Theta_Y(t - u) \mathbf{A}^{-1} \cdot \mathbf{K}[\vec{Q}(u), \vec{Q}(v) | Y(t_0) = \vec{w}] \cdot (\mathbf{A}^{-1})^T \Theta_Y(s - v) du dv \end{aligned} \quad (2.109)$$

It is also possible to specify this expressions for delta correlated excitations[40].

## 2.2.6 Direct stochastic analysis of linear systems

A more straightforward approach for the solution of the equations of motion is based on the direct derivation of deterministic differential equations involving the statistical properties of the system[40]. The big advantage of this method is that it does not introduce any hypothesis about the linearity at the beginning and so can be extended also to non-linear problems. However, for this thesis only the linear case is considered, assuming the design limits in linear field.

### Derivation of state space moments equations

Considering  $X(t)$  as the response of a generic linear system excited by a stochastic process  $F(t)$ , the equation of motion can be written in differential form as[40]:

$$\sum_{j=0}^n a_j \frac{d^j X(t)}{dt^j} = F(t) \quad (2.110)$$

Multiplying both the terms for  $X^k$  and averaging them gives:

$$\sum_{j=0}^n a_j \cdot E \left[ X^k(t) \cdot \frac{d^j X(t)}{dt^j} \right] = E[X^k(t) \cdot F(t)] \quad (2.111)$$

The obtained formulation is the moment equation in terms of cross products. This is only a possible form and other formulations can be obtained from (2.110). At different times:

$$\sum_{j=0}^n a_j \cdot E \left[ X^k(s) \cdot \frac{d^j X(t)}{dt^j} \right] = E[X^k(s) \cdot F(t)] \quad (2.112)$$

with the time derivative of  $X^k(t)$ :

$$\sum_{j=0}^n a_j \cdot E \left[ \dot{X}^k(t) \frac{d^j X(t)}{dt^j} \right] = E[\dot{X}^k \cdot F(t)] \quad (2.113)$$

with the product for  $F(t)$ :

$$\sum_{j=0}^n a_j \cdot E \left[ F^k(t) \cdot \frac{d^j X(t)}{dt^j} \right] = E[F^{k+1}(t)] \quad (2.114)$$

Similar expressions can be derived for the cumulants of the system, more details can be found on Muscolino[46] and Lutes & Sarkani[40]. By the state-space formulation of the equations of motion in (2.84) the analysis can be performed without any restrictive hypothesis about the shape of the damping matrix  $\mathbf{c}$  or the linearity of the response; this makes the direct stochastic analysis a powerful instrument for the study of random vibrations.

### Equations for first and second Moments and Covariance

A possible and widely used approach in the analysis is to derive the first and second order moments equations without doing any consideration about the distributions. The big advantage of this approach can be seen for the Gaussian processes that are completely determined by their first and second order moments. Considering that many processes can be modelled as Gaussian or nearly Gaussian, the direct stochastic integration can be applied with success in many cases.

The partial description of the response aims also to limit the computational effort and can be combined with the theory of filters exposed in sec.2.3 to obtain significant results.

To analyse the mean, both members of (2.84) are averaged, obtaining the following equation:

$$\mathbf{A} \vec{\mu}_Y(t) + \mathbf{B} \vec{\mu}_Y(t) = \vec{\mu}_Q(t) \quad (2.115)$$

The second order moments of the state variables are obtained by substituting in eq.(2.84) the term  $\Phi_{YY}(t, t) = E[\vec{Y}(t) \cdot \vec{Y}^T(t)]$  and calculate the derivatives respect to the time:

$$\frac{d}{dt} \Phi_{YY}(t, t) = E[\dot{\vec{Y}}(t) \cdot \vec{Y}^T(t)] + E[\vec{Y}(t) \cdot \dot{\vec{Y}}^T(t)] \quad (2.116)$$

The first term on the right hand side of this equation is obtained by multiplying both terms of eq.(2.84) for  $\vec{Y}^T(t)$  on the right and for  $\mathbf{A}^{-1}$  on the left, then, the expected value is calculated:

$$E[\dot{\vec{Y}}(t) \cdot \vec{Y}^T(t)] + \mathbf{D} \cdot \Phi_{YY}(t, t) = \mathbf{A}^{-1} E[\vec{Q}(t) \cdot \vec{Y}^T(t)] = \mathbf{A}^{-1} \Phi_{QY}(t, t) \quad (2.117)$$

Calculating the transpose of eq.(2.117), remembering that  $\Phi_{YY}(t, t)$  is symmetric, i.e.  $\Phi_{YY}(t, t) = \Phi_{YY}^T(t, t)$ , it becomes:

$$E[\vec{Y}(t) \cdot \dot{\vec{Y}}^T(t)] + \Phi_{YY}(t, t) \cdot \mathbf{D}^T = E[\vec{Y}(t) \cdot \vec{Q}^T(t)] (\mathbf{A}^{-1})^T = \Phi_{YQ}(t, t) (\mathbf{A}^{-1})^T \quad (2.118)$$

The final obtained equation is[40]:

$$\frac{d}{dt}\Phi_{YY}(t,t) + \mathbf{D} \cdot \Phi_{YY}(t,t) + \Phi_{YY}(t,t) \cdot \mathbf{D}^T = \mathbf{A}^{-1}\Phi_{QY}(t,t) + \Phi_{YQ}(t,t) (\mathbf{A}^{-1})^T \quad (2.119)$$

This equation takes commonly the name of *Lyapunov equation* and is widely used in the direct stochastic analysis. In (2.119) the matrices are symmetric, therefore, indicating with  $n_Y$  the state space vector components, the total number of scalar equations are  $n_Y \cdot (n_Y + 1)/2$  instead of  $n_Y^2$  and the system is determined. One equation of the system has the following form:

$$\begin{aligned} \frac{d}{dt}E[Y_j(t) \cdot Y_l(t)] + \sum_{r=1}^{n_Y} \sum_{s=1}^{n_Y} A_{jr}^{-1} B_{rs} \cdot E[Y_s(t) \cdot Y_l(t)] + \sum_{r=1}^{n_Y} \sum_{s=1}^{n_Y} E[Y_j(t) \cdot Y_r(t)] \cdot B_{rs} A_{ls}^{-1} = \\ \sum_{r=1}^{n_Y} A_{jr}^{-1} \cdot E[Q_r(t) \cdot Y_l(t)] + \sum_{r=1}^{n_Y} E[Y_l(t) \cdot Q_r(t)] \cdot A_{lr}^{-1} \end{aligned} \quad (2.120)$$

The moments obtained in this way take the name of *non-geometric spectral moments* in contrast with the methods exposed in sec.1.6.6.

### Simplifications for mean zero, delta-correlated process

The use of a delta-correlated input, combined with a proper filter, is a frequently used method to solve many dynamic problems by keeping a low complexity level. In the general case, without stationarity hypothesis, eq.(1.132) has to be slightly modified to get the variance of the excitation:

$$\mathbf{K}_{QQ}(t,s) = 2\pi \mathbf{S}_0 \cdot \delta(t-s) \quad (2.121)$$

where  $\mathbf{S}_0$  is the non-stationary auto-spectral density matrix for the external excitation  $\vec{Q}(t)$ . The mean square  $\Phi_{QQ}(t,t)$  is substituted by the variance  $\mathbf{K}_{QQ}(t,s)$  because for mean zero processes they are equivalent. The right hand side term of eq.(2.119) is simplified. Assuming for  $t_0 < t$ :

$$\vec{Y}(t) = \vec{Y}(t_0) + \int_{t_0}^t \vec{Y}(u) du \quad (2.122)$$

and solving eq.(2.84) for  $\vec{Y}$  gives:

$$\vec{Y}(t) = \vec{Y}(t_0) + \mathbf{A}^{-1} \int_{t_0}^t \vec{Q}(u) du - \mathbf{D} \int_{t_0}^t \vec{Y}(u) du \quad (2.123)$$

Transposing the equation and putting it into  $\mathbf{K}_{QY}(t,t)$  leads to:

$$\mathbf{K}_{QY}(t,t) = \mathbf{K}_{QY}(t,t_0) + \int_{t_0}^t \mathbf{K}_{QQ}(t,u) du (\mathbf{A}^{-1})^T - \int_{t_0}^t \mathbf{K}_{QY}(t,u) du \mathbf{D}^T \quad (2.124)$$

If the process is delta-correlated,  $\vec{Q}(t)$  is independent from  $\vec{Q}(u)$  for  $u < t$ . In the same way,  $\vec{Q}(t)$  is independent from  $\vec{Y}(t_0)$  for  $t > t_0$ ; in fact,  $\vec{Y}(t_0)$  is caused by an excitation at  $t_0$  from which  $\vec{Q}(t)$  is independent. Thus,  $\mathbf{K}_{QY}(t,t_0) = 0$ . Moreover:

$$\int_{t_0}^t \mathbf{K}_{QY}(t,u) du = \int_{T-\Delta t}^t \mathbf{K}_{QY}(t,u) du \quad (2.125)$$

where the time increment  $\Delta t$  can be taken as arbitrarily small. If  $\mathbf{K}_{QY}$  is finite, then the integral is of a finite quantity over an infinitesimal interval and is nil. Eq.(2.124) becomes:

$$\mathbf{K}_{QY}(t,t) = \int_{t_0}^t \mathbf{K}_{QQ}(t,u) du (\mathbf{A}^{-1})^T \quad (2.126)$$

Substituting the Dirac's delta function auto-covariance of eq.(2.121) in eq.(2.126) gives:

$$\int_{t_0}^t \mathbf{K}_{QQ}(t, u) du = 2\pi \int_{t_0}^s \mathbf{S}_0(t) \cdot \delta(t - u) du = 2\pi \mathbf{S}_0(t) \cdot U(s - t) \quad (2.127)$$

where  $U(s - t)$  is the unit step function of eq.(1.20). For  $s < t$  this integral is zero and for  $t > s$  is  $2\pi \mathbf{S}_0(t)$ <sup>1</sup>. The cross covariance is:

$$\mathbf{K}_{QY}(t, t) = \int_{t_0}^t \mathbf{K}_{QQ}(t, u) du (\mathbf{A}^{-1})^T \quad (2.128)$$

and its transpose:

$$\mathbf{K}_{YQ}(t, t) = \mathbf{A}^{-1} \int_{t_0}^t \mathbf{K}_{QQ}(u, t) du \quad (2.129)$$

By putting it in (2.119), the Lyapunov equation becomes:

$$\begin{aligned} \frac{d}{dt} \mathbf{K}_{YY}(t, t) + \mathbf{D} \cdot \mathbf{K}_{YY}(t, t) + \mathbf{K}_{YY}(t, t) \cdot \mathbf{D}^T = \\ = \mathbf{A}^{-1} \left( \int_{t_0}^t \mathbf{K}_{QQ}(t, u) du + \int_{t_0}^t \mathbf{K}_{QQ}(u, t) du \right) (\mathbf{A}^{-1})^T \end{aligned} \quad (2.130)$$

The right-hand side of eq.(2.130) can be rewritten in the Dirac's delta form of the auto-covariance in eq.(2.121):

$$\int_{t_0}^t \int_{t_0}^t \mathbf{K}_{QQ}(u, v) du dv = 2\pi \int_{t_0}^t \mathbf{S}_0(v) \cdot U(t - v) dv = 2\pi \int_{t_0}^t \mathbf{S}_0(v) dv, \quad \text{for } t_0 < t \quad (2.131)$$

The derivative of both sides respect to  $t$  is:

$$\int_{t_0}^t \mathbf{K}_{QQ}(t, v) dv + \int_{t_0}^t \mathbf{K}_{QQ}(u, t) du = 2\pi \mathbf{S}_0(t) \quad (2.132)$$

The right hand side of this equation can be substituted to the left hand of eq.(2.130). Therefore, the final equation of Lyapunov for the delta-correlated excitation  $\vec{Q}(t)$ , with non stationary auto-spectral density matrix  $\mathbf{S}_0(t)$ , is:

$$\frac{d}{dt} \mathbf{K}_{YY}(t, t) + \mathbf{D} \cdot \mathbf{K}_{YY}(t, t) + \mathbf{K}_{YY}(t, t) \cdot \mathbf{D}^T = 2\pi \mathbf{A}^{-1} \mathbf{S}_0(t) (\mathbf{A}^{-1})^T \quad (2.133)$$

This equation allows to get, by only algebraic calculations, the solution of the state space equation. To do that, a Schur decomposition[66] or the Kronecker tensor product can be used.

Given two matrices  $\mathbf{A}$  and  $\mathbf{B}$  of order, respectively,  $(p \times q)$  and  $(s \times t)$ , the *Kronecker tensor product* of  $\mathbf{A}$  for  $\mathbf{B}$  is indicated as  $\mathbf{A} \otimes \mathbf{B}$  and is a matrix of order  $(ps \times qt)$ , obtained by the multiplication of each element  $a_{ij}$  of  $\mathbf{A}$  for the entire matrix  $\mathbf{B}$ :

$$\mathbf{A} \otimes \mathbf{B} = \begin{bmatrix} a_{11} \mathbf{B} & a_{12} \mathbf{B} & \dots & a_{1q} \mathbf{B} \\ a_{21} \mathbf{B} & a_{22} \mathbf{B} & \dots & a_{2q} \mathbf{B} \\ \dots & \dots & \dots & \dots \\ a_{p1} \mathbf{B} & a_{p2} \mathbf{B} & \dots & a_{pq} \mathbf{B} \end{bmatrix} \quad (2.134)$$

<sup>1</sup>The value for  $s = t$  is more delicate to be treated, more details can be found on Lutes & Sarkani[40]

Muscolino[46] presents different properties of the Kronecker tensor product with a detailed exposition of the Kronecker's algebra. For this thesis, only this definition will be used.

It is possible to demonstrate that eq.(2.133) can be written in explicit form by defining[46]:

$$\mathbf{D}_2 = \mathbf{D}_n \otimes \mathbf{I}_n + \mathbf{I}_n \otimes \mathbf{D}_n \quad (2.135)$$

$$\mathbf{f}_2(t) = 2\pi S_0 \varphi^2(t) \cdot (\vec{v} \otimes \vec{v}) \quad (2.136)$$

where  $n$  indicates the number of nodal degrees of freedom,  $\varphi(t)$  is a modulating function that expresses the time variation of the delta-correlated process and  $\vec{v}$  is a vector that indicates the influence of the white noise excitation on the components of the second order moments  $\vec{m}_{2,Y}$ . The explicit Lyapunov equation can be written as:

$$\dot{\vec{m}}_{2,Y}(t) = \mathbf{D}_2 \cdot \vec{m}_{2,Y} + \mathbf{f}_2(t) \quad (2.137)$$

In the special case of stationary white noise,  $\dot{\vec{m}}_{2,Y}(t) = \vec{0}$  and  $\varphi(t) = 1$ , giving:

$$\vec{m}_{2,Y}(t) = -\mathbf{D}_2^{-1} \mathbf{f}_2 \quad (2.138)$$

The results are ordered in a  $(2 \cdot n)^2 \times 1$  vector, where  $n$  is the number of degrees of freedom:

$$\begin{aligned} \vec{m}_{2,Y}(t) = [ & m_{2,Y}^{X_1,X_1}, m_{2,Y}^{X_1,X_2}, \dots, m_{2,Y}^{X_1,X_n}, m_{2,Y}^{X_1,\dot{X}_1}, m_{2,Y}^{X_1,\dot{X}_2}, \dots, \dots, m_{2,Y}^{X_1,\dot{X}_n}, \\ & m_{2,Y}^{X_2,X_1}, m_{2,Y}^{X_2,X_2}, \dots, m_{2,Y}^{X_2,X_n}, m_{2,Y}^{X_2,\dot{X}_1}, m_{2,Y}^{X_2,\dot{X}_2}, \dots, \dots, m_{2,Y}^{X_2,\dot{X}_n}, \\ & m_{2,Y}^{X_n,X_1}, m_{2,Y}^{X_n,X_2}, \dots, m_{2,Y}^{X_n,X_n}, m_{2,Y}^{X_n,\dot{X}_1}, m_{2,Y}^{X_n,\dot{X}_2}, \dots, \dots, m_{2,Y}^{X_n,\dot{X}_n}, \dots \\ & m_{2,Y}^{\dot{X}_1,X_1}, m_{2,Y}^{\dot{X}_1,X_2}, \dots, m_{2,Y}^{\dot{X}_1,X_n}, m_{2,Y}^{\dot{X}_1,\dot{X}_1}, m_{2,Y}^{\dot{X}_1,\dot{X}_2}, \dots, \dots, m_{2,Y}^{\dot{X}_1,\dot{X}_n}, \\ & m_{2,Y}^{\dot{X}_2,X_1}, m_{2,Y}^{\dot{X}_2,X_2}, \dots, m_{2,Y}^{\dot{X}_2,X_n}, m_{2,Y}^{\dot{X}_2,\dot{X}_1}, m_{2,Y}^{\dot{X}_2,\dot{X}_2}, \dots, \dots, m_{2,Y}^{\dot{X}_2,\dot{X}_n}, \dots \\ & m_{2,Y}^{\dot{X}_n,X_1}, m_{2,Y}^{\dot{X}_n,X_2}, \dots, m_{2,Y}^{\dot{X}_n,X_n}, m_{2,Y}^{\dot{X}_n,\dot{X}_1}, m_{2,Y}^{\dot{X}_n,\dot{X}_2}, \dots, \dots, m_{2,Y}^{\dot{X}_n,\dot{X}_n}]^T \end{aligned} \quad (2.139)$$

### Non geometric odds spectral moments by direct stochastic integration

The odds spectral moments cannot be easily obtained as the even ones because the product  $E[\vec{Y}(t) \cdot \vec{Y}(t)]$  gives always an even power of the averaged terms. To avoid this, it is necessary to introduce the *Hilbert transform* of the white noise input in order to create a phase shift in the averaged terms  $E[\vec{Y}(t) \cdot \vec{\tilde{Y}}(t)]$ . Despite some mathematical delicate aspects[46], the Hilbert transform can be generally expressed as follow:

$$\tilde{a} = \text{Hilb} [a(t)] = \frac{1}{\pi} \int_{-\infty}^{+\infty} \frac{a(\rho)}{t - \rho} d\rho \quad (2.140)$$

this operation produces a time shift of the variable that becomes out of phase to its original form. By applying the Hilbert transform to eq.(2.92), the expression becomes:

$$\vec{\tilde{Y}}(t) = \int_{-\infty}^t \Theta(t-s) \mathbf{A}^{-1} \vec{Q}(s) ds \quad (2.141)$$

That, in the special case of delta-correlated process of (2.93), is:

$$\vec{\tilde{Y}}(t) = \int_{-\infty}^t \Theta(t-s) \mathbf{A}^{-1} \vec{v} \cdot \tilde{W}(s) ds \quad (2.142)$$

Applying this expression to the second order moments equation means:

$$\frac{d}{dt} E[\vec{Y}(t) \cdot \vec{Y}^T(t)] = E[\vec{Y}(t) \cdot \vec{Y}^T(t)] + E[\vec{Y}(t) \cdot \dot{\vec{Y}}^T(t)] \quad (2.143)$$

Starting from the state space equation (2.84) rewritten as:

$$\dot{\vec{Y}}(t) = \mathbf{D} + \vec{v} \cdot W(t) \quad (2.144)$$

and applying the solution to the state space problem in (2.93) for both  $\vec{Y}(t)$  and  $\vec{Y}(t)$  gives respectively:

$$\vec{Y}(t) = \int_{-\infty}^t \Theta_Y(t-s) \cdot \mathbf{A}^{-1} \cdot \vec{v} \cdot W(s) ds \quad (2.145)$$

$$\vec{Y}(t) = \int_{-\infty}^t \Theta_Y(t-s) \cdot \mathbf{A}^{-1} \cdot \vec{v} \cdot \tilde{W}(s) ds \quad (2.146)$$

Substituting the two equations in eq.(2.143) leads to the final form:

$$\begin{aligned} \frac{d}{dt} E[\vec{Y}(t) \cdot \vec{Y}^T(t)] &= \mathbf{D} \cdot E[\vec{Y}(t) \cdot \vec{Y}^T(t)] + E[\vec{Y}(t) \cdot \vec{Y}^T(t)] \cdot \mathbf{D}^T + \\ &+ \vec{v} \cdot E[W(t) \cdot \vec{Y}^T(t)] + E[\vec{Y}^T(t) \cdot \tilde{W}(t)] \cdot \vec{v}^T \end{aligned} \quad (2.147)$$

Eq.(2.147) is a generalization of the Lyapunov equation for the case of time shifted input by the Hilbert transform. The mixed terms  $E[W(t) \cdot \vec{Y}^T(t)]$  and  $E[\vec{Y}^T(t) \cdot \tilde{W}(t)]$  can be further developed as:

$$\begin{aligned} E[W(s) \cdot \vec{Y}^T(t)] &= E\left[\int_{-\infty}^t \Theta_Y(t) \cdot \mathbf{A}^{-1} \cdot \vec{v} \cdot W(t) \cdot \tilde{W}(s) ds\right] = \\ &= \int_{-\infty}^t \Theta_Y(t) \cdot \mathbf{A}^{-1} \cdot \vec{v} \cdot E[W(t) \cdot \tilde{W}(s)] ds = \\ &= \int_{-\infty}^t \Theta_Y(t) \cdot \mathbf{A}^{-1} \cdot \vec{v} \cdot R_{W\tilde{W}} ds \end{aligned} \quad (2.148)$$

and:

$$\begin{aligned} E[\vec{Y}^T(t) \cdot \tilde{W}(s)] &= E\left[\int_{-\infty}^t (\mathbf{A}^{-1})^T \cdot \Theta_Y^T(t) \cdot \vec{v} \cdot \tilde{W}(t) \cdot W(s) ds\right] = \\ &= \int_{-\infty}^t (\mathbf{A}^{-1})^T \cdot \Theta_Y^T(t) \cdot \vec{v} \cdot E[\tilde{W}(t) \cdot W(s)] ds = \\ &= \int_{-\infty}^t \Theta_Y(t) \cdot \mathbf{A}^{-1} \cdot \vec{v} \cdot R_{\tilde{W}W} ds \end{aligned} \quad (2.149)$$

The matrices of covariance of the white noise multiplied for their Hilbert transform have been determined by Caddemi and Muscolino[9] as:

$$R_{W\tilde{W}}(\tau) = -R_{\tilde{W}W} = \frac{2S_0}{t-s} = \frac{2S_0}{\tau} \quad (2.150)$$

Consequently, the (2.148) and (2.149) reduce to:

$$E[W(s) \cdot \vec{Y}^T(t)] = \int_{-\infty}^t \Theta_Y(t-s) \cdot \mathbf{A}^{-1} \cdot \vec{v} \cdot \left(\frac{2S_0}{t-s}\right) ds \quad (2.151)$$

and:

$$E[\vec{Y}^T(t) \cdot \vec{W}(s)] = \int_{-\infty}^t \Theta_Y(t-s) \cdot \mathbf{A}^{-1} \cdot \vec{v} \cdot \left( -\frac{2S_0}{t-s} \right) ds \quad (2.152)$$

These two forms, for the elision between the negative signs in the transfer matrix and in the second term, are equivalent. The obtained integral is not a convolution because there is not a time shift between the transfer matrix and the input force. The Lyapunov equation so defined can be however solved for the stationary case according to eq.(2.138), changing the definition of  $\mathbf{f}_2$ . The term  $\mathbf{f}_{img}$  is introduced as:

$$\mathbf{f}_{img}(t) = \int_{-\infty}^t (\vec{v} \otimes \mathbf{I}_n - \mathbf{I}_n \otimes \vec{v}) \Theta_Y(t) \cdot \mathbf{A}^{-1} \cdot \vec{v} \cdot \left( -\frac{2S_0}{t-s} \right) ds \quad (2.153)$$

where  $\mathbf{I}_n$  is a square identity matrix of size  $(n \times n)$ , where  $n$  is the number of nodal degrees of freedom. The Kronecker's products have to be solved before the integration to do not have divergent solutions. The final exciting term is:

$$\mathbf{f}_2(t) = 2\pi S_0 \varphi^2(t) \cdot (\vec{v} \otimes \vec{v}) + i \cdot \mathbf{f}_{img}(t) \quad (2.154)$$

where  $i$  is the imaginary unit. The obtained solution will be in the form of eq.(2.139), where the imaginary terms correspond to the odd spectral moments while the real ones correspond to the even spectral moments.

The calculation of the term  $\mathbf{f}_{img}(t)$  implies the major difficulties in the analysis. In fact, the transition matrix can be written in closed form only for the ordinary damped case in MDF systems (after performing a modal decomposition)[46]. Proceeding in this way, an analytic integration is possible to get the term  $\mathbf{f}_{img}(t)$  from eq.(2.154) and the odd spectral moments are obtained directly. For the not ordinary damped case the construction of the transition matrix requires a first ordinary modal analysis followed by a second complex one using the diagonalized matrices to get the final form of the transition matrix[46].

Being modal decomposition of overdamped system numerically difficult to be solved, Muscolino proposed an approximate numerical solution that corrects the classic damping transfer matrix along the integration domain at every step of integration. Unfortunately, this numerical approach is based on the assumption of a convolution between transfer matrix and external force, which is not the case of the integral that defines the imaginary part of spectral moments. A closed solution for the filtered, not classically damped case to the non-geometric spectral moments has not be found by the author for the actual state of art.

## 2.3 Theory of filters

All the presented methods are very effective if applied to delta-correlated excitations, otherwise, the formulations become quite complex and difficult to be handled numerically. Obviously, the delta-correlated process does not suit all the real existing actions and a way to describe them has to be found. To do that, one or more filters are used to transform the white noise input in a more realistic excitation. The big advantage of a filter approach to the study of random vibrations is that it aims both to keep a low level of complexity in the calculations (maintaining the white noise input) and to model a wide range of possible external actions (by properly defining the filter). An essential explanation of the theory is reported by Muscolino[46], from which the elements useful for this thesis are taken.

A filter is a set of differential equations of the type:

$$L[X(t)] = F(t) \quad (2.155)$$

The differential operator  $L[\bullet]$  describes the properties of the filter,  $X(t)$  is called *output* and  $F(t)$  *input*. The aim is to solve the differential equation to get  $X(t)$  by the reverse of (2.155):

$$X(t) = L^{-1}[F(t)] \quad (2.156)$$

The operation of eq.(2.156) is called *filtering* and the physical system crossed by the signal is the *filter*. The number of differential equations involved in the filtering defines the *order of the filter*, for example a set of two differential equations defines a second order filter.

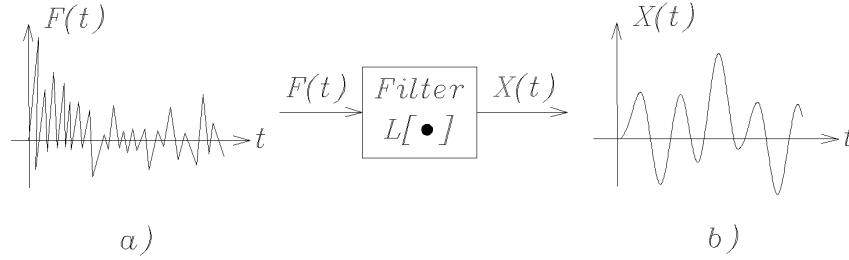


Figure 2.2: Schematic representation of the filtering[46]: a) input signal, filter, b) output signal.

A filter is said to be linear if it is the combination of more linear input signals:

$$F(t) = \sum_{k=1}^r a_k \cdot F_k(t) \quad (2.157)$$

to which corresponds an output signal:

$$X(t) = L^{-1}[F(t)] = \sum_{k=1}^r a_k \cdot L^{-1}[F_k(t)] = \sum_{k=1}^r a_k \cdot X_k(t) \quad (2.158)$$

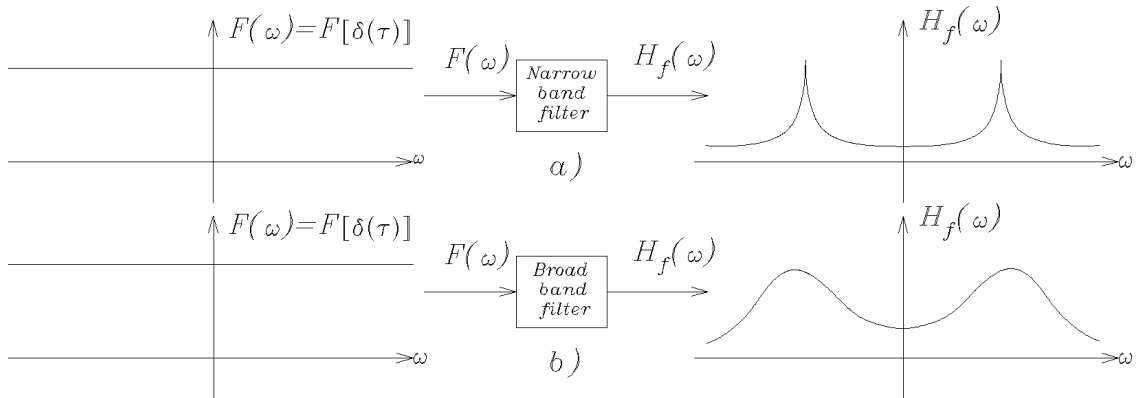


Figure 2.3: Schematic representation of the filtering operation[46]: a) Narrow band filter, b) Broad band filter.

The operator, for linear filter, is assumed of the type:

$$L[\bullet] = b_r(t) \frac{d^r}{dt^r} + \dots + b_2(t) \frac{d^2}{dt^2} + b_1(t) \frac{d}{dt} \quad (2.159)$$

If the filter is defined with constant coefficient, a representation of the filtering process in the frequency domain can be used:

$$X(\omega) = H_f(\omega) \cdot F(\omega) \quad (2.160)$$

$H_f(\omega)$  is the *filter transfer function* and is equal to the Fourier's transform of the filter output for a Dirac's delta function input:

$$H_f(\omega) = F(L^{-1}[\delta(t)]) \quad (2.161)$$

The filters are divided in broad band and narrow band depending on the magnified frequencies, in fig.2.3 an example is given.

There are different types of filter to better describe the real process in analysis. A first distinction is between:

- *mono correlated*: one input signal is spread between the different degrees of freedom of the final system;
- *multi correlated*: multiple input signals are linearly combined and enter in the filter. The latter can be furthermore distinguished in:
  - *mono varied*: just one modulating function  $\varphi(t)$  is used for all the entering signals;
  - *multi varied*: more modulating function  $\varphi(t)$  are used for each entering signal.

Thanks to the different options a wide set of natural actions can be modelled. For the goals of this study only mono correlated processes are considered, more details about the others can be found on Muscolino[46].

It is possible to modify the equation of order  $r$  of the mono-correlated, filtered, not stationary process to  $r$  equations of first order in a similar way to the state space analysis. The obtained equations are:

$$\begin{aligned} \vec{F}(t) &= \vec{a}^T(t) \cdot \vec{Z}_f(t) \\ \vec{Z}_f(t) &= \mathbf{D}_f(t) \cdot \vec{Z}_f(t) + \vec{v}_f \cdot \varphi(t) \cdot W(t) \end{aligned} \quad (2.162)$$

where  $\vec{a}(t)$ ,  $\vec{Z}_f(t)$  and  $\vec{v}_f$  are vectors of order  $(r \times 1)$  that characterize the filter,  $\mathbf{D}_f(t)$  is the system matrix of the filter of order  $(r \times r)$ ,  $\varphi(t)$  is a modulating deterministic function and  $W(t)$  a white noise, Gaussian signal with power spectrum  $S_0$ . The output of the filter is applied to the main system that in the state space is dynamically described as:

$$\vec{Y}(t) = \mathbf{D}_N \cdot \vec{Y}(t) + \vec{V}_N \cdot \vec{\tau} \cdot \vec{F}(t) \quad (2.163)$$

where:

$$\vec{Y}(t) = \begin{bmatrix} \vec{X}(t) \\ \vec{X}_f(t) \end{bmatrix}, \quad \mathbf{D}_N = \begin{bmatrix} \mathbf{0} & \mathbf{I}_n \\ -\mathbf{m}^{-1}\mathbf{k} & -\mathbf{m}^{-1}\mathbf{c} \end{bmatrix}, \quad \mathbf{V}_N(t) = \begin{bmatrix} \mathbf{0} \\ \mathbf{m}^{-1} \end{bmatrix} \quad (2.164)$$

Eq.(2.162) can be associated to eq.(2.163) to get a system of  $(2 \cdot n_{dof} + r)$  first order equations with the following form:

$$\vec{Y}(t) = \bar{\mathbf{D}}_N \cdot \vec{Y}(t) + \vec{v} \cdot \varphi(t) \cdot W(t) \quad (2.165)$$

with

$$\begin{aligned} \vec{Y}(t) &= \begin{bmatrix} \vec{Y}(t) \\ \vec{Z}_f(t) \end{bmatrix}, \quad \bar{\mathbf{D}}(t) = \begin{bmatrix} \mathbf{D}_N & \mathbf{D}_{Nf}(t) \\ \mathbf{0} & \mathbf{D}_f(t) \end{bmatrix} \\ \vec{v} &= \begin{bmatrix} \vec{0}_{2n} \\ \vec{v}_f \end{bmatrix}, \quad \mathbf{V}_N = \begin{bmatrix} \mathbf{0} \\ \mathbf{m}^{-1} \end{bmatrix}, \quad \mathbf{D}_{Nf}(t) = \mathbf{V}_N \cdot \vec{\tau} \cdot \vec{a}^T(t) \end{aligned} \quad (2.166)$$

A schematic representation of a mono correlated, mono varied, filter is given in fig.2.4, where  $k$  indicates the number of degrees of freedom. If necessary, it is also possible to diagonalize the state space equations and define a modal space version of the filtering process[46].

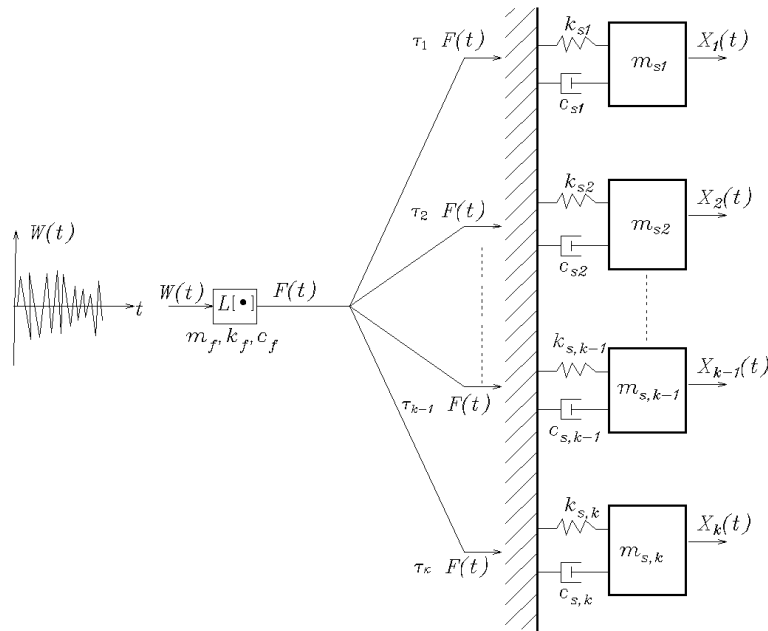


Figure 2.4: Filtering process for mono correlated, mono varied signal[46]

The filters aim to perform the study of a system by applying simple equations for the external forces (typically a white noise with mean zero and Gaussian distribution) to then filtering them to model properly the external actions. This leads to a huge simplification in the analysis and is the main reason for which different filters are constantly developed. It is interesting to see, from a different perspective, that the system itself constitutes a filter for the external forces that changes depending on the mechanical characteristics of the structure, with better or worse final effects depending on the cases.

## 2.4 Physical modelling of earthquakes

The physical modelling of the seismic action is a still debated problem and, despite the many studies performed, a definitive solution is still far to be determined. The effects that influence the measure of an history of acceleration are different and include: 1) the intensity of the earthquake (i.e. its magnitude), 2) the nature of the fracture in the hypocenter, 3) the path done by the seismic waves to reach the surface, 4) the physical and mechanical properties of the soils crossed, 5) the geotechnical properties of the soil on which the measure system is placed. Analytically, all this parameters determine the PSD of the seismic action adopted in the analysis.

The most commonly used spectrum for the seismic analysis are the *Fourier's spectrum* and the *response spectrum*[46]:

- The *Fourier's spectrum* is based on the analysis of the energy spectral density of the deterministic energetic content of the earthquake that is bound to its power spectral density (PSD). Assumed the hypothesis of  $\xi_0 = 0$  (no damping of the main system), by the PSD

of the excitation and the Duhamel integral, it is possible to calculate the response in terms of displacement, velocity and acceleration for different frequencies  $\omega_0$  and get the response spectrum for the specific earthquake. The main limit of the Fourier's spectrum is the assumption of nil damping that does not reflect the real behaviour of the structure. However, it is the only formulation that permits a full description of the seismic action although under simplified hypothesis.

- The *response spectrum* considers that the data of interest for the design are the maximum of the excitations rather than its full time history and proposes an easy formulation for their description. The maximum of the response, obtained by searching the max of the Duhamel's integral in the damped case, is plotted for different frequencies of the system  $\omega_0$  (or in terms of period  $T_0 = 2\pi/\omega_0$ ) once fixed the damping ratio  $\xi_0$ . Many considerations can be done about the spectrum defined in this way[46], the most interesting is that the spectrum of velocity for undamped system coincides, for the maximum values, with the Fourier's spectrum, showing that the response spectrum is connected to the energy content of the earthquake at the different frequencies.

### 2.4.1 Response and design spectrum

The first step in the definition of the response spectrum consists in the calculation of the maximum of displacement for a damped case by a Duhamel's integral. Assumed a SDF oscillator of natural frequency  $\omega_0$  and natural frequency  $\xi_0$ , subjected to an acceleration  $\ddot{x}_g$  along a time interval  $[0, t_f]$ , the maximum of response is:

$$\begin{aligned} x_{max}(t_f) &= \max |x(t)| = \max \left| \int_0^{t_f} h_x(t-s) \cdot \ddot{x}_g(s) ds \right| = \\ &= \max \left| \int_0^{t_f} \frac{e^{-\xi\omega_0(t-s)}}{m\omega_d} \sin[\omega_d(t-s)] ds \right|, \quad 0 \leq t \leq t_f \end{aligned} \quad (2.167)$$

Where  $\omega_d = \omega_0[1 - \xi^2]^{1/2}$  is the damped frequency. Analysing the expression, it is immediate that the maximum displacements depends both on the characteristics of the oscillator than on the ground acceleration applied. Therefore, for an assigned damping ratio and acceleration history, is defined a *response spectrum* that plots the maximum displacements over the period  $T_0$  (or the frequency  $\omega_0$ ):

$$S_s(\omega_0, \xi_0) \equiv S_s(T_0, \xi_0) = \max |x(t)|, \quad 0 \leq t \leq t_f \quad (2.168)$$

In a similar way, the response spectrum of velocity and absolute acceleration are defined:

$$S_v(\omega_0, \xi_0) \equiv S_v(T_0, \xi_0) = \max |\dot{x}(t)|, \quad 0 \leq t \leq t_f \quad (2.169)$$

The absolute acceleration is adopted because the inertial forces depend from the total value and not from the relative one:

$$S_a(\omega_0, \xi_0) \equiv S_a(T_0, \xi_0) = \max |\ddot{x}(t) + \ddot{x}_g(t)| \equiv \max |2\xi_0\omega_0 \cdot \dot{x}(t) + \omega_0^2 \cdot x(t)|, \quad 0 \leq t \leq t_f \quad (2.170)$$

Analysing the expressions leads to the following considerations:

- For  $\omega_0 \rightarrow \infty$  ( $T_0 \rightarrow 0$ ), the oscillator is infinitely rigid and the displacement, velocity and relative acceleration are nil, the structure follows the movements of the ground:

$$\begin{aligned} \lim_{T_0 \rightarrow 0} S_s(T_0, \xi_0) &= 0, & \lim_{T_0 \rightarrow 0} S_v(T_0, \xi_0) &= 0 \\ \lim_{T_0 \rightarrow 0} [\max |\ddot{x}(t)|] &= 0, & \lim_{T_0 \rightarrow 0} S_a(T_0, \xi_0) &= \ddot{x}_{g_0} \end{aligned} \quad (2.171)$$

where  $\ddot{x}_{g_0}$  indicates the *peak ground acceleration*, that is, the maximum value of the acceleration history at the ground level.

- For  $\omega_0 \rightarrow 0$  ( $T_0 \rightarrow \infty$ ), the oscillator is infinitely deformable and is not influenced by the movement of the ground:

$$\begin{aligned} \lim_{T_0 \rightarrow \infty} S_s(T_0, \xi_0) &= x_{g_0}, & \lim_{T_0 \rightarrow \infty} S_v(T_0, \xi_0) &= \dot{x}_{g_0} \\ \lim_{T_0 \rightarrow \infty} [\max |\ddot{x}(t)|] &= \ddot{x}_{g_0}, & \lim_{T_0 \rightarrow \infty} S_a(T_0, \xi_0) &= 0 \end{aligned} \quad (2.172)$$

where the terms  $x_{g_0}$ ,  $\dot{x}_{g_0}$  and  $\ddot{x}_{g_0}$  are the maximum values of the displacement, velocity and acceleration histories at the ground level; therefore, no inertial forces are transmitted.

Globally, these results are in accordance with the harmonic vibration determined in sec.1.2.1 and the frequency analysis done sec.2.1.3.

In the seismic engineering two other quantities are often used:

- the *pseudo-velocity spectrum*:

$$S_{pv} = (\omega_0, \xi_0) \equiv S_{pv}(T_0, \xi_0) = \omega_0 \cdot S_s(\omega_0, \xi_0) \equiv \frac{2\pi}{T_0} S_s(T_0, \xi_0) \quad (2.173)$$

The  $S_{pv}$ , differently from the  $S_v$ , tends to zero for  $\omega_0 \rightarrow 0$ ;

- the *pseudo-acceleration spectrum*:

$$S_{pa} = (\omega_0, \xi_0) \equiv S_{pa}(T_0, \xi_0) = \omega_0^2 \cdot S_s(\omega_0, \xi_0) \equiv \frac{4\pi^2}{T_0^2} S_s(T_0, \xi_0) \quad (2.174)$$

In ordinary damped structures the damping ratio  $\xi_0$  is negligible and the pseudo-acceleration is similar to the absolute acceleration spectrum:

$$S_a(\omega_0, \xi_0) \equiv \max |2\xi_0\omega_0 \cdot \dot{x}(t) + \omega_0^2 \cdot x(t)| \approx \max |\omega_0^2 \cdot x(t)| \equiv S_{pa} \quad (2.175)$$

These formulations are particularly useful because aim to calculate directly the displacements  $x(t)$  and then the elastic forces acting on the structure. Remembering the relation  $\omega_0 = k/m$ , the elastic forces are:

$$f_E(t) = -k \cdot x(t) = -m \cdot \omega_0^2 \cdot x(t) \quad (2.176)$$

Considering the (2.174), the maximum value of the elastic forces is:

$$\max |f_E(t)| = m \cdot \max |\omega_0^2 \cdot x(t)| = m \cdot S_{pa}(T_0, \xi_0), \quad 0 \leq t \leq t_f \quad (2.177)$$

where  $t_f$  is the duration of the event. Therefore, given a pseudo-acceleration spectrum and the participating mass of a modal shape, it is possible to get the global displacements associated to that mode and analyse the system. This pretty straightforward method relies on the assumption of negligible damping ratio, condition that is not satisfied in presence of external passive devices. In fig.2.5, the spectrum of acceleration and velocity are compared with the correspondent pseudo quantities for damping ratio  $\xi_0 = 0.05$  and acceleration histories: a) N-S El Centro (1940), b) S-E Taft (1952).

The response spectrum defined previously depends on the earthquake analysed, therefore, a method to give a possible expected seismic event for the zone has to be developed. The particular nature of the seismic event does not allow to determine the response spectrum of a future earthquake and statistic methods have to be used. The approach is to mediate and smooth the response spectra of many earthquakes and draw the *design elastic spectrum*. Seeds et al.[57] have

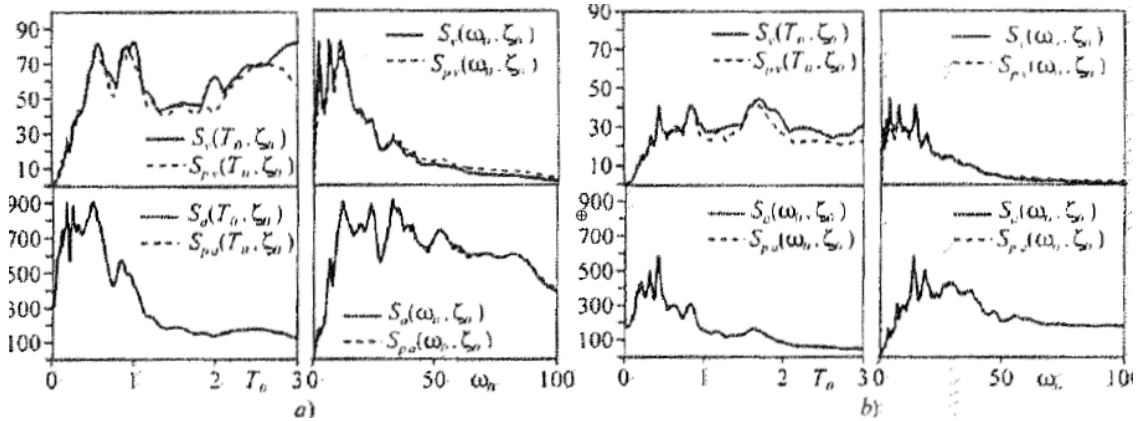


Figure 2.5: Comparison between  $S_a$ - $S_{pa}$  and  $S_v$ - $S_{pv}$  for damping ratio  $\xi_0 = 0.05$  and acceleration histories: a) N-S El Centro (1940), b) S-E Taft (1952)[46].

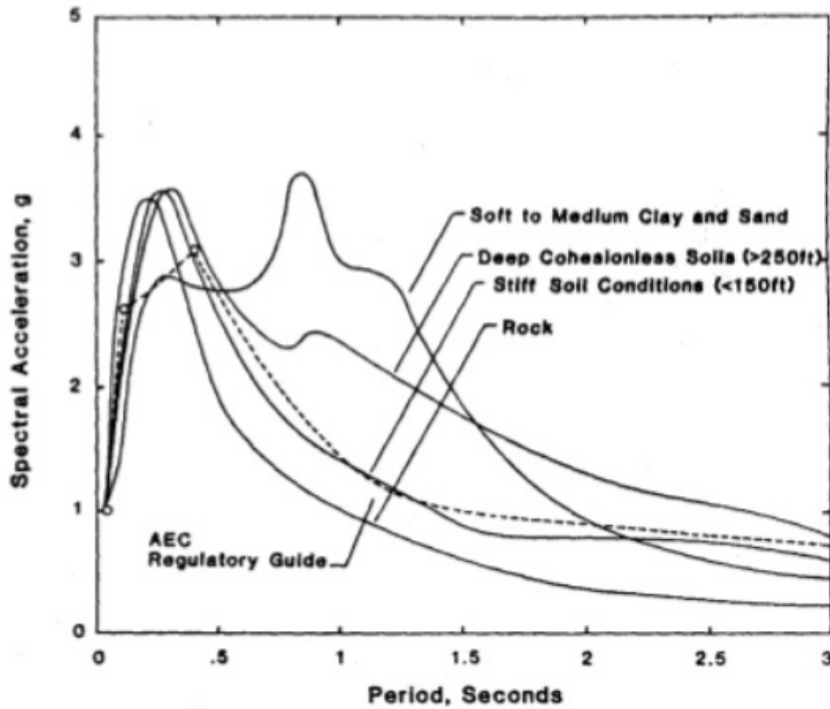


Figure 2.6: Average elastic response spectrum for different acceleration histories and different local conditions[57].

done this work for 104 different acceleration histories in different conditions, with the results of fig.2.6.

However, the average response spectrum shows all the limits connected to the brutal averaging of many events together. For this reason, many codes have introduced the use of *spectrum consistent* with the elastic response one. The idea is to bond the power spectrum, probabilistically analyzed, to the maximum of the average elastic response spectrum and draw a power spectral density graph usable for a probabilistic analysis[46].

## 2.4.2 Spectrum consistent with the design spectrum

In the majority of the codes is provided the possibility to use, instead of a design spectrum, a *consistent spectrum*, coherent with the latter. Recalling the process  $\{Y(T_s)\}$ , of maximums of the response  $\{X(t)\}$  along a time interval  $T_s$ :

$$\{Y(T_s)\} = \max\{|X(t)|\}, \quad 0 \leq t \leq T_s \quad (2.178)$$

The process can be seen as the inferior fractile  $p$  of the maximum absolute response peak to a mean zero, stationary process of a generic SDF damped oscillator:

$$X_{T_s,p}(T_0, \xi_0) = \zeta_X(T_s, p) \cdot \sigma_X \quad (2.179)$$

Where  $\zeta_X(T_s, p)$  is the peak factor, with probability  $p$ , in the time interval  $T_s$  of the maximums evaluation. The standard deviation of the displacement can be obtained by a frequency analysis of the PSD:

$$\sigma_X^2 = \int_{-\infty}^{+\infty} |H(\omega)|^2 S_{\ddot{X}_g}(\omega) d\omega = \int_0^{+\infty} |H(\omega)|^2 G_{\ddot{X}_g}(\omega) d\omega \quad (2.180)$$

where  $S_{\ddot{X}_g}(\omega)$  and  $G_{\ddot{X}_g}(\omega)$  are the PSD and unilateral PSD for the ground acceleration. The transfer function  $H^2(\omega)$  is the same of the SDF oscillator in eq.(2.35), except for the absence of the mass  $m$ , elided with the input  $m \cdot \ddot{X}_g$ :

$$H_x(\omega) = \frac{1}{(k + i\omega c - \omega^2 m)} = \frac{1}{(\omega_0^2 + 2i\xi_0\omega - \omega^2)} \quad (2.181)$$

To describe properly the PSD consistent with the design spectrum, it is necessary to define statistically the latter to extract the fractile of the peaks of interest. Being the design spectrum the averaging of different normalized response spectrum, it is reasonable to define  $S_s(\omega_0, \xi_0)$  as the mean value  $\mu_Y(T)$  of the maximum absolute peaks  $Y(T)$  of the process  $X(t)$  of unknown PSD. The following relation can be written:

$$S_s(\omega_0, \xi_0) \equiv S_s(T_0, \xi_0) = \mu_Y(T) \quad (2.182)$$

Assuming the approximation that the mean value of the non stationary process  $\{Y(T)\}$  of peaks of  $\{X(T)\}$  is approximatively the median  $X_{T,0.5}(T_0, \xi_0)$ , then, according to eq.(2.179), it is possible to write:

$$S_s(\omega_0, \xi_0) \equiv S_s(T_0, \xi_0) \approx X_{T,0.5}(T_0, \xi_0) = \zeta_X(T_s, p) \cdot \sigma_X \quad (2.183)$$

Similar values can be calculated for different fractiles  $p$ . In principle, the use of a Gaussian distribution for only positive values would be an error because, if the process of maximums  $\{Y(T)\}$  crosses the zero, biased values occur. However, assumed the peaks enough high so that the process would be always over the zero, the approximation seems acceptable.

The expression (2.183) gives directly a design spectrum once the PSD is given but the reverse process is not so straightforward. The PSD should be obtained from the peaks of the response process that depend from the PSD itself. An iterative method could be used, otherwise approximated formulations for independent or grouped up-crossings are available. The expression of Cacciola[46] gives a solution for the latter case:

$$G_{\ddot{X}_g}(\omega_0) = \frac{S_{pa}^2(\omega_0, \xi_0) - \zeta_X^2(T_s, 0.5) \int_0^{\omega_0} G_{\ddot{X}_g}(\omega) d\omega}{\omega_0 \cdot \zeta_X^2(T_s, 0.5) \left( \frac{\pi}{4\xi_0} - 1 \right)} \quad (2.184)$$

The peak factor can be approximately calculated as:

$$\zeta_X(T_s, 0.5) \approx \sqrt{2 \ln \left\{ 0.46 T_s \cdot \omega_0 \left[ 1 - \exp \left( -q^{1.2} \cdot \sqrt{\pi \ln(0.46 T_s \cdot \omega_0)} \right) \right] \right\}} \quad (2.185)$$

The calculation of the PSD has to be performed on a defined interval  $[0, \omega_S]$ , where  $\omega_S$  is a cut-off frequency depending on the energy content of the response at the higher frequencies. Practically,  $[0, \omega_S]$  is divided in  $m$  sub-intervals of amplitude  $\Delta\omega$ . The  $k^{th}$  value of the consistent PSD at the central frequency of the interval, i.e.  $\omega_k = \omega_i + (k - 0.5)\Delta\omega$ , is given by:

$$G_{\dot{X}_g}(\omega_k) = \frac{4\xi_0}{\omega_k \cdot \pi - 4\xi_0 \cdot \omega_{k-1}} \left( \frac{S_{pa}^2(\omega_0, \xi_0)}{\zeta_X^2(T_s, 0.5)} - \Delta\omega \sum_{j=1}^{k+1} G_{\dot{X}_g}(\omega_j) \right), \quad (k = 1, 2, \dots, m) \quad (2.186)$$

where  $\omega_i$  is the lower bound of the  $k^{th}$  interval of analysis for which the peak value is real. The expression gives the PSD at different frequencies once given the initial value  $G_{\dot{X}_g}(\omega)$ . The initial value is evaluated at  $\omega_i$ , considering nil the PSD in  $[0, \omega_i)$ . Of course, the smaller is the  $\Delta\omega$ , the more accurate is the integration. Once the PSD is given, the geometric spectral moments of response can be calculated according to what stated in sec.1.6.6 and the failure occurrence analysed. Another approach samples the PSD to generate a set of acceleration histories to be used for a statistic analysis[46]. To verify the consistency of the created acceleration histories, they have to be averaged to generate a new spectrum of acceleration that must not variate more than a value set according to the codes in order to be used.

### 2.4.3 Seismic acceleration as stationary, Gaussian, white, filtered random process

The theory of filters helps a lot in the definition of the seismic input action. Indeed, all the problem is reduced to adding a proper filter to the system that can model the earthquake. Unfortunately, the description of a proper filter is not simple and requires some simplifying assumption on the nature of the seismic action.

#### Seismic action as stationary process

The power spectral density characterizes completely a process only if it is Gaussian and stationary (otherwise, evolutive forms are necessary). Unfortunately, analysing some typical acceleration histories in fig.2.7, it is evident that the real nature of the seismic action is of a non-stationary mean zero process.

Despite this, a more accurate analysis of an acceleration history shows a *strong motion* phase of limited durance  $T_S$  in which the process may be approximated as stationary[46]. Husid[28] showed that, considering the ground acceleration  $\ddot{x}_g$ , it is possible to determine this time  $T_S$  by the function  $H(t)$ :

$$H(t) = \frac{\int_0^t \ddot{x}_g^2(t) dt}{\int_0^{t_f} \ddot{x}_g^2(t) dt}, \quad 0 \leq H(t) \leq 1 \quad (2.187)$$

where  $t_f$  is the total duration of the event and  $t$  a generic time instant along it.  $H(t)$  takes the name of *Husid's function*. For instance, the Husid function is plotted in fig.2.8 for the components: a) N-S of El Centro's earthquake (1940) and b) S-E of the Talt's earthquake (1952). The Husid function grows slowly at the beginning and end of the event, while increases quickly in the middle of it when the accelerations are bigger.

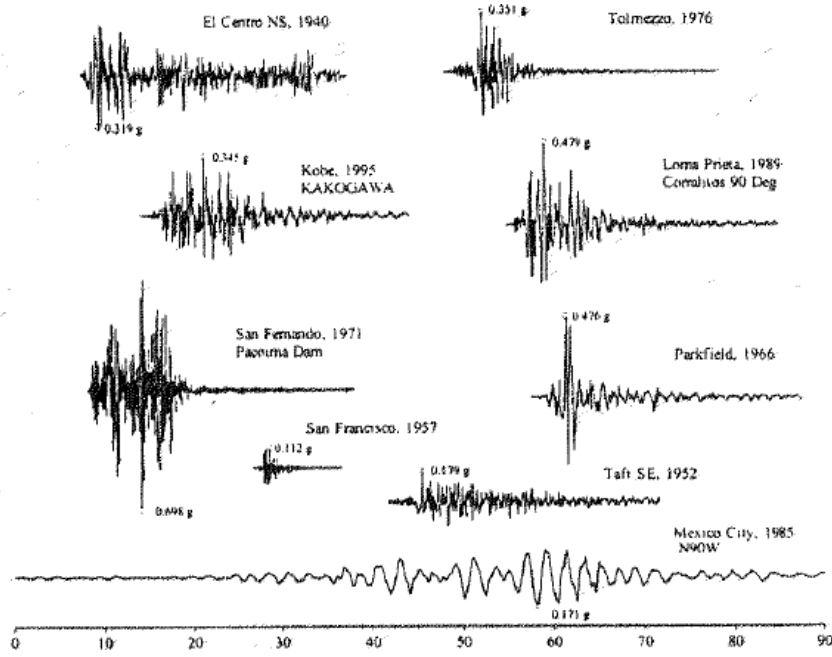


Figure 2.7: Acceleration histories in different sites with indication of the absolute peaks[46].

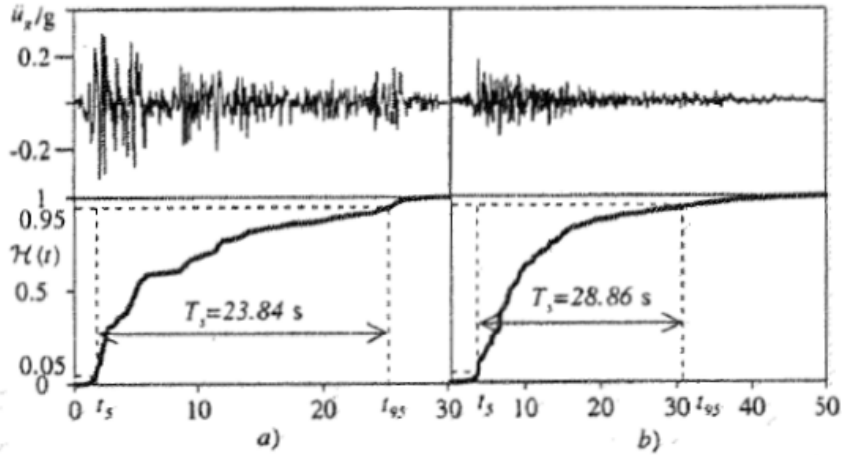


Figure 2.8: Acceleration histories and Husid function for the components: a) N-S of El Centro's earthquake (1940), b) S-E of the Talft's earthquake (1952)[46].

Considering this, the intermediate phase is generally defined as  $T_S = t_{95} - t_5$ , where the two times correspond to the instants in which the Husid function assumes the values 0.05 and 0.95 respectively.

If the time  $T_S$  is much bigger then the main period of the system ( $T_0 = 2\pi/\omega_0$ ), then, it is possible to consider the acceleration history and the response as mean zero stationary processes. Generally, the transient time of a SDF oscillator is considerable concluded after a time  $3/\xi_0\omega_0$ . Thus, if it is verified that:

$$T_S \gg \frac{3T_0}{2\pi\xi_0} \tag{2.188}$$

then, the transient phase ends before the strong motion phase  $T_S$  in which the acceleration process is assumed as stationary. The seismic process can be safely approximated as stationary and defined completely by a power spectral density function. However, the assumption of the seismic action as stationary remains a big approximation that in some specific cases shows even to be not conservative. Despite this, it aims to obtain some simple results to set a proper design.

### The Tajimi-Kanai filter

In the 1960 Tajimi, after the Kanai's studies in 1957, modelled the seismic acceleration process as a white filtered noise; assuming the equation of the filter as a SDF oscillator that schematizes the soil between the fault and the structure, while the white noise excitation is the acceleration at the hypocenter. The expression of the PSD of the ground acceleration takes the name of Tajimi-Kanai's spectral power density[59] and has the form:

$$S_{\ddot{X}_g} = \frac{(\omega_K^4 + \xi_K^2 \omega_K^2 \omega^2) S_0}{(\omega_K^2 - \omega^2)^2 + 4\xi_K^2 \omega_K^2 \omega^2} \equiv S_{TK}(\omega) \quad (2.189)$$

where  $S_0$  is the power spectrum of the white noise process and the lowercase  $K$  indicates the properties of the ground, while the others are the properties of the structure. For rigid grounds the values  $\omega_K = 4\pi \div 5\pi$  and  $\xi_K = 0.6$  are assumed. It is possible to relate the maximum acceleration peak of the ground to  $S_0$  by the following expression[8]:

$$S_0 = \frac{0.141 \xi_K \cdot \ddot{x}_{g0}^2}{\omega_K \sqrt{1 + 4\xi_K^2}} \quad (2.190)$$

By multiplying the (2.189) for  $1/\omega^2$  and  $1/\omega^4$  respectively, the PSD of velocity and acceleration of the ground motion are obtained.

Due to the fact that for  $\omega \rightarrow 0$  these PSD go to indefinite values, Clough and Penzien[13] proposed a modified version based on two consequential filters with parameters  $\omega_P, \xi_P$  and  $\omega_K, \xi_K$ :

$$S_{\ddot{X}_g} = S_{TK}(\omega) \cdot \frac{\omega^4}{(\omega_P^2 - \omega^2)^2 + 4\xi_P^2 \omega_P^2 \omega^2} \equiv S_{CP}(\omega) \quad (2.191)$$

where the parameters of the filters have to be determined experimentally by using registered acceleration histories. Despite the problem for low frequencies of the Tajimi-Kanai filter, the ordinary structures have main frequencies enough far from the zero and the filter has the main advantage of being able to describe the resonance between structure and seismic acceleration, differently from the Clough Penzien filter. This is due to the fact that it is described by only one oscillator of frequency  $\omega_K$  instead of the filter of Clough Penzien that requires a double filtering.

### Tajimi-Kanai filter in time domain

The expression in time domain of the Tajimi-Kanai filter is a second order filter with form[46]:

$$\begin{cases} \ddot{X}_g = -\omega_K^2 \cdot X_K(t) - 2\xi_K \omega_K \cdot \dot{X}_K(t) \\ \ddot{X}_K(t) + 2\xi_K \omega_K \cdot \dot{X}_K(t) + \omega_K^2 \cdot X_K(t) = -W(t) \end{cases} \quad (2.192)$$

The model considers an infinite mass oscillator as schematization of the ground, the SDF system is constrained over it and subjected to the motion transmitted. In the state space, the filter is described as follow:

$$\begin{cases} \dot{\vec{X}}_g(t) = \vec{a}_K^T \cdot \vec{Y}_K(t) \\ \dot{\vec{Y}}(t) = \mathbf{D}_K \cdot \vec{Y}_K(t) - \vec{V}_K \cdot W(t) \end{cases} \quad (2.193)$$

where

$$\vec{Y}(t) = \begin{bmatrix} \vec{X}(t) \\ \dot{\vec{X}}(t) \end{bmatrix}, \quad \mathbf{D}_K = \begin{bmatrix} 0 & 1 \\ -\omega_K^2 & -2\xi_K\omega_K \end{bmatrix}, \quad \vec{V}_K(t) = \begin{bmatrix} 0 \\ 1 \end{bmatrix}, \quad \vec{a}_K = \begin{bmatrix} -\omega_K^2 \\ -2\xi_K\omega_K \end{bmatrix} \quad (2.194)$$

In fig.2.9 a schematic representation of the filter is given.

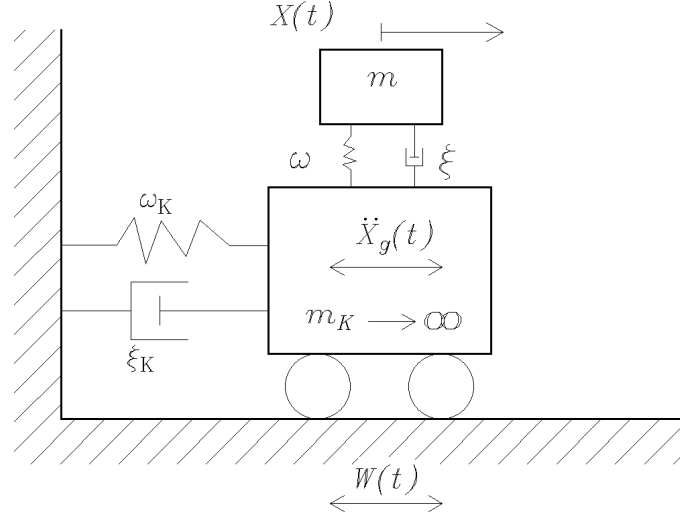


Figure 2.9: Tajimi-Kanai filter schematic representation[46].

#### 2.4.4 Non-stationary models of the seismic action

The seismic action should be modelled as non-stationary to have a correct description of its real behave, this implies that there are two elements to be modelled in addition:

- the variability in the amplitude of the seismic acceleration;
- the variability in the crossing rate of time.

If the first aspect can be easily modelled by a modulating function  $\varphi(t)$ , the second one is far more complex and requires the use of peculiar models. The modulation in amplitude of the process is obtained as:

$$\hat{\ddot{X}}_g^{(r)}(t) = \varphi(t) \cdot \ddot{X}_g^{(r)}(t) \quad (2.195)$$

where the term  $\ddot{X}_g^{(r)}(t)$  is the  $r^{th}$  sampled acceleration history from the defined PSD. Muscolino reports different forms of the modulating functions proposed to fit in the best way the measured accelerations during a real earthquake[46].

For the modulation in frequency, the solution is to model the seismic action as a filtered process with coefficients varying along time. For the Tajimi-Kanai filter for example:

$$\begin{cases} \ddot{X}_g(t) = \varphi(t) \cdot \vec{a}_K^T(t) \cdot \vec{Y}_K(t) \\ \vec{Y}(t) = \mathbf{D}_K(t) \cdot \vec{Y}_K(t) - \vec{V}_K \cdot W(t) \end{cases} \quad (2.196)$$

where:

$$\mathbf{D}_K = \begin{bmatrix} 0 & 1 \\ -\omega_K^2(t) & -2\xi_K\omega_K(t) \end{bmatrix} \quad (2.197)$$

The damping is supposed constant while the frequency of the state space matrix of the filter varies. There are different models for the time variation of the frequency that fit better the different seismic waves at their arrival time (primary, secondary and surface)[46]. The same approach is used if a PSD analysis is performed, varying along time the PSD parameters. For the Tajimi-Kanai filter the equation is:

$$S_{\ddot{x}_g}(t) = \frac{[\omega_K^4(t) + \xi_K^2 \omega_K^2(t) \omega^2] S_0}{[\omega_K^2(t) - \omega^2]^2 + 4\xi_K^2 \omega_K^2(t) \omega^2} \equiv S_{TK}(\omega) \quad (2.198)$$

## Chapter 3

# Optimization process

The constant improvements of materials and technologies in the last decades increased the possibilities that structures can reach and, together with that, the demand of efficient designs stretching their limits. Engineers today deal with a wide range of solutions and materials that come up every day and have to manage their implementation in new designs.

Despite this, the design approaches proposed by the codes are based on safety factors derived from the experience acquired on the field during time; a method that cannot keep up with the rapidly evolution of materials, IT and installation technologies. Moreover, from a sustainability point of view, the current approach shows its lacks in terms of costs, environmental impact and also aesthetic; especially out from the ordinary cases.

Many studies in the last years have focused on the research of better optimization systems, both reliable and robust, able to deal with safety and cost in a direct way. A big help in this process comes from IT technologies, that aim to manage the big amount of data required in this process. Thanks of them, the designer can focus on the inventive aspects while the computer covers the optimization of the possible solutions. This new field of study takes the name of computational design, a sector that uses the potential of IT to better perform in design.

However, if the flexibility of this approach aims to improve the performances, on the other hand it relies much more on the support of technology and requires hybrid specialist able to manage these algorithms to control the final results.

The optimization processes consist in the research of an optimum solution between all the possible ones that satisfy the design requirements, searching the minimum cost in terms of different parameters. Considering the nature of the optimization problem, computational design can be effectively applied to manage it. In structural design, there are some main requirements assumed typically: mechanical and functional efficiency, durability, reliability, robustness, economy and also aesthetic. The problem of facing optimization directly came up at the the beginning of the 19<sup>th</sup> century, it has been studied for many years and different approaches have been developed with the increase of computational possibilities.

In this chapter are presented the principles of limit state and performance design in order to set the basis for the optimization, then, the possible approaches are introduced to be later specified for the cases of single and multi-objective optimization. Finally, the probabilistic based optimization is investigated: both the robust and reliable one. Most of what is reported here is taken from Vangelis[60] that has done a wide study about the optimization procedures mostly used today.

### 3.1 Uncertain in structural analysis

An optimal design cannot leave apart the randomness of the main factors that characterize the problem. In the past, the different outcomes in an experiment were seen as limits of the mathematical model, but today is a fact that uncertainties affect every physical phenomena and cannot be eliminated completely. There are two classes of uncertainties[60]:

- *epistemic*: due to a lack of knowledge (in terms of model or available data) about the system;
- *aleatory*: due to the intrinsic randomness of the physical phenomena;

The two types can be treated either separately or together in the analysis. If the epistemic uncertainty can be reduced by the improvements in the models adopted, the aleatory uncertainty is part of the nature and a good project has to deal with it somehow.

In the structural field, the approach to design is based on the *limit states analysis*: a possible failure mechanism is defined and the probability of occurrence analysed in different way depending from the cases. A *failure mechanism* is defined as a possible state in which the system does not satisfy the design requirements any more. The codes set three classes of limit states:

- *ultimate limit states*: involve the collapse of the structure and risks for the human life;
- *serviceability limit states*: involve the loss of functionality and/or comfort of the structure;
- *fatigue limit states*: connected to the gradual damaging of the structure with a slow erosion of the safety margin;

To deal with the possible limit states, the actual codes have developed a method based on *partial safety factors*, depending on the experience in that field and affected by all the limits connected to this approach: 1) it is a slow process that has difficulty to keep up with the actual technologies, 2) the safety margin obtained is not quantifiable exactly and may be too big or unsuitable to particular design situations.

Thanks to the studies about probability, combined with the computational capacity reached by computers, a more accurate approach is not hard to be reached any more. The studies developed in the branches of *Computational Stochastic Mechanics* and *Structural Reliability* aim to express the reliability of a structure, not in terms of coefficients, but as a failure probability to be kept under a fixed threshold set by the codes.

This approach has many advantages, the most immediate is that aims to adapt quickly the codes to the changes in the state of art without waiting that for time consuming experiences on the field. In addition, it does not constraint the designer to specific prescription but gives a bigger flexibility in design as long as the performances correspond to the requirements. This approach requires a precise description of the limit state and introduces a bigger level of complexity but on the other hand is paid back by cheaper and safer designs that can be performed also for new and innovative applications. Considering this, the Computational Stochastic Mechanics will be soon a paradigm in the structural analysis.

## 3.2 Performance and limit state

The safety in probabilistic field is defined by a *performance function* (or *limit state function*)  $G = G(\vec{X})$ , where  $\vec{X} = [X_1, X_2, \dots, X_m]^T$  is a set of  $m$  random variables of which  $\vec{x} = [x_1, x_2, \dots, x_m]^T$  is a possible realization. The limit between failure,  $G(\vec{X}) \leq 0$ , and safety,  $G(\vec{X}) \geq 0$ , is called *limit state surface*  $G(\vec{X}) = 0$ . The safety domain, in  $\mathbb{R}^m$ , is defined as:

$$D_s = \{\vec{x} \in \mathbb{R}^m \mid G(\vec{x}) > 0\} \quad (3.1)$$

while the failure domain is:

$$D_f = \{\vec{x} \in \mathbb{R}^m \mid G(\vec{x}) \leq 0\} \quad (3.2)$$

Given the performance function, the failure probability is given by the integration of the joint PDF of random variables over the failure domain:

$$P_f(\vec{X}) = \int_{D_f} p_X(\vec{x}) d\vec{x} \quad (3.3)$$

where  $p_X(\vec{x}) : \mathbb{R}^m \rightarrow \mathbb{R}$  is the joint PDF of all the random variables involve in the analysis. A different way to express the performance function defines it as margin between the *structural resistance* (or *capacity*),  $R = R(\vec{X})$ , and the *external action effect* (or *demand*),  $S = S(\vec{X})$ :

$$G(\vec{X}) = R(\vec{X}) - S(\vec{X}) \quad (3.4)$$

Being them function of random variables, the capacity, the resistance and the safety functions are random variables as well.

### 3.2.1 Structural resistance and demand as independent normal variables

Considering a normal distribution for the limit state function  $G(\vec{X}) = R(\vec{X}) - S(\vec{X})$ , for linearity, the mean and variance are definable as:

$$\mu_G = \mu_R - \mu_S \quad (3.5)$$

$$\sigma_G = \sqrt{\sigma_R^2 + \sigma_S^2} \quad (3.6)$$

By them, the failure probability with the corresponding Gaussian PDF is calculated as:

$$p_G(x) = \frac{1}{\sqrt{2\pi}\sigma_G} \exp\left[-\frac{(x - \mu_G)^2}{2\sigma_G^2}\right] \quad (3.7)$$

The CDF is:

$$F_G(x) = \int_{-\infty}^x p_G(x) dx \quad (3.8)$$

For the definition of limit state surface, the failure occurs for  $G(\vec{X}) \leq 0$ , i.e., the CDF for  $x_p = 0$  gives the failure probability:

$$P_f(X) = F_G(0) = \int_{-\infty}^0 p_G(x_p) dx \quad (3.9)$$

The Gaussian PDF can be expressed in standard form:

$$p_G(z = 0) = \varphi\left(-\frac{\mu_G}{\sigma_G}\right) = \frac{1}{\sqrt{2\pi}} \exp\left(-\frac{\mu_G^2}{2 \cdot \sigma_G^2}\right) \quad (3.10)$$

This formulation leads to a failure probability equal to:

$$P_f(Z) = F_G(0) = \Phi\left(-\frac{\mu_G}{\sigma_G}\right) = \Phi(-\beta) \quad (3.11)$$

where  $\beta = \mu_G/\sigma_G$  takes the name of *reliability index* and measures the distance between the mean value of the performance function and the limit state surface. In general, the higher is  $\beta$ , the lower is the failure probability because the values are farther from the limit state surface. The analytical forms of the joint PDF for  $R$  and  $S$  are obtainable by using eq.(1.64) for the case of independent random variables<sup>1</sup> ( $\rho = 0$ ):

$$p_{S,R}(s, r) = \frac{1}{2\pi\sigma_S \cdot \sigma_R\sqrt{1-\rho^2}} \exp\left[-\frac{1}{2}\left(\frac{(r-\mu_R)^2}{\sigma_R^2} + \frac{(s-\mu_S)^2}{\sigma_S^2}\right)\right] \quad (3.12)$$

The obtained limit state curve is plotted in fig.3.1. The computational cost of a direct integration of a joint PDF with a high number of random variables  $m$  (as design uncertain parameters) is high. For this reason, mathematical methods have been developed to determine the solution to the problem in simplified forms:

- First and Second Order Reliability Method (FORM and SORM);
- Response Surface Method (RSM);
- Monte Carlo Simulation (MCS).

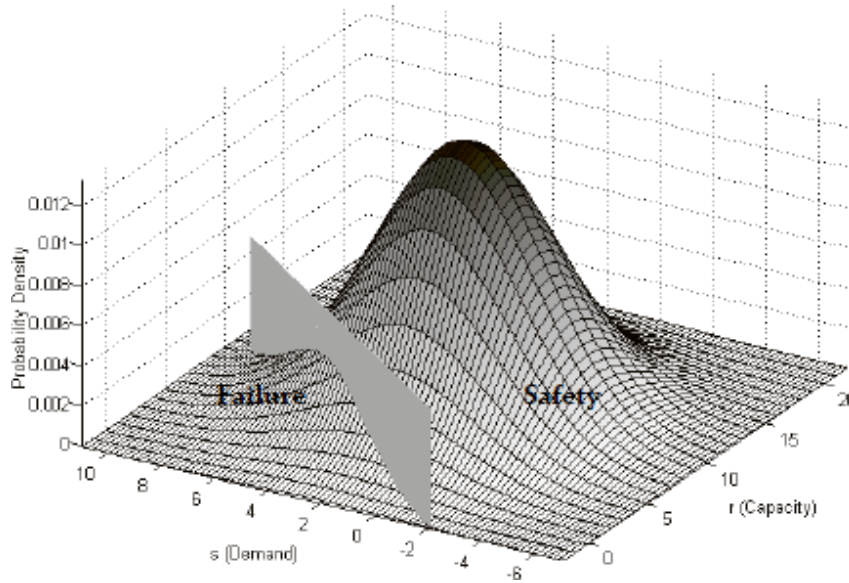


Figure 3.1: Gaussian joint PDF for capacity and demand cut by the limit state surface (corresponding to the plane  $r=s$ )[60].

<sup>1</sup>This assumption is not always true of course. For instance, increasing the section of an element involves changes both in the resistance and in the demand because the weight increases together with the resisting section. However, the obtained results do not change too much, while remarkable advantages come from this simplification.

### 3.2.2 First and Second Order Reliability Method (FORM and SORM)

The First and Second Order Reliability Methods are based on the approximation of the performance function in the standard Gaussian space by using a polynomial series. The failure surface is approximated at the point of highest failure probability to better describe it in the area which contributes most to the integral defining the probability of failure. Due to the symmetry of the PDF in the standard normal space, this point, called also  $\beta$ -point, is the nearest failure point to the origin having the highest probability density among all points in the failure domain. The methods require to know the mean and variance of each random variable and to have a differentiable failure function. The basic steps to implement the FORM and SORM are[55]:

1. transformation of the basic variables into standard and uncorrelated normal ones (in the *standard normal space*). In this way, the real joint probability density function is transformed into an "equivalent" multivariate normal density (with mean zero and identity covariance matrix).
2. Determination of the design point (MPP) in the standard normal space.
3. Approximation of the limit state surface in the standard normal space at the design point with the FORM or SORM principle.
4. Computation of the probability of failure in accordance with the approximation surface selected in step 3.

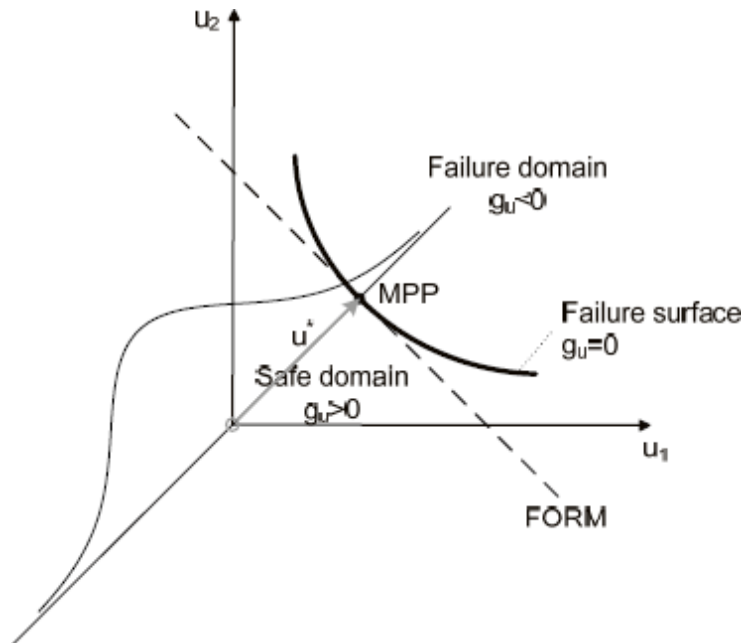


Figure 3.2: Graphical interpretation of the FORM principle[60].

Let consider an optimization problem defined in the form:

$$\vec{u}^* = \min\{\|\vec{u}\| \mid G(\vec{u}) = 0\} \quad (3.13)$$

where  $\vec{u}^* = [u_1^*, u_2^*, \dots, u_m^*]$  is the coordinate of the design point and  $G(\vec{u})$  the limit state function in the transformed standard normal space.

The FORM is based on the linearization of the failure surface in proximity of the design point  $\vec{u}^*$  in the transformed standard space by a Taylor series expansion:

$$G(\vec{u}) \cong G(\vec{u}^*) + \nabla_u G(\vec{u}^*)^T \cdot (\vec{u} - \vec{u}^*) \quad (3.14)$$

where  $\nabla_u G(\vec{u}^*)$  is the gradient of G at the design point  $\vec{u}^*$ ; of which the reliability index is:

$$\beta = \text{sign}(g_u(\vec{0}) \cdot \|\vec{u}^*\|) \quad (3.15)$$

The failure probability:

$$p_{FORM} = \Phi(-\beta) \quad (3.16)$$

Figure 3.2 shows graphically how the FORM approximates the safety function.

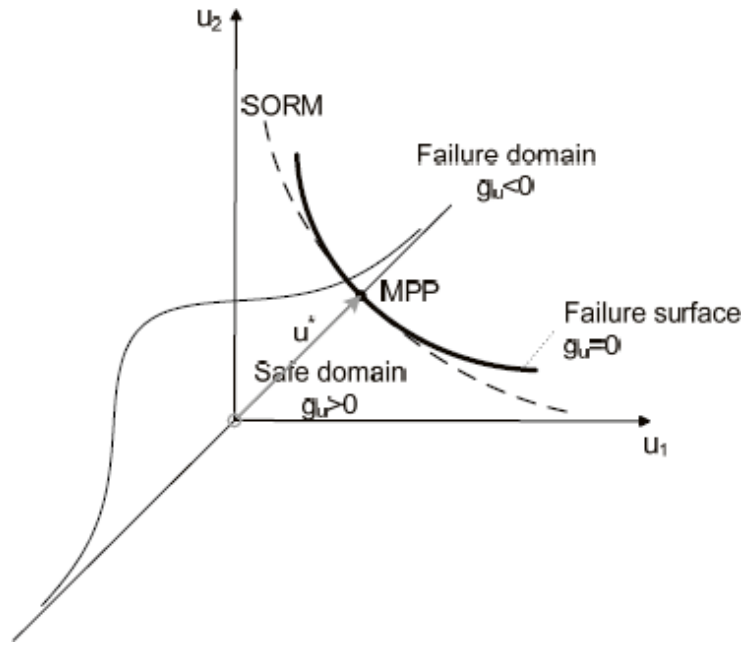


Figure 3.3: Graphical interpretation of the SORM principle[60].

The SORM is based on the approximation with a quadratic function of the failure surface in the design point  $\vec{u}^*$  in the transformed standard space by a Taylor series expansion:

$$G(\vec{u}) \cong G(\vec{u}^*) + \nabla_u G(\vec{u}^*)^T \cdot (\vec{u} - \vec{u}^*) + \frac{1}{2}(\vec{u} - \vec{u}^*)^T \cdot \nabla_u^2 G(\vec{u}^*)^T \cdot (\vec{u} - \vec{u}^*) \quad (3.17)$$

$\nabla_u G(\vec{u}^*)$  and  $\nabla_u^2 G(\vec{u}^*)$  are, respectively, the gradient and the Hessian matrix of G at the design point  $u^*$ . The failure probability is given in approximated form[26]:

$$p_{SORM} = \Phi(-\beta) \prod_{i=1}^{m-1} \frac{1}{\sqrt{1 + 2n(\beta) \cdot \lambda_i \beta}} \quad (3.18)$$

where  $\lambda_i = k_i/2$  and  $k_i$  are the main curvatures, taken positive for a concave limit state function, and  $n(\beta) = \varphi(\beta)/\Phi(-\beta)$ . The corresponding reliability index is:

$$\beta_{SORM} = -\Phi^{-1}(p_{SORM}) \quad (3.19)$$

Figure 3.3 shows graphically how the FORM approximates the safety function.

The main problem of the SORM and FORM methods is the presence of various local optima. Both methods are quite sensible to them and can stuck in a local optima rather than in the design point if the dominion is not convex. Moreover, the approximation in the design point neglects the contribute of its neighbourhoods that can be important for the determination of the failure probability.

### 3.2.3 Response Surface Method (RSM)

The response surface method defines a *meta-model* to determine the behaviour of the system in a defined domain. Generally, the vector  $\vec{X} = [X_1, X_2, \dots, X_m]$  and the performance function  $g(\vec{X})$  are not given in closed form and it is necessary to perform more experiments to define a response surface with sufficient level of accuracy. Each experiment is a point in the  $m$ -dimensional design space of the random variables for which a structural analysis is performed and one value of the function  $g$  calculated. With a polynomial interpolation the response surface is approximated between the calculated points with  $\tilde{g} : \mathbb{R}^m \rightarrow \mathbb{R}$  in the region of interest. The order of the polynomial and the number of points have to be carefully chosen. The degree of the polynomial approximation  $\tilde{g}$  must be less than or equal to the degree of  $g$  to avoid ill-conditioned problems, but higher order polynomials may induce errors out of the explored area of the response surface. Computational cost increases quickly with the polynomial order and the fact that the main contribute comes in proximity of the design point (where the probability density is higher) leads to use quadratic approximations in its neighbourhood.

The main advantages of using the RSM[11] are in the reduction of computational effort for the determination of the limit state surface (for a moderate number of random variables) and in the possibility to couple the reliability and optimization algorithms together to reach high efficiency. It could be also used to study approximatively the response of the system before applying other forms of optimization. Unfortunately, for a higher number of random variables, the computational cost for the multiples analysis necessary to determine the polynomial approximation becomes too high and the method is not convenient any more.

### 3.2.4 The Monte Carlo Simulation (MCS)

The MCS methods deal with high complexity problems characterized by a large number of degrees of freedom, significant uncertain on the input and complex boundary conditions. They are often used to test new models and study uncertainty propagation, where the goal is to determine how random variation, lack of knowledge, or errors affect the sensitivity, performance or reliability of the system.

The principle is quite simple, many experiments are simulated and the outcomes are used to define in detail the limit state surface. By the use of statistical sampling the discrete probabilistic characteristics of the system can be extracted. The mean is:

$$\mu_n(G) = \frac{1}{n} \sum_{k=1}^n g(X_j) \quad (3.20)$$

The variance is:

$$\sigma_n^2(G) = \frac{1}{n-1} \sum_{k=1}^n [g(X_j) - \mu_n(G)]^2 \quad (3.21)$$

that correspond to the Monte Carlo estimator of the real mean  $\mu$  and variance  $\sigma^2$ . It is demonstrated that as the simulations performed increase, the two estimators converge to the real values.

Let suppose a number  $n$  of experiments performed with different possible outcomes  $\vec{x}$  of the  $m$  elements of the set  $\vec{X} = [\vec{X}_1, \dots, \vec{X}_n]$  with a corresponding performance  $g_i(\vec{x}_i)$ . For each one, the failure occurrence is:

$$a_i = \begin{cases} 0, & \text{if } g(\vec{x}_i) > 0, \\ 1, & \text{if } g(\vec{x}_i) \leq 0, \end{cases} \quad \text{for } i = 1, \dots, n \quad (3.22)$$

The sum of elements of the sequence counts the samples for which the failure has occurred on the total number of samples  $n$ , giving the rate of occurrence equal to:

$$P_n(\vec{X}) = \frac{1}{n} \sum_{i=1}^n a_i \quad (3.23)$$

that converges for a high number of simulations to the failure probability  $P_f(\vec{X})$ .

The main advantage of the MCS[11] is the capability of handling any type of problem regardless of its complexity by simply repeating the same mechanical analysis several times, avoiding the necessity of modifications of the solution. On the other hand, it is a very computational expensive method and is subjected to noise during random sampling that may leads to problems in the response gradient analysis. Of course, every Monte Carlo simulation leads to different results, even if the same number of samples is used, i.e., the same outcome cannot be reproduced again.

To reduce the computational effort connected to the MCS many improved sampling techniques have been developed. The three most popular ones are:

- *importance sampling* (IS)[1]: the main problem in the ordinary MCS simulation is the high number of extractions necessary to describe the tails of the distribution due to rare events. A possible solution is to introduce changes in the probability distribution by weighting more these areas; such PDF is problem-dependent and in most cases difficult to find.

The IS technique generates a biased distribution which results in biased estimators if it is applied directly in the simulation. Therefore, the simulation outputs are weighted to correct this bias. The main drawback of the IS method is that requires prior knowledge of the system behaviour in order to determine the most effective sampling region, which for many practical problems is not clearly identifiable.

- *Latin Hypercube Sampling* (LHS)[19]: the samples extracted from the MCS have to describe the real distribution by inferences applied to the data extracted. Nevertheless, in most applications there is no relationship between successive extractions and the randomness of sampling is not crucial for the approximation because each extraction does not depend on the others. Thus, a random sampling is computational expensive and unnecessary, the main task is to cover the largest part of the limit state surface, not to acquire informations on the population.

The LHS method divides the range of each  $m$  uncertain variable in  $N$  non-overlapping segments of equal probability, defining a  $m$ -dimensional cubic parameter space partitioned in  $N^m$  cells. For every random variable, a value is chosen respect to the PDF in that partition, generally the mid one, and is used to get a set of  $N$  values used to describe the PDF of the performance function. The main advantage is that, fixed a beginning set of random variables, the LHS technique does not require more RV to describe better the PDF. In figure 3.4 and 3.5 are showed respectively a simple MCS and a LHS sampling; it is evident how with the same number of samples the LHS performs much better in the description of the limit state surface.

- *Descriptive Sampling* [56](DS): is a MCS technique based on a deterministic and purposive selection of the sample values and their random permutation in order describe the sampled distribution. This approach is justified by the fact that, in any Monte Carlo application, the sampled distribution must be assumed known a priori. The main purpose becomes descriptive (describe the known PDF) instead of inferential (acquire informations on the population). The DS can be seen as a limit case of th LHS where an high control selection on the samples is operated.

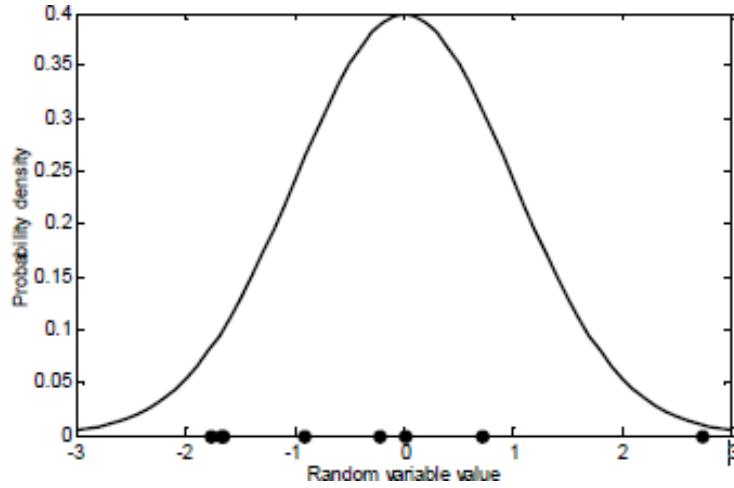


Figure 3.4: MC sampling for the normal distribution with 8 samples[60].

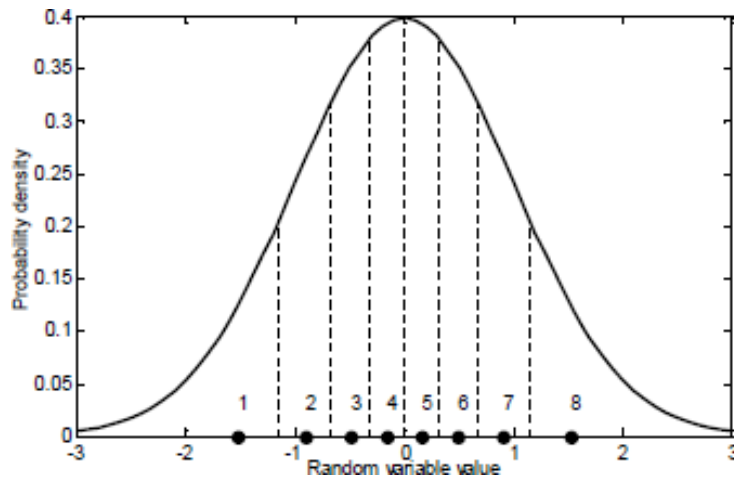


Figure 3.5: Latin Hypercube sampling for the normal distribution with 8 samples[60].

### 3.3 Optimization

The optimization process aims to obtain, between many possible solutions, the best one which satisfies the design constraints, i.e., the limit state surface surpassing,  $G(\bar{X}) = 0$ , together with the constraints on the design parameters. The main elements involved in the optimization are:

- the *design parameters*: geometric, mechanical, dynamical, etc.;
- the *design constraints*: acceptable stresses, strains, displacements, forces, ductility, resistance to brittle collapse and so on;
- an *objective function*: to be optimized as cost, resistance, weight, ductility, etc.

The optimization problem can be divided in two phases: 1) the mathematical formulation (design variables, definition of an objective function and corresponding constraint functions) and 2) the application of a computer optimization algorithm to it. The designer's experience plays still a key role in this process in order to use the algorithm efficiently by formulating the problem in a correct manner and have valuable results. The recent develops of high capacity IT has allowed to define algorithms of increasing complexity that can deal with many design parameters and constraints with a contained computational effort.

There are several ways to approach the optimization problem, a first division is between:

- *enumerative methods*: they consider all the possible solutions to the problem and then select the best one. It is a very onerous approach and generally not used;
- *heuristic methods*: they search a solution that may not be the optimum but is significant and rapid to be found.

A second classification divides the optimization processes in:

- *analytics*: they express by analytic functions the laws that rule the problem and get the solution by finding one or more zeros of them. They give an exact solution (if the equations are solvable) and require the use of mathematical analysis;
- *evolutive methods*: they search sequential solutions that fit progressively better the problem once the fixed initial values are set by the designer. The obtained results are not in general exact but the methods have the big advantage of being applicable also to empiric laws. Moreover, they are easy to be implemented on the calculator.

The classes stated before enter all in a general division between:

- *single optimization*: where all the parameters to be optimized converge to the same optimum and they can be pooled in a single design vector;
- *multiple optimization*: where one or more parameters to be optimized diverge to different optimum and they cannot be pooled in a single design vector. The approach is to define a Pareto n-dimensional set to compare the solutions and choose a trade-off between the possible optimums.

In structural engineering the main types of optimization problems involve:

- *sizing optimization*, where the aim is to minimize the weight of the structure under constraints over the stresses and displacements. The trade-off is between costs, aesthetic requirements and the safety of the structure, considering together the standardization of the elements adopted.

- *Shape optimization*, where the boundaries and the shape of the structure have to be modified. The design variables are some key points coordinates in the structure or other parameters influencing the shape.
- *Topology optimization*, where the design parameter is the type of structure used by the designer to best suit the conditions to solve the problem. Generally, the approach is to define a topology optimization on an initial layout of the structure to then operate on the shape optimization to refine it.
- *External devices optimization* (as the vibration control ones) they can be optimized referring to the comparison of performances between protected and unprotected case.

### 3.4 Single Objective Optimization

The single objective optimization problem, in the deterministic field, can be formulated as:

- find the *design vector*  $\vec{x} = [x_1, x_2, \dots, x_n] \in \mathbb{R}^n$  (discrete, continuous or mixed, depending on the problem), bounded in a domain  $\vec{x}_L \leq \vec{x} \leq \vec{x}_U$ , where  $(\vec{x}_L, \vec{x}_U)$  are the lower and upper bounds of the design variables fixed by shape, typology of the structure, etc.;
- in  $X_i$ , the set of  $x_i$ , which may be continuous, discrete or integer. The whole design space for the  $n$  design variables can be denoted as  $\vec{X}$ ;
- that minimizes an *objective function*  $f(\vec{x})$ , corresponding to a design limit in displacements, tension, etc. ( $f \in \mathbb{R}$ );
- subjected to *inequality constraints*  $g_i(\vec{x}) \leq 0$ , where  $i = 1, 2, \dots, p$  are the number of inequality constraints ( $\vec{g} \in \mathbb{R}^p$ );
- and to *equality constraints*  $h_j(\vec{x}) = 0$ , where  $j = 1, 2, \dots, q$  are the number of equality constraints ( $\vec{h} \in \mathbb{R}^q$ );

In a synthetic way the problem can be written as:

$$\begin{aligned}
 & \min[f(\vec{x})], \quad \vec{x} = [x_1, x_2, \dots, x_n], \quad f \in \mathbb{R} \\
 & \text{subjected to:} \\
 & \vec{g}(\vec{x}) \leq 0, \quad \vec{g} \in \mathbb{R}^p \\
 & \vec{h}(\vec{x}) = 0, \quad \vec{h} \in \mathbb{R}^q \\
 & x_i \leq X_i \quad \text{for } i=1, \dots, n \\
 & \text{bounded by:} \\
 & \vec{x}_L \leq \vec{x} \leq \vec{x}_U
 \end{aligned} \tag{3.24}$$

A set of design vectors  $\vec{x}$  that satisfy the constraints in (3.24) is called *feasible set*,  $\vec{F}$ , and is a subset of  $\vec{X}$  ( $\vec{F} \in \vec{X}$ ):

$$\vec{F} = \{\vec{x} \in \vec{X} \mid \vec{g}(\vec{x}) \leq 0, \vec{h}(\vec{x}) = 0\} \tag{3.25}$$

The image of  $\vec{F}$  is called *criterion space*,  $V_F = f(\vec{F})$ . All equality constraints (regardless of the value of  $\vec{x}$  used) are considered active at all points of the feasible set  $\vec{F}$ . The design vector  $\vec{x}^* \in \vec{F}$  to which corresponds the minimum objective function  $f(\vec{x}^*) \leq f(\vec{x}), \forall \vec{x} \in \vec{F}$ , is called *global minimizer*, and the corresponding value of the objective function is called *global minimum*. A *local minimizer* is a design vector  $\vec{x}' \in \vec{F}$  for which exists a neighbourhood  $\vec{\chi}$  such that  $f(\vec{x}') \leq f(\vec{x}), \forall \vec{x} \in \vec{\chi}$ . The corresponding value  $f(\vec{x}')$  is called *local minimum*.

### 3.4.1 Convex and not-convex problems

One of the main problem in the formulation of the optimization process is the presence of local optima in which the algorithm may be trapped during the analysis. This depends on the convexity of the optimization domain. A *convex set*  $C$  in the real or complex space is such that for all  $x$  and  $y$  in  $C$  and all the  $t$  in the interval  $[0,1]$ , the point:

$$(1 - t) \cdot x + t \cdot y \tag{3.26}$$

is also in  $C$ . In other words, every point of the line segment connecting  $x$  and  $y$  is in  $C$ . A function in the real space is said to be *convex* if, for any two points  $x$  and  $y$  in its domain and any  $t$  in the interval  $[0,1]$ :

$$f[t \cdot x + (1 - t) \cdot y] \leq t \cdot f(x) + (1 - t) \cdot f(y) \tag{3.27}$$

A function  $f$  is said to be *concave* if  $(-f)$  is convex. The function is instead say to be *strictly convex* if for any  $x \neq y$  and any  $t$  in the interval  $[0,1]$

$$f[t \cdot x + (1 - t) \cdot y] < t \cdot f(x) + (1 - t) \cdot f(y) \tag{3.28}$$

Fig.3.6 shows the effect of the presence of local minimums in the optimization process of not-convex functions. In general, a global minimizer is also a local minimizer while the converse is not necessarily true unless all the functions involved are convex.

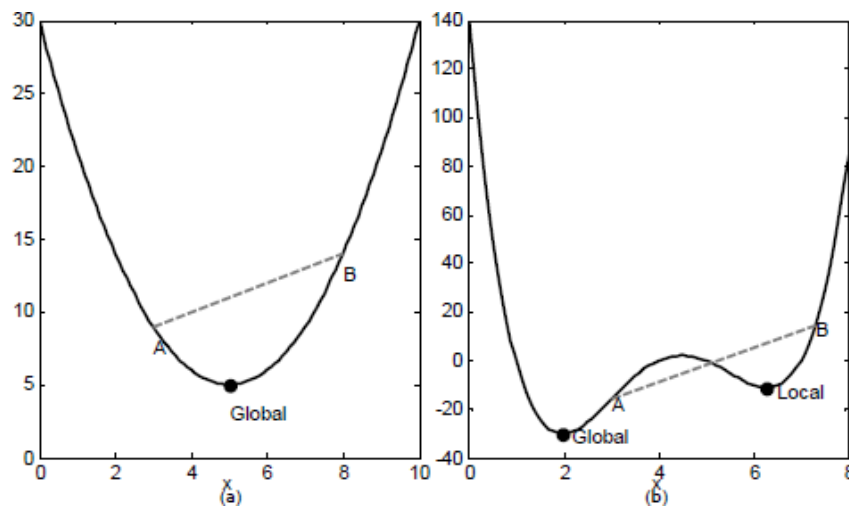


Figure 3.6: a) a convex one-variable function with a global minimum, b) a non-convex one-variable function with a global and a local minimum[60].

### 3.5 Single Objective optimization Problem (SOP)

Several methods have been proposed to solve the Single Objective Optimization Problem (SOP), a first rough separation can be done between:

- deterministic methods;
- probabilistic methods;

Of course, the use of probabilistic methods involves a higher complexity, but aims to manage the uncertainties by the instruments of probability and is definitively the best approach for a safe and sustainable design.

It has been demonstrated by Wolpert and Macready[62], with the *No Free Lunch* theorem, that it does not exist an algorithm able to perform the best in every optimization problem, for every case there is a better approach depending on its characteristics. There are three main typologies of optimization algorithms: the *mathematical programming*, entering in the analytical class, the *genetic algorithms* and the *particle swarm*, entering in the heuristic methods.

## 3.6 Mathematical Programming (MP)

The *mathematical programming* (MP) methods, and particularly the method of the gradient, had been used widely until when the heuristic algorithms were developed. They adopt an analytical approach to the solution and are considered *local methods* because they use local curvature informations of the objective function together with a gradient evaluation. The main advantage of these methods is that, using the gradient informations to guide the search, the convergence rate is faster toward the optimum. On the other hand, relying only on the local informations, they are sensible to local optima of not convex domains and require that the designer defines a first estimation of the solution in order to control the final results. The general structural optimization problems are quite complex, with multiple local optima and several constraints to be satisfied that make the MP not really effective for the real design situation.

### 3.6.1 Sequential Mathematical Programming

The most popular method adopted for mathematical programming is the *Sequential Quadratic Programming* (SQP), used generally to solve *Non-Linear Programming* problems. The method uses local curvature informations to search a local minimum once the objective function is linearised respect to the design variables at different points calculated during the process.

Generally, the non-linear constraints are difficult to be treated directly in a gradient search and indirect methods to consider them need to be introduced. A penalty function is used to transform the problem and remove the constraints, obtaining an *unbounded optimization problem* that may be solved by the following procedure.

Considering the optimization problem in eq.(3.24) for a continuous case, the SQP converts the non linear-programming problem in a sequence of *Quadratic Programming* (QP) sub-problems, based on a quadratic approximation of the Lagrangian function:

$$L(\vec{x}, \vec{\lambda}) = f(\vec{x}) + \sum_{k=1}^m \lambda_k \cdot g_k(\vec{x}) \quad (3.29)$$

where  $\lambda_k$  is the  $k^{th}$  Lagrange multiplier under the non-negativity restriction for the inequality constraints assumed in the analysis and  $g_k$  the non linear inequality constraints which are linearised (the equality constraints are generally not encountered in structural optimization).

The  $l^{th}$  QP sub-problem is formulated in the following form:

$$\begin{aligned} & \min \left\{ \frac{1}{2} \vec{p}^T \cdot \mathbf{H}_l \cdot \vec{p} + \nabla f(\vec{x}_l)^T \cdot \vec{p} \right\}, \quad \vec{p} \in \mathbb{R}^n \\ & \text{Subject to:} \\ & [\nabla g_k(\vec{x}_l)]^T \cdot \vec{p} + g_k(\vec{x}_l) \leq 0, \quad k = 1, \dots, m \end{aligned} \quad (3.30)$$

where  $l$  indicates the step of the iteration,  $\vec{p}$  is the search direction and  $\mathbf{H}_l$  is the approximation of the Hessian matrix of the Lagrangian function in eq.(3.29). The steps of the procedure are:

1. solution of the QP sub-problem to find the search direction  $\vec{p}$ ;
2. line search along the direction;
3. update of the Hessian matrix for the changing of direction.

The formulation of eq.(3.30) allows to remove, at each iteration, the inequality constraints by penalizing the objective function near the points that violate these limits and take the name of *transformations with penalty*. To construct the Jacobian and Hessian matrices of the QP sub-problem, the derivatives of the objective and constraint functions have to be determined during the sensitivity analysis phase, either analytically or numerically with a global finite difference method.

### Line search and merit function

The direction  $\vec{p}$  is changed at every resolution of the QP sub-problem in eq.(3.30). The line search consists in the research along the line containing the current point  $x_l$ , parallel to the search direction, and the new design point calculated as:

$$x_{l+1} = x_l + a_l \cdot \vec{p}_l \quad (3.31)$$

where  $a_l$  is the step length parameter, determined so that a sufficient decrease in a *merit function* is obtained. The form of this function is:

$$\Phi(\vec{x}) = f(\vec{x}) + \sum_{k=1}^m r_k \cdot \max\{0, g_k(\vec{x})\} \quad (3.32)$$

where  $r_k$  are the penalty parameters defined as:

$$r_k = (r_{l+1})_k = \max_{(k)} \left\{ \lambda_k, \frac{(r_l)_k + \lambda_k}{2} \right\}, \quad k = 1, \dots, m \quad (3.33)$$

The penalty parameter have to be fixed at an initial value to start the procedure. Typically:

$$r_k = \frac{\|\nabla f(\vec{x})\|}{\|g(\vec{x})\|} \quad (3.34)$$

### Hessian update

The updating of the Hessian matrix is performed according to the following formulation[21]:

$$\mathbf{H}_{l+1} = \mathbf{H}_l + \frac{\vec{q}_l \cdot \vec{q}_l^T}{\vec{q}_l^T \cdot \vec{s}_l} - \frac{\mathbf{H}_l \cdot \vec{s}_l^T \cdot \vec{s}_l \cdot \mathbf{H}_l}{\vec{s}_l^T \cdot \mathbf{H}_l \cdot \vec{s}_l} \quad (3.35)$$

where  $l$  denotes the current SQP iteration. The terms  $\vec{s}_l$  and  $\vec{q}_l$  are, respectively, the difference between the value and the product of gradient at the actual and next step design point:

$$\vec{s}_l = \vec{x}_{l+1} - \vec{x}_l \quad (3.36)$$

$$\vec{q}_l = \left( \nabla f(\vec{x}_{l+1}) + \sum_{k=1}^m \lambda_k \cdot \nabla g_k(\vec{x}_{l+1}) \right) \cdot \left( \nabla f(\vec{x}_l) + \sum_{k=1}^m \lambda_k \cdot \nabla g_k(\vec{x}_l) \right) \quad (3.37)$$

This formulation requires that  $\vec{q}_l^T \cdot \vec{s}_l$  is positive and that the Hessian is initialized as positive definite to be maintained in the same way. If the quadratic function is convex, then the Hessian is positive definite, or positive semi-definite, and the solution obtained will be a global optimum. Else, if the quadratic function is non-convex, then the Hessian is indefinite and, if a solution exists, it is in general a local optimum.

### Sensitivity analysis

The most important part of the SQP procedure consists in the sensitivity analysis to determine the derivatives of the objective function used for the gradient update. The sensitivity coefficients of the function are calculated by applying small perturbations to each design variable. Two methodologies can be adopted: *discrete* and *variational*.

The discrete methods use a finite element (FE) analysis to calculate the gradient of characteristic functions (stresses, displacements, etc.) by equilibrium equations and are divided in:

- *global finite difference method*: that performs a full FE analysis for each design variable. Its accuracy depends strongly on the value of the perturbation applied to the design variables and it is the most computational expensive method. Despite this, it is very easy to be used, requiring just to perform several analysis of the same problem.
- *Semi-analytical methods*: the stiffness matrix of the initial finite element solution is retained during the computation of the sensitivities. The effect is a small increase of the algorithm complexity with the advantage of an improve in its efficiency.
- *Analytical method*: the finite element equations, the objective and the constraint functions are differentiated analytically. This method works only for analytic formulations.

Due to the high computational costs related to the resolution of the equilibrium equations, the efficiency of the discrete algorithm for the sensitivity analysis is really important and has to be chosen carefully depending on the nature of the problem.

The *perturbational methods* define a sensitivity coefficient as derivative respect to the parameters that influence the result that is evaluated in the design point. The same methods are also used for the analysis of the effects of uncertainties on the objective function.

## 3.7 Evolving Algorithms methods (EA)

The limits showed by the mathematical programming in handling complex problems with many design parameters and local optimums have lead the research of new solutions out from the ordinary analytical field. These methods, called heuristics because not based on rigorous analytical demonstrations, are able to deal with highly non-linear and complex problems as was not possible before. The *evolving algorithms* (EA) are a promising group of heuristic methods that deal with many types of optimization problems being not based on analytical calculations. Furthermore, their heuristic nature makes them less sensitive to local optima. The most popular EA methods used today are:

- The *genetic algorithms*: set an initial ensemble of design parameters converted in fixed-length strings (binary or real valued) on which the natural selection principle is applied by using recombination and mutation operators together with a fitness function. The recombination operator creates new offsprings and the mutation keeps the diversity of specimen, while the fitness function determines the survived individuals to get a result that satisfies the design requirements within a fixed tolerance.
- The *particle swarm methods*: similar to the genetic algorithms, instead that on natural selection they are based on social contexts. A group of particles is selected and their experience is built by tracking and memorizing the best position encountered by the particles "flight" along the design space. The process has a memory and the global optimum is obtained by keeping into account the previous velocity together with the best ever position of the single particle and of the global swarm.

- *Hybrid optimization methods*: since every algorithm has its own strength and weakness, some approaches combine them together to get more effective solutions. For instance, using the evolving algorithms to explore the entire design space and roughly localize an optimal area then explored by a sequential programming.

This thesis will use the genetic algorithm to perform the optimization, thus a detailed description about them is presented. More details about the particle swarm and hybrid methods are given by Vangelis[60].

The main difficulty encountered in these methods is the managing of the constraints for which many techniques have been developed. Also the step for the exploration of the design space has to be chosen carefully, a too small step requires a high computational effort, while a too big one may be inaccurate in the optimum. Possible solutions are the use of sequential evolving algorithms that change gradually the step while the optimum is approached or adopt hybrid methods. Despite these difficulties, heuristic methods have a big potential for the resolution of problems out of the ordinary analytic field, as discrete or non-linear optimizations, and are today widely used. The EAs work differently respect to the usual optimization methods:

- instead of the usual deterministic operators, they use randomized operators of mutation, selection and recombination;
- instead of a single design point, they work simultaneously with a population of design points in the space of design variables;
- they can handle continuous, discrete or mixed optimization problems;

The EAs show a fast rate of convergence at the beginning towards the area of global optimum but when they reach the optimal zone they slow down and several steps are necessary to converge, however, their computational effort is contained because they do not require a gradient calculation. Overall, their limits are acceptable compared to the potential to deal with the majority of optimization problems and, in addition, they can be used in hybrid methods.

### 3.8 Genetic algorithms (GA)

Based on the evolution theory formulated by Darwin, the *Genetic Algorithms* (GA) have grown in popularity in many optimization applications thanks to their flexibility, computational economy and ability to deal with high complexity problems due to their heuristic nature.

The basic GA operate on fixed-sized bit strings which are mapped to the values of the design variables. The operators of recombination and mutation allow to keep the diversity of the population and, consequently, of the design space. The performance of each group is measured by using apposite fitness functions at each step of the optimization. The idea is that by building together the blocks that characterize the nature of the population it is possible to reach the best solution. The characteristics that do not suit the fitness function are eliminated while the best ones remain toward the best fit for the problem. The optimization procedure was first set by Goldberg[22] as follow:

1. *Initialization step*: random generation of an initial population of vectors of the design variables  $\vec{x}_j (j = 1, \dots, n_{pop})$  which can be encoded in binary strings or keep real valued.
2. *Analysis step*: solve the structural analysis problem, in a FE analysis the displacements  $\vec{u}$  calculation: given the stiffness matrix  $\mathbf{k}$  and the forces  $\vec{F}$ , the displacements are:

$$\mathbf{K}(x^j) \cdot \vec{u}^j = \mathbf{F}, \quad (j = 1, \dots, n_{pop}) \quad (3.38)$$

3. *Fitness evaluation step*: each member of the population is evaluated by computing the representative penalized objective and the corresponding fitness functions, using an appropriate penalty function.
4. *Selection step*: a selection operator is applied to the current population to create an intermediate one to which the genetic operators will be applied.
5. *Generation step*: in order to create the next generation, crossover and mutation operators are applied to the intermediate population to create the next one  $\vec{t}_j (j = 1, \dots, n_{pop})$ .
6. *Analysis-Fitness evaluation step*: solve the analysis problem; for the FE problem stated before,  $\mathbf{K}(\vec{t}_j) \cdot \vec{u}_j = \mathbf{F}$ , ( $j = 1, \dots, n_{pop}$ ).
7. *Convergence check*: if satisfied stop, else go to step 4.

Each of the operators adopted in the process (mutation, crossover and fitness) can be defined by different functions, either analytic or heuristic depending on the type of problem. According to the choice, different evolving algorithms have been developed.

The optimal size of the initial population, in order to grant enough diversity of the samples but also an acceptable convergence time, was suggested by Goldberg[22] as:

$$n_{pop} = 2^k \cdot (\xi/k) \quad (3.39)$$

where  $\xi$  is the length of the binary string and  $k$  the average size of the schema. The size of the schema corresponds to the dimension of the design parameters  $\vec{x}$ , while the length of the binary strings is obtained by encoding the real data to binary ones.

### 3.8.1 Encoding

If converted in binary strings, the design parameters require an encoding to convert the real values that characterize them, the *phenotype*, in linear strings  $\vec{x}_j$  ( $j = 1, \dots, n_{pop}$ ), the *genotype*. The binary strings are divided in  $n$  segments, corresponding to the number of design variables, the decoding then returns them to real values at the end of the analysis. In the case of discrete design variables, each discrete value is assigned to a binary string, while in the case of continuous design variables, the design space is expressed in binary base by dividing it into a power of 2 number of intervals.

### 3.8.2 Fitness function

To each member of the population is assigned a fitness function that measures its suitability compared to the other individuals. Every string is analyzed independently and then compared to the others in order to find the parents of the next generation of chromosomes. In basic genetic algorithms, the penalized objective function  $F'_i$ , associated with the string, and the average penalized objective function value of all the strings population,  $\bar{F}'$ , are compared by the ratio  $F'_i/\bar{F}'$ . The fitness function may be also assigned by other methods, for instance to rank of strings in the population or by the sampling techniques exposed in the following section.

### 3.8.3 Selection

Among the several ways to perform the selection of the strings, the most popular are *tournament selection*, *roulette wheel* and *ranking selection*. The tournament method selects randomly subgroups of population from which the best sample becomes part of an intermediate subgroup. The roulette wheel places the population in random order in a pie graph where for each individual a

space is assigned in proportion to its fitness. An outer roulette wheel is placed around the pie with  $n_{pop}$  equally spaced pointers, a single spin of the roulette wheel simultaneously picks all  $n_{pop}$  members of the intermediate population. The ranking scheme classifies the population in ranks according to the fitness function value to then performs the selection according to them. Another popular but slightly different technique is the *elitism*: the best chromosome is selected and directly copied to the next generation without genetic operators. The big advantage of elitism is the increasing performance of the algorithm avoiding the risk of losing the best solution in the genetic operations.

### 3.8.4 Genetic Operators

The two basic genetic operators are *crossover* and *mutation*. The crossover operators emulate reproduction by combining parts of two "parent" chromosomes and can be divided in: 1) one point, 2) two point, 3) multi-point and 4) uniform crossover. Both single and multi-point crossover define a locus where chromosomes can split. Uniform crossover generalizes this scheme by randomly creating a crossover mask, having the same length as the parent chromosomes, that defines which parent will contribute its corresponding bit to the offspring chromosome.

The main purpose of the mutation operator is to maintain diversity within the population and inhibits premature convergence. It is a reproduction operator that forms a new chromosome by making small alterations to the values of genes in a copy of a single parent chromosomes and serves only to recover lost alleles (the allele is the value of a gene). For binary encoding each gene may have an allele of 0 or 1.

## 3.9 Evolution Strategies (ES)

The evolution strategies reproduce the natural behave by applying a crude simplified evolution mechanism. Although these simplifications, they have proved to perform really well, especially in some seismic applications. They can be formulated for both continuous and discrete problems, with some differences in the two approaches.

### 3.9.1 Continuous problems

There are two ES continuous methods: 1) two-membered and 2) multi-membered evolution strategies. The *two membered evolution strategies* are based on a population of individuals that produce only one offspring, building the minimal scheme for the ES. The two operators of mutation and selection are used, respectively, to variate the parameters and to recurse the iteration sequence. The method works in two steps[60]:

1. *mutation*: the parent  $\vec{x}^{p(g)}$  of the generation  $g$  produces an offspring  $\vec{x}^{0(g)}$  with a genotype slightly different from its parents:

$$\vec{x}^{0(g)} = \vec{x}^{p(g)} + \vec{z}^{(g)} \quad (3.40)$$

where the vector  $\vec{z}^{(g)} = [z_1^{(g)}, z_2^{(g)}, \dots, z_n^{(g)}]^T$  is a random vector of *mutation*.

2. *selection*: by evaluating the feasibility of the design, the best individuals between both parents and offspring are chosen to survive:

$$\vec{x}^{p(g+1)} = \begin{cases} \vec{x}^{0(g)}, & \text{if the design } \vec{x}^{0(g)} \text{ is feasible and } f(\vec{x}^{0(g)}) \leq f(\vec{x}^{p(g)}) \\ \vec{x}^{p(g)}, & \text{otherwise} \end{cases} \quad (3.41)$$

The mutations are random, purposeless events, which occur very rarely. Therefore, a PDF that gives high frequency to small changes and lower to the big ones has to be adopted. In analogy with the natural evolution, the following requirements have to be satisfied:

1. the expected mean value  $\mu_i$ , for the  $i^{th}$  component  $z_i^{(g)}$ , has to be zero;
2. the variance  $\sigma_i^2$  has to be small;

Considering a normally distributed variable, the PDF is:

$$p(z_i^{(g)}) = \frac{1}{\sqrt{2\pi} \cdot \sigma_i} \cdot \exp\left[-\frac{(z_i^{(g)} - \mu_i)^2}{2\sigma_i^2}\right] \quad (3.42)$$

Setting  $\mu_i = 0$ , the  $(0, \sigma_i)$  distribution is obtained. The value of  $\sigma_i$  can be seen as the average value of the length of the random steps of mutation. If the step is too large, the optimum can be only largely approached or the objective function may even stuck far away from the global optimum. If the step is too small, the computational effort required increases. The choice is an important part of the optimization and is closely linked to the convergence ratio.

The *multi-membered evolution strategies* use a population of  $\xi$  parents that produce  $\lambda$  offsprings. The procedure is defined as follow[60]:

1. *Recombination and mutation*: the population of  $\xi$  parents at the  $g^{th}$  generation produces  $\lambda$  offsprings with a genotype slightly different from their parents.
2. *Selection* is evaluated in two ways:
  - $(\xi + \lambda)$ -ES: the best  $\xi$  individuals between both parents and offsprings are chosen to survive between a temporary population of  $(\xi + \lambda)$  individuals. The survivors will form the parents of the next generation;
  - $(\xi, \lambda)$ -ES: the  $\xi$  individuals produce  $\lambda$  offsprings ( $\xi < \lambda$ ) and a new set of  $\xi$  individual is defined only from the  $\lambda$  offsprings. Considering that an individual cannot "live" for more than one generation, this method seems more in accordance to the real natural selection. This allows to perform better on problems with an optimum moving overtime, or on problems where the objective function is noisy.

To create the offsprings in the mutation phase, a vector of temporary parents  $\vec{\tilde{x}} = [\tilde{x}_1, \dots, \tilde{x}_n]^T$  is built by recombination operator. Defined  $x_i^a$  and  $x_i^b$  as the  $i^{th}$  components of the genotype vector of the two parents selected from the population randomly, the possible recombinations are:

$$\tilde{x}_i = \begin{cases} x_i^a \text{ or } x_i^b, & \text{randomly} \\ 1/2(x_i^a + x_i^b) \\ x_i^{rand} \\ x_i^a \text{ or } x_i^{rand}, & \text{randomly} \\ 1/2(x_i^a + x_i^{rand}) \end{cases} \quad (3.43)$$

where  $x_i^{rand}$  is the  $i^{th}$  random component selected from all the parents population  $\xi$ . From the temporary parents  $\vec{\tilde{x}}$ , an offspring is created in the same way as the two-membered ES by eq.(3.40). A termination criteria has to be fixed, there are two options[60]:

- the absolute or relative difference between the best and the worst objective function values is less than a given threshold value  $\varepsilon_1$ ;
- the mean of the objective values from all parent vectors in the last  $2n$  generations has not been improved by less than a given threshold value  $\varepsilon_2$ .

### 3.9.2 Discrete optimization problems

The discrete nature of the design variables used in the practical cases requires to define a method to perform a discrete optimization. The differences from the continuous case lie mostly in the mutation and recombination operators.

The mutation is similar to what stated in eq.(3.40), but in the discrete version of ES the random vector  $\vec{z}^{(g)}$  is properly generated in order to force the offspring vector to move to another set of discrete values. The requirement that the variance  $\sigma_i^2$  has to be small cannot be fulfilled if the difference between two adjacent values is relatively large. For this reason, a used approach is to not change all the components of parent vectors but only a number  $l$  randomly chosen at every generation. This implies that the remaining  $(n - l)$  components of  $\vec{z}^{(g)}$  will have zero value and, given  $\delta_{x_i}$  as the difference between two adjacent discrete values, the mutation vector is:

$$\vec{z}^{(g)} = \begin{cases} (k + 1) \cdot \delta_{x_i}, & \text{for } l \text{ randomly chosen components} \\ 0, & \text{for the } (n - l) \text{ other components} \end{cases} \quad (3.44)$$

In eq.(3.44),  $k$  is a random integer number, which follows the Poisson distribution:

$$p(k) = \frac{\gamma^k}{k!} \cdot \exp(-\gamma) \quad (3.45)$$

in this way, the selected values are only the ones nearer to each other. The components  $l$  are selected by using a uniform distribution in every generation; the number of elements depends from the problem size, generally 1/5 of the total number of design variables.

The selection is performed in the same way as the continuous case and the procedure iterates until one of the following criteria is satisfied[60]:

- when the best value of the objective function in the last  $4n \cdot \xi/\lambda$  generations remains unchanged;
- when the mean of the objective values from all parent vectors in the last  $2n \cdot \xi/\lambda$  generations has not been improved by less than a threshold value  $\varepsilon_b$ , generally 0.0001;
- when the relative difference between the best OF (Objective Functions) value and the mean value of the OF from all parent vectors in the current generation is less than  $\varepsilon_c$ , generally 0.0001;
- when the ratio  $\xi_d/\xi$  reaches a given value  $\varepsilon_d$ , e.g.  $\varepsilon_d = 0.5 \div 0.8$ , where  $\xi_d$  is the number of the parent vectors in the current generation with the best objective function value.

### 3.9.3 Techniques to handle the constraints

As said before, the optimization algorithms are not able to deal directly with the boundary conditions and, in general, with constraints applied to the design dominion. Therefore, different techniques to handle them have been developed both for ES and SQP. Considering a set of constraints, for example displacements or stresses limits, the difference between number of constraints and design variables gives the degrees of freedom of the optimization problem. If all the (equality and inequality) constraints are removed and the degrees of freedom remain the same, then the number of variables decreases. The obtained reduced problem is called *unbounded optimization* and can be solved by the previous algorithms. However, the constraints cannot be simply removed and a method to consider them has to be adopted.

A way to work in proximity of the border is to penalize the objective function near the points that violate these limits, by sequential transformations of the objective function. These transformations take the name of *transformations with penalty*. The problem, e.g. the FE analysis, is performed without constraints and then for the obtained values the constraints violation is checked. If any of them are violated, a penalty is applied to the objective function with a value related to the degree of violation. Mathematically speaking, a given constraint  $k$  in the structural optimization can be expressed in the form:

$$g_k(\vec{x}) = |q_k(\vec{x})| - q_{\text{allow},k} \leq 0 \quad (3.46)$$

where  $q_k(\vec{x})$  is a response measure for the design vector  $\vec{x}$  (as stresses or displacements) and  $q_{\text{allow},k}$  is the maximum allowable absolute value of  $q_k(\vec{x})$ . The optimization problem subjected to this constraint is written as:

$$\min [f(\vec{x})], \quad \text{with the bound } g_k(\vec{x}) \leq 0 \quad (3.47)$$

The same problem can be expressed in its transformed form:

$$\min [f_p(\vec{x}, \vec{d})] = f(\vec{x}) \cdot \max\{\Phi(\vec{x})\}, \quad k = 1, \dots, m \quad (3.48)$$

$\Phi(\vec{x})$  is a *penalty function* that depends on the *vector of control parameters*  $q_k$ . For the sequential transformation  $\Phi_k(\vec{x})$  is defined as:

$$\Phi_k(\vec{x}) \begin{cases} 1, & \text{if } \frac{|q_k(\vec{x})|}{q_{\text{allow},k}} \leq 1 \\ \frac{|q_k(\vec{x})|}{q_{\text{allow},k}}, & \text{if } \frac{|q_k(\vec{x})|}{q_{\text{allow},k}} > 1 \end{cases} \quad (3.49)$$

the value  $q_k(\vec{x})$  is taken as the maximum (the worst) value between all the elements. For example, in a FE analysis this means that the value of the worst node is taken. In fig.3.7 an analytic representation of the penalty function is showed.

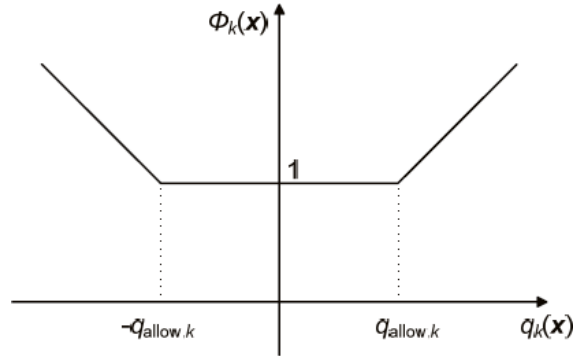


Figure 3.7: A multiple linear segment penalty function[60].

### 3.10 Multi-Objective optimization (MOP)

The real world design problems are long way from the straightforward single optimization case, involving many objective functions often in contrast between each other and require to the designer to make choices in order to select one of the multiple optimal solutions. For instance, cost and safety of a structure cannot strive toward the same solution, but this is not the only case, also some physical parameters are not compatible between each other and have to be treated separately. Whatever is the case, if the objective functions cannot be pooled in a single vector that converges to a unique optimum, the problem has to be considered as a *multi-objective optimization* (MOP). Since a unique solution does not exist, a trade-off between the possible designs has to be adopted and an *Optimum Pareto* generated to compare and select the optimal solutions. Many methods are possible to solve the multi-objective optimization problem, the most popular are:

- *perturbation method*: for each parameter a Pareto set is generated with one objective minimized while the others are constant.
- *Min-max method*: the Pareto set is generated by minimizing the distance between the values of the objective function and its possible maximum or the ensemble of objective values.
- *Programmed end method*: the optimization is performed with one objective fixed as maximum priority while the others are assumed as constrictions. The same is repeated for the minimum priority objective with the constraints that the optimal solution is fixed as maximum priority. Repeating this for every parameter generates a Pareto set.
- *Weighted sum method*: a weight factor is assigned to every objective depending on the designer sensibility. The weights have to be normalized and will give different Pareto curves from the unweighted case.
- *Space investigation parameters (PSI)*: an ensemble of design solutions that cover the entire design space is generated and, for each design, the objective functions are analysed generating restrictions. In this region an acceptable Pareto set is generated.

The formulation of the multiple-objective optimization problem is slightly different from the single-objective case:

- find the *design vector*  $\vec{x} = [x_1, x_2, \dots, x_n] \in \mathbb{R}^n$  (discrete, continuous or mixed depending on the problem), bounded in a domain  $\vec{x}_L \leq \vec{x} \leq \vec{x}_U$ , where  $(\vec{x}_L, \vec{x}_U)$  are the lower and upper bounds of the design variables on shape, typology of the structure, etc.;
- in  $X_i$ , the set of  $x_i$ , which may be continuous, discrete or integer. The whole design space for the  $n$  design variables can be denoted as  $\vec{X}$ ;
- that minimizes a vector of *objective functions*  $\vec{f}(\vec{x})$  that correspond to a design parameter, for example a limit in displacements, tension, etc. ( $\vec{f} \in \mathbb{R}^m$ );
- subjected to *inequality constraints*  $g_i(\vec{x}) \leq 0$ , where  $i = 1, 2, \dots, p$  are the number of inequality constraints ( $\vec{g} \in \mathbb{R}^p$ );
- and to *equality constraints*  $h_i(\vec{x}) = 0$ , where  $j = 1, 2, \dots, q$  are the number of equality constraints ( $\vec{h} \in \mathbb{R}^q$ );

In a synthetic way, the problem can be written as:

$$\begin{aligned}
 & \min[\vec{f}(\vec{x})], \quad \vec{x} = [x_1, x_2, \dots, x_n], \quad \vec{f} \in \mathbb{R}^m \\
 & \text{subjected to:} \\
 & \vec{g}(\vec{x}) \leq 0, \quad \vec{g} \in \mathbb{R}^p \\
 & \vec{h}(\vec{x}) = 0, \quad \vec{h} \in \mathbb{R}^q \\
 & x_i \leq X_i \quad \text{for } i=1, \dots, n \\
 & \text{bounded by} \\
 & \vec{x}_L \leq \vec{x} \leq \vec{x}_U
 \end{aligned} \tag{3.50}$$

A set of design vectors  $\vec{x}$  that satisfies the constraints of (3.50) is called *feasible set*,  $\vec{F}$ , and is a subset of  $\vec{X}$  ( $\vec{F} \in \vec{X}$ ):

$$\vec{F} = \{\vec{x} \in \vec{X} \mid \vec{g}(\vec{x}) \leq 0, \vec{h}(\vec{x}) = 0\} \tag{3.51}$$

The image of  $\vec{F}$  is called the *criterion space*  $\vec{V}_F = f(\vec{F})$ . All equality constraints (regardless of the value of  $\vec{x}$  used) are considered active at all points of the feasible set  $\vec{F}$ . A *feasible design* is a design vector  $\vec{x}$  that belongs to the feasible set  $\vec{F}$ .

### 3.10.1 Pareto distribution of the optimal solutions

In the multi-objective optimization (MOP) the concept of optimum is slightly different from the single-objective optimization (SOP). In SOP the feasible set is completely ordered according to the single value of the objective function  $f$  and can be easily compared in order to get the searched optimum. In MOP, instead, the solutions can be only partially ordered and more possible optimum have to be considered.

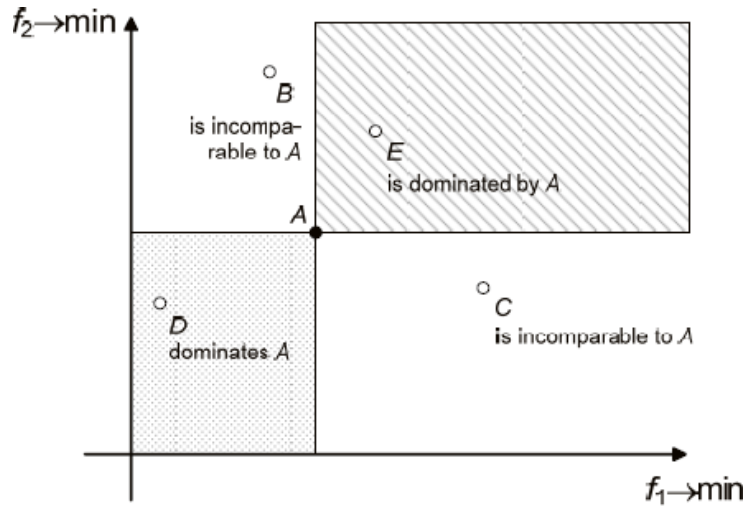


Figure 3.8: Dominated, dominating and incomparable regions with respect to point A in the objective space[60].

In fig.3.8 a two dimensional objective function vector  $\vec{f} = [f_1, f_2]$  is considered. A Pareto dominance in the design space between the different solutions is investigated, considering that the best value for a single term  $f_i$  of the objective function vector  $\vec{f}$  is the nearest to the corresponding

axis. Taking a reference point  $x^A$  represented on the criterion space by A, abbreviation of  $\vec{f}(x^A)$ , there are four areas defined by it.

For any point in the area dominated by A there are only worse solution  $\vec{f}(x^E)$  to the problem, while for any point in the area that dominates A every solution  $\vec{f}(x^D)$  is better than  $\vec{f}(x^A)$ . The points out of these two areas are not comparable to  $\vec{f}(x^A)$  because they are better (or worse) in only one element of the vector.

Mathematically, this concept is expressed by defining the Pareto notation[60]:

- *weak Pareto dominance*: an objective vector  $\vec{u}$  is said to *weakly dominate* the objective vector  $\vec{v}$  ( $\vec{u} \succeq \vec{v}$ ), if and only if:

$$u_i \leq v_i \quad \forall i = 1, \dots, n; \quad (3.52)$$

- *Pareto dominance*: an objective vector  $\vec{u}$  is said to *dominate* the objective vector  $\vec{v}$  ( $\vec{u} \succ \vec{v}$ ), if and only if:

$$u_i \leq v_i \quad \forall i = 1, \dots, n \quad (3.53)$$

and  $u_i < v_i$  for at least one value of  $i = 1, \dots, n$ ;

- *strict Pareto dominance*: an objective vector  $\vec{u}$  is said to *strictly dominate* the objective vector  $\vec{v}$  ( $\vec{u} \succ \vec{v}$ ), if and only if:

$$u_i < v_i \quad \forall i = 1, \dots, n; \quad (3.54)$$

- *incomparability*: two objective vectors  $\vec{u}$  and  $\vec{v}$  are *incomparable* ( $\vec{u} \not\prec \vec{v}$ ) if neither  $\vec{u} \succ \vec{v}$  nor  $\vec{v} \succ \vec{u}$ ;
- *rank*: the rank of an individual indicates the order of dominance respect to the others. A rank 1 individual is not dominated by any other, a rank 2 is dominated by the rank 1 individuals, a rank 3 by the 1 and 2 and so on;
- *local Pareto optimality*: a design vector  $\vec{x}' \in \vec{F}$  is said to be a *local Pareto optimal design vector* if, and only if, there is a neighbourhood  $\vec{\chi}$  of  $\vec{x}'$  in which there exists no other  $\vec{x} \in \vec{\chi}$  such that  $\vec{f}(\vec{x}) \succ \vec{f}(\vec{x}')$ ;
- *global Pareto optimality*: a design vector  $\vec{x}^* \in \vec{F}$  is said to be a *global Pareto optimal design vector* if, and only if, there exists no other  $\vec{x} \in \vec{F}$  such that  $\vec{f}(\vec{x}) \succ \vec{f}(\vec{x}^*)$ . Or also, there is no other  $\vec{x} \in \vec{F}$  such that:

$$f_i(\vec{x}) \leq f_i(\vec{x}^*) \quad \forall i = 1, \dots, n \quad (3.55)$$

with  $f_i(\vec{x}) < f_i(\vec{x}^*)$  for at least one objective function  $i$ . Of course, a global Pareto optimum is also a local Pareto optimum while the reverse is not necessarily true;

- *Pareto set  $P^*$* : is the set of all the Pareto optimal design vector  $\vec{x}^* \in \vec{F}$ . That is, the group of all the non-dominated objective vectors that satisfy:

$$P^* = \{\vec{x}^* \in \vec{F} \mid \text{there is no } \vec{x} \text{ such that } \vec{f}(\vec{x}) \succ \vec{f}(\vec{x}^*)\} \quad (3.56)$$

- *Pareto front*: is the image of a Pareto set  $P^*$  in the objective function space. The fig.3.9 shows a Pareto front for a bidimensional objective function. In the feasible region, the empty dots show the dominated solutions while the solid ones the incomparable solutions.

From this analysis, it is evident that, in the multi-objective optimization, there is not a single optimal solution but many possible ones to choose from and that the designer has to accept and define a trade-off between them.

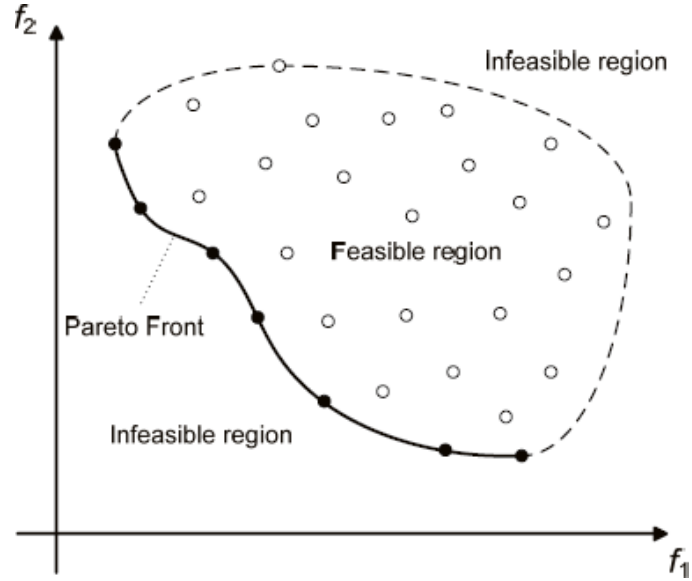


Figure 3.9: Dominated, feasible region and corresponding Pareto Front in the objective space for a bidimensional problem[60].

### 3.10.2 Selection criteria

The choice of the optimal solution in the MOP can be done according to different criteria formulated to define in a clearer way the problem and the trade-offs. Remarking that these criteria have to be applied only if a form of conflict exist between the solutions, here are stated some definitions about conflict:

- *local collinearity*: two OFs  $f_i$  and  $f_j$  are said to be *local collinear* with a no conflict point  $\vec{x}$ , if there is a  $c > 0$  such that

$$\nabla f_i(\vec{x}) = c \cdot \nabla f_j(\vec{x}) \quad (3.57)$$

otherwise, the functions are called *locally conflicting* at point  $\vec{x}$ . According to this definition, any two OFs are locally conflicting at a point of the design space if their maximum improvement is achieved in different directions;

- *global conflict*: two objective functions  $f_i$  and  $f_j$  are *globally conflicting* in the feasible region  $\vec{F}$  of the design space if the two single-objective optimization problems:

$$\min f_i(\vec{x}), \quad \vec{x} = [x_1, \dots, x_n]^T, \quad \vec{x} \in \mathbb{R} \quad (3.58)$$

$$\min f_j(\vec{x}), \quad \vec{x} = [x_1, \dots, x_n]^T, \quad \vec{x} \in \mathbb{R} \quad (3.59)$$

have different optimal solutions in the feasible region  $\vec{F}$  of the design space.

There are two phases in the solving of MOP: the *search* and the *decision making*[27]. During the search, the group of optimal solutions in the feasible set for Pareto is found. Decision making consists instead in choosing a suitable compromise among the Pareto optimal solutions and can be done in different way:

- *decision making before search*: the objectives of the MOP are aggregated and the multi-objective problem is transformed in a single-objective one. This option requires a profound

knowledge of the solution domain because each choice in this sense influences significantly the final results;

- *decision making after search*: the analysis is performed without any preference given. After that, the designer chooses a trade-off and a final design among the possible ones. For unexplored domain it is the best approach although it implies an increase of complexity;
- *decision making during search*: after each optimization step a number of alternative trade-offs is presented and the decision maker specifies further preferences informations, guiding the search process. The final results are heavily influenced by the adopted choices that sometimes may be obscure to the designer being hidden in the optimization process.

### 3.10.3 Standard methods to solve the MOP

According to Marler and Arora[43], in the light of the decision making process previously stated, the multi-objective optimization methods can be divided in:

- methods with a priori articulation of preferences;
- methods with a posteriori articulation of preferences;
- methods with no articulation of preferences.

The a priori methods are attractive because they transform the multi-objective problem in a single-objective one with different weights of the objective functions. These methods are called *standard methods* and are not necessary initially fixed by the designer but may also change during the analysis automatically. The main limits in this approach are that:

- some techniques may be sensitive to the shape of the Pareto Front;
- problem knowledge is required to perform the analysis;
- many analysis have to be performed and this may become cumbersome for the complex practical applications.

However, when the size of the problem increases, the non a priori methods become inapplicable because too many variables are involved and the designer would not be able to make decisions directly. Below are reported some popular standard methods adopted in the MOP.

#### Linear Weighting Method (LWM)

The LWM[14] combines all the objectives into a single scalar parametrized objective function by using weighting coefficients. A coefficient  $w_i$  is adopted for every  $i^{th}$  OF ( $i = 1, \dots, m$ ) and the optimization problem of eq.(3.50) can be written as:

$$\min \sum_{i=1}^m w_i \cdot f_i(\vec{x}), \quad \vec{x} \in \vec{F} \quad (3.60)$$

The weighting coefficients have to be normalized so that  $\sum_{i=1}^m w_i = 1$ . The weight of every function corresponds to its importance and every combination of weighting coefficients corresponds theoretically to a single Pareto optimal solution. In this way, a full a set of Pareto optimal solutions is generated. If the weights are not already normalized, the following formulation can be used:

$$\tilde{w}_i = \frac{w_i}{\sum_{j=1}^m w_j} \quad (3.61)$$

and if the optimized functions have different physical dimension (for example costs and displacements) they have to be normalized in the following way:

$$\tilde{f}_i(\vec{x}) = \frac{f_i(\vec{x}) - f_{i,min}}{f_{i,max} - f_{i,min}}, \quad \tilde{f}_i(\vec{x}) \in [0,1] \quad (3.62)$$

where  $f_{i,max}$  and  $f_{i,min}$  are, respectively, the maximum and minimum value that the function can assume in the design space.

The main disadvantage of the LWM is that it relies on the weights assigned by the designer that can influence significantly the results of the analysis. The optima for a fixed distribution have not necessary an equal Pareto set of a not weighted one and, moreover, this method can be applied only to convex problems. In fact, the use of weights may trap the solution in local optima and a proper Pareto set could not be generated.

### Distance Function Method (DFM)

The distance methods[65] are based on the minimization of the distance between the set of OF values and a group of chosen reference points  $\vec{z}^{id} = [z_1, \dots, z_m]^T$  in the criterion space  $\vec{V}_f = f(\vec{F})$ . The technique, applied in the structural field, results in transforming eq.(3.50) in:

$$\min d_p(\vec{x}), \quad \vec{x} \in \vec{F} \quad (3.63)$$

where  $d_p(\vec{x})$  is a distance function expressed as

$$d_p(\vec{x}) = \left[ \sum_{i=1}^m w_i \cdot (f_i(\vec{x}) - z_i)^p \right]^{1/p} \quad (3.64)$$

where  $p$  is an integer number. The reference points take also the name of *utopian points* and are selected by the designer. A typically used reference point is:

$$\vec{z}^* = [f_1^*, \dots, f_m^*] \quad (3.65)$$

that collects the optimum solutions of each single optimization problem  $f_i^*$  ( $i = 1, \dots, m$ ), treating each  $f_i$  as a single objective separated case. The normalization criteria of eq.(3.61) can be used if necessary. In the special case of  $p = \infty$ , eq.(3.63) becomes:

$$\min \{ \max [w_i \cdot f_i(\vec{x})] \}, \quad \text{for } i = 1, \dots, m \quad (3.66)$$

and takes the name of *minimax optimization*. If instead  $p = 1$ , the DFM becomes equivalent to the LWM when the reference point used is zero ( $\vec{z}^{id} = 0$ ). For  $p = 2$  the method is called *Weighted Quadratic Method*.

### Constraints method

The constraint method[24] replaces the original  $m$  dimensional MOP with a scalar one with  $m$  objectives. Chosen the main objective  $f_k$ , only this function is kept and all the other  $(m - 1)$ , called additional objectives, are moved into the constraints. A set of parameters  $\varepsilon_i$  ( $i = 1, \dots, m$ , with  $i \neq k$ ) and the corresponding  $(m - 1)$  constraints are written as:

$$f_i(\vec{x}) \leq \varepsilon_i, \quad i = 1, \dots, m \text{ with } i \leq k \quad (3.67)$$

The resulting equivalent single-objective optimization problem is:

$$\begin{aligned}
 & \min[f_k(\vec{x})], \quad \vec{x} = [x_1, x_2, \dots, x_n], \quad f_k \in \mathbb{R} \\
 & \text{subjected to:} \\
 & \vec{g}(\vec{x}) \leq 0, \quad \vec{g} \in \mathbb{R}^p \\
 & \vec{h}(\vec{x}) = 0, \quad \vec{h} \in \mathbb{R}^q \\
 & f_i(\vec{x}) \leq \varepsilon_i, \quad i = 1, \dots, m \text{ with } i \leq k \\
 & x_i \leq X_i \quad \text{for } i=1, \dots, n \\
 & \text{bounded by:} \\
 & \vec{x}_L \leq \vec{x} \leq \vec{x}_U
 \end{aligned} \tag{3.68}$$

Every solution is a point of the Pareto Front of the original MOP. By using various parameters  $\varepsilon_i$  a full Pareto set can be drawn. This technique has the big advantage to be not biased towards convex portion of the Pareto front and is able to obtain solutions associated with non-convex parts of the trade-off curve.

### 3.10.4 Evolutionary Algorithms for solving multi-objective optimization problems

The standard gradient methods proposed to solve the MOP have been recently flanked by the EAs methods that allows to handle large search spaces and generate multiple alternative trade-offs in a single optimization run, avoiding the difficulties encountered by the standard methods. By working simultaneously on a population of design points, instead of a single one, EAs have a great potential in finding the full Pareto front and are less computationally onerous. Overall, EAs outperform the gradient methods in most MOP applications and are enough flexible to apply the standard methods but also more elaborated approaches out form the analytical field.

#### Evolution strategies combined with LWM

The application of the Evolution strategies combined with LWM method consists is a popular solution for the analysis of MOP problems despite the limits stated before. A set of parent design vectors is defined with their weighting coefficients to combine all the objectives in a single scalar parametrized function. The weighting coefficients are not set by the designer but are systematically varied by the optimizer after a Pareto optimal solution has been achieved. An outer loop varies the parameters of the parametrized function, called *decision making loop*. The inner loop consists in the classical ES algorithm that starts with an initial set of parents vectors modified until when a feasible design is reached, then, the offsprings are generated and their belonging to the feasible region checked. Using the  $(\xi, \lambda)$  or  $(\xi + \lambda)$  method the selection is operated; this procedure is repeated until the chosen termination criteria is satisfied. The general algorithm is showed in tab.3.1.

Table 3.1: Evolution strategies LWM algorithm[60]

---

**Evolution strategies LWM algorithm**

---

**Outer loop - Decision Making**  
Set the parameters  $w_i$  of the parametrized objective function

**Inner loop - ES loop**

1. *selection step*: selection of  $x^i$  ( $i = 1, \dots, \xi$ ) parent vectors of the design variables;
2. *analysis step*;
3. evaluation of the *parametrized objective function*;
4. *constraints check*: all parent vectors become feasible to perform the control;
5. *offspring generation*: generate  $x^j$  ( $j = 1, \dots, \lambda$ ) offspring vectors of the design variables;
6. *analysis step*;
7. evaluation of the *parametrized objective function*;
8. *constraints check*: if satisfied continue, else change  $x^j$  and go to step 5;
9. *selection step*: of the next generation parents according to  $(\xi, \lambda)$  or  $(\xi + \lambda)$  scheme;
10. *convergence check*: if satisfied stop, else go to step 5.

**End of Inner Loop**

**End of Outer Loop**

---

### 3.11 Probabilistic based design optimization

The *performance based design* defines explicitly the performances required to the system by setting a *performance function* in terms of value, class or level of behave of the system or of one of its sub-parts. This approach is widely adopted today and provided by the codes since it aims to quantify directly the satisfaction of every design requirement. In this framework, considerations about the uncertain of the parameters entering in the design cannot be neglected since they influence significantly the performance: epistemic and aleatory uncertainties affect either resistance and actions, leading the behaves far from the prefixed target. Even if the design parameters might be determined accurately, they would however change along the service life for ageing or changing in the utilization of the structure itself. The *deterministic optimization* shows all its limits in a performance approach, operating at the limits of the design space by not keeping into account the possible fluctuations around the design point with the possibility to cause unreliable designs with catastrophic effects. Considering that, two forms of probabilistic optimization have been developed:

- *Reliability Based Design Optimization*(RBDO): the reliable design aims to keep low the probability of exceeding a fixed threshold (generally corresponding to the system failure) by satisfying an objective function of minimum costs coupled with limitations on the allowable limit failure probability;
- *Robust Design Optimization*(RBO): the robust design is capable to contain the variation of the performance function under the uncertainties that may affect the design parameters.

#### 3.11.1 Reliability Based Design Optimization (RBDO)

The RBDO aims to reach the lowest failure probability for the minimum costs of the structure and is formally a multi-objective optimization. Indeed, it is possible to consider the reliable design as a multi-criteria optimization where the bi-dimensional OF vector contains the costs and the failure probability. More often, the two functions are pooled by using the LWM explained in sec.3.10.3 and optimized together. The RBDO is characterized by two steps:

1. characterize the uncertain variables and the failure modes using statistical models. It is important to grant a reliability respect to each of the critical failure modes, thus the definition phase is fundamental for a correct optimization;
2. perform the optimization by substituting the critical failures of the deterministic case with constraints on the probability of failure corresponding to each of the failure driven modes or with a single constraint on the probability of failure of the system.

The RBDO is more efficient than a normal deterministic optimization and yields to safer and cheaper designs. On the other hand, the solution of the RBDO is not easy, even for simple structures, due to the high computational effort that implies the analysis of several distributions of design parameters. It is difficult to characterize every parameter from the probabilistic point of view and every error in this sense may induce big differences in the final failure probability. Indeed, the reliability design method may not be so practical if there are not enough data to characterize the system properly.

### Formulation of the RBDO problem

In a synthetic way the problem RBDO can be written as:

$$\begin{aligned}
 & \min[f(\vec{x})], \quad \vec{x} = [x_1, x_2, \dots, x_n], \quad \mathbf{F} \in \mathbb{R}^m \\
 & \text{subjected to:} \\
 & \vec{g}(\vec{x}) \leq 0, \quad \vec{g} \in \mathbb{R}^p \\
 & \vec{h}(\vec{x}) = 0, \quad \vec{h} \in \mathbb{R}^q \\
 & P[y(\vec{x}, \vec{R}) \leq 0] \leq P_f, \quad \vec{R} \in \mathbb{R}^m \\
 & x_i \leq X_i \quad \text{for } i=1, \dots, n \\
 & \text{bounded by} \\
 & \vec{x}_L \leq \vec{x} \leq \vec{x}_U
 \end{aligned} \tag{3.69}$$

where:

- $\vec{x} = [x_1, x_2, \dots, x_n]^T$  are the  $n$  deterministically fixed design parameters;
- $\vec{R} = [R_1, R_2, \dots, R_m]^T$  are the  $m$  random variables entering in the design;
- $X_i$  is the set of  $x_i$ , which may be continuous, discrete or integer. The whole design space for the  $n$  design variables can be denoted as  $\vec{X}$ ;
- $f(\vec{x})$  is a scalar function to be minimized;
- $g_i(\vec{x}) \leq 0$ , where  $i = 1, 2, \dots, p$  are the number of inequality constraints ( $\vec{g} \in \mathbb{R}^p$ );
- $h_j(\vec{x}) = 0$ , where  $j = 1, 2, \dots, q$  are the number of equality constraints ( $\vec{h} \in \mathbb{R}^q$ );
- $P[y(\vec{x}, \vec{R})]$  denotes the design probability of failure assumed  $y(\vec{x}, \vec{R})$  as the limit state function of the system;
- $P_f$  is the threshold value for the probability of failure.

The final aim is that the system does not exceed a fixed threshold of failure probability in its life-cycle. In the RBDO problem some of the parameters may be both design variables and random variables of the problem. In this case, the mean value of the parameter is assumed as design variable for the calculation of the objective function and the deterministic constraints, while the PDF of the parameter is used for the calculation of the probability of failure using a stochastic analysis process.

### 3.11.2 Robust Design Optimization (RDO)

The main limits of the RBDO approach are in the difficulties of an accurate description of the distributions of parameters that enter in the analysis. Considering that a small difference in these distributions may implies significant changes in the results, it is necessary a big effort in order to characterize properly these data and perform a correct reliable design. The RDO overcomes this problem by focusing on limiting the sensitivity of the structure to changes that enter in the design parameters. The literature sets three steps to perform the robust optimization:

1. the conceptual project with the develop and the configuration of the system;
2. the design of the system parameters by the identification of the control ones;
3. the project of the acceptable tolerances in the design variables.

Each designed element is prone to variations from the initial design configuration, either due to changes in the expected actions or to the degradation of its properties along the service life. The Japanese engineer Taguchi introduced in the 1986 the concept of *robust optimization* as "*the state in which the performance of a product or a process is sensible in the minimum measure to the external factors that cause this variability*". A specific terminology was introduced to describe the robust optimization:

- *failure mode*: of the system that may occur;
- *noise parameters*: on which the designer has not control of the nominal value, they are imposed either by the environment or by the unacceptable costs for their control;
- *control parameters*: on which the designer has control of the nominal value and have to be optimized in order to minimize the sensitivity to the noise;
- *critical parameter*: that affects mostly the final performance of the product or that is difficult to be kept on the design nominal value.

The design parameters that can influence the final performances of the system take the name of *signal parameters* and are then divided in *basic design parameters* and *derived design parameters* if dependent to other ones or not. In the structural field the basic design parameters are: the geometry, the mechanical properties of the material (Poisson coefficient, shear modulus, yielding and ultimate strength, etc.) and the environmental factors (moisture, temperature, loads, etc.).

In simple words, the robust approach is reduced to the minimization of the ratio noise over signal for the variation of every parameter of design in a defined range. Although this ratio is easy to be obtained, the number of parameters may be difficult to be handle in terms of simulation and many statistical techniques have been developed to reduce the consequent computational effort. As first approximation, instead of defining an entire distribution of the parameters, only the mean and variance of the objective function are analysed. In fig.3.10 a graphical representation of a robust design compared with a deterministic one is showed: considering on the horizontal axis the objective function (OF) to be minimized and on the vertical axis the PDF of the OF, the two design approaches are compared.

The curve a) (dashed) shows the typical result of a deterministic optimization: the mean of the OF is minimized but the the outcomes are spread along the axis either in better than in negative design configurations. The curve b) (continue) is an example of robust approach to design: the OF mean,  $\mu_{OF}$ , is optimised together with its standard deviation,  $\sigma_{OF}$ , the two parameters are in conflict and a MOP has to be performed. The final result is that the RDO is worse than the deterministic optimization in terms of mean value due to the chosen trade-off between performance and deviation but better perform on the latter. In the figure, the characteristic fractile ( $p_f = 0.95$ ) is extracted for both cases, showing that the RDO results definitively in a more reliable design.

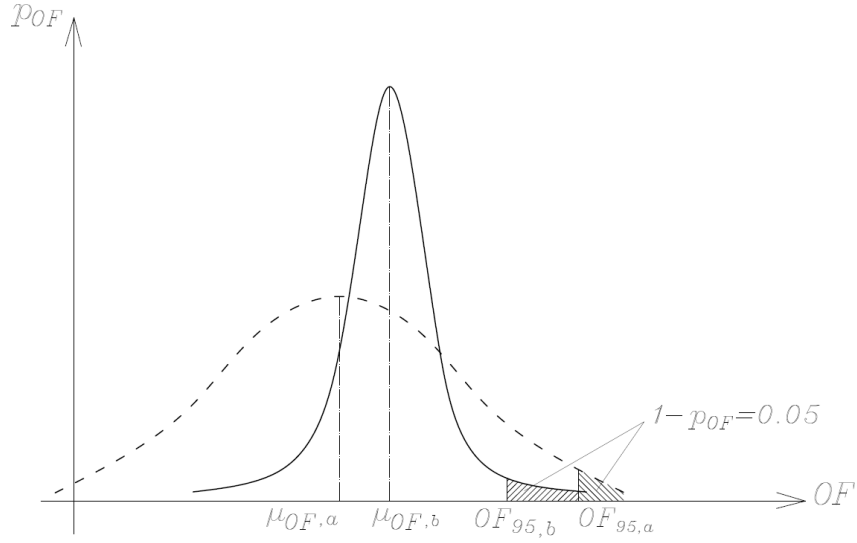


Figure 3.10: Approaches to the design: a) deterministic design approach (dashed line), b) robust design approach (solid line).

### Formulation of the RDO

Mathematically, the RDO can be defined as a multi-objective optimization involving the mean and standard deviation of the OF:

$$\begin{aligned}
 & \min [f(\vec{x}), \sigma_u(\vec{x}, \vec{R})], \quad \vec{x} = [x_1, x_2, \dots, x_n], \quad f \in \mathbb{R}, \sigma_u \in \mathbb{R} \\
 & \text{subjected to:} \\
 & \vec{g}(\vec{x}) \leq 0, \quad \vec{g} \in \mathbb{R}^p \\
 & \vec{h}(\vec{x}) = 0, \quad \vec{h} \in \mathbb{R}^q \\
 & x_i \leq X_i \quad \text{for } i=1, \dots, n \\
 & \text{bounded by:} \\
 & \vec{x}_L \leq \vec{x} \leq \vec{x}_U
 \end{aligned} \tag{3.70}$$

where:

- $\vec{x} = [x_1, x_2, \dots, x_n]^T$  are the  $n$  design parameters (or control parameters);
- $\vec{R} = [R_1, R_2, \dots, R_m]^T$  are the  $m$  random variables that enter in the design (or noise parameters);
- $X_i$  is the set of  $x_i$ , which may be continuous, discrete or integer. The whole design space for the  $n$  design variables can be denoted as  $\vec{X}$ ;
- $f(\vec{x})$  is a scalar function to be minimized;
- $g_i(\vec{x}) \leq 0$ , where  $i = 1, 2, \dots, p$  are the number of inequality constraints ( $\vec{g} \in \mathbb{R}^p$ );
- $h_j(\vec{x}) = 0$ , where  $j = 1, 2, \dots, q$  are the number of equality constraints ( $\vec{h} \in \mathbb{R}^q$ );
- $\sigma_u(\vec{x}, \vec{R})$  is the standard deviation of the response measure to be minimized.

The key passage in the robust design is the definition of the objective function, once that this has been done the solution can be treated by the use of statistical instruments.

### **RDO and RBDO comparisons**

RDO method primarily seeks to reduce the probability of failure at the tails of the distribution while RBDO method tries to control the spread around the mean value. Since the two approaches are not mutually exclusive, they can be considered as complementary, that is, a good project have to be both robust and reliable. Referring to fig.3.10, the effect pursued by RBDO can be indirectly obtained by applying RDO because a reduction of the spread implies a reduction of the failure probability. However, a quantitative direct comparison is not possible because they optimize different parameters.

## Chapter 4

# Tuned Mass Dampers

The first formalization of the *Tuned Mass Damper* (TMD) technology dates at the beginning of the 19th century by Frahm[20] as a simple added mass properly tuned with the main system. Since then, the TMD has been developed and applied in many designs and nowadays is an established technology in many fields. The TMD enters in the group of vibrations reduction external devices and aims to deal with a wide range of problems, from mechanic machineries to space applications, including many structural aspects concerning wind, seismic actions or traffic. The major attractiveness of TMDs are to be inherently stable and in the possibility to perform several times, both in exercise conditions than during the major earthquakes, without necessity of any connection to the ground.

The basic concept behind TMD is to add a small mass, of the order of 5% ÷ 10% of the mass of the main system, properly tuned with the latter. In resonance conditions the TMD moves out of phase from the main system and reduces its vibrations. The use of simply an added mass would only shift the resonance and the system is usually coupled with damping devices that allows the dissipation of the energy transferred from the main system to the TMD. The technology is quite effective but sensible to deviations from the design target with the risk of uneven amplifications, therefore, an accurate design has to be performed.

In this chapter, the main aspects of control of vibrations are briefly presented, then an historical description of TMD technology and of its recent develops are exposed, followed by an analysis of the dynamic of TMD with some applications in the structural field. After that, the robust optimization of TMD is presented together with the direct perturbation method adopted for it.

### 4.1 Control of vibrations

The dynamic actions are more onerous than the static ones adopted in design: they are difficult to predict, dependent on the characteristics of the structure and involve stricter design constrictions. Nevertheless, the costs of an ordinary stiffening of the structure are often unacceptable either from an aesthetic than sustainable point of view. To overcome this problem, the use of external dissipative devices has been introduced in control of vibrations. Let consider the energetic contributes that enter in the energy balance of a system subjected to dynamic excitation:

$$E_{in} = E_k(t) + E_c(t) + E_h(t) + E_{el}(t) \quad (4.1)$$

where:

- $E_{in}$  is the total energy introduced in the system by external dynamic actions;

- $E_k$  is the quote of input energy converted in kinetic due to the motion of the system that causes inertial forces and displacements;
- $E_c$  is the quote of energy absorbed by the system for elastic viscous effects;
- $E_h$  is the quote of energy absorbed by the system for hysteretic friction effects;
- $E_{el}$  is the quote of energy absorbed by the system for elastic deformations;

An ordinary civil structure presents a damping ratio  $\xi_0 \approx 0.05$ ; remembering that the latter includes contributes from  $E_c(t) + E_h(t)$ , this means that a structure relies mostly on the elastic contribute  $E_{el}$  and  $E_k$  to balance the introduced energy. The final effects are high displacements and inertial forces involving wide damages and, eventually, the collapse.

In seismic design, the typical approach for ordinary structures is to increase significantly the term  $E_h(t)$  by defining a controlled sequence of collapse. Lots of energy is dissipated during destructive earthquakes, leaving the structure heavily damaged but not collapsed, while for weaker events the structure remains in elastic field and only small damages occur. This approach, called *capacity design*, constitutes a good compromise compared to the costs of an elastic design for high magnitude earthquakes. However, if a spread damage is accepted in ordinary buildings, it is not the same for strategic structures and infrastructures. In hospitals, civil protection centres or bridges, that are fundamental during the civil defence operations, the operativity must be granted to allow the rescue operations to be performed. There are also situations in which architectural constraints would not allow a particularly stiff construction and the limits in design can be only surpassed by optimizing the response of the system to the dynamic actions: high rise buildings, slender bridges and similar structures would be economically unacceptable and, moreover, ugly, without the use of supplemental devices. To all these cases have to be added the existing structures and infrastructures that were not designed with the actual codes and need to be adequate to the current state of art in dynamic design.

For all the previous reasons, in many cases, it is necessary to introduce external devices to reduce the expected dynamic actions. A first classification divides them between:

- *passive systems*: they act when the excitation is applied without any activation device, changing the dynamic response of the system permanently;
- *semi-active systems*: they use the motion of the structure to generate control forces and are activated by electric or magneto-electric systems. During the event, the electronic system controls the forces to adapt the configuration to the external actions;
- *active systems*: they use a system of actuators that generate the control forces and are activated by electric or magneto-electric systems. During the event, the electronic system controls the forces to adapt the configuration to the external action recorded, while the electric power supplies the actuator;

The active and semi-active systems are more flexible solutions thanks to the adaptability to the evolution of the external action; on the other hand, they are sensible to damages in the electronic system and require an electric energy supply (especially the active one that may require megawatt or even gigawatt of power depending on the structure).

Either in passive, active or semi-active form, the most used technologies today are:

- *dissipative added systems*: they increase the term  $E_h$  of eq.(4.1) by the introduction of added mechanisms of dissipation as steel yielding, viscous fluids compression, friction mechanisms and so on. According to their configuration, these systems may even add a stiffness to the structure by moving its period to higher values far from the resonance (see fig.1.4).

- *Insulation systems*: they act directly on the term  $E_{in}$  of eq.(4.1) by adding an intermediate high deformability element between foundations and structure. The element acts as filter to the lower frequencies and lets pass only the higher ones that are far from the resonance. The effect is that the first mode is prevalently translational, with a low energy content and involves the 90% of the mass of the structure. This system is passive and works only for base excitations.
- *Tuned Mass Dampers*: the technology adds one or more masses to the system. If properly designed, the motion of this elements is out of phase respect to the structure, with the effect of a significant reduction of vibrations. The system acts on the term  $E_c$  of eq.(4.1), adding a damping contribute (for this reason sometimes it is coupled with other dissipative systems) and on  $E_k$  and  $E_{el}$ , by adding to the system an elastic and inertial force.

The focus of this study is on Tuned Mass Dampers, remanding the reader to the wide bibliography produced about the others for further details.

## 4.2 Historical development of TMD

The first applications of TMD were performed by Frahm in the 1909 that received a US patent for his projects[20]. He considered a simple system with stiffness  $k_s$  and mass  $m_s$  excited by an harmonic excitation  $f(t) = f_0 \cdot \sin(\omega_f \cdot t)$ , as showed in fig.4.1. An added mass  $m_t$  is connected to the main system by a spring of stiffness  $k_t$  without any damping device. Frahm demonstrated that the main system motion could be totally stationary if the absorber frequency is set on  $\omega_t = \sqrt{k_t/m_s}$ , i.e., the frequency of the excitation.

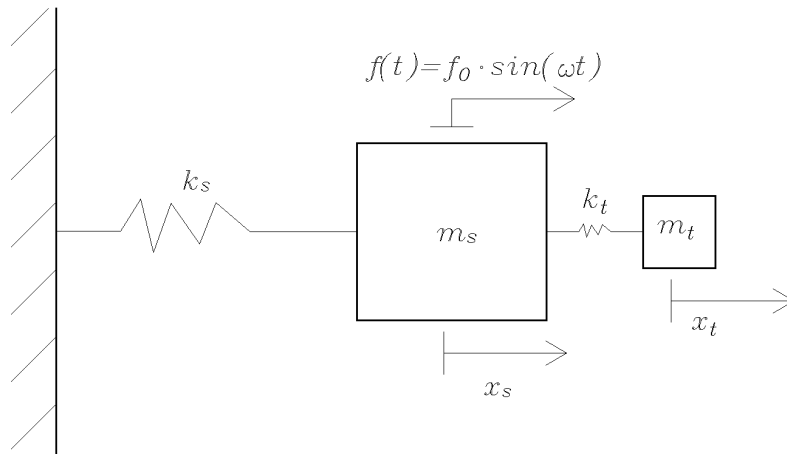


Figure 4.1: Model of the Frahm absorber system.

The first studies about the use of damped absorber were performed by Dean Hartog in 1929[49], with the hypothesis of negligible main system damping, setting the basis design principles. He performed a study with damped and undamped absorber showing that, even if the results on the main system were satisfactory, the undamped one vibrated with too high amplitude and the resonance was not avoided but only shifted in frequency(fig.4.2).

The introduction of a damping system limits the sensitivity to changes in the main system frequency from the design target. By balancing two fixed points in the frequency response, Den

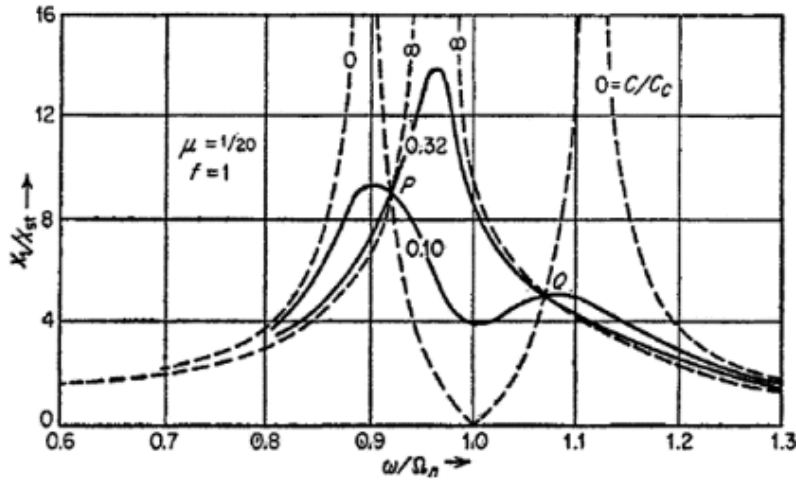


Figure 4.2: Magnification factor of displacement  $D = X_f/X_{st}$  for different damping ratio  $\xi = C/C_c$  and frequency ratio  $\beta = \omega/\Omega_n$ [17]. The mass ratio is fixed at  $\mu = 1/20 = 5\%$  and the TMD is perfectly tuned,  $f = \omega_{tmd}/\Omega_n = 1$ .

Hartog demonstrated that the optimal tuning ratio  $\rho_t = \omega_t/\omega_s$  and damping ratio  $\xi_t$  for an auxiliary single mass attached to an undamped SDF system are:

$$\rho_t^{opt} = \frac{1}{1 + \gamma_t} \quad (4.2)$$

$$\xi_t^{opt} = \sqrt{\frac{3\gamma_t}{8(1 + \gamma_t)}} \quad (4.3)$$

where  $\gamma_t = m_t/m_s$  is the mass ratio. The damping of the main system was introduced only later by Welbourn and Bishop that performed many analysis on STMD and introduced the possibility to use more tuned masses (MTMD)[5]. The reasons for the use of more absorbers were the operative limitations in the installation of a single TMD, the very narrow band of suppression frequency and sensitivity to fluctuation in the tuning operations. The mistuning of the STMD decreases significantly the effectiveness of the system with the risk to create undesired amplifications[37]. The first applications about the use of a double mass damper were studied by Iwanami and Seto[29]. Other solutions considers the use non-linear springs to extend the frequency response range but with a complication in the iterative optimization techniques.

### 4.3 Recent developments in TMDs analysis

The studies about TMDs have focused in recent years on the parameters that may affect the final performances and the best choices for the optimization balancing the computational costs of the analysis. Overall, all these studies are in accordance about the fact that MTMD has similar or better performances compared to STMD depending on the objective function assumed, and always higher robustness. Increasing the mass ratio improves the performances, decreases the necessary damping ratio, widens the bandwidth and decreases the tuning ratio of the TMDs. Increasing the damping ratio of the main system implies a diminution of effectiveness because the system already behaves well under dynamic actions. Fixed these points, the researches attained similar results but not always in accordance between each other, depending also from the analysis parameters.

Xu and Igusa[63] proposed a model for the use of MTMD with distributed natural frequencies that was then studied by many others.

Joshi and Jangid[30] calculated the equivalent added damping for different tuning ratio, bandwidth and damping ratio of a uniformly distributed MTMD applied to a generic SDF system, using the Root Mean Square (RMS) of displacement for separated modal shapes under a white noise excitation. Increasing the mass ratio led to smaller damping ratios and higher uniform tuning ratio of TMDs, especially for the MTMD rather than the single TMD.

Based on the various combinations available of stiffness, mass, damping coefficient and damping ratio in the MTMD, the five MTMD models have been presented by Li and Qu[36]. Li showed also, by using optimization techniques, that the MTMD with the identical stiffness and damping coefficient, but unequal mass and damping ratio, provides better effectiveness and wider optimum frequency spacing (identical to higher robustness against the change of the estimation error in the structural controlled natural frequency) with respect to the rest of the MTMD models[35]. The studies conducted by Lin opened a further branch of research in the field of MTMD, considering different combinations of parameters to reach a higher efficiency.

Wu and Ghenda[61] separated in groups the TMDs in a structure according to the modal shapes suppressed by them and optimized each group in terms of tuning ratio, damping ratio and position respect to the variance of response under a seismic input. According to the modal shape studied, or to the global RMS of the displacements, different better positions were found.

Zuo and Nayef[67] optimized the stiffness and damping of the MTMD applied on a SDF system referring to the RMS of displacement under a base acceleration. They also showed that the high frequencies peaks are better suppressed by the system respect to lower ones.

Hoang and Warnitchai[25] used a gradient search for the tuning and damping ratio of a MTMD system for either uniform and free parameters under a white band excitation. Overall, the bigger the uncertainties on the system parameters, the wider was the bandwidth and the higher the damping ratio required to the TMDs. They showed also that the behave for fixed uniform damping ratio for the dampers is not so far from having free parameters, while imposing uniform tuning ratio affects significantly the performances of the MTMD.

Similar results have been found by Patil and Jangid[52] in the optimization of bandwidth, tuning ratio and mass ratio on the 1<sup>st</sup> modal shape of a 40 storeys benchmark building excited by wind. Between the results, they showed also that increasing the number of TMDs over a certain values does not lead to better performances. Similar results were found later by Patil et al.[51], in a comparison of single TMD and MTMD, optimizing the mass ratio and number of dampers.

Lee et al.[33] proposed an iterative method for a generic building to optimize damping and stiffness for different positions of the dampers. They demonstrated the consistency of the method with the previous literature and the adaptability to different design conditions.

Dehghan et.al[18] compared robustness of different number of MTMD with a minimax method applied to displacements and accelerations under a seismic excitation, calculating the flatness of the spectrum and the presence of new peaks out of the tuning frequency. They showed that a higher number of TMDs increases robustness while maintaining the same effectiveness.

Lewandoski[34] compared the robustness of TMD and MTMD for a shear type frame subjected to wind, calculating the correspondent transfer function for the main modal shape. Overall, the MTMD showed to be similarly effective to STMD and less sensible to uncertainties.

Chey and Kim[12] studied a parametric formulations for the optimal damping and tuning ratio to minimize the Dinamic Magnification Factor (DMF) of acceleration and displacement under a white noise input. They showed that, nevertheless the two criteria lead to similar optimal parameters, the control of displacements is more difficult than on acceleration, especially for higher mass ratio.

Yang and Esmailzadeh[64] presented an optimization technique applied to a MDF system based only on the mass ratio while the other parameters were kept uniform, minimizing the DMF

of acceleration. They proved the technique to be more robust than others and that the optimal masses were distributed around a central one tuned with the main system. Also in this case, over a certain number, increasing the TMDs did not improve the performance.

Bozer and Saban[6] used an artificial bee colony algorithm to perform a free parameters analysis of the optimal MTMD minimizing the norm of the harmonic transfer function, showing that for increasing number of TMDs the damping ratio required is smaller and the natural frequencies of the TMDs more closely spaced. They also found that the robustness of the MTMD is not significantly improved by increasing over 3 the number of dampers.

Bibiana and Leticia[4] performed a free parameters optimization of stiffness, mass ratio and number of TMDs for a 40 storeys benchmark building under a wind excitation for both acceleration and displacements. A search group algorithm was used to show that the two OFs lead to similar results and that for small mass ratio the tuning becomes fundamental, while for high mass ratio is the damping ratio that determines the performances.

Although a free parameters optimization has showed to be more effective, the presence of a defective damper may involves significant loss of performance. From this point of view, the uniform MTMD is more robust also if less effective than the not uniform MTMD.

However, the nature of the excitation and of the protected system themselves play an important role in the final performance of the TMD. Therefore, some authors focused on the effects of the slenderness of the structure and the soft or stiff nature of the soil in case of seismic excitations.

Murudi and Mane[45] used a genetic algorithm to optimize the damping ratio and tuning ratio for a Tajimi-Kanai modulated spectrum used to generate 20 acceleration histories with different parameters. They analysed the response by a central difference method in terms of DMF of the acceleration. Overall the TMD worked better near the resonance and especially at higher frequencies, slender structures showed to be more difficult to protect while the Peak Ground Acceleration (the intensity) of the event showed to not influence the TMD performances.

Marano and Greco[41] compared the performances of slender and stiffer structures placed on stiff and soft soils for a single TMD under a Tajimi-Kanai input with the purpose of optimizing its damping and tuning ratio to contain the displacement and absolute acceleration. The stiffer soils proved to be better for the limitation of displacements while the softer one were better for the control of absolute accelerations. Moreover, they concluded that very stiff structures lead to a fail of the TMD system because tuning becomes difficult.

Marano et al.[42] performed a robust optimization based on displacements of a single MTMD implemented on a SDF system, showing that increasing uncertainties request a bigger damping ratio of the dampers. For what concerns the tuning ratio: for frequency ratio between excitation and system over 1 the TMD had higher frequencies, while for frequency ratio between excitation and system less than 1, the TMD worked well for lower frequencies.

Mohebhi et al.[44] performed a constrained optimization of mass, stiffness and damping of TMDs, resolving the global equation of motion of the entire MDF system. In slender buildings the higher frequencies modes may be as important as the first one in case of high frequency seismic input, applying this approach, all modes can be analyzed together. Assumed a stiff soil, a genetic algorithm was applied to optimize the accelerations and displacements. Overall, the efficiency of the MTMD has proved to be dependent from the analyzed earthquake and the displacements were easier to be controlled, moreover, some TMDs need to be tuned to the second mode of vibration, showing that attention should be paid on the tuning frequencies of interest.

Khatibinia et al.[32] optimized the stiffness, damping ratio and mass of a benchmark building of 40 storeys by applying a particle swarm optimization to the system structure plus soil to control absolute acceleration and displacements. They showed that the characteristics of the soil influence the effectiveness of the TMD significantly.

## 4.4 Dynamic principles of MTMD

To explain the behaviour of a TMD system implemented in a structure, let consider the system in fig.4.3 and analyse its dynamic in terms of displacements and energy balance[23].

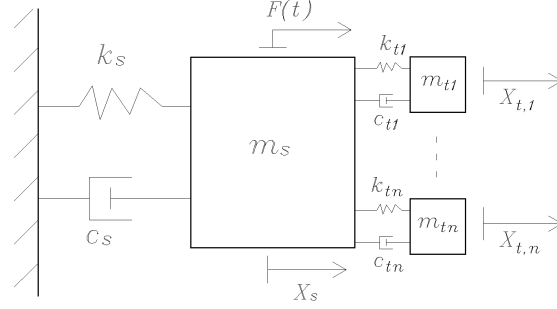


Figure 4.3: Dynamic scheme of MTMD system for a SDF structure

Defined  $m_s$ ,  $c_s$  and  $k_s$  as the mass, damping and stiffness of the main system, the vector  $\vec{X}_t(t)$  contains  $n$  values corresponding to the displacements of each TMD,  $X_s(t)$  is a scalar that indicates to the only degree of freedom of the main system and  $F(t)$  is a force applied to it. For the system of MTMD, the main characteristics are definable as diagonal matrices:

$$\mathbf{m}_t = \text{diag}(\vec{\gamma}_t \cdot m_s) = \begin{bmatrix} m_1 & 0 & \dots & 0 \\ 0 & m_2 & 0 & \vdots \\ \vdots & & \ddots & 0 \\ 0 & \dots & 0 & m_n \end{bmatrix}, \quad (4.4)$$

$$\mathbf{c}_t = \begin{bmatrix} c_1 & 0 & \dots & 0 \\ 0 & c_2 & 0 & \vdots \\ \vdots & & \ddots & 0 \\ 0 & \dots & 0 & c_n \end{bmatrix}, \quad \mathbf{k}_t = \begin{bmatrix} k_1 & 0 & \dots & 0 \\ 0 & k_2 & 0 & \vdots \\ \vdots & & \ddots & 0 \\ 0 & \dots & 0 & k_n \end{bmatrix} \quad (4.5)$$

There is no interaction between the TMDs because they are not connected between each other. A vector  $\vec{\gamma}_t$  of dimension  $[n \times (n_{dof} = 1)]$  assigns a mass ratio to each TMD.

The SDF system with no TMD can be studied as an equivalent MDF one with  $(n + n_{dof})$  degrees of freedom. The global matrices of the mechanical characteristics of the system are defined as follow. The mass:

$$\mathbf{m} = \begin{bmatrix} m_1 & 0 & \dots & \dots & 0 \\ 0 & m_2 & 0 & \dots & \vdots \\ \vdots & & \ddots & & \vdots \\ & & & m_n & 0 \\ 0 & \dots & \dots & 0 & m_s \end{bmatrix}, \quad (4.6)$$

the damping:

$$\mathbf{c} = \begin{bmatrix} c_1 & 0 & \dots & \dots & -c_1 \\ 0 & c_2 & 0 & \dots & -c_2 \\ \vdots & & \ddots & & \vdots \\ & & & c_n & -c_n \\ -c_1 & -c_2 & \dots & -c_n & c_s + \sum_{i=1}^n c_i \end{bmatrix}, \quad (4.7)$$

the stiffness:

$$\mathbf{k} = \begin{bmatrix} k_1 & 0 & \dots & \dots & -k_1 \\ 0 & k_2 & 0 & \dots & -k_2 \\ \vdots & & \ddots & & \vdots \\ & & & k_n & -k_n \\ -k_1 & -k_2 & \dots & -k_n & k_s + \sum_{i=1}^n k_i \end{bmatrix}, \quad (4.8)$$

where the terms of the  $\mathbf{c}$  matrix in the column  $(n + 1)$  correspond to the damping transmitted by the main system to the dampers  $\vec{c}_{st}$  and the row  $(n + 1)$  to the damping transmitted by each dampers to the main system  $\vec{c}_{ts}$ ; the last cell  $[(n + 1), (n + 1)]$  is the total damping of the main system increased by the contributes of TMDs. The same is valid for the  $\mathbf{k}$  matrix.

The final equations of motion defines a system of  $(n + 1)$  dynamic equilibriums:

$$\begin{cases} m_s \cdot \ddot{\vec{X}}_s(t) + c_s \cdot \dot{\vec{X}}_s(t) + \sum_{i=1}^n c_i \cdot \vec{X}_t(t) + k_s \cdot X_s(t) + \sum_{i=1}^n k_i \cdot \vec{X}_t(t) = F(t) \\ \mathbf{m}_t \cdot \ddot{\vec{X}}_t(t) + \mathbf{c}_t \cdot \dot{\vec{X}}_t(t) + \vec{c}_{st} \cdot \dot{\vec{X}}_s(t) + \mathbf{k}_t \cdot X_t(t) + \vec{k}_{st} \cdot \dot{\vec{X}}_s(t) = \vec{0} \end{cases} \quad (4.9)$$

In case of a base ground acceleration applied, eq.(4.9) becomes:

$$\begin{cases} m_s \cdot \ddot{\vec{X}}_s(t) + c_s \cdot \dot{\vec{X}}_s(t) + \sum_{i=1}^n c_i \cdot \vec{X}_t(t) + k_s \cdot X_s(t) + \sum_{i=1}^n k_i \cdot \vec{X}_t(t) = -m_s \cdot \ddot{X}_g(t) \\ \mathbf{m}_t \cdot \ddot{\vec{X}}_t(t) + \mathbf{c}_t \cdot \dot{\vec{X}}_t(t) + \vec{c}_{st} \cdot \dot{\vec{X}}_s(t) + \mathbf{k}_t \cdot X_t(t) + \vec{k}_{st} \cdot \dot{\vec{X}}_s(t) = -\vec{\gamma}_t m_s \cdot \ddot{X}_g(t) \end{cases} \quad (4.10)$$

where  $-\vec{\gamma}_t m_s \cdot \ddot{X}_g(t)$  is the effect of the ground acceleration on the TMDs, proportional to their mass.

Analysing the equation of motion (4.9) or (4.10), in both cases the MTMD adds a damping term to the main system and shift the frequency to lower values due to a mass increase. It is possible to find the particular case of single TMD from the previous equation by reducing the matrix  $\mathbf{m}_t$ ,  $\mathbf{k}_t$  and  $\mathbf{c}_t$  to scalar terms. The main parameters entering in the efficiency of the system are:

- the mass ratio  $\gamma_t$ ;
- the damping ratio of the TMDs  $\xi_t$ ;
- the *tuning ratio*  $\rho = \omega_t/\omega_s$  between the frequency of the TMD and the structure.

Consequently, the related parameters  $\mathbf{m}$ ,  $\mathbf{c}$ ,  $\mathbf{k}$  are adoptable as design variables too. The general approach is fixing the mass ratio according to the costs and installation requirements and optimize the other two parameters. In fact, as big is the mass of the TMDs, as high is the defectiveness if the other parameters are correctly set. However, values over a certain (around 5%) have showed to produce few improvements compared to the costs and are generally not recommended.

In fig.4.4 the damping effect produced by the single TMD and the MTMD are compared for a response spectrum similar to the one in fig.1.4. The MTMD shows a number of peaks equal to

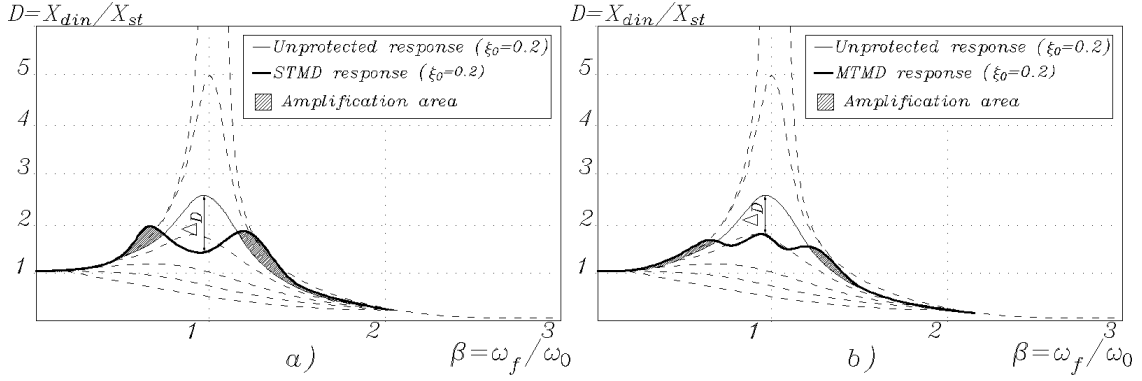


Figure 4.4: Response spectre of the system: a) with a single TMD and b) with MTMD.

the original degrees of freedom plus the ones added by the dampers. The band of suppression is wider and less sharp, therefore, more robust than a STMD.

A single TMD produces a high damp concentrated on a narrow band of frequencies and is typically tuned to the main mode of vibration of a structure. However, the system may have a conspicuous energy content at higher frequencies modes, implying a lack of flexibility of the STMD; moreover, the uncertainties on the main system parameters may shift the resonance frequency with a significant loss of effectiveness. A MTMD system is instead able to cover a wider range of frequencies by tuning properly the dampers, gaining in robustness.

As stated before, adding a TMD to the main structure produces an increase in the dissipated energy  $E_c$  in eq.(4.1). To express this mathematically, let write the equations of motions (4.10) in compact form by introducing the vector  $\vec{X}(t) = [\vec{X}_t(t), X_s(t)]^T$ [23].

$$\mathbf{m} \cdot \ddot{\vec{X}}(t) + \mathbf{c} \cdot \dot{\vec{X}}(t) + \mathbf{k} \cdot \vec{X}(t) = -\mathbf{m} \cdot \ddot{\vec{X}}_g(t) \quad (4.11)$$

To obtain the energy balance for the unprotected case let consider the equation of motion for the main system without dampers:

$$m_s \cdot \ddot{X}_s(t) + c_s \cdot \dot{X}_s(t) + k_s \cdot X_s(t) = -m_s \cdot \ddot{X}_g(t) \quad (4.12)$$

Multiplying it for  $\dot{X}_s(t)$  gives the power balance at a fixed instant of time[23]:

$$m_s \cdot \ddot{X}_s(t) \cdot \dot{X}_s(t) + c_s \cdot \dot{X}_s^2(t) + k_s \cdot X_s(t) \cdot \dot{X}_s(t) = -m_s \cdot \ddot{X}_g(t) \cdot \dot{X}_s(t) \quad (4.13)$$

Eq.4.13 takes the name of *relative power equation*. The terms represent:

- $m_s \cdot \ddot{X}_s(t) \cdot \dot{X}_s(t) = dE_k/dt$ , the rate of kinetic energy at time  $t$ ;
- $c_s \cdot \dot{X}_s^2(t) = dE_d/dt$ , the rate of dissipated energy at time  $t$ , including both viscous and dissipative contributes;
- $k_s \cdot X_s(t) \cdot \dot{X}_s(t) = dE_{el}/dt$ , the rate of elastic energy at time  $t$ ;
- $m_s \cdot \ddot{X}_g(t) \cdot \dot{X}_s(t) = dE_{in}/dt$ , the rate of introduced energy at time  $t$ ;

Integrating along two generic time extremes equation (4.13) gives an energy balance:

$$\begin{aligned} & \int_0^t m_s \cdot \ddot{X}_s(t) \cdot \dot{X}_s(t) dt + \int_0^t c_s \cdot \dot{X}_s^2(t) dt + \\ & + \int_0^t k_s \cdot X_s(t) \cdot \dot{X}_s(t) dt = \int_0^t (-m_s) \cdot \ddot{X}_g(t) \cdot \dot{X}_s(t) dt \end{aligned} \quad (4.14)$$

or, in compact form:

$$E_k(t) + E_d(t) + E_{el}(t) = E_{in}(t) \quad (4.15)$$

There is a time  $t_q$  in which all the energy is dissipated and the motion stops:

$$E_d(t_q) = E_{in}(t_q), \quad E_k(t_q) = E_{el}(t_q) = 0 \quad (4.16)$$

This dissipation may occur either due to viscous or friction damaging effects. Unfortunately, the viscous resources of ordinary civil structures are minimal and this quote of energy is covered mainly by damaging mechanisms, compromising the performance of the structure.

To consider the energy balance in the protected case it is possible to proceed in a similar way of the previous develops on eq.(4.11). Multiplying for  $\vec{X}^T(t)$  gives a power balance:

$$\vec{X}^T(t) \cdot \mathbf{m} \cdot \ddot{X}(t) + \vec{X}^T(t) \cdot \mathbf{c} \cdot \dot{X}(t) + \vec{X}^T(t) \cdot \mathbf{k} \cdot X(t) = -\vec{X}^T(t) \cdot \mathbf{m} \cdot \ddot{X}_g(t) \quad (4.17)$$

where each term has exactly the same meaning of (4.13) but applied to the system with the TMDs. Integrating between two generic time extremes gives an energy balance:

$$\int_0^t \vec{X}^T(t) \cdot \mathbf{m} \cdot \ddot{X}(t) dt + \int_0^t \vec{X}^T(t) \cdot \mathbf{c} \cdot \dot{X}(t) dt + \int_0^t \vec{X}^T(t) \cdot \mathbf{k} \cdot X(t) dt = - \int_0^t \vec{X}^T(t) \cdot \mathbf{m} \cdot \ddot{X}_g(t) dt \quad (4.18)$$

or in compact form:

$$E_k(t) + E_d(t) + E_{d,tmd}(t) + E_{el}(t) = E_{in}(t) \quad (4.19)$$

where the term  $E_d(t) + E_{d,tmd}(t) = \int_0^t \vec{X}^T(t) \cdot \mathbf{c} \cdot \dot{X}(t) dt$  includes the dissipative contributes of both system and TMDs. Therefore, the introduction of TMDs adds a source of dissipation and eq.(4.16) becomes:

$$E_d(t_q) + E_{d,tmd}(t_q) = E_{in}(t_q), \quad E_k(t_q) = E_{el}(t_q) = 0 \quad (4.20)$$

The damages on the structure are contained because the dissipative energy is supplied by the damping introduced by the TMDs. Analysing the term  $E_{in}(t)$  shows an increment of the energy introduced in the system due to the added mass by the TMDs (this happens only in case of imposed acceleration), but on the other hand the term  $E_{d,tmd}(t)$  increases much more the dissipation with positive effects on the final performances of the system.

Remembering that the response at the resonance is determined mostly by damping, it means that if the TMDs are properly tuned, then the main dissipation occurs at the higher energy content frequencies and the system is effectively protected.

To find the tuning frequency in the simplest case of single tuned mass damper let consider eq.(4.10) for  $n_{tmd} = 1$ . The two equations become:

$$\begin{cases} m_s \cdot \ddot{X}_s(t) + c_s \cdot \dot{X}_s(t) - c_t \cdot \dot{X}_t(t) + k_s \cdot X_s(t) - k_t \cdot X_t(t) = -m_s \cdot \ddot{X}_g(t) \\ m_t \cdot \ddot{X}_t(t) + c_t \cdot \dot{X}_t(t) + k_t \cdot X_t(t) = -\gamma_t m_s \cdot \ddot{X}_g(t) \end{cases} \quad (4.21)$$

Summing linearly the two equations gives:

$$(m_s + m_t) \cdot \ddot{X}_s(t) + c_s \cdot \dot{X}_s(t) + k_s \cdot X_s(t) = -m_s \cdot \ddot{X}_g(t) - \gamma_t m_s \cdot \ddot{X}_g(t) - \gamma_t m_s \cdot \ddot{X}_t(t) \quad (4.22)$$

Forcing terms are added: the motion of the TMDs,  $\gamma_t m_s \cdot \ddot{X}_g$ , and the effects of acceleration of the TMD on the main system,  $\gamma_t m_s \cdot \ddot{X}_t$ . If the external force input is stationary, the (4.22) can be expressed in power form by calculating the time average of the terms multiplied for  $\dot{X}_s$ :

$$\begin{aligned} & (m_s + m_t) \cdot E[\dot{X}_s(t) \cdot \dot{X}_s(t)] + c_s \cdot E[\dot{X}_s^2(t)] + k_s \cdot E[X_s(t) \cdot \dot{X}_s(t)] = \\ & -m_s \cdot E[\ddot{X}_g(\tau) \cdot \dot{X}_s(t)] - \gamma_t m_s \cdot E[\ddot{X}_g(\tau) \cdot \dot{X}_s(t)] - \gamma_t m_s \cdot E[\ddot{X}_t(\tau) \cdot \dot{X}_s(t)] \end{aligned} \quad (4.23)$$

where  $\tau = t_2 - t_1$  is the difference between two generic instants of time. If the response  $X_s(t)$  is stationary too, then  $E[\dot{X}_s(t) \cdot \dot{X}_s(t)] = E[X_s(t) \cdot \dot{X}_s(t)] = 0$  because they are the mean of out of phase processes. The (4.23) becomes:

$$c_s \cdot E[\dot{X}_s^2(\tau)] = -m_s \cdot E[\ddot{X}_g(\tau) \cdot \dot{X}_s(\tau)] - \gamma_t m_s \cdot E[\ddot{X}_g(\tau) \cdot \dot{X}_s(\tau)] - \gamma_t m_s \cdot E[\ddot{X}_t(\tau) \cdot \dot{X}_s(\tau)] \quad (4.24)$$

Let analyse the terms of this equations:

- $c_s \cdot E[\dot{X}_s^2(\tau)]$  is the power dissipated by the structural damping;
- $-m_s \cdot E[\ddot{X}_g(\tau) \cdot \dot{X}_s(\tau)] - \gamma_t m_s \cdot E[\ddot{X}_g(\tau) \cdot \dot{X}_s(\tau)]$  is the power introduced in the system by the external force;
- $-\gamma_t m_s \cdot E[\ddot{X}_t(\tau) \cdot \dot{X}_s(\tau)]$  indicates the power transferred from the main system to the MTMD and is a measure of the effectiveness of the latter;

The maximum of the last term is reached when the acceleration of the TMD is in phase with the velocity of the main system and the term  $E[\ddot{X}_t(\tau) \cdot \dot{X}_s(\tau)] = \max$ . In this case, the total dissipated power coincides with the energy transmitted to the TMD and it increases the total effective damping  $c_{eq}$  of a term:

$$c_{eq} = c_s + \gamma_t m_s \frac{E[\ddot{X}_t(\tau) \cdot \dot{X}_s(\tau)]}{E[\dot{X}_s^2(\tau)]} \quad (4.25)$$

There is also an added energy to the system,  $-\gamma_t m_s E[\ddot{X}_g(\tau) \cdot \dot{X}_s(\tau)]$ , but this term is generally small compared to the power dissipated by the TMD. The result is a significant increase of the dissipated energy and, consequently, of the performance. This is a simple tuning criteria that depends on the energy content but there are many possible reference parameters adoptable for the design: transfer function, dynamic magnification factor, displacements and acceleration of the final system and so on. Despite the differences of final performances obtained, the criteria tend to the similar optimal parameters of the TMDs.

## 4.5 Applications in the structural field

The TMD technology was developed for mechanical purposes but immediately showed its potential in the structural applications: bridges, skyscrapers, towers, power lines and chimneys are only the most common structures that can benefit from the use of TMDs. Different sources of vibration can be managed as: traffic, wind, earthquakes and so on. The system is typically placed in the point of highest displacements of the structure (the top of the building or the middle of the longest span of a bridge) and can be passive, active or semi-active, with actuators and controlling devices.

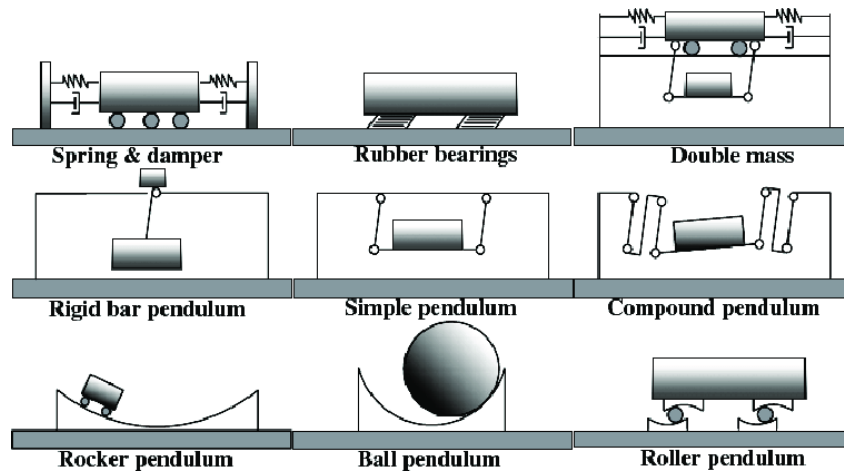


Figure 4.5: Most common typologies of TMD[53].

The TMDs are often coupled with other dissipative systems as shock absorbers or viscous systems in different typologies to increase the damping, as showed in fig.4.5.

The different typologies of dampers are usually divided in:

- *horizontals*: used in slender buildings, communication towers, spires and the like; they are composed of viscodampers and leaf springs or pendulum suspensions to deal with horizontal and torsional excitations.
- *Vertical*: applied in long span horizontal structures such as bridges, floors and walkways. They are a combination of coil springs and viscodampers that mitigate vertical vibrations.

Overall, both the TMD and MTMD technologies have the following advantages:

- if used as passive system they do not depend necessarily from external energy supply, although some semi-active solutions may use it;
- they are able to respond to small excitations too;
- they can be properly adjusted in situ and require low maintenance;

and disadvantages:

- their use is limited by the large mass (and volume consequently) that has to be installed on the site, although MTMD aims to distribute the mass on more devices;
- their effectiveness depends on the tuning with the main frequencies of the structure that cannot be predicted with great accuracy.

#### 4.5.1 Some applications for TMDs

In this section some examples of uses of the TMD in past and modern applications are presented to give an idea of the potential of this technology and the possibilities reachable in the current state of design.

### The Horyu-Ji temple in Japan

Despite the mechanical principles behind it were systematized just in the last century, the TMD, in its first configurations, is far more ancient. Indeed, some studies performed on the effect of earthquakes on the Pagoda ancient structures in Japan has showed that this peculiar building may rely on a principle very similar to the TMD[47].

The structure of a Pagoda can be described as a series of wood boxes implied with pillars interrupted at each storey and no rigid connections between the inner elements. At the centre of the structure is placed a thick wood pillar that rises from the foundation until the roof of the building without any intermediate connection (fig.4.6). This element takes the name of Shin-bashira and is a fundamental part of the structure of a Pagoda. During an earthquake, the Shin-bashira moves with a different period from the wood structure around it and damps the vibrations induced on the latter.

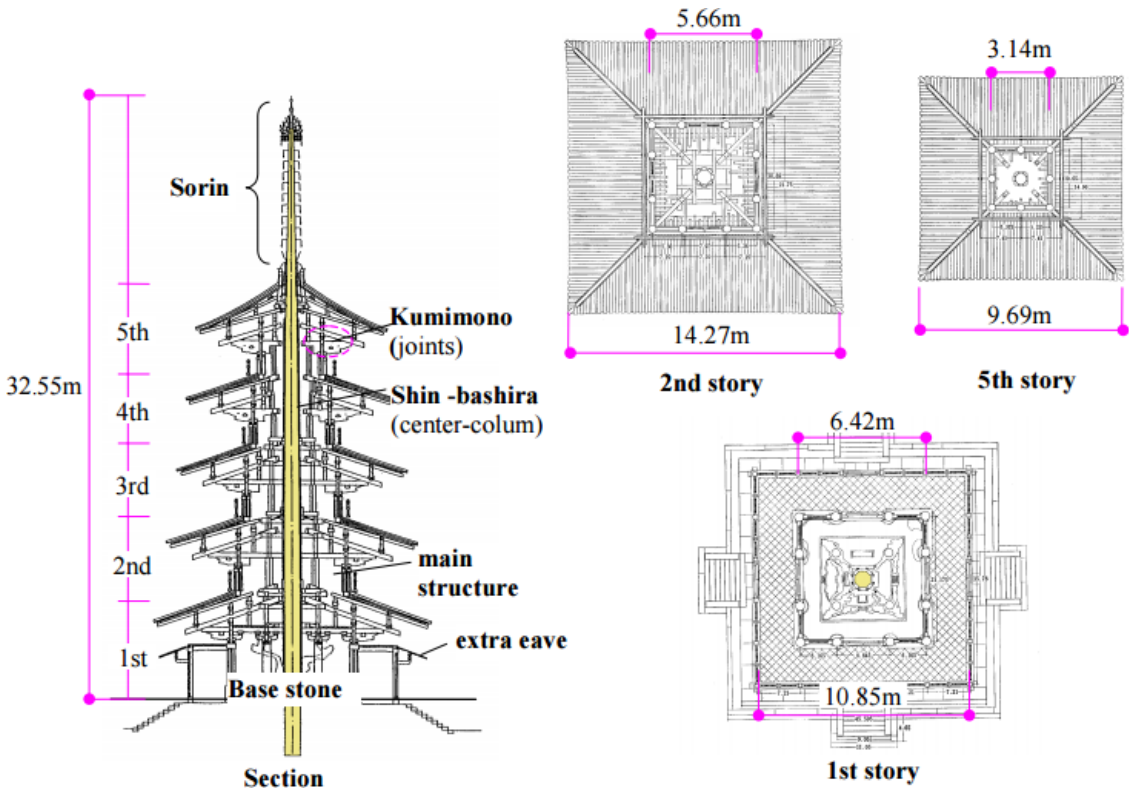


Figure 4.6: Plan and sectional view of the five-storeys pagoda structure of the Horyu-Ji temple in Japan[47].

However, this is not the only contribute to the seismic resistance, it seems that the Pagodas were the precursors of many anti-seismic solutions for modern buildings.

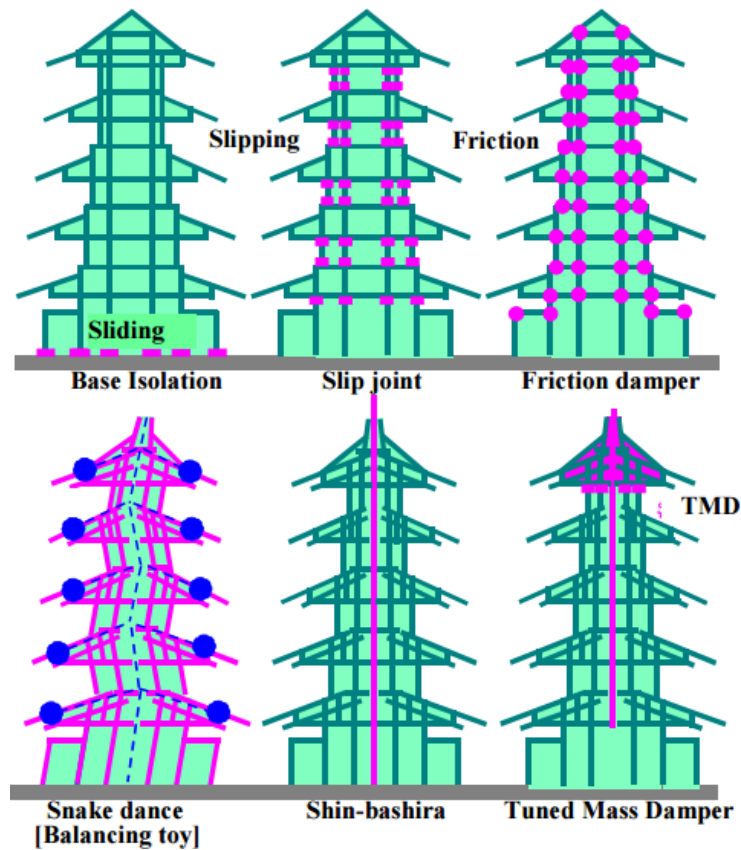


Figure 4.7: Vibration control mechanisms of the pagoda[47].

Nakahara et al.[47] individuate many mechanisms that overall reduce the seismic effects on the building (fig.4.7):

- sliding between the base stones and columns, contributing to the earthquake resistance (base isolations);
- slipping and gaps in the wooden joints;
- friction damping effect of wooden joints;
- balancing toy effect (due to deep eaves);
- oscillation of the whole structure like a snake dance;
- collision between the center column and the main structure, making a bolt effect;
- center column TMD effect;

All this elements shows that probably the constructors of the past known more than it could be expected about seismic design.

### The Hancock Tower in Boston

The use of MTMD has showed to be an efficient and robust solution to deal with complex structure characterized by uncertainties on their effective behaviour. Built between 1965 and 1969, the Hancock tower is one of the most famous high rise building of our period (344 m). Despite this, it suffered many problems during and after its construction, included a despicable fall of the windows panels of its peculiar facade. An article of the Boston Globe in 1995[10] reported an analysis of the story of the building. For what concern the TMDs, it came out that the torsional and translational period interacted under the action of wind, causing the building to sway too much. William LeMeussier, an engineer of Cambridge, studied a MTMD system constituted by two boxes in lead of 5.60 square meters and 1.00 m high for 300 tons of weight for each one, placed at the 58<sup>th</sup> floor of the building. The use of two dampers aims to deal with the two modes of vibration along the main direction of the building. All the system lies on an lubricated surface and is connected by springs and shock absorbers to the building. The TMDs, with periodically maintenance operations, are still operative today.

### The Taipei 101

The TMD can be used in different configurations according to the design necessity (fig.4.5); a popular solution in high rise building are the pendol systems, used for example in the Taipei 101. With its 101 floors for a total 508 meters high, the Taipei 101 has been for a period after its construction (ended in 2004) the tallest building Worldwide[54]. The particular frame structure makes it very stiff compared to a normal 101 storeys building. The frame is constituted of steel boxes super columns built up with plate of 50 to 80 mm of thickness with full penetration welded splices and filled with 69 MPa resistance concrete where extra stiffness is needed; in addition, the braced core is encased in concrete walls from the foundation until the eighth level.

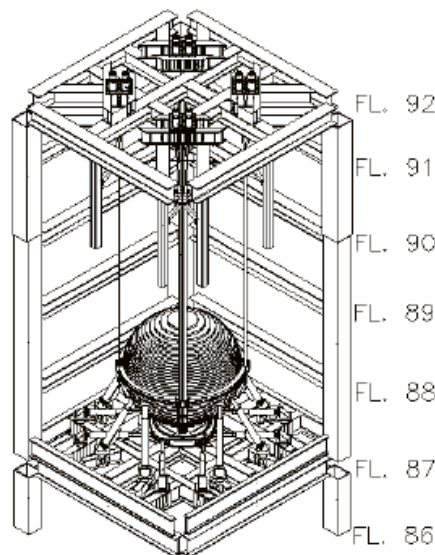


Figure 4.8: The pendulum of the main TMD system of the Taipei 101[54].

The final effect is a building with a sway period of 9 sec, very high if compared to the 7 sec of the other similar height building. However, the problem of vibrations remained because the lower amount of damped energy could not deal with the wind input energy at the higher storeys.

A semi-active TMD system of 726 tons (24% of the total building mass), in stacked steel and coupled with shock absorber has been installed (see fig.4.8). The damping effect of the sealed dashpots varies with the square of the velocity of the mass. Therefore, a small wind velocity would create a small resistance and the mass would swing, but the system would fail under a strong event as an earthquake that may induce a sort of lock-on effect. For this reason, bumping devices have been placed in the building to support the the main system.

### The Millennium Bridge in London

The TMD can also be coupled with other protection systems to better perform in particularly vulnerable structures, the Millennium bridge in London is one of these cases[16]. Built in 1999 for the celebration of the new Millennium together with other buildings in London (as the famous Millennium Dome), the bridge presents an unordinary shallow suspension method for a continuous beam structure. Two groups of four 120 mm diameter locked coil cables span from bank to bank over two river piers. The lengths of the three spans are 81 m for the north span, 144 m for the main span between the piers and 108 m for the south span. The sag of the cable profile is 2.3 m in the main span, around six times shallower than a more conventional suspension bridge structure. The intermediate river piers are quite slender and cannot provide stiffness comparable to that of the massive abutments, causing the spans to interact. Fig.4.9 illustrates the plan view of the bridge with already the configuration of the dampers showed.

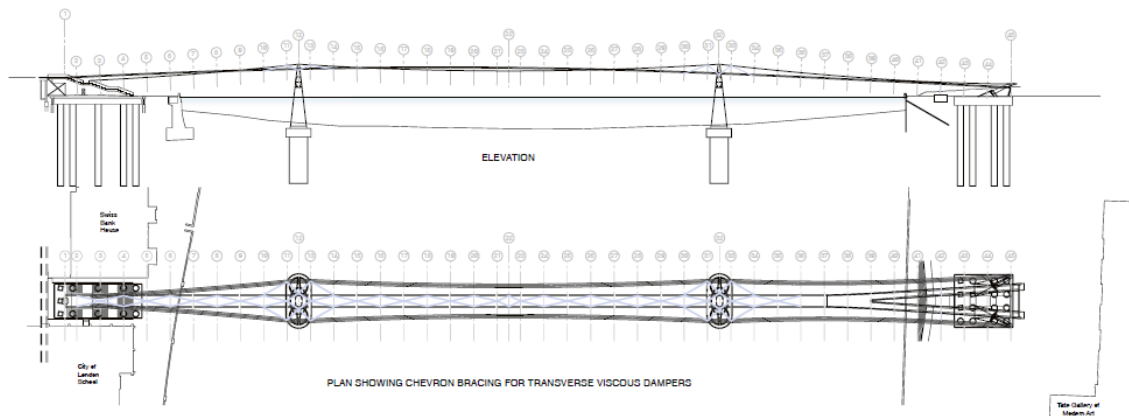


Figure 4.9: Plan and elevation of the bridge showing the arrangement of dampers[16].

During the day of the opening, on the 10<sup>th</sup> of June 2002, a big crowd crossed the bridge, estimated between 80 000 and 100 000 people. Unexpected torsional vibrations showed on the different spans at frequencies lower than 1 Hz. The vibrations occurred only during the crowd peaks and when all the pedestrian moved on the bridge, otherwise, the motion stopped. The studies performed showed an interaction between the vertical load applied by the crowd and the lateral response of the bridge. Indeed, the vertical load interacted with the lateral response increasing the motion of all the modes of vibration, in particular the ones with a good percentage of torsional coupling. Moreover, the general people's behavior follows the motion of the bridge creating a resonance effect.

To solve the problem, a complex damping system was installed:

- Tuned mass dampers and tuned slosh dampers<sup>1</sup>;
- Visco-elastic dampers, fluid-viscous dampers and friction dampers;
- Active control systems.

The TMD were placed on each transverse beam and connected to the other devices according to the schemes in fig.4.10 and 4.11. The studies performed on the bridge brought to light the problem of synchronous lateral excitation on slender bridges with a lateral frequency below 1.3 Hz and loaded with a sufficient number of pedestrians.

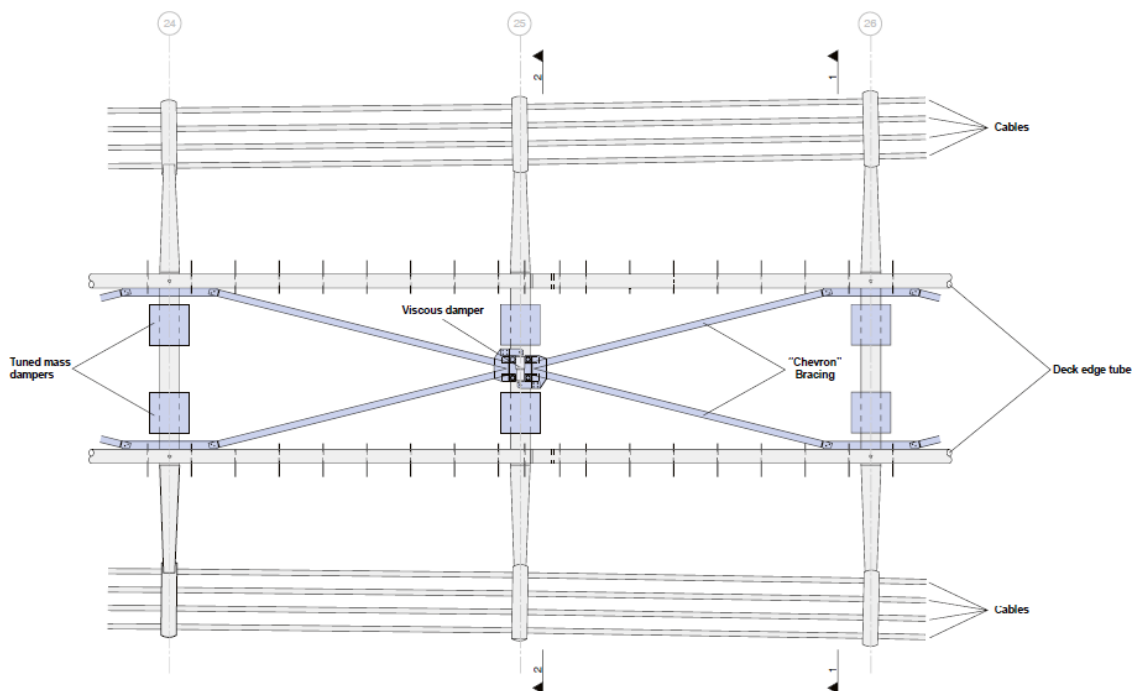


Figure 4.10: Plan view of a typical 16 m length of deck showing viscous dampers and tuned mass dampers[16].

## 4.6 Optimization of MTMD systems

As said before, the TMDs systems act as added masses that move out of phase and cut down the magnification factor of the structure at a desired frequency. If the system is well designed, the frequencies of cut down are in the range of resonance and the damp is maximum. Unfortunately, the different parameters entering in the design are affected by uncertainties that can significantly move the resonance frequency from the design point, with effects that may even be negative on the final response with undesired amplifications. In the following sections, the uncertain analysis and the approach to the robust design of MTMD are presented.

<sup>1</sup>A system similar to TMD that uses a liquid in a tube instead of a mass. The damping is introduced by an oscillating liquid column that passes through an orifice.

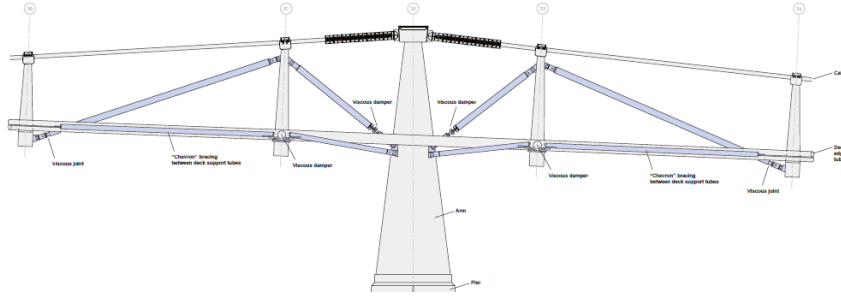


Figure 4.11: Viscous dampers in plane between cables and deck at piers[16].

In the different studies during the years many parameters have been considered for the search of an optimum of the TMDs system

- minimum displacements of the main structure;
- maximum stiffness of the main structure;
- maximum effective damping of the combined system structure-TMD;
- minimum displacement for the frequency tuning while the damping of TMD is used for the maximum damping of the system;
- minimum velocity of the main structure;
- minimum forces on the frame of the structure;
- minimum absolute acceleration of the main structure.
- minimum dynamic magnification factor;
- minimum transfer function;
- minimum drift of storeys.

These criteria often lead to quite different solutions but generally toward the similar optimal parameters. For instance, the components of the high frequencies are influenced primarily by the acceleration while the displacements determine the low frequencies response (sec.2.1.3) and the two criteria of optimization cannot coincide. In fact, in the case of harmonic external forces, the acceleration of the system  $\ddot{x}$  is proportional to the corresponding displacement  $x$  by the square of the natural frequency  $\omega^2$ :

$$\ddot{x} = \omega^2 \cdot x \tag{4.26}$$

Assumed  $x_{st}$  as the stationary response, the magnification factor of the acceleration is bond to the displacements by:

$$\left( \frac{\ddot{x}}{\omega_f^2 \cdot x_{st}} \right) = \left( \frac{\omega_s^2 \cdot x}{\omega_f^2 \cdot x_{st}} \right)_{max} = \left( \beta^2 \frac{x_s}{x_{st}} \right) \tag{4.27}$$

where  $\beta^2 = \omega_f^2/\omega_s^2$  is the frequency ratio. Many formulations have tried to optimize the acceleration together with the displacements as the analysis of Brock in the case of perfect tuning[7]. An example of mixed criteria was applied by Luft[39] to get an approximative closed form.

To give a better idea of how these approaches work, the simplified analysis of Den Hartog[17] for sinusoidal force is presented. Considering fig.4.2, in absence of damping there are two divergent

resonance frequencies for the coupled system, but in the ideal condition of infinite damping, instead, the two masses can be considered as a SDF oscillator with total mass given by  $m_s + m_t = 1.05 \cdot m_s$  and divergent magnification factor  $D$ . Between these two extremes, a value of  $\xi_t$  optimal, for which  $D$  is minimum, must exist. Den Hartog demonstrated that there are two movable points P and Q that define the shape of every response spectrum. The minimum  $D$  can be obtained by changing the tuning ratio  $\rho = \omega_t/\omega_s$  to fix them at the same level and is:

$$\rho_{opt} = \frac{1}{1 + \gamma_t} \quad (4.28)$$

that corresponds to:

$$D = \sqrt{1 + \frac{2}{\gamma_t}} \quad (4.29)$$

and to a value of  $\xi_t^{opt}$  equal to:

$$\xi_t^{opt} = \sqrt{\frac{3\gamma_t}{8(1 + \gamma_t)}} \quad (4.30)$$

Many studies searched similar values for different kind of external forces and considering the damping of the main system (see sec.4.2). However, to perform a good optimization it is necessary to consider the probabilistic nature of the problem, both in actions than in the parameters for the modelling of the system.

#### 4.6.1 Parameters uncertain in random vibrations

Generally, the uncertainties assumed in the analysis of random vibrations are connected only to the input excitation assumed as stochastic. However, it is well know that this does not correspond to the real behave of a structure because also the estimated parameters as stiffness, damping and mass (with the derived frequency  $\omega$  and damping ratio  $\xi$ ) are affected by uncertain. Due to the nature of dynamic excitation, all the previous parameters influence the final actions on the system and their variability cannot be neglected. In order to model these aspects, the perturbational methods exposed by Lutes and Sarkani[40] are used in this thesis.

Analysing the system parameters shows their variable nature:

- the mass  $m$  depends on the structure usage and may variate significantly. In very light structures, as the Millenium bridge for example, the oscillation of the crowd over it may lead to coefficient of variation of the order of the unity;
- the stiffness  $k$  depends in a good part from the non-structural elements that various studies tried to consider in the dynamic analysis; considering the complexity of modelling these effects, they can be assumed as epistemic uncertainties. Moreover, thermal excursions or other imposed actions may variate the stiffness significantly;
- the damping  $c$  is one of the most difficult parameter to be determined, it involves different mechanisms as internal dissipation, frictions, viscous effects, etc. The approach is typically to assume it as epistemic uncertain.

The costs of a detailed modelling of all these parameters is quite high and, moreover, they may variate along the service life of a structure due to degradation or change of service conditions. The most convenient approach is to abandon the deterministic assumption for these parameters and consider them as uncertain in the analysis.

### 4.6.2 Perturbational methods

The perturbational methods are a wide group of approaches used for the analysis of uncertainties that are based on the introduction of a small perturbation in the design parameters to then study the effects on the final response.

Let define a *vector of uncertainties*  $\vec{r}$ , which contains all the uncertain parameters, and a *response of interest*  $Q = Q(\vec{r})$ , function of the them. For instance, considering a FE analysis that aims to get the displacements from the stiffness  $\mathbf{K}$  and the external forces  $\vec{F}$ , the uncertain vector is  $\vec{r} = [\mathbf{K}, \vec{F}]$  and the relation  $Q = K^{-1} \cdot F$ . An exact description of the relationship  $Q$  (that is generally non linear) is very complex to be done and often simplified linearised formulations are adopted. In order to consider the uncertain on each parameter involved, a *sensitivity coefficient*  $\beta_l$  is defined:

$$\beta_l = \left( \frac{\partial Q}{\partial r_l} \right)_{\vec{r}=\vec{r}_0} \quad (4.31)$$

where  $\vec{r}_0$  is the original design point in the space of parameters and  $r_l$  the  $l^{th}$  uncertain parameter. It means that a change of  $\Delta_{r_l}$  in  $r_l$  implies a change of  $\beta_l \cdot \Delta_{r_l}$  in  $Q$ . Particular attention is required in case of a non-linear dependence from  $r_l$  because the modifications to  $Q$  may be not finite.

As for the previous analysis, the following notation will be adopted: capital letters indicate the general uncertain parameters and small letters a possible extraction of them.

Therefore, considering mass, stiffness and damping as uncertain, the following elements are introduced:

- the vector of the uncertain parameters  $\mathbf{R} = [\mathbf{M}, \mathbf{C}, \mathbf{K}]$ ;
- the possible extraction from the vector of the uncertain parameters  $\mathbf{r} = [\mathbf{m}, \mathbf{c}, \mathbf{k}]$ ;
- the *design point*  $\mathbf{r}_0 = [\mathbf{m}_0, \mathbf{c}_0, \mathbf{k}_0]$  used when neglecting the uncertainties. Typically, is fixed as coincident with the mean value ( $\mathbf{r}_0 = \boldsymbol{\mu}_r$ )

$\mathbf{R}$  is a vector containing the matrices of uncertain parameters and is, therefore, a matrix. Generally, the uncertain parameters are dependent and non-linearly connected. For instance, increasing the base of the pillars in a shear-type frame would increase linearly the mass while the stiffness would increase with a cubic relation; for what concern the damping, even less can be said about it. Modelling of such dependencies is complex and still not affordable with even complex effects on the estimation of uncertainties. For these reasons, the independence between these parameters is typically assumed and all possible variations considered singularly. The alternative is adopting a numerical analysis, varying the design parameters several times and performing multiple analysis in order to inference a distribution for the response. However, the computational cost of this approach, in complex systems with many degrees of freedom, becomes very high.

If  $\mathbf{R}$  is a random variable, then,  $Q(\mathbf{R})$  is a random variable too. Unfortunately, the analytical definition of the distribution of  $Q(\mathbf{R})$  is quite complicated and the study of the uncertainties is generally limited to the mean  $\boldsymbol{\mu}_{Q(\mathbf{R})}$  (deviation of  $Q$  from the design point) and the covariance matrix  $\mathbf{K}_{QQ}$  (oscillation of  $Q$  around  $\boldsymbol{\mu}_Q$ ). In fact, there are no clues on which could be a possible applicable distribution and generally a principle of maximum entropy is assumed. A truncated Gaussian or a truncated uniform distribution may be used, but these distributions assign significant probability to the extreme values (especially the uniform). The truncated Gaussian has some problems with negative values in conflicts with the physical nature of parameters as mass or stiffness; moreover, if the relation of  $\mathbf{R}$  with the response  $Q$  is inversely proportional, it is not possible to invert it.

A possible solution is to use a *log-normal distribution*, so that the  $\log(\mathbf{R})$  is distributed as Gaussian. There are many advantages in this choice as the elimination of negative values and that  $\mathbf{R}^{-1}$  remains Gaussian too. The problem is that the results of  $\log^{-1}[Q(\mathbf{R})]$  do not give the same values of a normal Gaussian analysis because the relation is not linear. Moreover, a log-normal distribution is not easy to be handled for more complex relations between  $\mathbf{R}$  and  $Q$ .

In conclusion, the choice between the previous distributions depends basically on which fits better the experimental data and requires to know the bond between parameters and response together with the expected extreme values. These data are not always available or easy to be modelled. Fortunately, many applications do not require to define a complete distribution but only the mean and the variance that can be obtained, with a significant computational reduction, by using the *direct perturbation method*.

### 4.6.3 Direct perturbation method

The direct perturbation method is based on the linearisation of response by using a polynomial Taylor series around the mean value  $\boldsymbol{\mu}_R$  (assumed as coincident with the design point  $\mathbf{r}_0$ ). Thanks to this approach, as complex could be the relation between  $\mathbf{R}$  and  $Q$ , it can always be approximated and simplified. In the linear form the Taylor series is:

$$Q_{lin} = Q(\boldsymbol{\mu}_R) + \sum_{l=1}^R \left( \frac{\partial Q(\mathbf{r})}{\partial r_l} \right)_{\mathbf{r}=\boldsymbol{\mu}_R} \cdot (R_l - \mu_{Rl}) \quad (4.32)$$

In the quadratic form it can be written as:

$$Q_{quad} = Q_{lin} + \frac{1}{2} \sum_{l=1}^R \sum_{k=1}^R \left( \frac{\partial^2 Q(\mathbf{r})}{\partial r_k \partial r_l} \right)_{\mathbf{r}=\boldsymbol{\mu}_R} \cdot (R_l - \mu_{Rl}) \cdot (R_k - \mu_{Rk}) \quad (4.33)$$

where  $R$  indicates, in this case, the number of uncertain parameters. Set  $\boldsymbol{\mu}_R = \mathbf{r}_0$ , the derivatives of the series correspond to the sensitivity coefficient:

$$\beta_l = \left( \frac{\partial Q(\mathbf{r})}{\partial r_l} \right)_{\mathbf{r}=\boldsymbol{\mu}_R=\mathbf{r}_0} \quad (4.34)$$

$$\beta_{lk} = \left( \frac{\partial^2 Q(\mathbf{r})}{\partial r_k \partial r_l} \right)_{\mathbf{r}=\boldsymbol{\mu}_R=\mathbf{r}_0} \quad (4.35)$$

Thus, eq.(4.32) and (4.33) become:

$$Q_{lin} = Q(\mathbf{r}_0) + \sum_{l=1}^R \beta_l \cdot (R_l - r_{l,0}) \quad (4.36)$$

$$Q_{quad} = Q_{lin} + \beta_{lk} \cdot (R_l - r_{l,0}) \cdot (R_k - r_{k,0}) \quad (4.37)$$

For the probabilistic parameters, set  $Q_0 = Q(\mathbf{r}_0)$ , this corresponds to:

$$E[Q_{lin}] = Q_0 \quad (4.38)$$

$$\text{Var}[Q_{lin}] = \sum_{l=1}^R \sum_{k=1}^R \beta_l \beta_k \cdot \text{Cov}[R_l, R_k] \quad (4.39)$$

If the parameters are uncorrelated, the equations are simplified as:

$$E[Q_{lin}] = Q_0 \quad (4.40)$$

$$\text{Var}[Q_{lin}] = \sum_{l=1}^R \beta_{lk}^2 \cdot \sigma_{Rl}^2 \quad (4.41)$$

The quadratic approximation is a bit more complex than the linear one:

$$E[Q_{quad}] = Q_{lin} + \frac{1}{2} \sum_{l=1}^R \sum_{k=1}^R \beta_{lk} \cdot \text{Cov}[R_l, R_k] \quad (4.42)$$

For the variance determination the moments of 3<sup>rd</sup> and 4<sup>th</sup> order are necessary:

$$\begin{aligned} \text{Var}[Q_{quad}] = & \text{Var}[Q_{lin}] + \sum_{l=1}^R \sum_{k=1}^R \sum_{j=1}^R \beta_j \beta_{lk} \cdot E[(R_l - r_{l,0}) \cdot (R_k - r_{k,0}) \cdot (R_j - r_{j,0})] + \\ & + \frac{1}{4} \sum_{l=1}^R \sum_{k=1}^R \sum_{j=1}^R \sum_{i=1}^R \beta_{lk} \beta_{ji} \left( E[(R_l - r_{l,0}) \cdot (R_k - r_{k,0}) \cdot (R_j - r_{j,0}) \cdot (R_i - r_{i,0})] + \right. \\ & \left. - \text{Cov}[R_l, R_k] \cdot \text{Cov}[R_j, R_i] \right) \end{aligned} \quad (4.43)$$

Also these formulations are simplified for uncorrelated parameters:

$$E[Q_{quad}] = Q_{lin} + \frac{1}{2} \sum_{l=1}^R \beta_{ll}^2 \cdot \sigma_{R_l}^2 \quad (4.44)$$

$$\begin{aligned} \text{Var}[Q_{quad}] = & \text{Var}[Q_{lin}] + \sum_{l=1}^R \sum_{l=1}^R \sum_{j=1}^R \beta_l \beta_{ll} \cdot E[(R_l - r_{l,0})^3] + \\ & + \frac{1}{4} \sum_{l=1}^R \beta_{ll}^2 \left( E[(R_l - r_{l,0})^4] - \sigma_{R_l}^4 \right) + \sum_{l=1}^R \sum_{k=1}^{l-1} \beta_{lk}^2 \cdot \sigma_{R_l}^2 \sigma_{R_k}^2 \end{aligned} \quad (4.45)$$

Of course, the quadratic approximation is more accurate but implies higher computational costs. Due to the difficulty in the determination of the 3<sup>rd</sup> and 4<sup>th</sup> order moments (that require detailed distribution), sometimes mixed incoherent methods are used with the mean determined by a quadratic method and the variance by a linear method.

The big advantage of the direct perturbation method is that does not require to fix a distribution of probability and, therefore, the mean and variance of  $Q$  can be determined with limited data. However, a distribution becomes necessary if more informations about the response have to be found. Sometimes, a distribution is adapted to the obtained moments, typically a log-normal, a  $\gamma$  or a  $\beta$  distribution.

For indirect relations, as  $Q = f(s, r)$  and  $s = g(r)$ , the chain derivation rule can be used:

$$\frac{dQ}{dr} = \frac{df}{dr} + \frac{df}{ds} \cdot g'(r) \quad (4.46)$$

A normalized form is sometimes preferred because easy to be handled. Given the uncertain parameters  $[K, C, M]$  the following normalised values are used:

$$\mathbf{R}_1 = M/m_0, \quad \mathbf{R}_2 = C/c_0, \quad \mathbf{R}_3 = K/k_0 \quad (4.47)$$

In this way, once set the mean coincident with design values of parameters,  $\mathbf{R} = E[\mathbf{R}] = \mathbf{r}_0$ , the mean of the design value is unitary,  $Q_0 = 1$ . Consequently, the deviation of  $E(Q)$  from the unity is an indication of the non-linearity of the problem and may be useful to define how good is the linear approximation adopted. In fact, the linear perturbation method has the big limit of not being able to model the non-linearity of the process (especially for big uncertainties) and to be dependent from the chosen distribution for quadratic or higher orders cases.

There are also other formulations of the method as the logarithmic one[40]. The latter has the disadvantage of requiring a particular form of the  $R_l$  distributions of parameters because the expected value and variance of the power of them have to be found. This requires to describe properly the distributions of the parameters with all the problems previously stated.

### Linear perturbation solution for delta-correlated excitation applied to a SDF system

The analysis of the delta-correlated excitation applied to a SDF system gives an easy solution useful to understand how the linear perturbation method works and also to have a benchmark for more complex analysis. Considering the SDF solutions for the variance of the process in eq.(2.4) and (2.8), with the unit pulse response (1.28) for the system in fig.1.6, gives:

$$\sigma_X^2 = \frac{\pi S_0}{2m^2 \xi \omega_0^3} = \frac{\pi S_0}{k} \quad (4.48)$$

$$\sigma_{\dot{X}}^2 = \frac{\pi S_0}{2\xi \omega_0^3} = \frac{\pi S_0}{mc} \quad (4.49)$$

Introducing the uncertainties in the analysis by defining a vector  $\vec{R} = [M, C, K]$  (but also the choice  $\vec{R} = [\xi, \omega]$  is possible), after the normalization of the parameters as done in eq.(4.47), the relation  $Q(\vec{R})$  for the displacements becomes:

$$Q = \frac{\sigma_X^2}{(\sigma_X^2)_0} = R_1^2 R_2^{-1} R_3^{-1} \quad (4.50)$$

For the speed instead is:

$$Q = \frac{\sigma_{\dot{X}}^2}{(\sigma_{\dot{X}}^2)_0} = R_1^{-1} R_2^{-1} \quad (4.51)$$

Calculating the sensitivity coefficient as in eq.(4.31) for each parameter and applying eq.(4.38) and (4.39), the obtained results for the displacement are:

$$E(Q) = 1 \quad (4.52)$$

$$\text{var}(Q) = 4\sigma_{R_1}^2 + \sigma_{R_2}^2 + \sigma_{R_3}^2 = 4\frac{\sigma_M^2}{m_0^2} + \frac{\sigma_C^2}{c_0^2} + \frac{\sigma_K^2}{k_0^2} \quad (4.53)$$

The speed instead is:

$$E(Q) = 1 \quad (4.54)$$

$$\text{var}(Q) = \sigma_{R_1}^2 + \sigma_{R_2}^2 = \frac{\sigma_M^2}{m_0^2} + \frac{\sigma_C^2}{c_0^2} \quad (4.55)$$

It is also possible to assign a log-normal distribution to the uncertain parameters and get different results. As said before, the choice is connected to the model assumption and, if there are no clues about the possible distributions, the use of a linear perturbation analysis may be justified remembering that it does not describe the non-linearities.

The application of the direct perturbation method to a failure analysis is not different from other relations. By using the chain rule it is possible to find the final sensitivity coefficient, both for the first-passage failure than of the fatigue analysis[40]. The obtained derivatives for the sensitivity analysis of the first-passage failure are:

$$P_f(t) = \int_0^t \eta_X(u, s) ds, \quad \frac{\partial}{\partial r} P_f(t) = P_f(t) \cdot \int_0^t \frac{\partial}{\partial r} \eta_X(u, s) ds \quad (4.56)$$

$$\frac{\partial^2}{\partial r^2} P_f(t) = P_f(t) \cdot \left( \left[ \frac{\partial}{\partial r} P_f(t) \right]^2 + \int_0^t \frac{\partial^2}{\partial r^2} \eta_X(u, s) ds \right) \quad (4.57)$$

From them, the mean and variance of the uncertain process can be calculated.

#### 4.6.4 Optimization approach for MTMD systems

To perform the optimization in a correct manner, the first important step is define exactly how every factor enters in the analysis (see sec.3.11.2). In the optimization of TMD or MTMD a possible formulation of the problem considers:

- *failure mode*: a fixed threshold of displacements or absolute accelerations of the system;
- *control parameters*: TMDs mechanical characteristics (frequency  $\vec{\omega}_t$  and damping ratio  $\vec{\xi}_t$ );

- *noise parameters*: the main system parameters (frequency  $\omega_s$  and damping ratio  $\xi_s$ ) and the external force parameters, generally expressed by a filter on which the uncertain falls (frequency  $\omega_f$  and damping ratio  $\xi_f$ ). The mass ratio  $\gamma_t$  of the MTMD enters in this group because connected to the total mass of the main system that may variate as well;
- *objective function*: the ratio between protected and unprotected response, in terms of displacements, acceleration or also failure probability. To them is associated the standard deviation of the OF to perform the robust optimization.

This is only one of the possible formulations of the optimization problem. Other parameters as the ones presented in chapter 4.2 can be investigated to get an optimum that will be similar from the one obtained from this analysis.

An observation should be done about the system parameters for the uncertain analysis: the direct assumption of frequency and damping as uncertain is acceptable only in SDF systems. If a MDF system has to be investigated, the uncertainties have to be considered on the  $\mathbf{K}$ ,  $\mathbf{M}$  and  $\mathbf{C}$  matrices, this because a modal analysis would have to be performed and the uncertain would affect the obtained frequencies and modal shapes together.

However, the typical approach in TMDs optimization problem is to neglect variations induced by the TMDs on the modal analysis and tune the latter to the main modal shape of the unprotected structure to limit the complexity of the analysis. In fact, being the structure overdamped, the matrix  $\mathbf{C}$  is not diagonal and the equations of motions with TMDs have to be decoupled by a complex modal analysis with complications in the analysis.

The problem of optimization in the random vibration field was first formulated by Nigam[48] as follow:

- Find the *design vector*  $\vec{d} = (\vec{\omega}_t, \vec{\xi}_t) \in \Omega_d$  (where  $\Omega_d$  is the admissible space of the design parameters);
- that minimizes the *objective function* bi-dimensional vector  $\vec{OF} = [\mu_{OF}, \sigma_{OF}]$ , containing the mean and standard deviation (or sensitivity) of the ratio between protected and unprotected response;
- given the *constraints*  $g_i(\vec{d}) \leq 0$  for  $i = 1, 2, \dots, k$ , where  $k$  is the number of constraints.

The ratio assumed as  $OF$  takes the name of *index of vibration protection effectiveness*. A value smaller than one indicates that the protection is effective, while a value bigger than the unity means a worsening of the performance, as small is the index as big is the improvement.

## Chapter 5

# Robust optimization of MTMD systems

The single TMD shows its limits in the high sensitivity to the changes in design parameters. Theoretically, a single TMD properly tuned could be able to damp the vibrations of one degree of freedom of the structure. Practically, the changes in the initial design parameters affect the performance of the system by inducing even negative effects as undesirable amplifications. The use of MTMD is a good solution in terms of robustness, being the system able to deal with many frequencies and to reduce sensitivities to the variation of the design parameters while maintaining similar performances. The drawback is in the correct tuning of all the TMDs that has a bigger computational cost and is overall more difficult requiring often a numerical approach.

The proposed method aims to perform, with a lower computational cost, a robust optimal design of a SDF system with a variable number of TMDs of assigned total mass ratio  $\gamma_t$ . The system is excited by a stationary seismic load, modelled by the Tajimi-Kanai filter. The uncertainties are assumed on the main system properties: natural frequency  $\omega_s$ , damping ratio  $\xi_s$ , mass ratio of the TMDs  $\gamma_t$ , and on the seismic excitation described by the filter: circular frequency  $\omega_K$  and damping ratio  $\xi_K$ . To consider the sensitivity of the system, the direct perturbation method is applied respect to every uncertain parameter. Then, a multi-objective optimization, based on genetic algorithms, is performed and a Pareto front investigated to get an optimal design.

The choice of the Tajimi-Kanai model, defined by a SDF oscillator, aims to describe properly the resonance effects on the system. The assumption of stationariness is justified according to sec.2.4.3, considering only the strong motion phase. The direct perturbation method determines the sensitivities by only knowing the moments of the distributions instead of providing a full description that would be onerous and sensible to small errors. The use of a SDF (corresponding to a mode of vibration of the structure with its proper frequency) allows to describe in detail the effects of the uncertain in terms of frequencies and distance from the resonance. In practice, once the predominant mode is founded by a modal decomposition, the optimization algorithm can be applied for its frequency.

The analysis performed considers some simplifications in the description of the response. Despite this, the main objective of the study is not to describe in detail the behave of the system but to perform an optimization and, therefore, also a simplified analysis can give significant results. Moreover, the standard deviation of the process is connected to the failure probability of the peak values and the final results would not be particularly different from more detailed, but also more onerous, reliability analysis.

First a deterministic optimization is performed, showing how the nature of external action and main system influence the optimal configuration of TMDs, especially for what concerns the number of dampers. The absolute acceleration shows to be less sensitive to the variation of these parameters, differently from the displacements, as will be shown by the spectrum. After that, for a rigid soil and stiff structure (conditions more restrictive for a displacement reduction), a robust optimization is performed to get the optimal parameters and number of dampers and to compare it with a deterministic optimization.

### 5.1 Dynamic random vibrations analysis of the system

The system in exam is showed in fig.5.1. A white noise, Gaussian, mean zero signal, filtered by the Tajimi-Kanai oscillator, is applied;  $\vec{\tau}$  is the vector of influence of the filter on the different degrees of freedom. The SDF system with  $n$  TMD is transformed in an equivalent system with  $(n + 2)$  degrees of freedom given by the ones of the main system plus the  $n$  degrees of freedom added by the dampers and the single degree of freedom of the filter.

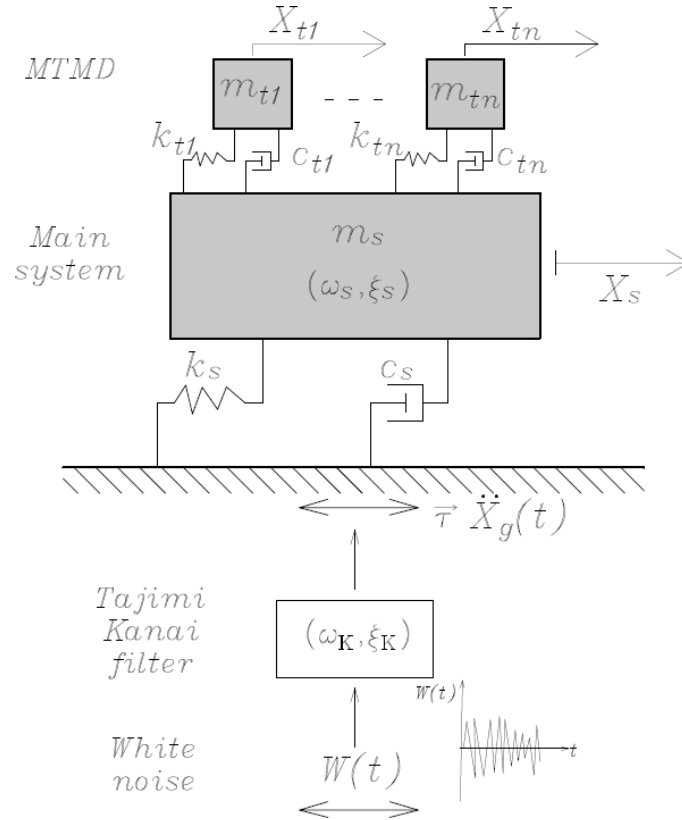


Figure 5.1: Dynamic scheme of MTMD system for a SDF structure.

The main uncertain characteristics of the system are: the mass  $m_s$ , damping  $c_s$  and stiffness  $k_s$ . The vector  $\vec{X}(t)$  contains  $(n+2)$  values corresponding to the displacements of the main system, of the TMDs and of the filter.  $X_s(t)$  is a scalar corresponding to the only degree of freedom of the main system and  $W(t)$  is the white noise applied to the filter.

For the system of MTMD the main characteristics are described in diagonal matrices:

$$\mathbf{M}_t = \text{diag}(\vec{\gamma}_t m_s) = \begin{bmatrix} m_1 & 0 & \dots & 0 \\ 0 & m_2 & 0 & \vdots \\ \vdots & & \ddots & 0 \\ 0 & \dots & 0 & m_n \end{bmatrix}, \quad (5.1)$$

$$\mathbf{C}_t = \begin{bmatrix} c_1 & 0 & \dots & 0 \\ 0 & c_2 & 0 & \vdots \\ \vdots & & \ddots & 0 \\ 0 & \dots & 0 & c_n \end{bmatrix}, \quad \mathbf{K}_t = \begin{bmatrix} k_1 & 0 & \dots & 0 \\ 0 & k_2 & 0 & \vdots \\ \vdots & & \ddots & 0 \\ 0 & \dots & 0 & k_n \end{bmatrix} \quad (5.2)$$

There is no interaction between the TMDs because they are connected to the main system but not between each other. The matrix  $\mathbf{M}_t$  is defined by a  $(n \times 1)$  vector  $\vec{\gamma}_t$  that assigns a mass ratio to each TMD, where 1 is the only degree of freedom of the main system.

The global matrices of the mechanical characteristics of the equivalent  $(n+1) \times (n+1)$  system are as follow. The mass:

$$\mathbf{M} = \begin{bmatrix} m_1 & 0 & \dots & \dots & 0 \\ 0 & m_2 & 0 & \dots & \vdots \\ \vdots & & \ddots & & \vdots \\ & & & m_n & 0 \\ 0 & \dots & \dots & 0 & m_s \end{bmatrix}, \quad (5.3)$$

the damping:

$$\mathbf{C} = \begin{bmatrix} c_1 & 0 & \dots & \dots & -c_1 \\ 0 & c_2 & 0 & \dots & -c_2 \\ \vdots & & \ddots & & \vdots \\ & & & c_n & -c_n \\ -c_1 & -c_2 & \dots & -c_n & c_s + \sum_{i=1}^n c_i \end{bmatrix}, \quad (5.4)$$

the stiffness:

$$\mathbf{K} = \begin{bmatrix} k_1 & 0 & \dots & \dots & -k_1 \\ 0 & k_2 & 0 & \dots & -k_2 \\ \vdots & & \ddots & & \vdots \\ & & & k_n & -k_n \\ -k_1 & -k_2 & \dots & -k_n & k_s + \sum_{i=1}^n k_i \end{bmatrix}, \quad (5.5)$$

where the terms of the  $\mathbf{C}$  matrix in the column  $(n+1)$  correspond to the damping transmitted by the main system to the dampers  $\vec{C}_{st}$  and the row  $(n+1)$  to the damping transmitted by each dampers to the main system  $\vec{C}_{ts}$ ; the last element  $(n+1, n+1)$  is the total damping of the main system increased by the contribute of TMDs. The same is valid for the  $\mathbf{K}$  matrix.

The equation of motions for system and TMDs are, respectively:

$$\begin{cases} m_s \cdot \ddot{X}_s(t) + c_s \cdot \dot{X}_s(t) + \sum_{i=1}^n c_i \cdot \dot{X}_i(t) + k_s \cdot X_s(t) + \sum_{i=1}^n k_i \cdot X_i(t) = -m_s \cdot \ddot{X}_g(t) \\ \mathbf{M}_t \cdot \ddot{\vec{X}}_t(t) + \mathbf{C}_t \cdot \dot{\vec{X}}_t(t) + \vec{C}_{st} \cdot \dot{X}_s(t) + \mathbf{K}_t \cdot \vec{X}_t(t) + \vec{K}_{st} \cdot X_s(t) = -\vec{\gamma}_t m_s \cdot \ddot{X}_g(t) \end{cases} \quad (5.6)$$

In eq.(5.6),  $-\vec{\gamma}_t \cdot \ddot{X}_g(t)$  is the effect of the ground acceleration on the TMDs which is given by the Tajimi Kanai-filter equations:

$$\begin{cases} \ddot{X}_g = -\omega_K^2 \cdot X_K(t) - 2\xi_K \omega_K \cdot \dot{X}_K(t) \\ \ddot{X}_K(t) + 2\xi_K \omega_K \cdot \dot{X}_K(t) + \omega_K^2 \cdot X_K(t) = -W(t) \end{cases} \quad (5.7)$$

In the state space the filter is described as follow:

$$\begin{cases} \ddot{X}_g(t) = \vec{a}_K^T \cdot \vec{Y}_K(t) \\ \vec{Y}_K(t) = \mathbf{D}_K \cdot \vec{Y}_K(t) - \vec{v}_K \cdot W(t) \end{cases} \quad (5.8)$$

where  $W(t)$  is a mean zero, Gaussian, white noise process representing the excitation at the bedrock. The stationary covariance of the white noise excitation is  $E[W(t) \cdot W(t - \tau)] = 2\pi S_0 \cdot \delta(t - \tau)$ , where  $\delta(t - \tau)$  is the delta of Dirac and  $S_0$  the power spectrum of the white noise. The other terms in eq.(5.8) are:

$$\vec{Y}_K(t) = \begin{bmatrix} \vec{X}_K(t) \\ \dot{\vec{X}}_K(t) \end{bmatrix}, \quad \mathbf{D}_K = \begin{bmatrix} 0 & 1 \\ -\omega_K^2 & -2\xi_K\omega_K \end{bmatrix}, \quad \vec{v}_K(t) = \begin{bmatrix} 0 \\ 1 \end{bmatrix}, \quad \vec{a}_K = \begin{bmatrix} -\omega_K^2 \\ -2\xi_K\omega_K \end{bmatrix} \quad (5.9)$$

Grouping the displacements in a vector  $\vec{X}(t) = [X_1(t), \dots, X_n(t), X_s(t)]^T$ , the equation of motion (5.6) can be rewritten in the state space once the state space vector  $\vec{Y}(t)$  is defined:

$$\vec{Y}(t) = [\vec{X}_t(t), X_s(t), \dot{\vec{X}}_t(t), \dot{X}_s(t)]^T \quad (5.10)$$

The dynamic equilibrium equation becomes:

$$\mathbf{A} \cdot \vec{Y}(t) + \mathbf{B} \cdot \dot{\vec{Y}}(t) = \vec{p}(t) \quad (5.11)$$

where:

$$\mathbf{A} = \mathbf{I}_{2n} = \begin{bmatrix} \mathbf{I}_n & \mathbf{0} \\ \mathbf{0} & \mathbf{I}_n \end{bmatrix}, \quad \mathbf{B} = \begin{bmatrix} \mathbf{0} & \mathbf{I}_n \\ -\mathbf{M}^{-1}\mathbf{K} & -\mathbf{M}^{-1}\mathbf{C} \end{bmatrix}, \quad \vec{p}(t) = \begin{bmatrix} \vec{0} \\ \mathbf{M}^{-1}\vec{F}(t) \end{bmatrix}, \quad (5.12)$$

$$\mathbf{D} = \mathbf{A}^{-1}\mathbf{B} = \begin{bmatrix} \mathbf{0} & \mathbf{I}_n \\ -\mathbf{M}^{-1}\mathbf{K} & -\mathbf{M}^{-1}\mathbf{C} \end{bmatrix} \quad (5.13)$$

Once that the system matrices are set, the theory of filters can be used to perform the analysis of the second order moments of the system. The final state space equation is:

$$\dot{\vec{Y}}(t) = \bar{\mathbf{D}}_N \cdot \vec{Y}(t) + \vec{v} \cdot \varphi(t) \cdot W(t) \quad (5.14)$$

where  $\varphi(t) = 1$  for a stationary input and the other terms are:

$$\begin{aligned} \vec{Y}(t) &= \begin{bmatrix} \vec{Y}(t) \\ \vec{Y}_K(t) \end{bmatrix}, \quad \bar{\mathbf{D}}(t) = \begin{bmatrix} \mathbf{D}_N & \mathbf{D}_{Nf}(t) \\ \mathbf{0} & \mathbf{D}_f(t) \end{bmatrix} \\ \vec{v} &= \begin{bmatrix} \vec{0}_{2n} \\ \vec{v}_K \end{bmatrix}, \quad \mathbf{V}_N = \begin{bmatrix} \mathbf{0} \\ \mathbf{M}^{-1} \end{bmatrix}, \quad \mathbf{D}_{Nf}(t) = \mathbf{V}_N \cdot \vec{\tau} \cdot \vec{a}_K^T(t) \end{aligned} \quad (5.15)$$

The Lyapunov equation is applied to get the covariance matrix of the state space vector of response, remembering that, for stationary mean zero processes, correlation and covariance coincide. For the case of delta-correlated, stationary, mean zero input, the equation can be written as:

$$\bar{\mathbf{D}} \cdot \mathbf{R}_{YY}(\tau, \tau) + \mathbf{R}_{YY}(\tau, \tau) \cdot \bar{\mathbf{D}}^T = 2\pi \mathbf{A}^{-1} S_0(\tau) (\mathbf{A}^{-1})^T \quad (5.16)$$

Defining  $\mathbf{P} = 2\pi \mathbf{A}^{-1} S_0(t) (\mathbf{A}^{-1})^T$ , the (5.16) becomes:

$$\mathbf{D} \cdot \mathbf{R}_{YY}(\tau, \tau) + \mathbf{R}_{YY}(\tau, \tau) \cdot \mathbf{D}^T = \mathbf{P} \quad (5.17)$$

where  $\tau = t_2 - t_1$  is the difference of time and  $\mathbf{R}_{YY}$  the stationary covariance corresponding to the matrix form of the second order moments  $\vec{m}_{2,Y}(t)$  (remembering that the mean of the response is zero). Eq.(5.17) can be solved by the defining the following matrices:

$$\bar{\mathbf{D}}_2 = \bar{\mathbf{D}}_{n+1} \otimes \mathbf{I}_{n+1} + \mathbf{I}_{n+1} \otimes \bar{\mathbf{D}}_{n+1} \quad (5.18)$$

$$\mathbf{f}_2(t) = 2\pi S_0 \varphi^2(t) \cdot (\vec{v} \otimes \vec{v}) \quad (5.19)$$

The second order moments are given by:

$$\dot{\vec{m}}_{2,Y}(t) = \bar{\mathbf{D}}_2 \cdot \vec{m}_{2,Y}(t) + \mathbf{f}_2(t) \quad (5.20)$$

that in the stationary case becomes:

$$\vec{m}_{2,Y}(\tau) = \bar{\mathbf{D}}_2^{-1} \cdot \mathbf{f}_2(\tau) \quad (5.21)$$

Otherwise, a Shur decomposition can be used[66]. The covariance of the acceleration is obtained from the state space equation (5.11):

$$\dot{\vec{Y}}(t) = \mathbf{A}^{-1} \mathbf{B} \cdot \vec{Y}(t) + \mathbf{A}^{-1} \vec{p}(t) = \mathbf{D} \cdot \vec{Y}(t) + \vec{p}(t) \quad (5.22)$$

that in expanded form becomes:

$$\dot{\vec{Y}}(t) = \begin{bmatrix} \dot{\vec{X}}(t) \\ \dot{\vec{X}}(t) \end{bmatrix} = \begin{bmatrix} \mathbf{0} & \mathbf{I}_n \\ -\mathbf{M}^{-1} \mathbf{K} & -\mathbf{M}^{-1} \mathbf{C} \end{bmatrix} \cdot \begin{bmatrix} \vec{X}(t) \\ \vec{X}(t) \end{bmatrix} + \begin{bmatrix} \vec{0} \\ \mathbf{M}^{-1} \vec{F}(t) \end{bmatrix} \quad (5.23)$$

where the applied force is the ground acceleration output of the filter,  $\mathbf{M}^{-1} \vec{F}(t) = -\vec{X}_g$ . Let take the second term of the equation and expand it:

$$\vec{X} = [-\mathbf{M}^{-1} \mathbf{K} \quad -\mathbf{M}^{-1} \mathbf{C}] \cdot \begin{bmatrix} \vec{X}(t) \\ \vec{X}(t) \end{bmatrix} - \vec{X}_g \quad (5.24)$$

The inertial forces induced on the structure depend on the absolute acceleration  $\vec{X}_{tot} = \vec{X} + \vec{X}_g$ . Therefore, the total acceleration is:

$$\vec{X}_{tot} = [-\mathbf{M}^{-1} \mathbf{K} \quad -\mathbf{M}^{-1} \mathbf{C}] \cdot \begin{bmatrix} \vec{X}(t) \\ \vec{X}(t) \end{bmatrix} = \mathbf{V} \cdot \vec{Y} \quad (5.25)$$

Applying the linear operator mean to the product  $(\vec{X}_{tot} \cdot \vec{X}_{tot}^T)$  gives the covariance matrix of the absolute acceleration:

$$E[\vec{X}_{tot} \cdot \vec{X}_{tot}^T] = \mathbf{R}_{\vec{X}_{tot} \vec{X}_{tot}} = \mathbf{V} \cdot \begin{bmatrix} \mathbf{R}_{XX} \\ \mathbf{R}_{\dot{X}\dot{X}} \end{bmatrix} \cdot \mathbf{V}^T \quad (5.26)$$

Following the method of sec.4.6.4, the analysis is performed both for the protected and unprotected case, then the objective functions are defined as ratio between them, i.e., as the *index of vibration protection effectiveness*.

A minimum of the index corresponds to an optimum of the system performance in terms of displacements:

$$OF_{displ} = \frac{\sigma_{XX}}{\sigma_{XX,0}} \quad (5.27)$$

absolute accelerations:

$$OF_{acc} = \frac{\sigma_{\ddot{X}_{tot} \ddot{X}_{tot}}}{\sigma_{\ddot{X}_{tot} \ddot{X}_{tot},0}} \quad (5.28)$$

or threshold associated to an acceptable failure probability:

$$OF_{Pf} = \frac{u}{u_0} \quad (5.29)$$

In the next paragraph considerations about the determination of the design threshold are reported.

### 5.1.1 Proposed approaches to determine the failure probability

To perform an analysis of peaks an acceptable failure probability has to be set, then, for the fixed probability, a distribution of peaks is assumed. Despite the limits illustrated by the Poisson formulation, as higher is the threshold and as much the distribution fits the real behave. Therefore, for a first passage analysis the Poisson approximation may be justified if the failure value is high enough. A characteristic value is assumed with a failure probability sets to 95%. Considering initial rest conditions, the double threshold failure probability after a time  $T_X$  is given by:

$$p_{T_X} = \nu_{|X|}^+(u) \cdot \exp[-\nu_{|X|}^+(u) \cdot T_X] \quad (5.30)$$

where  $u$  is the fixed threshold corresponding to the assigned probability. The term  $\nu_{|X|}^+$  is the double threshold rate of up-crossing, that in the stationary Gaussian process is equal to:

$$\nu_{|X|}^+ = 2 \cdot \nu_X^+ = \frac{1}{\pi} \frac{\sigma_{\dot{X}}}{\sigma_X} \exp\left(-\frac{u^2}{2\sigma_X^2}\right) \quad (5.31)$$

Inverting this formulation gives:

$$u = \sqrt{-2\sigma_X^2 \cdot \ln\left[-\frac{\pi}{T_X} \left(\frac{\sigma_X}{\sigma_{\dot{X}}}\right) \cdot \ln(1 - p_{T_X})\right]} \quad (5.32)$$

that indicates the threshold  $u$  corresponding to the assigned failure probability. The assumption of Gaussian stationary response is justified by the linearity of the problem: a mean zero, stationary Gaussian input gives a mean zero, stationary Gaussian output if the system behaves linearly.

Unfortunately, the independent up-crossing approximation is not generally acceptable. In fact, referring to the spectrum in fig.4.4, it is evident how the unprotected SDF system subjected to a seismic acceleration behaves as a narrow band process while the use of TMDs flattens the spectrum and the behave tends to broad band. The assumption of independent up-crossing is conservative for narrow band processes while more realistic for broad band and this would create a biased descriptor of the effectiveness of devices.

To have a correct description of the failure probability, the more general failure probability formulation has to be adopted:

$$P_{X_T} = L_X(u, t) = L_0 \cdot \exp[-\eta_X(u) \cdot t], \quad \text{for large } t \quad (5.33)$$

Where  $L_0 = 1.0$ , initial rest conditions. Using the Vanmarcke formulation :

$$\frac{\eta_X(u)}{\nu_{|X|}^+} \approx \left[1 - \exp\left(-\left(1 - q_X^2\right)^{0.6} (\pi/2)^{0.5} \frac{u}{\sigma_X}\right)\right] \cdot \left[1 - \exp\left(\frac{-u^2}{2\sigma_X^2}\right)\right]^{-1} \quad (5.34)$$

where the bandwidth has to be determined as:

$$q_X = \sqrt{1 - \frac{\lambda_{X,1}^2}{\lambda_{X,0}\lambda_{X,2}}}, \quad 0 \leq q_X \leq 1 \quad (5.35)$$

Therefore, to determine the failure probability according to the Vanmarcke's distribution of peaks, the odds spectral moments have to be determined. In this study, different approaches have been considered but every one presented limitations in its application to the problem in exam.

The first adopted approach has been the calculation of the non geometric odds spectral moments according to sec.2.2.6, but the not classical damping of the system created many problems in the modelling of an adequate transfer matrix  $\Theta_Y$  that cannot be found directly.

A second adopted approach considers the geometric spectral moments calculation, the latter also provides the possibility to model more accurately the seismic excitation as non-stationary modulated input consistent with the design spectrum. In the simple stationary case, the spectral moments are obtained by the PSD integration:

$$\lambda_{j,X} = \int_0^{+\infty} \omega^j \mathbf{H}(\omega) \cdot G_{\ddot{X}_g}(\omega) d\omega \quad (5.36)$$

where:

$$\mathbf{H}(\omega) = [\mathbf{k} - \omega^2 \mathbf{m} + i\omega \mathbf{c}]^{-1} \quad (5.37)$$

and the input Tajimi-Kanai PSD is:

$$S_{\ddot{X}_g} = \frac{1}{2} G_{\ddot{X}_g} = \frac{(\omega_K^4 + \xi_K^2 \omega_K^2 \omega^2) S_0}{(\omega_K^2 - \omega^2)^2 + 4\xi_K^2 \omega_K^2 \omega^2} \equiv S_{TK}(\omega) \quad (5.38)$$

A cut-off frequency  $\omega_s$  for the integration has to be chosen, either if it is performed numerically or analytically. The choice depends on finding a value of  $\mathbf{H}(\omega)$  negligible after  $\omega_s$ . Being the problem characterized by uncertain on the system parameters it could be a reasonable approach to calculate the deviation of the harmonic transfer matrix  $\mathbf{H}(\omega)$  and fix the cut-off frequency according to the worst value. Whatever the case, a loss of informations has to be accepted as trade-off. Another problem of this approach relies in the application of the direct perturbation method[40]: as the exciting process is narrow band, as the effect of uncertainties on the spectrum is big because it is basically more sharp and, therefore, sensible to variations. The direct perturbation may fail in the description of highly non-linear behaves as in the PSD of displacements. Better results may come from the use of approximations of second order, but they often become cumbersome and difficult to be determined. The use of simple matrix operations, by the state space approach, eliminates the problems related to the integration of these sharp PSDs.

Barone et.al[3] proposed an interpolated closed form for the sampling of the design spectrum according to its different branches. Then, a closed form recursive calculation is used for the determination of the spectral moments after an ordinary modal analysis (unfortunately, not the case of TMDs). The method is particularly effective in order to avoid onerous numerical integrations that for optimization aims become computationally cumbersome. The sensitivity analysis would be simplified too because only analytical expressions are used; uncertain has to be consider on mass, stiffness and damping matrices because a modal analysis has to be performed.

Andreucci and Muscolino[2] proposed a more general approach valid also for not ordinary damped structures that requires a numerical integration of a generalized form of eq.(5.36), considering a not-classically damped structure. A numerical frequency integration has to be performed for the uncoupled complex modes, presenting the same problems of the stationary approach of eq.(5.36). It is worth noting that in this case too it is possible to consider an uncertain on the harmonic transfer function  $\mathbf{H}(\omega)$  to determine the cut-off frequency of integration.

Combining a description of the consistent PSD according to Barone et.al[3] with the integration proposed by Andreucci and Muscolino[2] it is possible to determine in a quite straightforward way the response of the system by only performing a numerical integration in frequency domain while the others formulations are in closed form. Overall, this method gives a better description of the final response in order to perform the optimization, but has the same problem related to the uncertain on the cut-off frequency for the PSD analysis and is numerically onerous in iterative optimization problems.

## 5.2 Direct perturbation method and uncertain

To obtain the sensitivity of the system, that is, the standard deviation from the design value of the response, the direct perturbation method is applied. The uncertain parameters assumed are:

- the natural frequency of the main system  $\omega_s$ ;
- the damping ratio of the main system  $\xi_s$ ;
- the frequency of the Tajimi-Kanai filter  $\omega_k$ ;
- the damping ratio of the Tajimi-Kanai filter  $\xi_k$ ;
- the mass ratio of the tuned mass dampers;  $\gamma_t$ ;

that are all collected in the vector of uncertain parameters  $\vec{d} = [\omega_s, \xi_s, \omega_k, \xi_k, \gamma_t]$ . The dependence between these parameters is small, but in general not nil. However, the assumption of statistically independent parameters is often accepted because otherwise the calculation would become cumbersome. Once the derivatives respect to these parameters are set, the sensitivity of the objective function is determined assuming a linear approximation:

$$E[Q_{lin}] = Q_0 = \mu_Q \quad (5.39)$$

$$Var[Q_{lin}] = \sum_{l=1}^R \beta_{lk}^2 \cdot \sigma_{Rl}^2 \quad (5.40)$$

where the mean value is assumed coincident with the target design,  $\beta_{lk}$  are the sensitivity coefficients and  $\sigma_{Rl}^2$  the variance of each design parameter. The use of the linear perturbation method allows to work still in the field of linearity and after performing the previous analysis obtain again a mean zero, stationary Gaussian output, given a mean zero, stationary Gaussian input.

The derivatives of the objective functions in eq.(5.27) and (5.28) are respectively:

$$(OF_{displ})_{d_i} = \frac{-(\sigma_{XX})_{d_i} \cdot \sigma_{XX,0} + (\sigma_{XX,0})_{d_i} \cdot \sigma_{XX}}{\sigma_{XX,0}^2} \quad (5.41)$$

$$(OF_{acc})_{d_i} = \frac{-(\sigma_{\ddot{X}_{tot}\ddot{X}_{tot}})_{d_i} \cdot \sigma_{\ddot{X}_{tot}\ddot{X}_{tot},0} + (\sigma_{\ddot{X}_{tot}\ddot{X}_{tot},0})_{d_i} \cdot \sigma_{\ddot{X}_{tot}\ddot{X}_{tot}}}{\sigma_{\ddot{X}_{tot}\ddot{X}_{tot},0}^2} \quad (5.42)$$

The standard deviation in the previous equations is obtained from the variance as:

$$\sigma_{XX} = \sqrt{\sigma_{XX}^2} \quad (5.43)$$

Consequently, the derivative is:

$$(\sigma_{XX})_{d_i} = -\frac{1}{2} \frac{(\sigma_{XX}^2)_{d_i}}{\sqrt{\sigma_{XX}^2}} \quad (5.44)$$

and the same for  $(\sigma_{\dot{X}\dot{X}})_{d_i}$  and  $(\sigma_{\ddot{X}_{tot}\ddot{X}_{tot}})_{d_i}$ . For what concerns the variance of acceleration, it depends linearly from the other variance, as stated in eq.(5.26), and its derivative is:

$$\mathbf{R}_{\ddot{X}_{tot}\ddot{X}_{tot}} = 2 \cdot (\mathbf{V})_{d_i} \cdot \begin{bmatrix} \mathbf{R}_{XX} \\ \mathbf{R}_{\dot{X}\dot{X}} \end{bmatrix} \cdot \mathbf{V}^T + \mathbf{V} \cdot \begin{bmatrix} \mathbf{R}_{XX} \\ \mathbf{R}_{\dot{X}\dot{X}} \end{bmatrix}_{d_i} \cdot \mathbf{V}^T \quad (5.45)$$

The derivative of the Lyapunov equation is calculated considering the linearity of the operator, grouping all the linear operations in  $\text{lyap}(\bullet)$ . In this way, it can be written as:

$$\mathbf{R}(\vec{d}) = \text{lyap}(\vec{d}) \quad (5.46)$$

and its derivative respect to the  $i^{\text{th}}$  uncertain parameter is:

$$(\mathbf{R}(\vec{d}))_{d_i} = \left( \frac{\partial[\mathbf{R}(\vec{d})]}{\partial d_i} \right)_{\vec{d}=\vec{\mu}_d} = \left( \frac{\partial[\text{lyap}(\vec{d})]}{\partial d_i} \right)_{\vec{d}=\vec{\mu}_d} \quad (5.47)$$

Applying this to eq.(5.17) gives:

$$\mathbf{D} \cdot (\mathbf{R}_{YY})_{d_i} + (\mathbf{R}_{YY})_{d_i} \cdot \mathbf{D}^T + \mathbf{H}_i = \mathbf{0}, \quad \mathbf{H}_i = (\mathbf{D})_{d_i} \cdot \mathbf{R}_{YY} + \mathbf{R}_{YY} \cdot (\mathbf{D}^T)_{d_i} + (\mathbf{P})_{d_i} \quad (5.48)$$

the term  $(\mathbf{P})_{d_i} = \mathbf{0}$  because it is independent from the uncertain parameters. Applying the operator  $\text{lyap}(\bullet)$  to eq.(5.48) gives the derivative of the variance  $(\mathbf{R}_{YY})_{d_i}$  respect to each uncertain parameter. The derivatives of  $(\mathbf{D})_{d_i}$  respect to each element of the vector  $\vec{d}$  have been calculated both for the protected and unprotected case, the results are reported in the appendix A.

Once the sensitivity coefficient  $\beta$  is determined, the mean and the variance are given by eq.(5.39) and (5.40). From the variance, the standard deviation is calculated as its square root and a bi-dimensional robust optimization vector is set. It contains the mean and standard deviation (sensitivity) of the index of protection effectiveness:

$$\vec{OF} = [\mu_{OF}, \sigma_{OF}] \quad (5.49)$$

## 5.3 Optimization algorithm

The first step in the optimization is checking if the design domain is convex or not in order to adopt the best algorithm for the analysis. Either for the mean value that for the standard deviation, the design space is not convex due to the peaks and valleys that characterize the response with more TMDs. Therefore, the optimization cannot be performed properly by an ordinary gradient analysis but an heuristic method has to be applied. In this thesis, a genetic algorithm with not articulated preferences is used. The main advantage of this approach is to avoid influences on the Pareto front shape and possible biases induced by wrong evaluations done by the designer.

### 5.3.1 Adopted algorithm

The adopted algorithm is an unbounded, controlled, elitist genetic algorithm, variant of the NSGA-II method[31]. An elitist GA always favours individuals with better fitness value (rank), but also favours individuals that can help to increase the diversity of the population even if they have a lower fitness value.

The individuals are ordered in *ranks* according to their dominance position and the algorithm tracks the *crowding distance*: a measure of the closeness of an individual to its nearest neighbours of the same rank in the objective function space. The distance of individuals at the extreme positions are set to infinity. For the remaining ones, the distance is taken as a sum over the dimensions of the normalized absolute distances between the individual's sorted neighbours. Mathematically, for a problem of dimension  $m$  and sorted, scaled individual  $i$ , the distance  $d(i)$  is:

$$d(i) = \sum_{i=1}^m [x(m, i+1) - x(m, i-1)] \quad (5.50)$$

The algorithm sorts each dimension separately, so the neighbours are intended in each dimension. Individuals of the same rank with a higher distance have more chances of selection (because the distance grants the population diversity). The crowding distance is also one factor in the calculation of the spread, which is part of a stopping criterion and is used as a tie-breaker in tournament selection when two selected individuals have the same rank.

The *spread* is a measure of the movement of the Pareto set. To calculate it, the algorithm first evaluates  $\sigma$ , the standard deviation of the crowding distance of the points that are on the Pareto front. The algorithm then evaluates  $\mu$ , the sum over the  $k^{th}$  objective function indices of the norm of the difference between the current minimum value Pareto point for that index and the value in the previous iteration. The spread is then:

$$\text{spread} = \frac{\mu + \sigma}{\mu + k \cdot \sigma} \quad (5.51)$$

The value is small when the extreme objective function values do not change much between iterations (that is,  $\mu$  is small) and when the points on the Pareto front are spread evenly (that is,  $\sigma$  is small).

### Initialization

The first step in the algorithm is to generate an initial population. In this case, a uniform distributed initial population is created. The recommended population size for this algorithm is {50} when the number of variables is less or equal to 5 and {200} otherwise. In this case the size of the problem variates according to the number of TMD adopted:

- $n_{tmd} + 1$  if a parameter is fixed (either frequency or damping ratio of the TMDs);
- $2 n_{tmd}$  if the parameters are freely chosen;

Whatever the case, a value of {200} has been adopted.

### Iterations

The main iteration of the algorithm proceeds as follows:

1. select the parents for the next generation using the binary tournament method;
2. create the children from the selected parents by mutation and crossover:
  - *crossover*: an heuristic crossover has been adopted, it returns a child that lies on the line containing the two parents, a small distance away from the parent with the better fitness value in the direction away from the parent with the worse fitness value. A default value of 1.2 has been adopted for the distance ratio  $R$ . Taking two parents,  $p_1$  and  $p_2$ , where  $p_1$  has the better fitness value, the function returns the child  $c$ :

$$c = p_2 + R \cdot (p_1 - p_2) \quad (5.52)$$

- *mutation*: being fixed the extreme values of the design vector, an adapt feasible criteria has been used for the mutation in order to not violate the boundaries (that is, physically unacceptable negative values of the design parameters). The algorithm randomly generates directions that are adaptive with respect to the last successful or unsuccessful generation. The mutation direction and step length variates at every iteration to satisfy bounds and linear constraints;

3. score the children by calculating their objective function values and feasibility;
4. combine the current population and the children into one matrix of the extended population by applying the  $(\xi + \lambda)$  method;
5. compute the rank and crowding distance for all individuals in the extended population;
6. trim the extended population to have the initially set population size by retaining the appropriate number of individuals of each rank.

### Stopping criteria

When one of the stopping criteria occurs the algorithm is stopped and the Pareto set drawn. The stop occurs when:

- maximum number of generations exceeded. The assumed value is  $100 \cdot (\text{number of variables})$ ;
- the average relative change in the best fitness function value over stall generations is less than or equal to a function tolerance assumed as  $10^{-4}$  for the multi-objective case and  $10^{-6}$  for the single objective case;
- the set time limit has been exceeded. No time limit has been set for this algorithm;
- the set stall generation time limit has been exceeded. No stall generation time limit has been set for this algorithm;

At the end of the analysis, taking all the individuals of the first rank, the Pareto front is drawn to compare all the non dominated solutions.

### Single-objective optimization

For the single-objective analysis the same procedure is adopted but the rank is defined more easily according to the only criteria of comparison. At the end of the analysis the specimens are ordered and the unique best individual is given.

## 5.4 Obtained results

In this section are presented the obtained results from some benchmark examples. All the tabulated results are reported in appendix-B, while the graphs are showed and discussed in this section.

### 5.4.1 Deterministic analysis

A deterministic analysis is performed for both displacements and absolute accelerations, considering different frequencies of the main system. The size of the problem is  $(n_{tmd} + 1)$  for one fixed parameter and  $(2 \cdot n_{tmd})$  for free parameters. As first approach, for equal optimal damping of the TMDs and fixed filter frequency  $w_K$ , a varying frequency  $\omega_s$  is investigated. As stated by different authors ([67] and [25]), and verified later, fixing equal damping ratio does not leads to particularly different results from a free parameters analysis. Indeed, for free parameters the optimum TMD tents to assume a spread tuning ratio at a fixed value of damping ratio. The solution has been adopted also for the sake of clarity in the graphic representation that would be too spread for free parameters. Defined the *frequency ratio*  $\psi$  between main system and filter, remembering the definition of tuning ratio  $\rho$ :

$$\psi = \frac{\omega_s}{\omega_K}, \quad \rho = \frac{\omega_t}{\omega_s} \quad (5.53)$$

and assumed medium soil conditions ( $\omega_K = 12.5$  rad/s,  $\xi_K = 0.4$ ), the optimization is performed. The adopted data are reported in table 5.1. The analysis has been performed for a number of dampers varying from 1 to 10 either for absolute accelerations that for displacements.

Table 5.1: Initial data for the deterministic optimization with varying  $\psi$

$\omega_s$ (rad/s)	$\xi_s$ (-)	$\gamma_t$ (-)	$\omega_K$ (rad/s)	$\xi_K$ (-)	$S_0$ (cm <sup>2</sup> /s <sup>3</sup> )
[2.5, 20.0]	0.02	0.05	12.5	0.4	1000

Referring to the displacements, in figure 5.2a are reported the frequency values for different number of dampers and frequency ratio  $\psi$ , while in fig.5.2b are reported the OF values. In accordance with Marano et al.[42], for frequency ratios  $\psi > 1$ , the frequencies of the optimal TMDs increase, while they decrease for  $\psi < 1$  (except for low values of  $\psi$  where the tuning becomes difficult). For what concerns the absolute acceleration, in figure 5.3a are reported the frequencies values for different number of dampers and frequency ratio  $\psi$ , while in fig.5.3b are reported the OF values.

The numerical values assumed by the OFs are also tabled in appendix B. As expected, when the frequency ratio is near to the resonance, i.e  $\psi \approx 1$ , the performances improve. The performances in terms of displacements worsen if the number of dampers is increased, leading to a failure of the protection system after a certain number. The absolute acceleration performances instead benefit from the increase of the number of dampers except when the frequency ratio assumes low values ( $\psi \leq 0.4$ ), that is, the main mode of the system is characterized by a low frequency and the structure is slender.

In general, both the acceleration and displacements performances are worsen in slender structures by the use of more TMDs due to a difficult in tuning properly the system. This may be explained by the shape of the PSD of the system for the Tajimi-Kanai spectrum defined in eq.(2.189). The difficult tuning of displacements at the increasing of the number of dampers can be seen if the the transfer function  $H_X(\omega)$  is analysed.

The variance of displacements has a quadratic relation with the PSD:

$$\sigma_{\ddot{X}}^2 = \int_{-\infty}^{+\infty} |H_X(\omega)|^2 \cdot S_{\ddot{X}_g}(\omega) d\omega = \int_0^{+\infty} |H_X(\omega)|^2 \cdot G_{\ddot{X}_g}(\omega) d\omega \quad (5.54)$$

For a SDF system the harmonic transfer matrix takes the form:

$$H_X(\omega) = [k - \omega^2 m + i\omega c]^{-1} = \frac{1}{(\omega_s^2 + 2i\xi_s\omega - \omega^2)} \quad (5.55)$$

In the single degree of freedom case the relation between displacements and acceleration harmonic transfer matrices is given by  $H_{\ddot{X}}(\omega) = \omega^2 \cdot H_X(\omega)$ , while for MDF systems is necessary a modal decomposition but with similar results. For the SDF system it becomes:

$$H_{\ddot{X}}(\omega) = \frac{\omega^2}{(\omega_s^2 + 2i\xi_s\omega - \omega^2)} \quad (5.56)$$

The associated variance is:

$$\sigma_{\ddot{X}}^2 = \int_{-\infty}^{+\infty} |\omega^2 \cdot H_{\ddot{X}}(\omega)|^2 S_{\ddot{X}_g}(\omega) d\omega = \int_0^{+\infty} |\omega^2 \cdot H_{\ddot{X}}(\omega)|^2 G_{\ddot{X}_g}(\omega) d\omega \quad (5.57)$$

The PSD of the Tajimi-Kanai spectrum,  $S_{\ddot{X}_g}$  is reported in fig.5.4. The correspondent PSD of acceleration,  $S_{\ddot{X}\ddot{X}}$  is plotted for the system parameters in fig.5.5. The Tajimi-Kanai PSD of

displacements diverges for values of  $\omega \rightarrow 0$ , this is not a problem in a time analysis but becomes so if the spectrum are used; for sake of clarity, a correspondent Clough-Penzien spectrum is given in fig.5.6 with the associated  $S_{XX}(\omega)$  of displacements in fig.5.7. Another limits of the Tajimi-Kanai spectrum is also the fact that, for  $\omega \rightarrow 0$ ,  $S_{\ddot{x}\ddot{x}}$  does not go to zero too. However, for intermediate frequencies, the spectrum can be used without problems and gives an immediate picture of the resonance effects.

The PSD of acceleration shows a wider band of magnified frequencies compared to the PSD of displacements. As the number of TMDs increases, as the tuning ratio of part of them decreases, while only some are tuned to higher values (see fig.5.2a and fig.5.3a); overall, the bandwidth increases. The TMDs cannot actually be tuned to the same frequency of a STMD because the system increases of degrees of freedom and this modifies the behaviour of the structure, with more peaks and valleys in the response due to the different modal shapes. The very narrow band nature of the PSD of displacements makes difficult a proper tuning of a MTMD with an increasing bandwidth and the performance worsen because there are amplifications of the PSD (of which the subtended area corresponds to the variance of the process). In the case of acceleration, the more broad band nature of the PSD makes the MTMD better perform as the bandwidth increase. For very slender structures, ( $\psi \rightarrow 0$ ), the PSD of acceleration flattens, while the PSD of displacements shows a very sharp peak; both the phenomena are a reason for the worsening of performance as the number of dampers increases: a sharp peak is difficult to be covered without undesired amplification in its neighbourhood, while a flat curve is difficult to be managed by a MTMD with more peaks and valleys that may up-cross it. Actually, the PSD integration is not the adopted approach for the analysis but yet it can explain the physical aspects behind the results.

As demonstrated by Marano et al.[41], this behaviour is also influenced by the nature of the soil, in fact, soft soils imply wider displacements while stiff soils involve bigger accelerations.

In the light of what stated before, a sample stiff structure on a stiff soil is analysed in order to determine the best number of dampers to control displacement and acceleration in the worst conditions for the first (that is the most sensible parameter). The data adopted for the analysis are reported in tab.5.2. The analysis has been performed for: a) uniform damping ratio, free tuning ratio, b) uniform tuning ratio, free damping ratio and c) free parameters.

Table 5.2: Deterministic optimization initial data for the analyzed case

$\omega_s$ (rad/s)	$\xi_s$ (-)	$\gamma_t$ (-)	$\omega_K$ (rad/s)	$\xi_K$ (-)	$S_0$ (cm <sup>2</sup> /s <sup>3</sup> )
13.96	0.02	0.05	18.62	0.4	1000

### Displacements control

Fig.5.8, fig.5.9 and fig.5.10 show the parameters space values for the case a), b) and c). In fig.5.11 the performances of all three cases are compared together.

Increasing the number of TMDs only some dampers are tuned to higher frequencies while the others assume a narrow spacing at lower frequencies. Being the frequency ratio  $\psi < 1$ , the tuning ratio  $\rho < 1$ , similarly to what demonstrated by Marano et al.[42] for the single TMD .

For fixed damping the performances are not too far from adopting free parameters, with an increasing difference with the number of TMDs, until a maximum of 10% for 10 dampers. At this point the performances are not any more acceptable and until when the system works properly the differences are less than 5%. Moreover, it should be kept in account that the uniform MTMD

is more robust than the non uniform one because the loss of one damper does not compromise significantly the performance.

Fixing an uniform damping ratio instead leads to far worse performances: all the TMDs frequencies collapse to the inferior limit of design and the tuning is not possible, all the protection is given by the damping ratio that has to be increased significantly.

For the free parameters optimization, the points are more spread but also in this case only some dampers are tuned to higher frequencies while the others assume a narrow spacing and lower frequency values. The latter are not working as tuned devices and so the performances are granted by their damping ratio that has to be increased.

Overall, increasing the number of dampers worsen the performances of the system because only part of them are properly tuned while the others work as damping devices. The reasons for that have been already stated in the previous section.

### Absolute accelerations control

Fig.5.12, fig.5.13 and fig.5.14 show the parameters space values for the case a), b) and c). In fig.5.15 the performances of the three cases are compared together.

As for the displacements, increasing the number of TMDs, they assume a narrow spacing, lower frequencies and a wider bandwidth. Being the ratio  $\psi < 1$ , the tuning ratio  $\rho < 1$  too as for the displacements.

For fixed damping ratio, the performances are not so far from the free parameters, the difference increases with the number of TMDs until a 2% for 10 dampers but the uniform MTMD has the advantage of being more robust.

Instead, fixing an uniform tuning ratio leads to worse performances: the TMDs cannot be properly tuned because the frequencies are constrained, the damping ratio however remains low because the control of performance is still granted by the tuning.

For the free parameters optimization, the points are more spread but in general some dampers are tuned to uniform frequencies while the others assume a narrow frequency spacing and lower frequency values. Overall, increasing the dampers leads to better performances for the reasons stated in the previous section.

### Displacements and acceleration comparison

The curves of displacements and acceleration are compared for case a), b) and c) in fig.5.16. Overall, for stiff structures the choice of the number of dampers is not immediate because the accelerations and displacements diverge in the optimal choice. If for the displacement in any case increasing the dampers is problematic for the previously stated reasons, the absolute accelerations suffer only for lower system frequency. Consequently, a trade-off between the two parameters has to be adopted in the design.

## 5.4.2 Robust optimization

Referring to a deterministic analysis is limitative. As already said, the aleatory nature of the system may induce dangerous deviations from the design target. For the robustness purpose, these deviation have to be quantified and contained. Therefore, a robust optimization of both displacements and absolute acceleration is performed for the same data of tab.5.2 and the coefficient of variation of the uncertain parameters,  $\eta = \sigma/\mu$ , in tab.5.3. The design parameters are the same,  $\omega_t$  and  $\xi_t$ . The size of the problem is  $(n_{tmd} + 1)$  for one fixed parameter and  $(2 \cdot n_{tmd})$  for free parameters. The Pareto fronts are considered for a number from 1 to 10 dampers and some values extracted from the curves for comparison. On the same graphs are plotted the results obtained by adopting the optimal deterministic parameters in an analysis which takes in account

the uncertainties. As expected, the points are at the extreme of the Pareto fronts, maximizing only the effectiveness with the worst values in robustness.

Table 5.3: Coeff. of variation,  $\eta = \sigma/\mu$ , of the uncertain parameters in the analyzed case

$\omega_s (-)$	$\xi_s (-)$	$\gamma_t (-)$	$\omega_K (-)$	$\xi_K (-)$
0.15	0.20	0.05	0.15	0.10

### Displacements robust control

In fig.5.17, fig.5.18 and fig.5.19 are showed the parameters space values for the case a), b) and c) at the varying number of TMDs. In fig.5.20, 5.21 and 5.22 the Pareto fronts of the three cases are plotted.

In the displacements control the curves are quite flat, showing that every solution has a similar level of robustness. For instance, for 3 TMDs and fixed damping ratio, a decrease of 20% in the mean value implies just an increase of 2% in sensitivity. The system is generally more sensible when the tuning ratio is fixed, implying skewer curves, while between free parameters and fixed damping ratio the results are similar.

For the single TMD, higher damping ratios and lower tuning ratios correspond to more robust but less effective solutions. Increasing the number of dampers, the bandwidth, and consequently the robustness, increase, while the effectiveness worsen. In contrast, increasing the damping ratios improves robustness while worsen the effectiveness. As for the deterministic case, only part of the TMDs is tuned to higher frequencies while the others remain closely spaced at lower tuning ratios. This means a lower tuned mass and worse performance of the MTMD compared to the TMD. After a certain number of dampers the tuning becomes difficult and both effectiveness and robustness worsen.

In fig.5.24, 5.26 and 5.28 the three cases are reported for a number from 1 to 5 dampers to have better comparable curves. The correspondent space parameters values are reported in fig.5.23, fig.5.25 and fig.5.27 with some marked reference points. The points are tabled in appendix B.

### Accelerations robust control

In fig.5.29, fig.5.30 and fig.5.31 are showed the parameters space values for the case a), b) and c) for varying number of TMDs. In fig.5.32, 5.33 and 5.34 the Pareto fronts of the three cases are plotted together with the values from the optimal deterministic design parameters.

In the accelerations control the curves are very skew, showing that a small gain in terms of effectiveness is paid expensively in terms of robustness. For instance, for 3 TMDs and fixed damping, a decrease of 10% in the mean value implies an increase of 2% of sensitivity. However, in the analysed case, the performances, either in terms of mean and standard deviation, are better than displacements. For instance, considering a number between 1 and 5 TMDs, the reduction of acceleration arrives until the 65% compared to only a 35% in terms of displacements, while the sensitivity is kept between the 1% and 3% compared to a 1% to 10 % for displacements. Curiously, the use of a single TMD results in a two fragments front, where the choice is between high performances with low robustness or vice versa. Increasing the number of TMDs leads to more compact curves, resolving this problem.

The system is similarly sensible but less effective when the tuning ratio is fixed, with the fronts shifted on the right, while between free parameters and fixed damping ratio the results are similar. For the single TMD, higher damping ratios and lower tuning ratios correspond to more robust but less effective solutions. Increasing the number of dampers, the bandwidth collapse

and small variations in damping lead to great gains in robustness, showing that MTMD better performs respect to the single TMD. In fact, all the TMDs are tuned to higher frequencies and remain closely spaced.

Overall, increasing the number of TMDs aims to attain a higher level of robustness and performances. In fig.5.36, 5.38 and 5.40 the three cases are reported for a number from 1 to 5 dampers to have better comparable curves. The correspondent space parameters values are reported in fig.5.35, fig.5.37 and fig.5.39 with some marked reference points. The points are tabled in the appendix B.

### 5.4.3 Concluding remarks

As for the deterministic case, the best performance in term of acceleration or displacements are not attained in the same direction. Increasing the number of dampers always leads to more robust solutions but after a certain number the performance of displacements are no more acceptable due to the impossibility of a proper tuning. Overall, the correct choice depends on the required performances for displacements and acceleration, coupled together with a necessary level of robustness. However, an extended study about the influence of the soil nature, and/or the type of external action, on more samples has to be done before to generalize these observations.

## 5.5 Conclusions

The develops in the technologies, materials and building techniques of the recent years have stretched the limits that structures can reach, causing a rapidly increase of the demand of optimized designs. The current approaches set by the codes limit the possibility of the designer by using imprecise and slow adapting coefficients for rapidly evolving aims. A comprehensive study of dynamic cannot preclude the uncertain nature of real actions and of design parameters, a problem that can be addressed only in the field of random vibrations. The limits of a deterministic optimization has been widely described and basically consist in a lack of control on the obtained results, for this reason, a probabilistic approach has to be adopted. In particular, the nature of the TMD systems makes them particularly suitable for a robust optimization that can manage and quantify directly the deviations from the design target.

At this aim, the use of the Lyapunov equation in stationary field, combined with the direct perturbation method, limit the computational cost for the application of an iterative optimization algorithm. Despite the approximation assumed, being the main goal to perform an optimization and not to describe the system, the method leads however to significant results.

The use of a genetic algorithm, an heuristic method with not articulated preference analysis aims to deal with the many local optima of the analysed problem. In this way, after that all the optimal solutions are plotted in the Pareto set, the designer can choose the best one with a clear picture of the situation. This approach leaves a wide space to the designer, without any prescriptive indication and only requiring a certain performances, saving time from reiterative hand made optimization and guiding directly to the best design. All these elements, applied the optimization of tuned mass dampers systems, are realized in an effective robust approach that gives a quantitative indication of the performance and deviations from it. Although the MTMD has showed to be more robust than the single TMD, the nature of the structure and external actions influence significantly the response, leading to difficulties in a proper design, especially in the choice of the number of dampers. At last, the use of a uniform damping ratio MTMD has demonstrated to give similar performances to the not uniform one, with big advantages from the point of view of production and design .

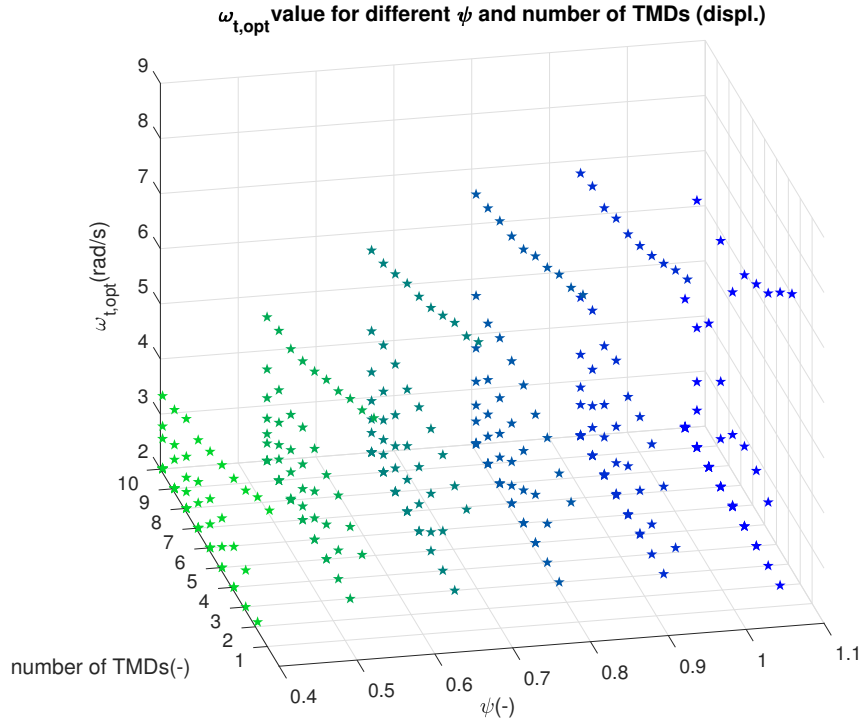
In conclusion, the optimal mechanical parameters (tuning and damping ratio) and number of dampers for the MTMD have to be chosen in accordance to all the previous aspects that can be

evaluated by the presented methods: balancing robustness, performance and practical problems connected to the installation of devices according to the design requirements.

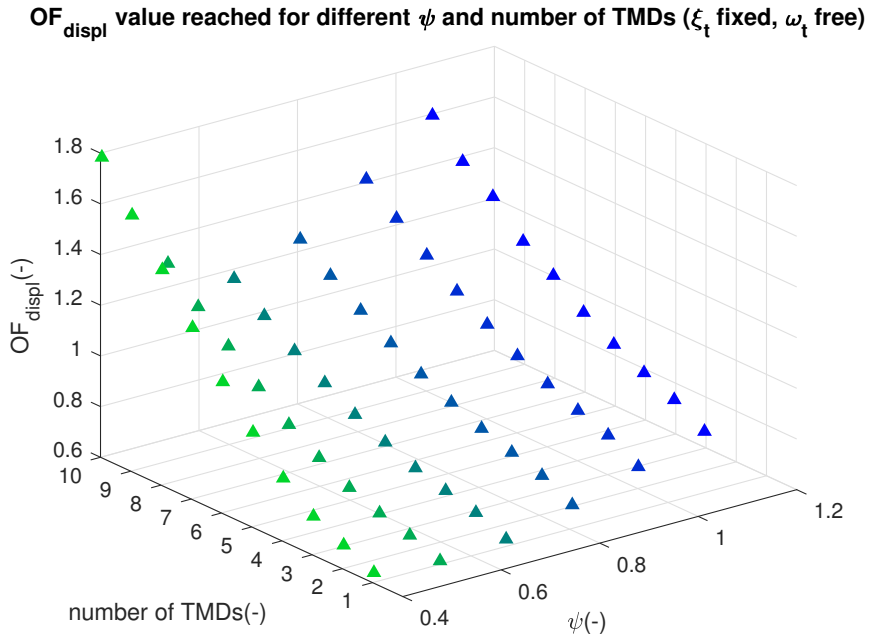
## **5.6 Future develops**

The proposed method assumed many approximations, some of which are very rough but useful to keep a low computational cost for the iterative optimization process. However, a better description of the dynamic process should be the next step for the optimization, applying a Vanmarcke analysis to the failure threshold. Unfortunately, the Lyapunov time domain equation shows many problems in the calculation of the odds spectral moments necessary for the Vanmarcke approach in the case of not ordinary damped filtered systems. A possible solution, either analytical or numerical, has not be found by the author in the literature. The study of the geometric spectral moments, based on the Spectral Power Density, could be a way once a proper spectrum is defined because it avoids the definition of an impulsive transition matrix in complex field. The assumption of stationarity is also a rough approximation, even if the phase of strong motion can be seen in such way, therefore, a not stationary spectrum consistent with the spectrum of design should be used. However, being the construction of such spectrum numerical, also the sensitivity could be investigated only in that way, implying an increase of computational cost.

At last, the presented results are restricted to a specific case and an extended research on the behaves of MTMD system for different combinations of soil conditions, input actions and properties of the structure should be performed in order to get generalized results for the design of the MTMD.



(a)  $\omega_{t,opt}$  dipl. deterministic optimal values for varying  $\psi$  and number of TMDs.



(b) OF dipl. deterministic optimal values for varying  $\psi$  and number of TMDs

Figure 5.2: Optimal parameters and  $OF_{displ}$  for varying frequency ratio  $\psi$  and number of TMDs

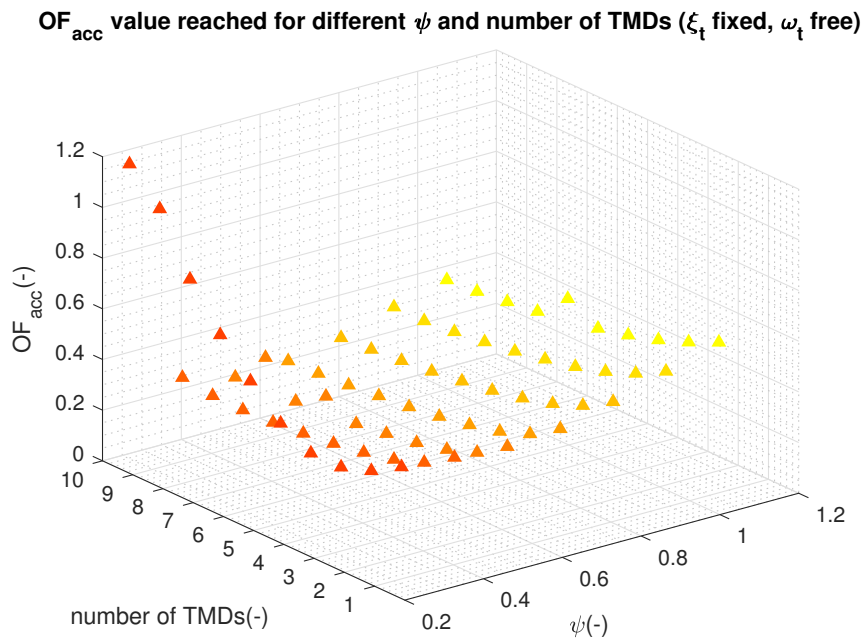
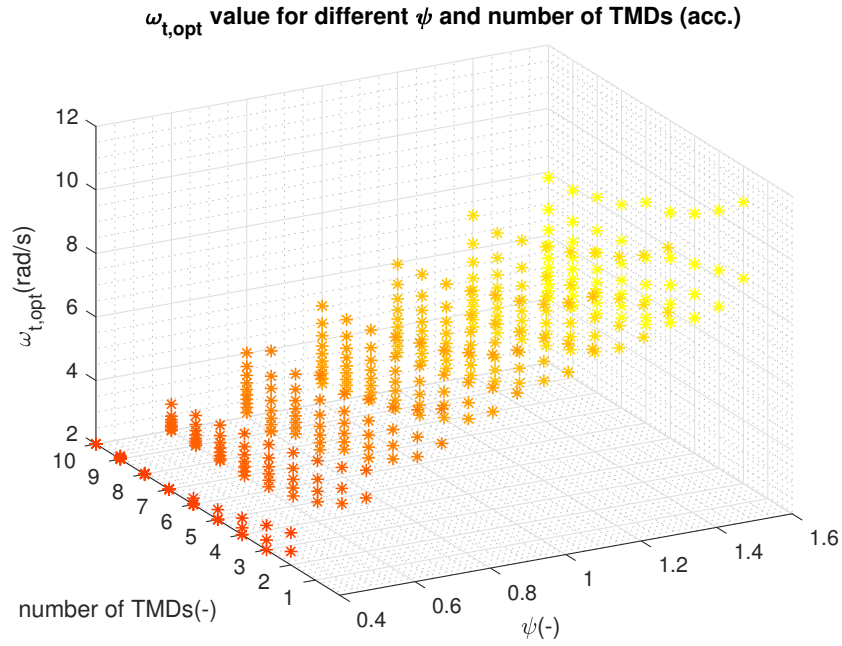


Figure 5.3: Optimal parameters and  $OF_{acc}$  for varying frequency ratio  $\psi$  and number of TMDs

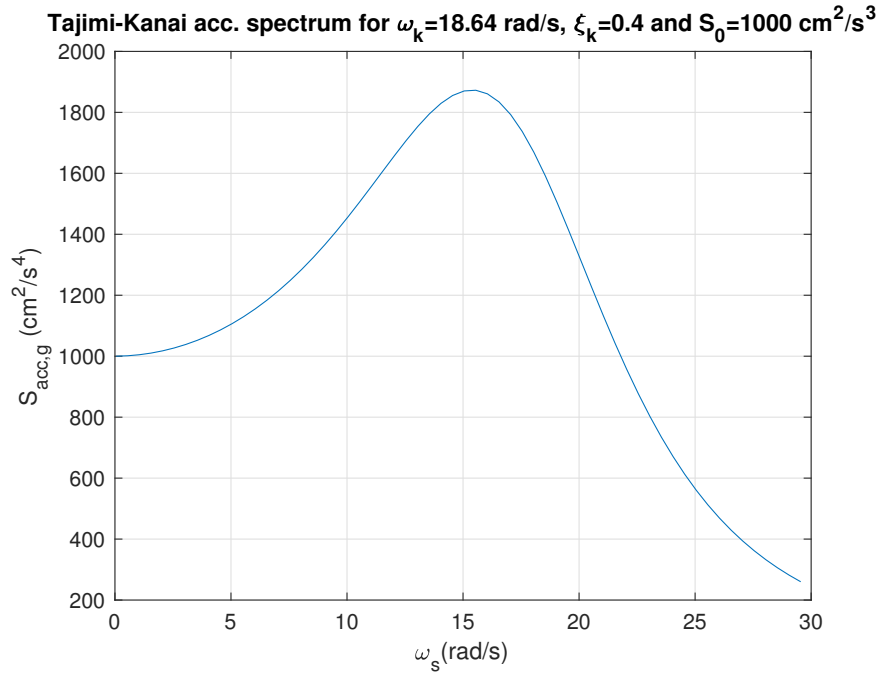


Figure 5.4: Tajimi-Kanai PSD for  $\omega_K = 18.64$  rad/s,  $\xi_K = 0.4$  and  $S_0 = 1000$  cm<sup>2</sup>/s<sup>3</sup>.

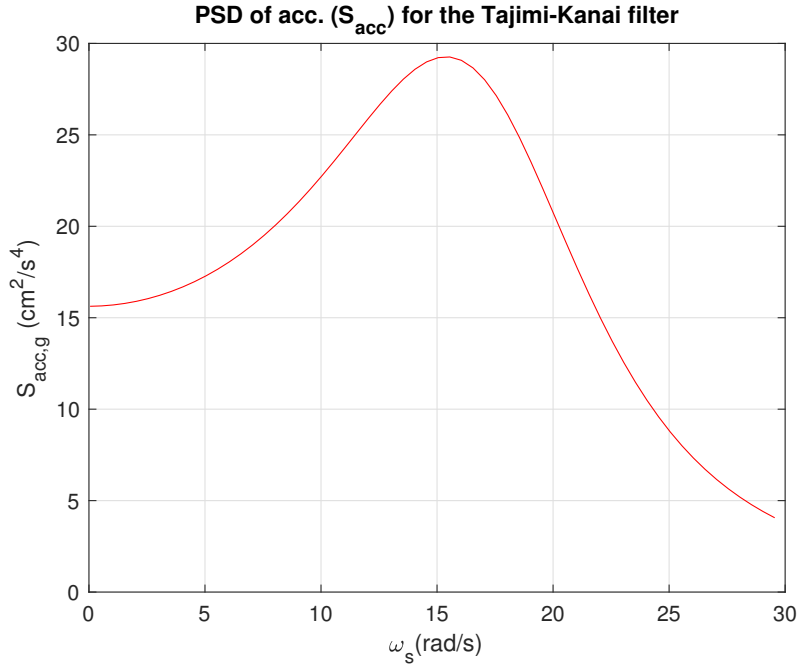


Figure 5.5: PSD of acc.  $S_{\ddot{x}\ddot{x}}$ , for the Tajimi-Kanai spectrum in fig.5.4,  $\omega_s = 13.96$  rad/s and  $\xi_s = 0.05$ .

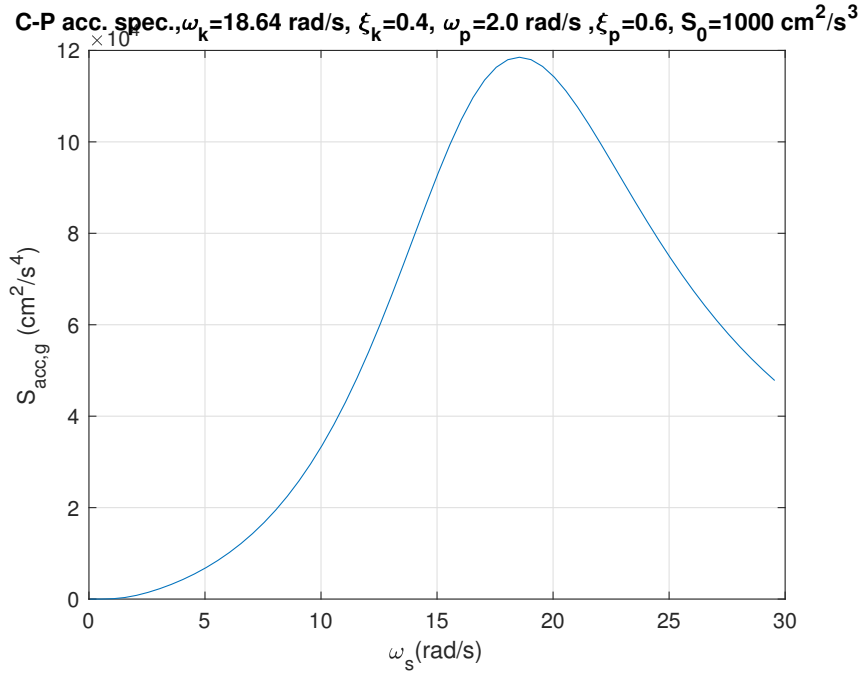


Figure 5.6: Clough-Penzien PSD for  $\omega_K = 18.64$  rad/s,  $\xi_K = 0.4$ ,  $\omega_P = 2.0$  rad/s,  $\xi_P = 0.6$  and  $S_0 = 1000$  cm<sup>2</sup>/s<sup>3</sup>.

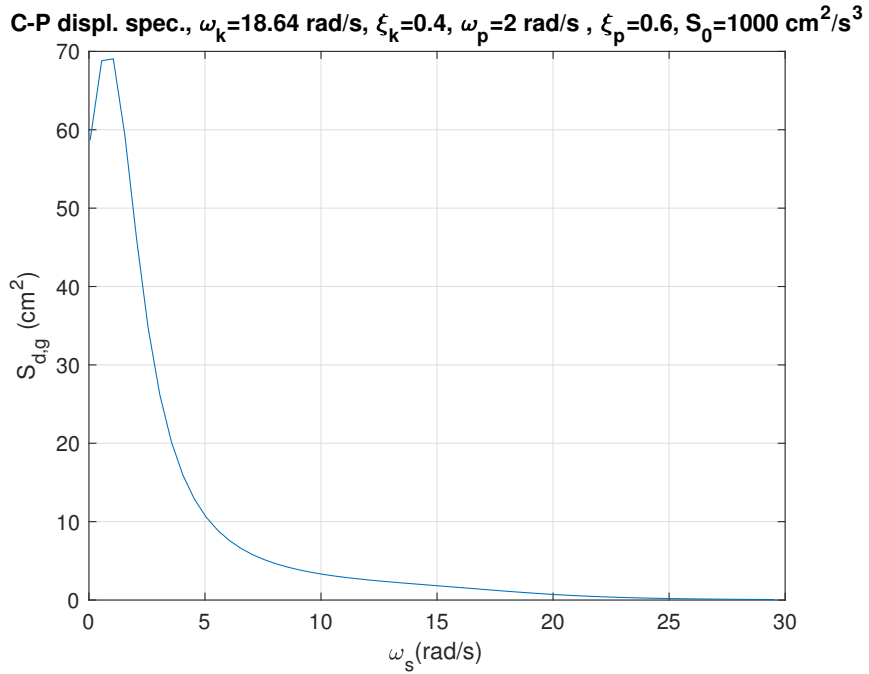


Figure 5.7: PSD of displ.,  $S_{XX}$ , for the Clough-Penzien spectrum in fig.5.6,  $\omega_s = 13.96$  rad/s and  $\xi_s = 0.05$ .

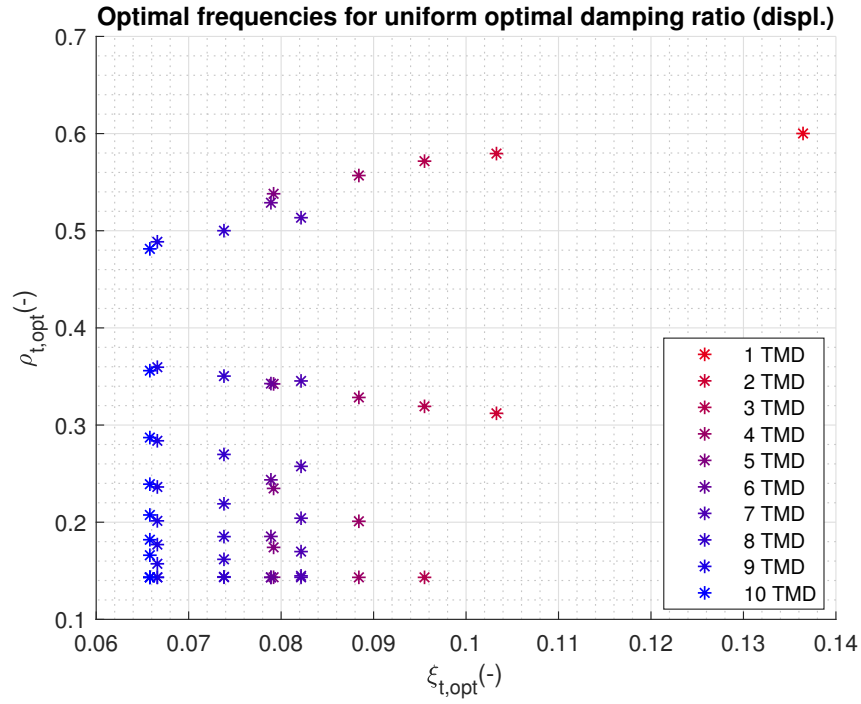


Figure 5.8: Deterministic optimal tuning ratios for uniform damping ratio (displ.).

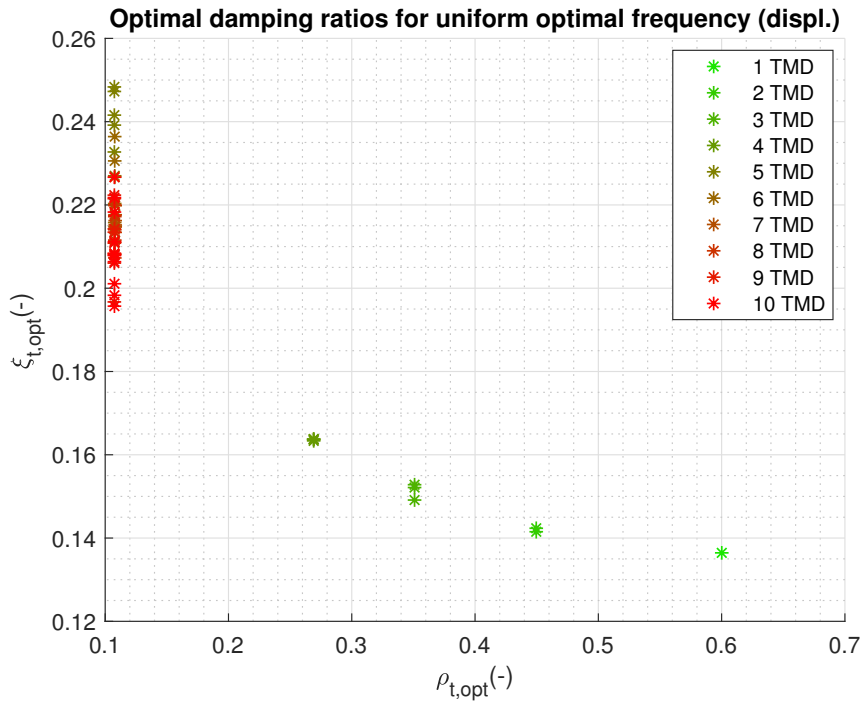


Figure 5.9: Deterministic optimal damping ratios for uniform tuning ratio (displ.).

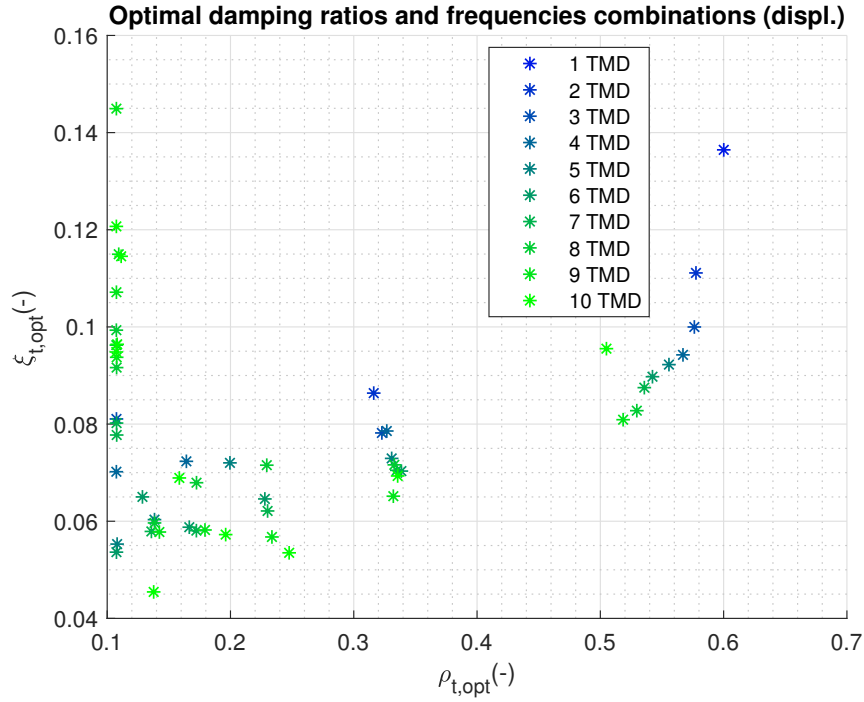


Figure 5.10: Deterministic optimal combinations of tuning and damping ratio (displ.).

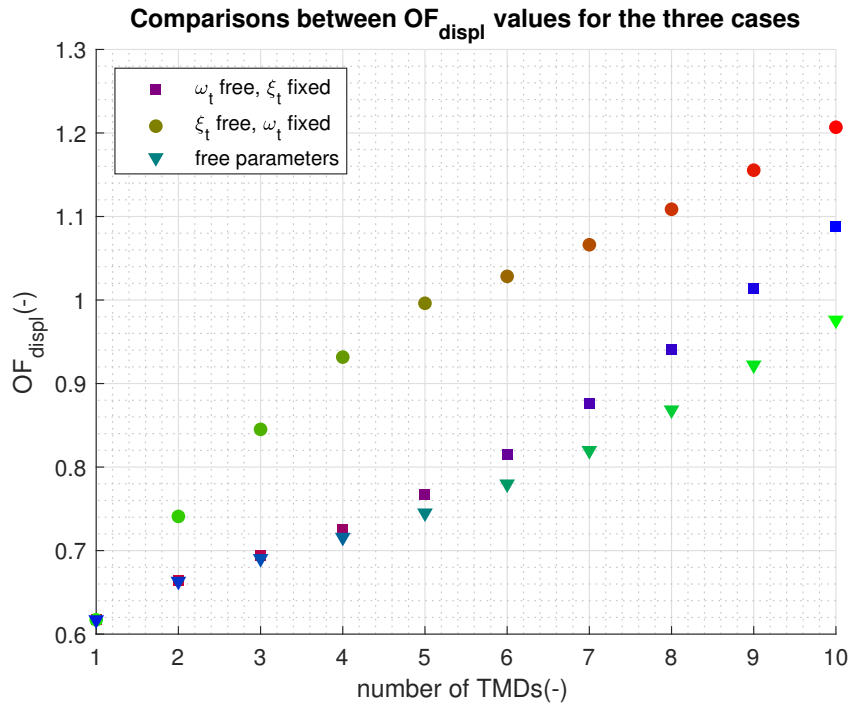


Figure 5.11:  $OF_{displ}$  deterministic analysis comparison between fixed damping ratio, fixed tuning ratio and free parameters.

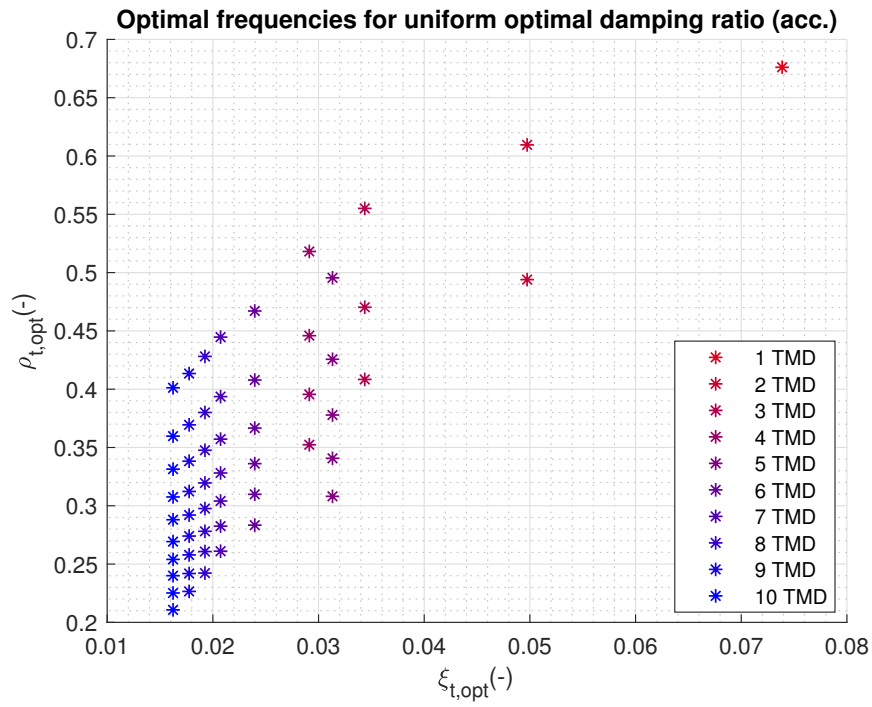


Figure 5.12: Deterministic optimal tuning ratios for uniform damping ratio (acc.).

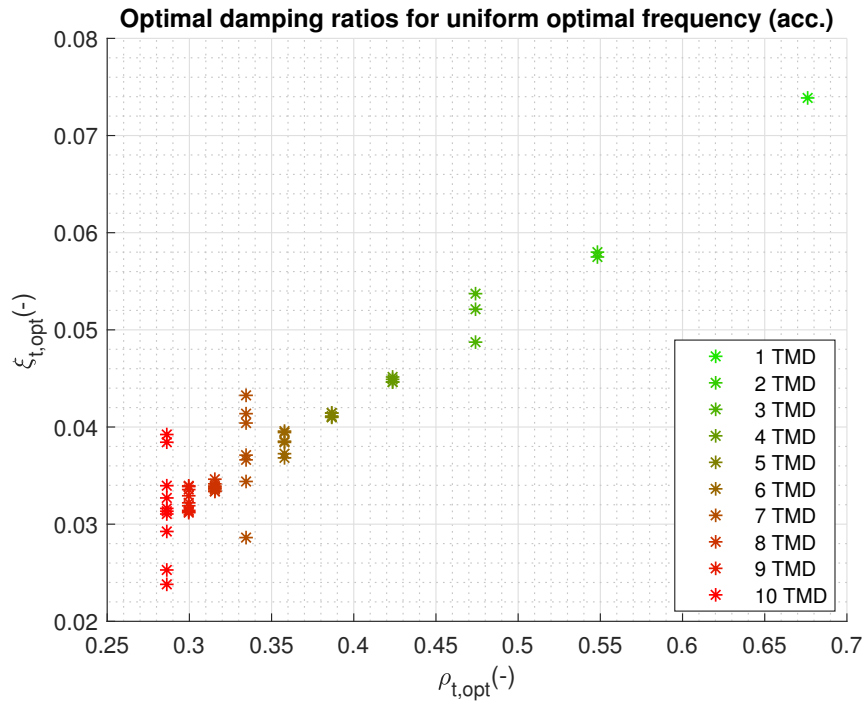


Figure 5.13: Deterministic optimal damping ratios for uniform tuning ratio (acc.).

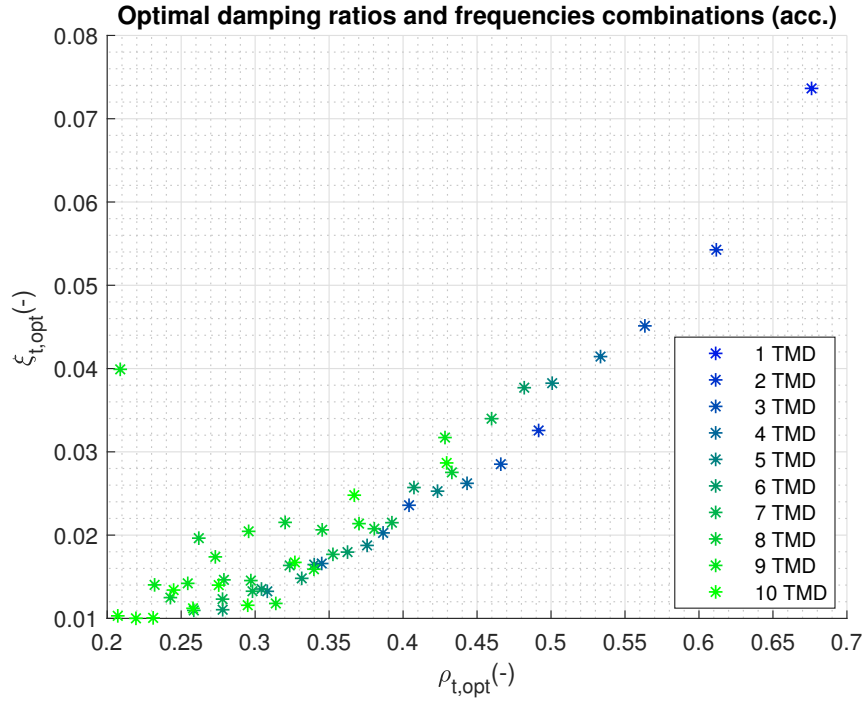


Figure 5.14: Deterministic optimal combinations of tuning and damping ratio (acc.).

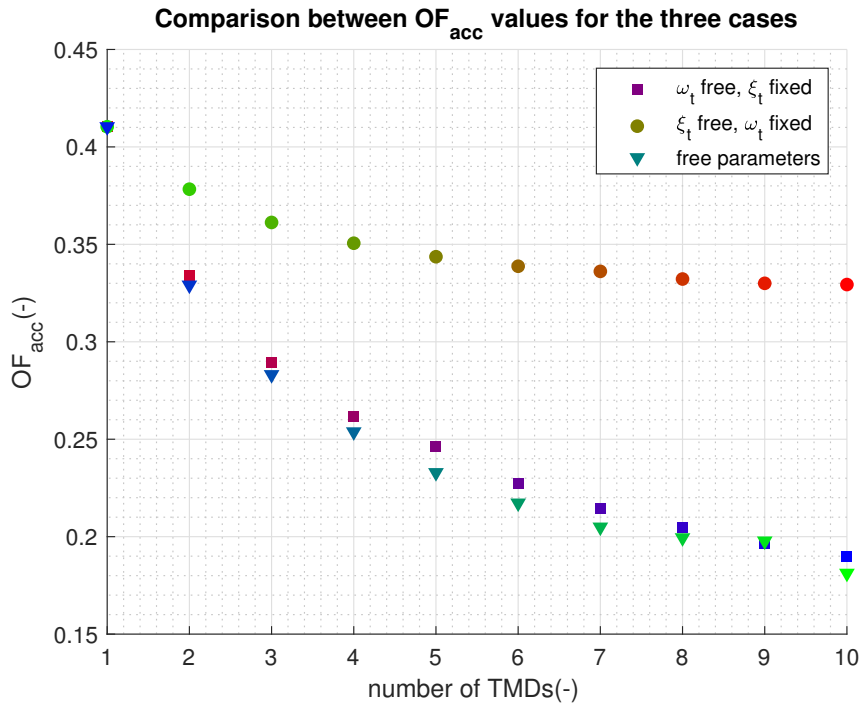


Figure 5.15:  $OF_{acc}$  deterministic analysis comparison between fixed damping ratio, fixed tuning ratio and free parameters.

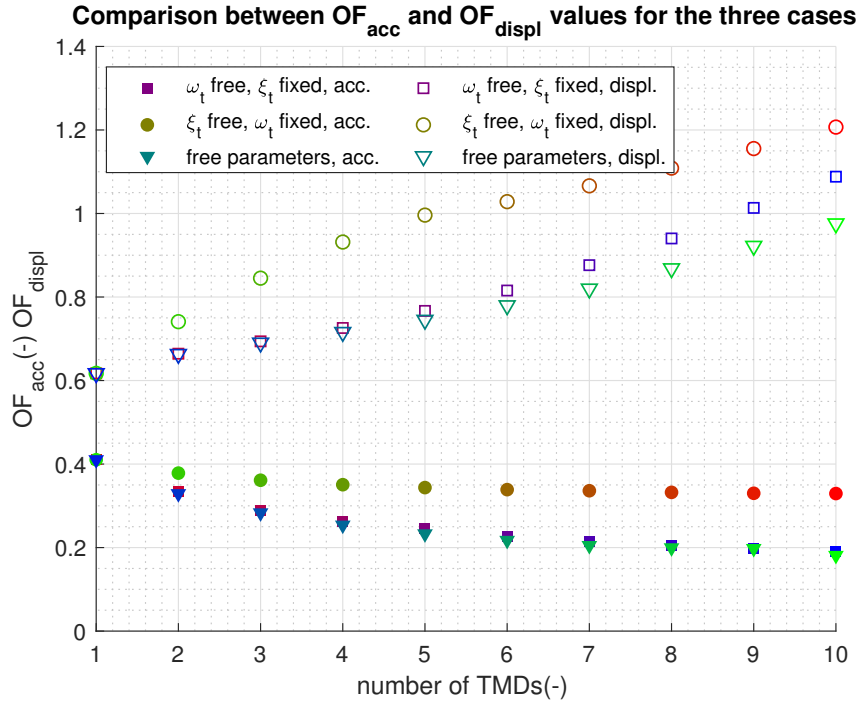


Figure 5.16:  $OF_{displ}$  (empty points) and  $OF_{acc}$  (solid points) deterministic analysis comparison between fixed damping ratio, fixed tuning ratio and free parameters.

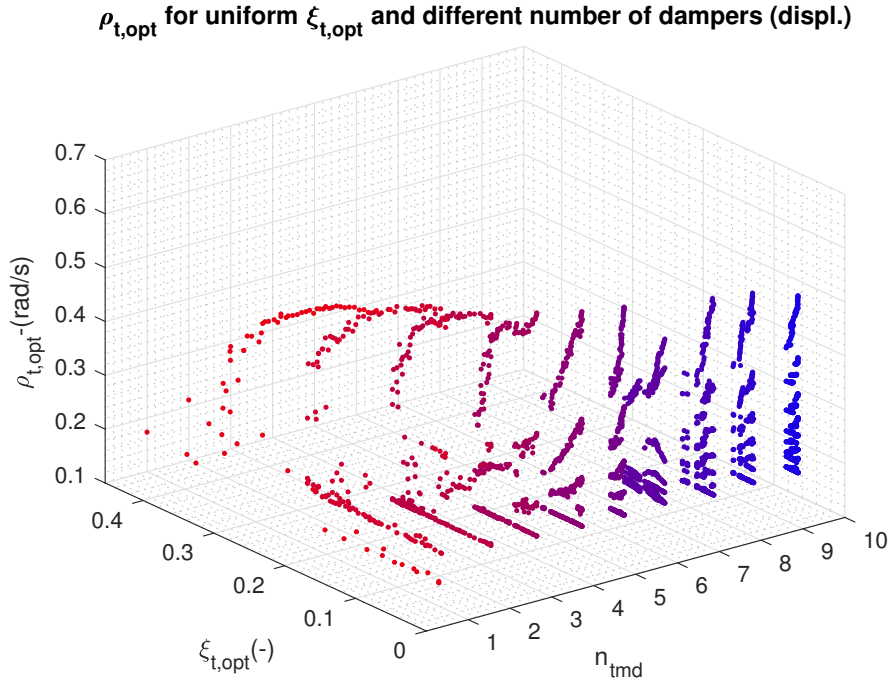


Figure 5.17: Robust optimal frequencies for uniform damping ratio (displ.).

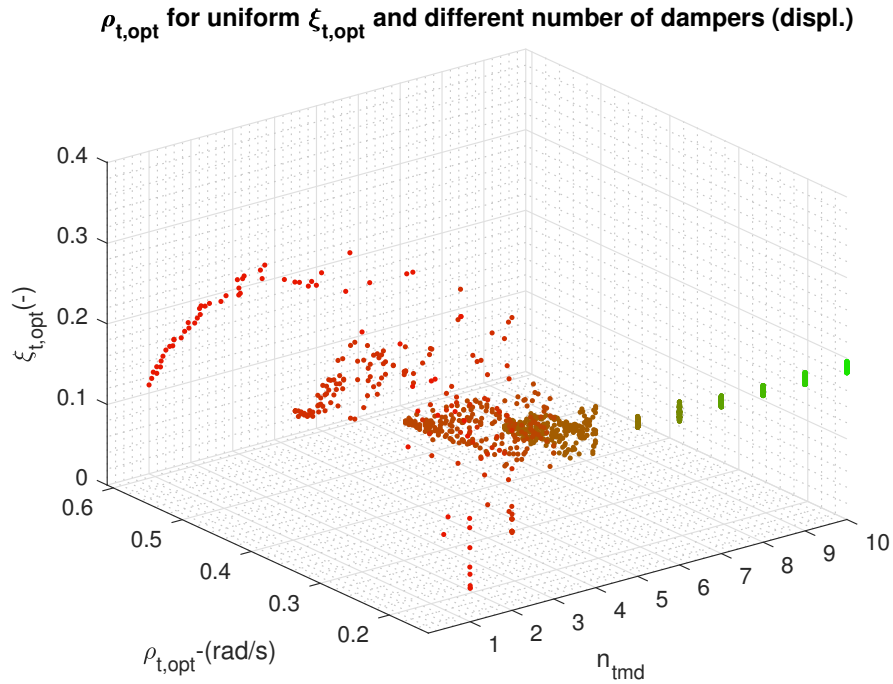


Figure 5.18: Robust optimal damping ratios for uniform frequency (displ.).

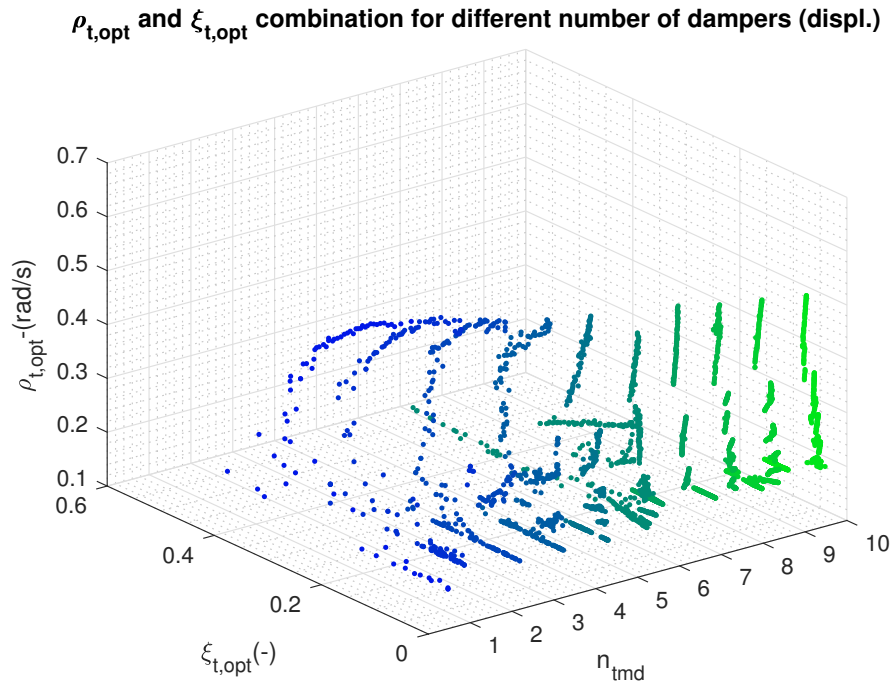


Figure 5.19: Robust optimal combinations of parameters (displ.).

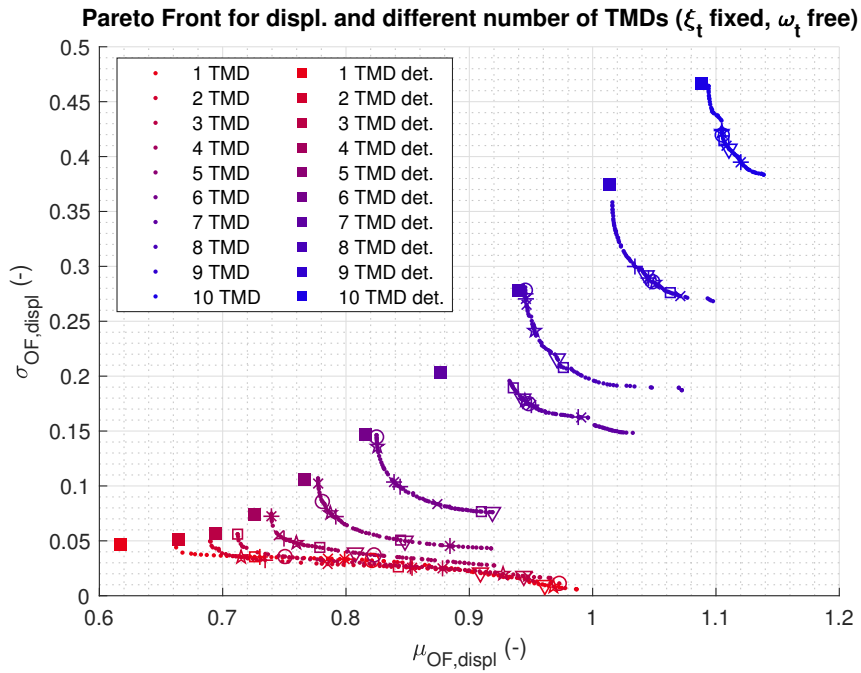


Figure 5.20: Pareto front for uniform damping ratio (displ.).

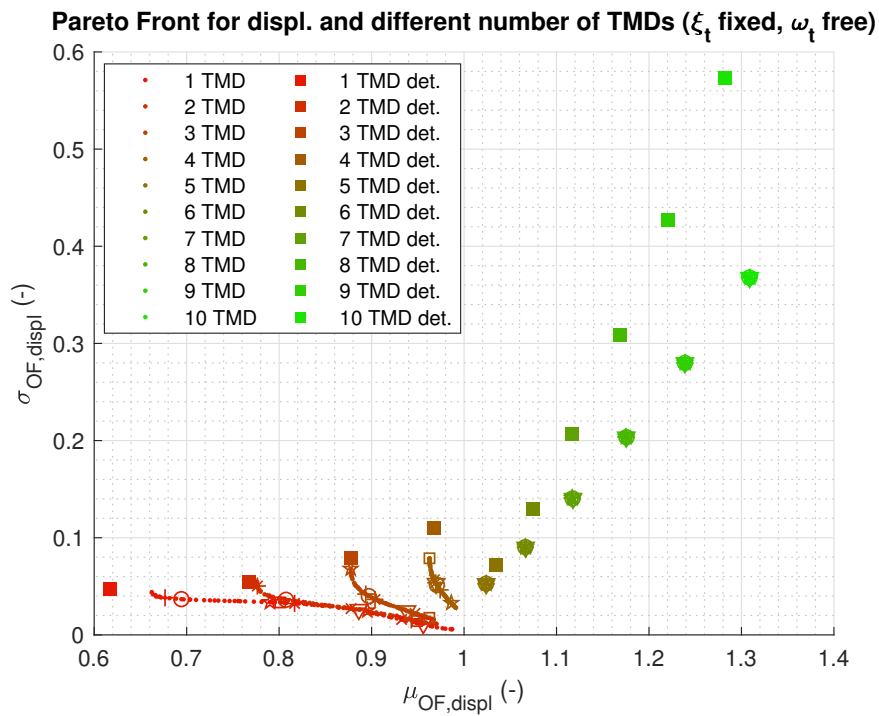
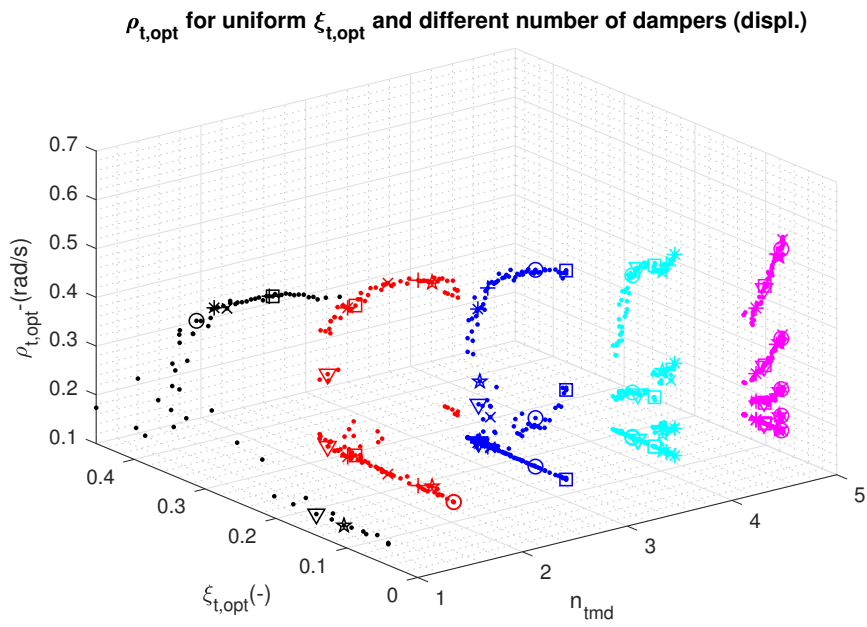
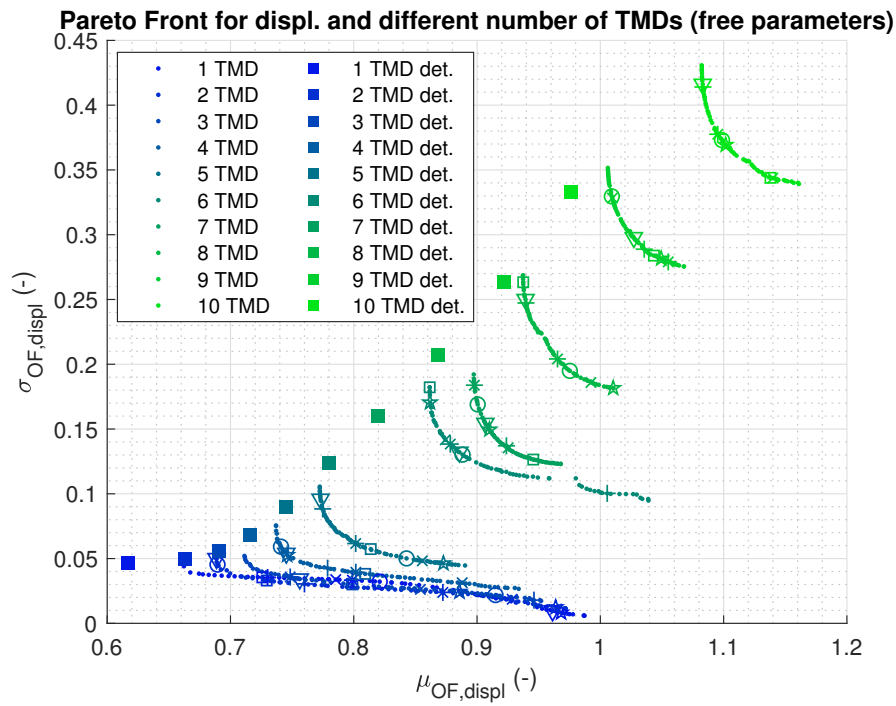


Figure 5.21: Pareto front for uniform frequency (displ.).



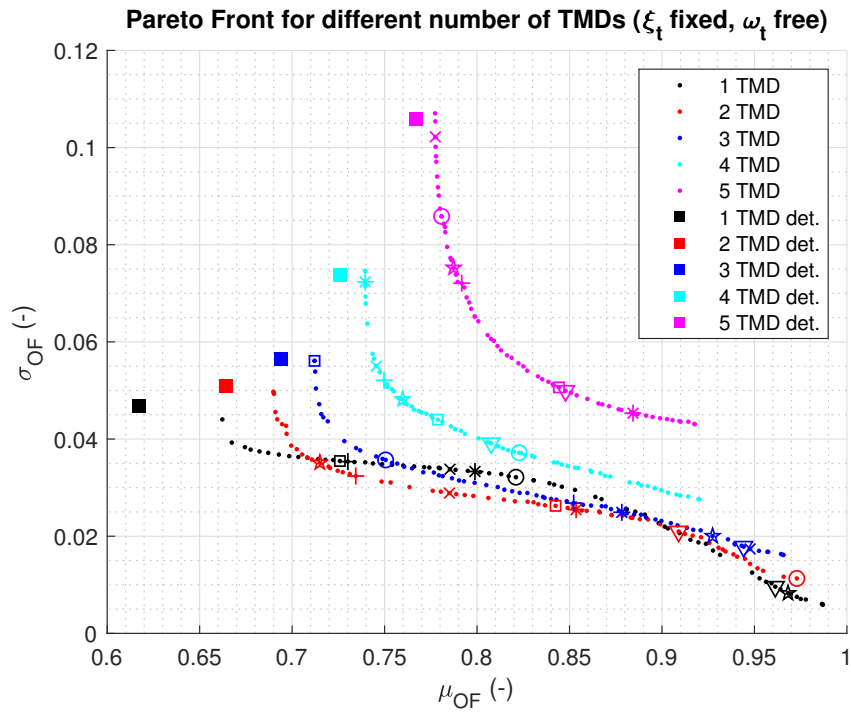


Figure 5.24: Reduced Pareto front for uniform damping ratio (displ.)

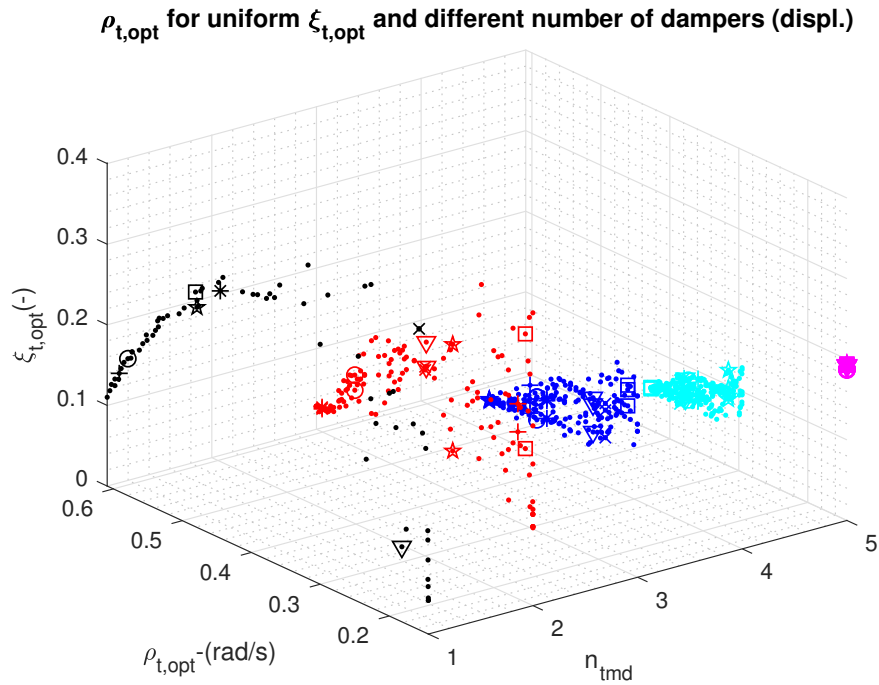


Figure 5.25: Reduced robust optimal damping ratio for uniform frequencies (displ.)

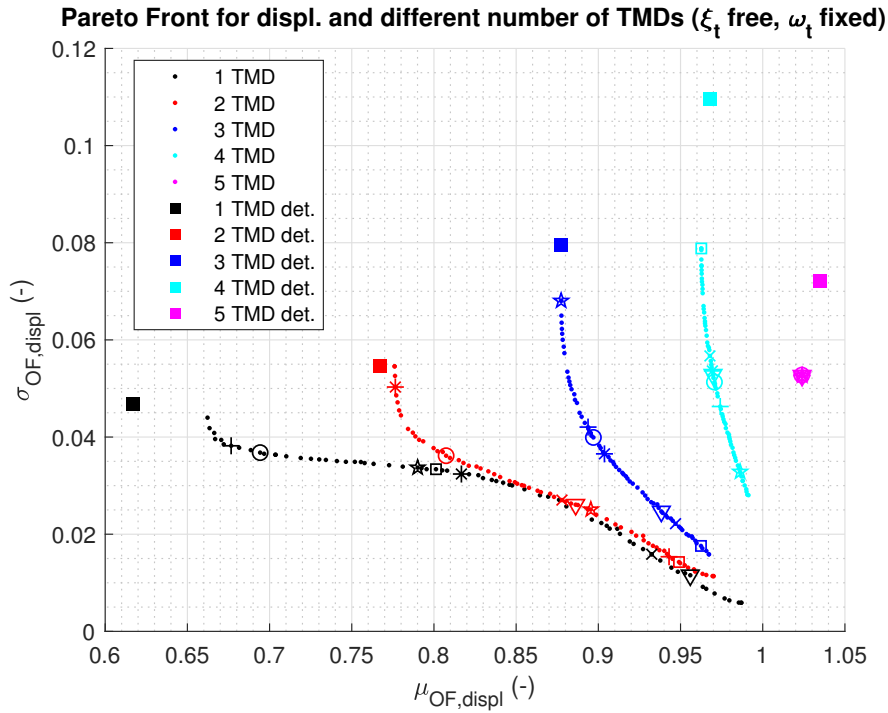


Figure 5.26: Reduced Pareto front for uniform frequency (displ.)

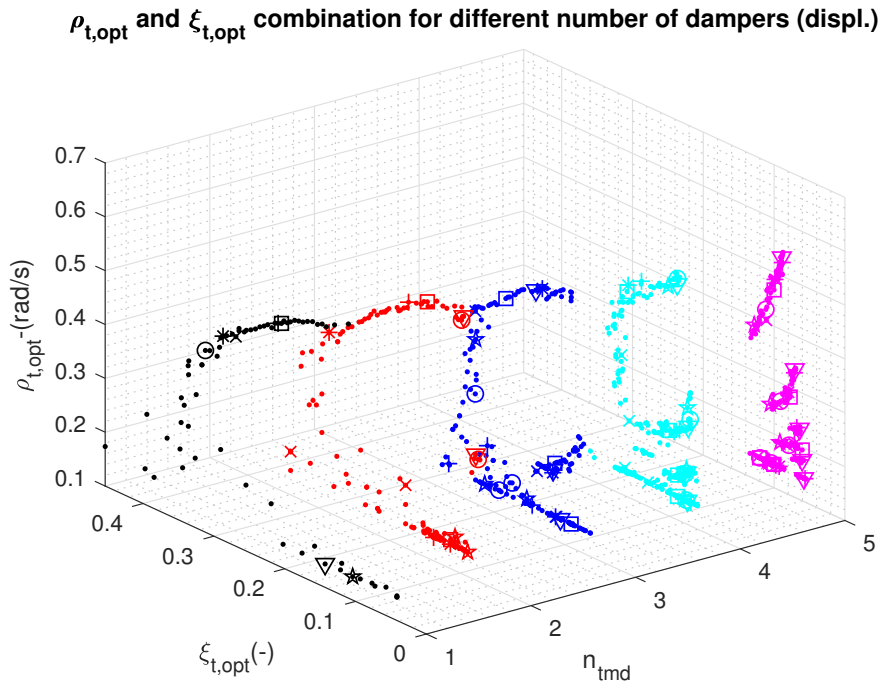


Figure 5.27: Reduced robust optimal combinations of parameters (displ.)

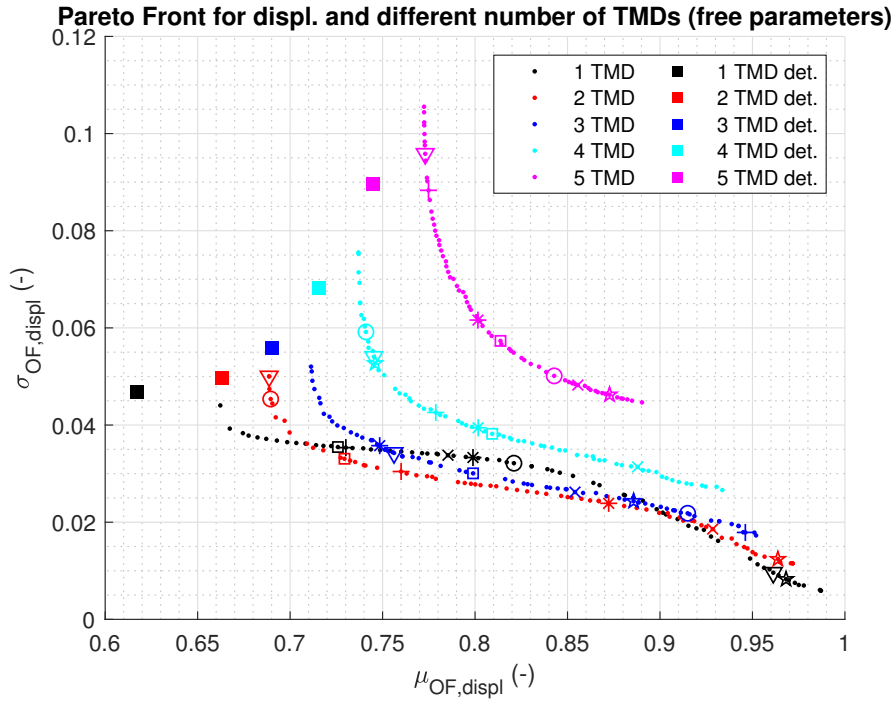


Figure 5.28: Reduced Pareto front for free parameters (displ.)

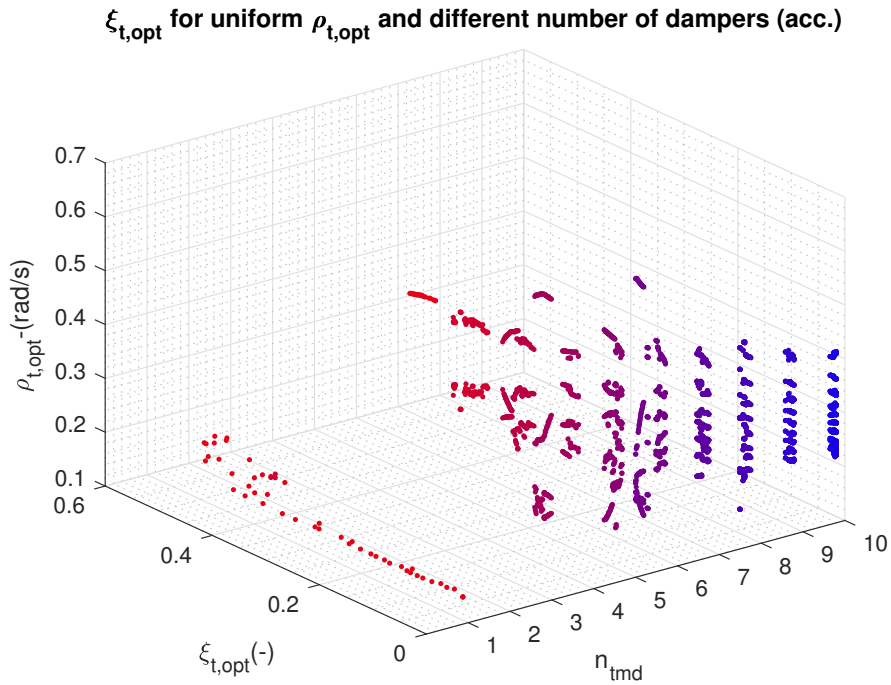


Figure 5.29: Robust optimal frequencies for uniform damping ratio (acc.)

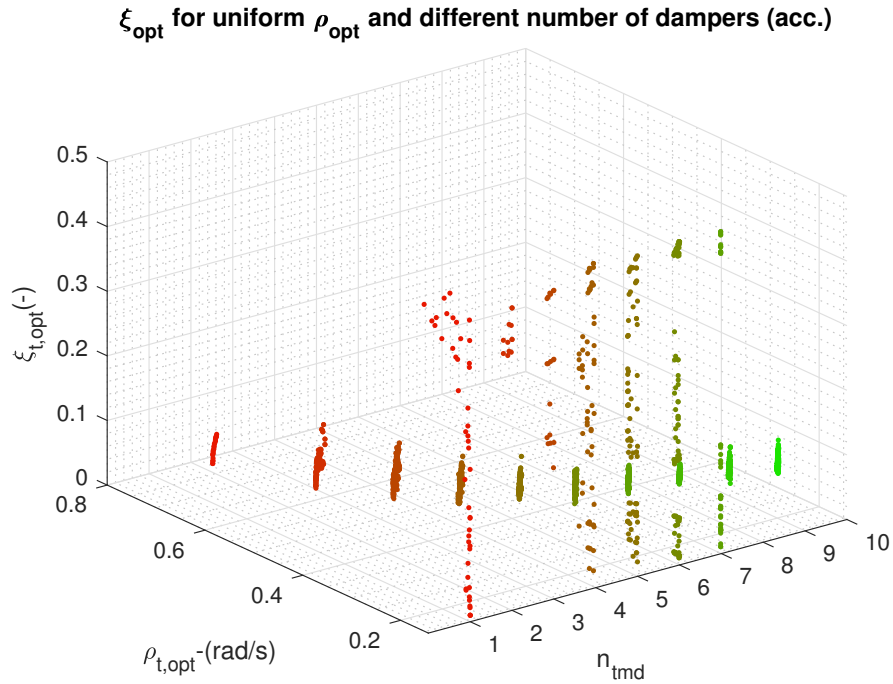


Figure 5.30: Robust optimal damping ratios for uniform frequency (acc.)

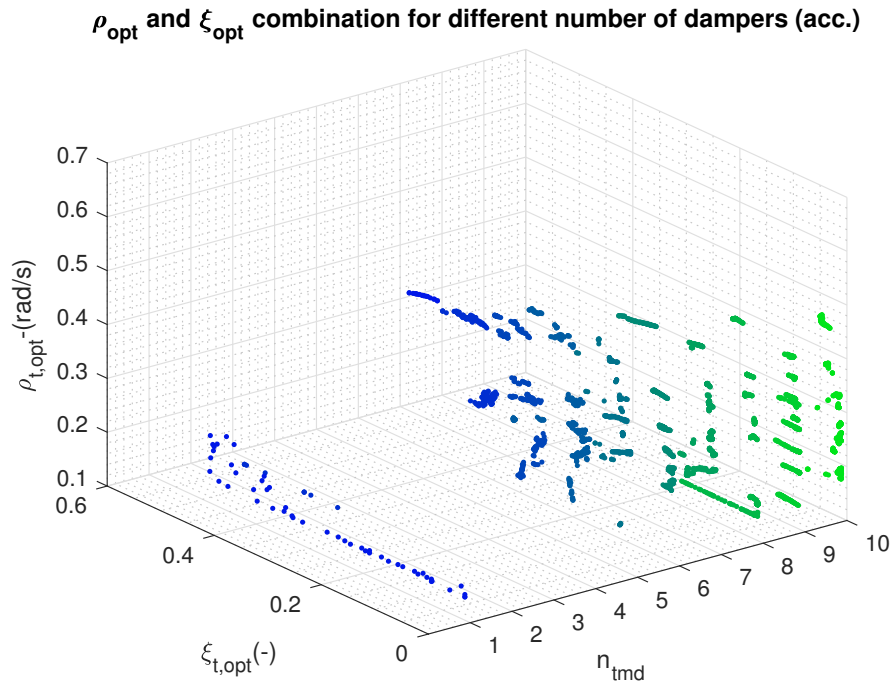


Figure 5.31: Robust optimal combinations of parameters (acc.)

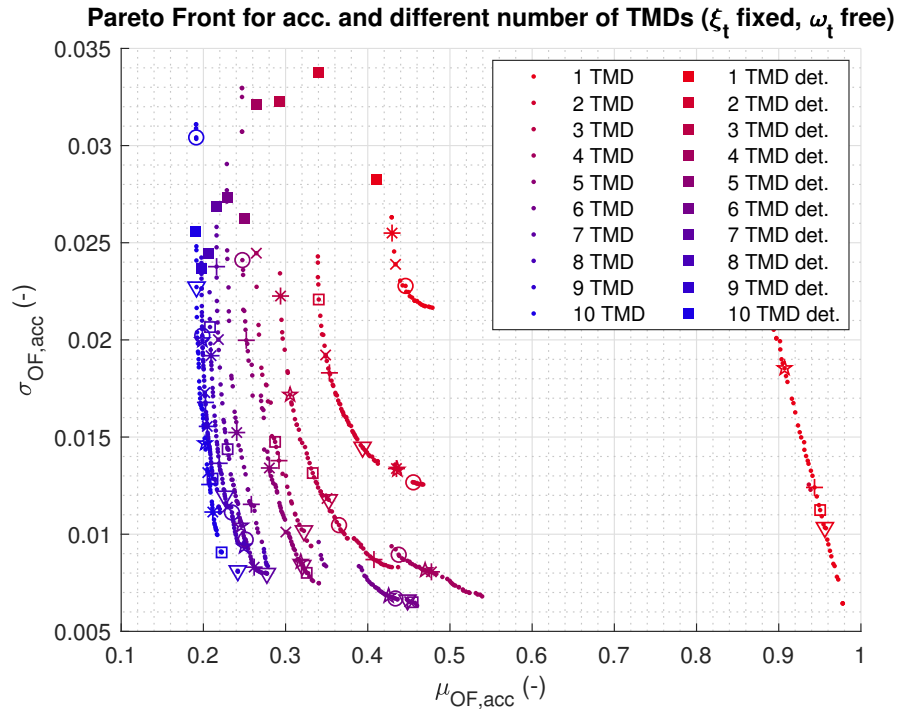


Figure 5.32: Pareto front for uniform damping ratio (acc.)

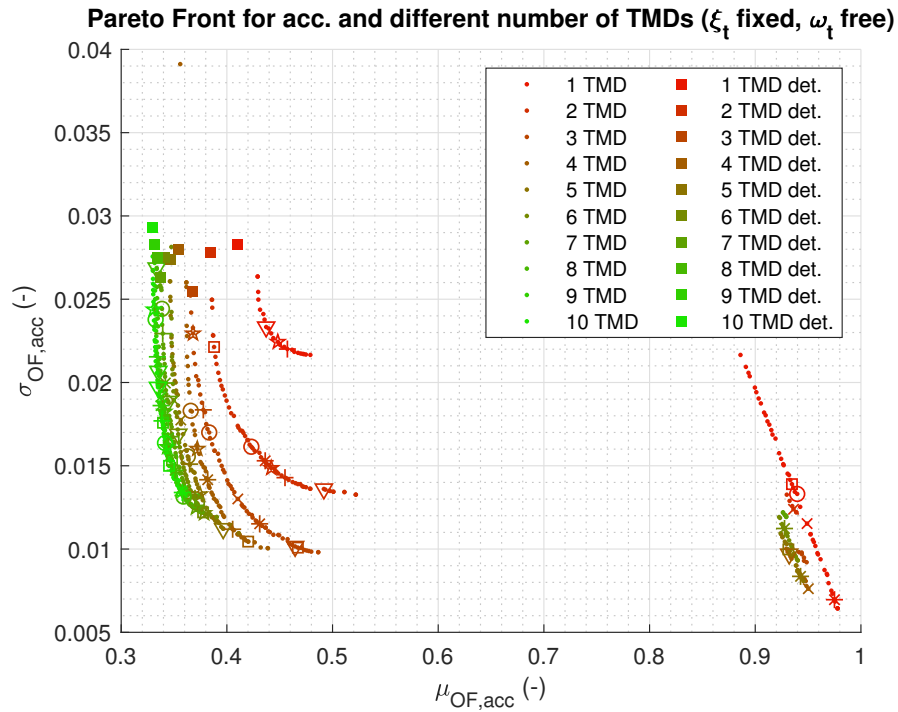


Figure 5.33: Pareto front for uniform frequency (acc.)

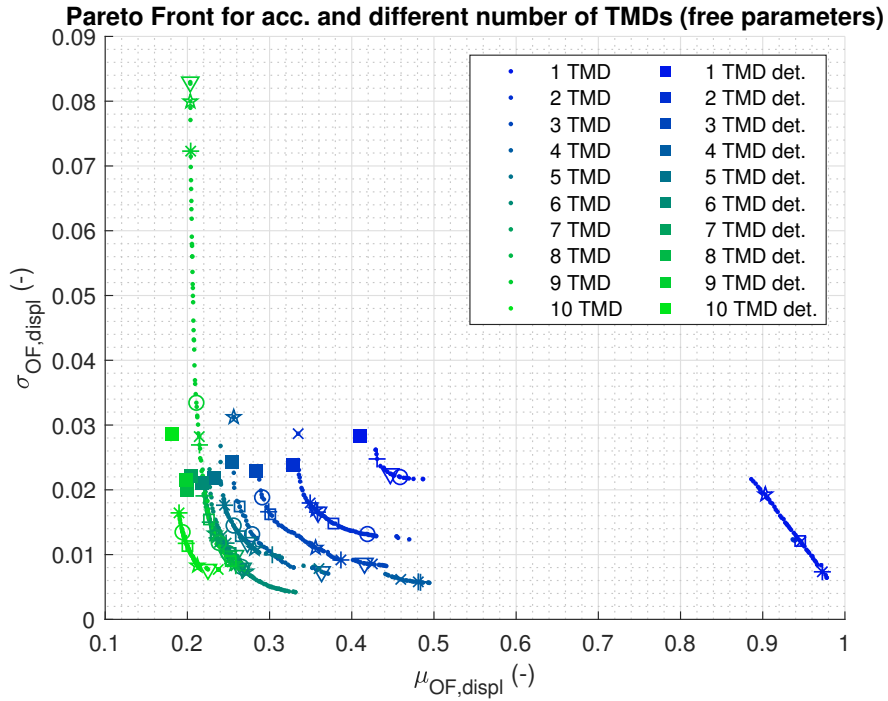


Figure 5.34: Pareto front for free parameters (acc.)

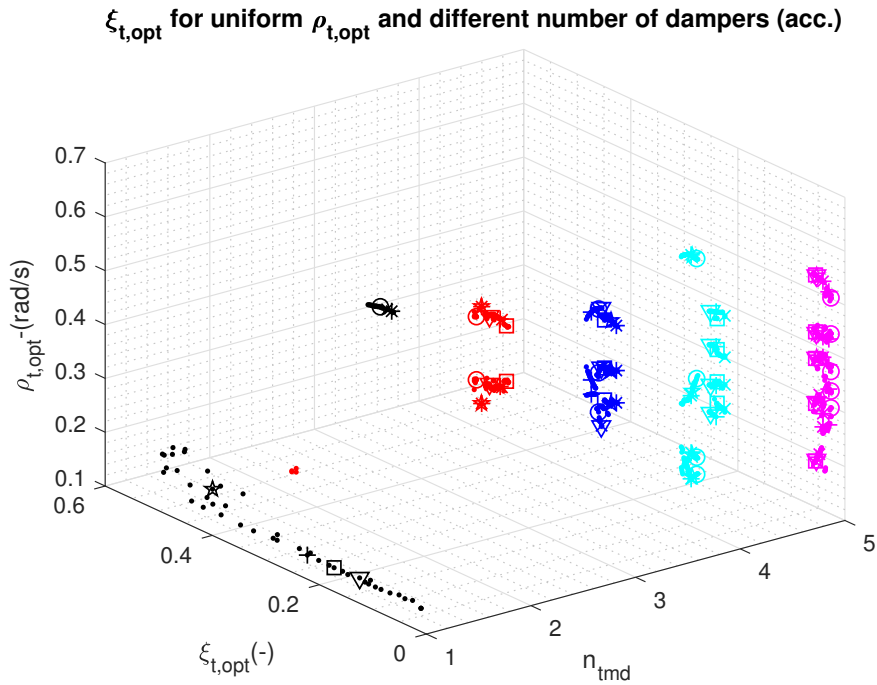


Figure 5.35: Reduced robust optimal frequencies for uniform damping ratio (acc.)

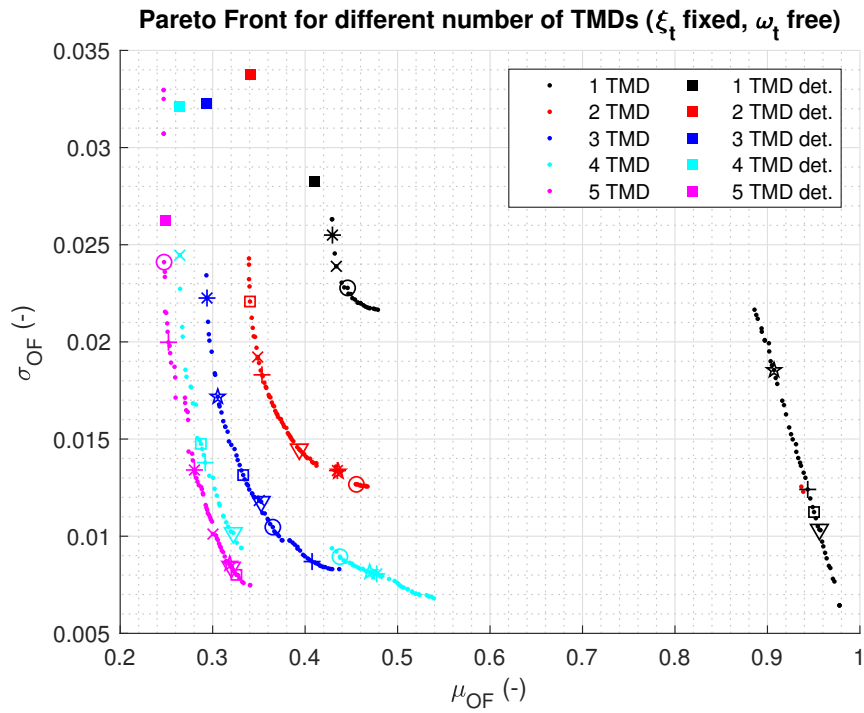


Figure 5.36: Reduced Pareto front for uniform damping ratio (acc.)

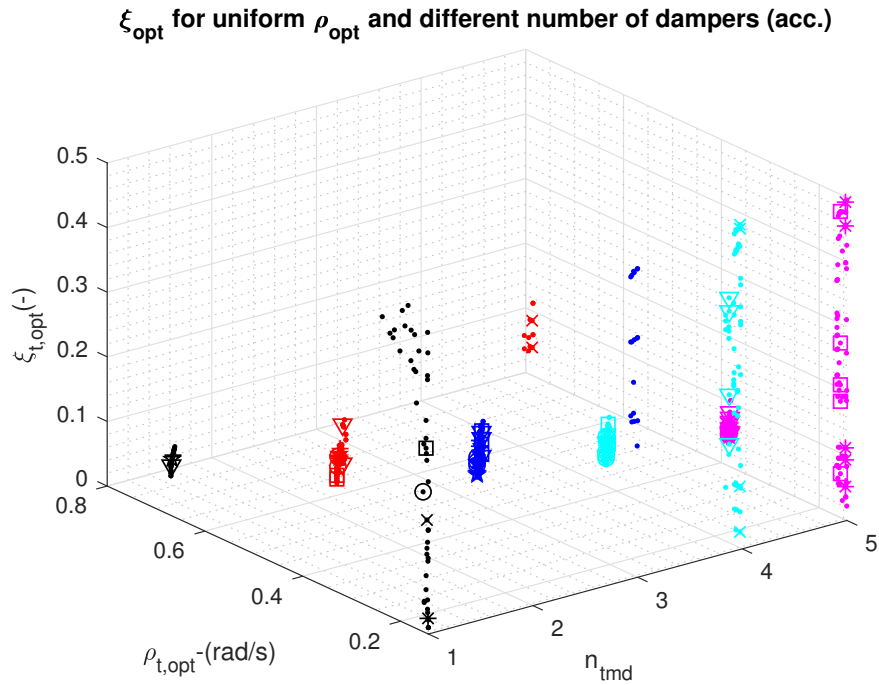


Figure 5.37: Reduced optimal damping ratio for uniform frequencies (acc.)

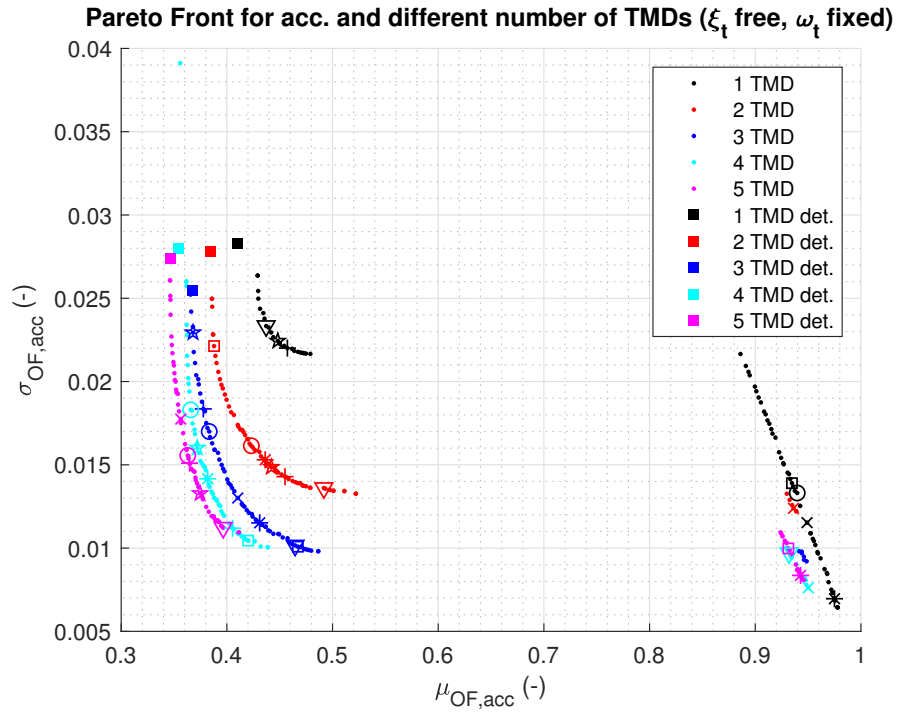


Figure 5.38: Reduced Pareto front for uniform frequency (acc.)

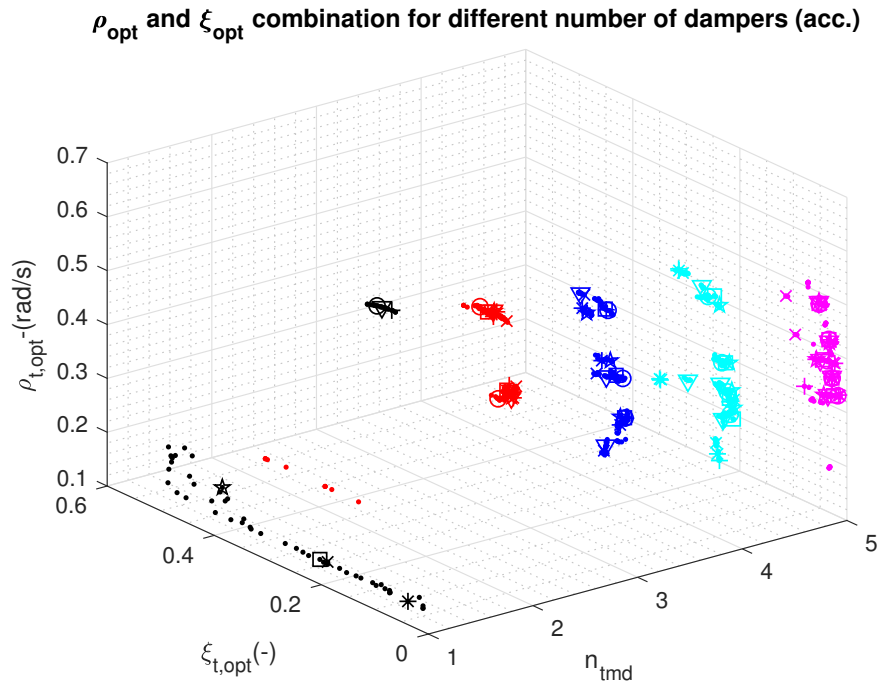


Figure 5.39: Reduced robust optimal combinations of parameters (acc.)

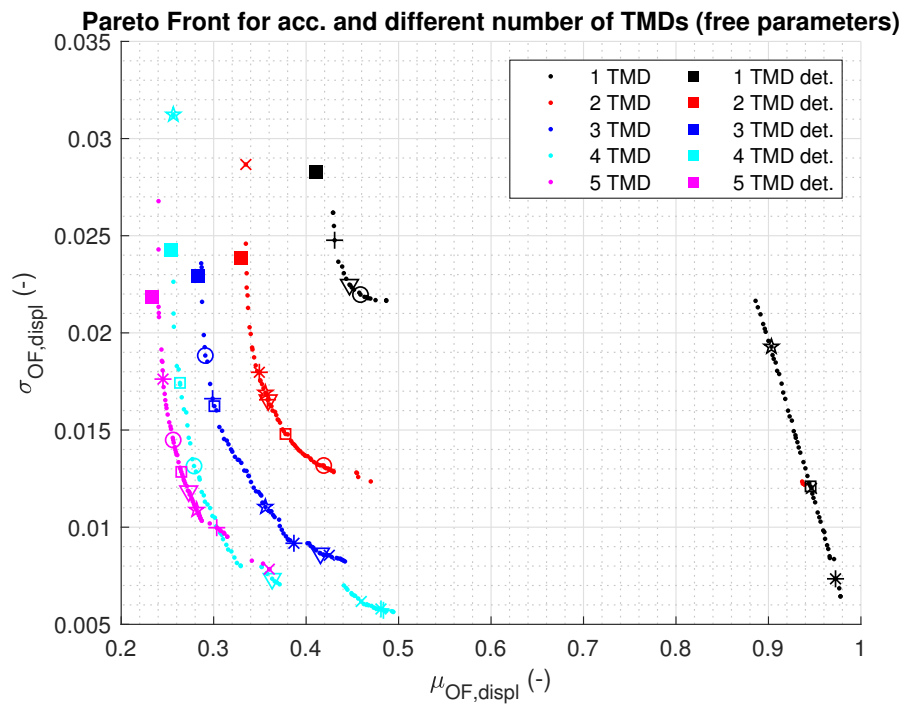


Figure 5.40: Reduced Pareto front for free parameters (acc.)

# Appendix A-System matrices and their derivatives

## Protected case

The system matrix obtained from eq.(5.15) has the following form:

$$\bar{\mathbf{D}} = \begin{bmatrix} \mathbf{D}_N & \mathbf{D}_{Nf} \\ \mathbf{0} & \mathbf{D}_f \end{bmatrix}$$

In the protected case the system matrix of the SDF oscillator plus the tuned mass dampers is a  $[2(1+n)] \times [2(1+n)]$  matrix (where  $n$  is the number of TMDs) of the following form:

$$\mathbf{D}_N = \begin{bmatrix} 0 & \dots & \dots & 0 & 1 & \dots & \dots & 0 \\ \vdots & \ddots & & \vdots & \vdots & \ddots & & \vdots \\ \vdots & & \ddots & \vdots & \vdots & & \ddots & \vdots \\ 0 & \dots & \dots & 0 & 0 & \dots & \dots & 1 \\ -\omega_1^2 & \dots & 0 & \omega_1^2 & -2\xi_1\omega_1 & \dots & 0 & 2\xi_1\omega_1 \\ \vdots & \ddots & \vdots & \vdots & \vdots & \ddots & \vdots & \vdots \\ 0 & \dots & -\omega_n^2 & \omega_n^2 & 0 & \dots & -2\xi_n\omega_n & 2\xi_n\omega_n \\ \gamma_1 \cdot \omega_1^2 & \dots & \gamma_n \cdot \omega_n^2 & \omega_s^2 + \sum_{i=1}^n \gamma_i \cdot \omega_i^2 & \gamma_1 \cdot 2\xi_1\omega_1 & \dots & \gamma_n \cdot 2\xi_n\omega_n & 2\xi_s\omega_s + \sum_{i=1}^n \gamma_i \cdot 2\xi_i\omega_i \end{bmatrix}$$

The system matrix of the Tajimi-Kanai filter is a  $(2 \times 2)$  matrix of this form:

$$\mathbf{D}_f = \mathbf{D}_K = \begin{bmatrix} 0 & 1 \\ -\omega_K^2 & -2\xi_K\omega_K \end{bmatrix}$$

The matrix  $\mathbf{D}_{Nf}$ , that indicates the influence of the filter on the system, is a  $[(n+1) \times 2]$  rectangular matrix of the form:

$$\mathbf{D}_{Nf} = \begin{bmatrix} m_1^{-1} \cdot \omega_K^2 & m_1^{-1} \cdot 2\xi_K\omega_K \\ \vdots & \vdots \\ m_n^{-1} \cdot \omega_K^2 & m_n^{-1} \cdot 2\xi_K\omega_K \\ m_s^{-1} \cdot \omega_K^2 & m_s^{-1} \cdot 2\xi_K\omega_K \end{bmatrix}$$

The derivatives of the matrix  $\bar{\mathbf{D}}$  respect to the  $i^{th}$  component  $d_i$  of the design parameters is calculated by derivation of the sub matrices that compose it:

$$(\bar{\mathbf{D}})_{d_i} = \begin{bmatrix} (\mathbf{D}_N)_{d_i} & (\mathbf{D}_{Nf})_{d_i} \\ \mathbf{0} & (\mathbf{D}_f)_{d_i} \end{bmatrix}$$

The derivatives respect each element of  $\vec{d} = [\omega_s, \xi_s, \omega_K, \xi_K, \gamma_t]$  are reported below.

$$(\mathbf{D}_N)_{\omega_s} = \begin{bmatrix} 0 & \dots & \dots & 0 & 0 & \dots & \dots & 0 \\ \vdots & \ddots & & \vdots & \vdots & \ddots & & \vdots \\ \vdots & & \ddots & \vdots & \vdots & & \ddots & \vdots \\ 0 & \dots & \dots & 0 & 0 & \dots & \dots & 0 \\ 0 & \dots & 0 & 0 & 0 & \dots & 0 & 0 \\ \vdots & \ddots & \vdots & \vdots & \vdots & \ddots & \vdots & \vdots \\ 0 & \dots & 0 & 0 & 0 & \dots & 0 & 0 \\ 0 & \dots & 0 & 2\omega_s & 0 & \dots & 0 & 2\xi_s \end{bmatrix}$$

$$(\mathbf{D}_N)_{\xi_s} = \begin{bmatrix} 0 & \dots & \dots & 0 & 0 & \dots & \dots & 0 \\ \vdots & \ddots & & \vdots & \vdots & \ddots & & \vdots \\ \vdots & & \ddots & \vdots & \vdots & & \ddots & \vdots \\ 0 & \dots & \dots & 0 & 0 & \dots & \dots & 0 \\ 0 & \dots & 0 & 0 & 0 & \dots & 0 & 0 \\ \vdots & \ddots & \vdots & \vdots & \vdots & \ddots & \vdots & \vdots \\ 0 & \dots & 0 & 0 & 0 & \dots & 0 & 0 \\ 0 & \dots & 0 & 0 & 0 & \dots & 0 & 2\omega_s \end{bmatrix}$$

$$(\mathbf{D}_N)_{\omega_K} = \begin{bmatrix} 0 & \dots & \dots & 0 & 0 & \dots & \dots & 0 \\ \vdots & \ddots & & \vdots & \vdots & \ddots & & \vdots \\ \vdots & & \ddots & \vdots & \vdots & & \ddots & \vdots \\ 0 & \dots & \dots & 0 & 0 & \dots & \dots & 0 \\ 0 & \dots & 0 & 0 & 0 & \dots & 0 & 0 \\ \vdots & \ddots & \vdots & \vdots & \vdots & \ddots & \vdots & \vdots \\ 0 & \dots & 0 & 0 & 0 & \dots & 0 & 0 \\ 0 & \dots & 0 & 0 & 0 & \dots & 0 & 0 \end{bmatrix}$$

$$(\mathbf{D}_N)_{\xi_K} = \begin{bmatrix} 0 & \dots & \dots & 0 & 0 & \dots & \dots & 0 \\ \vdots & \ddots & & \vdots & \vdots & \ddots & & \vdots \\ \vdots & & \ddots & \vdots & \vdots & & \ddots & \vdots \\ 0 & \dots & \dots & 0 & 0 & \dots & \dots & 0 \\ 0 & \dots & 0 & 0 & 0 & \dots & 0 & 0 \\ \vdots & \ddots & \vdots & \vdots & \vdots & \ddots & \vdots & \vdots \\ 0 & \dots & 0 & 0 & 0 & \dots & 0 & 0 \\ 0 & \dots & 0 & 0 & 0 & \dots & 0 & 0 \end{bmatrix}$$

$$(\mathbf{D}_N)_{\gamma_t} = \begin{bmatrix} 0 & \dots & \dots & 0 & 0 & \dots & \dots & 0 \\ \vdots & \ddots & & \vdots & \vdots & \ddots & & \vdots \\ \vdots & & \ddots & \vdots & \vdots & & \ddots & \vdots \\ 0 & \dots & \dots & 0 & 0 & \dots & \dots & 0 \\ 0 & \dots & 0 & 0 & 0 & \dots & 0 & 0 \\ \vdots & \ddots & \vdots & \vdots & \vdots & \ddots & \vdots & \vdots \\ 0 & \dots & 0 & 0 & 0 & \dots & 0 & 0 \\ \omega_1^2 & \dots & \omega_n^2 & \sum_{i=1}^n \omega_i^2 & 2\xi_1\omega_1 & \dots & 2\xi_n\omega_n & \sum_{i=1}^n 2\xi_i\omega_i \end{bmatrix}$$

$$(\mathbf{D}_K)_{\omega_s} = \begin{bmatrix} 0 & 0 \\ 0 & 0 \end{bmatrix}, \quad (\mathbf{D}_K)_{\xi_s} = \begin{bmatrix} 0 & 0 \\ 0 & 0 \end{bmatrix}, \quad (\mathbf{D}_K)_{\omega_K} = \begin{bmatrix} 0 & 0 \\ 2\omega_K & 2\xi_K \end{bmatrix}$$

$$(\mathbf{D}_K)_{\xi_K} = \begin{bmatrix} 0 & 0 \\ 0 & 2\omega_K \end{bmatrix}, \quad (\mathbf{D}_K)_{\gamma_t} = \begin{bmatrix} 0 & 0 \\ 0 & 0 \end{bmatrix}$$

$$(\mathbf{D}_{Nf})_{\omega_s} = \begin{bmatrix} 0 & 0 \\ \vdots & \vdots \\ 0 & 0 \\ 0 & 0 \end{bmatrix}, \quad (\mathbf{D}_{Nf})_{\xi_s} = \begin{bmatrix} 0 & 0 \\ \vdots & \vdots \\ 0 & 0 \\ 0 & 0 \end{bmatrix}, \quad (\mathbf{D}_{Nf})_{\omega_K} = \begin{bmatrix} m_1^{-1} \cdot 2\omega_K & m_1^{-1} \cdot 2\xi_K \\ \vdots & \vdots \\ m_n^{-1} \cdot 2\omega_K & m_n^{-1} \cdot 2\xi_K \\ m_s^{-1} \cdot 2\omega_K & m_s^{-1} \cdot 2\xi_K \end{bmatrix}$$

$$(\mathbf{D}_{Nf})_{\xi_K} = \begin{bmatrix} 0 & m_2^{-1} \cdot 2\omega_K \\ \vdots & \vdots \\ 0 & m_n^{-1} \cdot 2\omega_K \\ 0 & m_s^{-1} \cdot 2\omega_K \end{bmatrix}, \quad (\mathbf{D}_{Nf})_{\gamma_t} = \begin{bmatrix} 0 & 0 \\ \vdots & \vdots \\ 0 & 0 \\ 0 & 0 \end{bmatrix}$$

## Unprotected case

In the unprotected case the system matrix has the following form:

$$\bar{\mathbf{D}}_0 = \begin{bmatrix} \mathbf{D}_{N,0} & \mathbf{D}_{Nf,0} \\ \mathbf{0} & \mathbf{D}_f \end{bmatrix}$$

The system matrix of the SDF oscillator is a  $2 \times 2$  matrix of the following form:

$$\mathbf{D}_{N,0} = \begin{bmatrix} 0 & 1 \\ -\omega_s^2 & -2\xi_s\omega_s \end{bmatrix}$$

The system matrix of the Tajimi-Kanai filter does not change, it is a  $(2 \times 2)$  matrix of this form:

$$\mathbf{D}_f = \mathbf{D}_K = \begin{bmatrix} 0 & 1 \\ -\omega_K^2 & -2\xi_K\omega_K \end{bmatrix}$$

The matrix  $\mathbf{D}_{Nf,0}$  that indicates the influence of the filter on the system is a  $(1 \times 2)$  rectangular matrix of the form:

$$\mathbf{D}_{Nf} = [m_s^{-1} \cdot \omega_K^2 \quad m_s^{-1} \cdot 2\xi_K\omega_K]$$

The derivatives of the matrix  $\bar{\mathbf{D}}_0$  respect to the component  $d_i$  of the design parameters is given by the derivation of the sub matrices that compose it:

$$(\bar{\mathbf{D}}_0)_{d_i} = \begin{bmatrix} (\mathbf{D}_{N,0})_{d_i} & (\mathbf{D}_{Nf,0})_{d_i} \\ \mathbf{0} & (\mathbf{D}_f)_{d_i} \end{bmatrix}$$

The derivatives respect each element of  $\vec{d} = [\omega_s, \xi_s, \omega_K, \xi_K, \gamma_t]$  are reported below.

$$(\mathbf{D}_{N,0})_{\omega_s} = \begin{bmatrix} 0 & 0 \\ -2\omega_s & -2\xi_s \end{bmatrix}, \quad (\mathbf{D}_{N,0})_{\xi_s} = \begin{bmatrix} 0 & 0 \\ 0 & -2\omega_s \end{bmatrix}, \quad (\mathbf{D}_{N,0})_{\omega_K} = \begin{bmatrix} 0 & 0 \\ 0 & 0 \end{bmatrix}$$

$$(\mathbf{D}_{N,0})_{\xi_K} = \begin{bmatrix} 0 & 0 \\ 0 & 0 \end{bmatrix}, \quad (\mathbf{D}_{N,0})_{\gamma_t} = \begin{bmatrix} 0 & 0 \\ 0 & 0 \end{bmatrix}$$

$$(\mathbf{D}_K)_{\omega_s} = \begin{bmatrix} 0 & 0 \\ 0 & 0 \end{bmatrix}, \quad (\mathbf{D}_K)_{\xi_s} = \begin{bmatrix} 0 & 0 \\ 0 & 0 \end{bmatrix}, \quad (\mathbf{D}_K)_{\omega_K} = \begin{bmatrix} 0 & 0 \\ 2\omega_K & 2\xi_K \end{bmatrix}$$

$$(\mathbf{D}_K)_{\xi_K} = \begin{bmatrix} 0 & 0 \\ 0 & 2\omega_K \end{bmatrix}, \quad (\mathbf{D}_K)_{\gamma_t} = \begin{bmatrix} 0 & 0 \\ 0 & 0 \end{bmatrix}$$

$$(\mathbf{D}_{Nf,0})_{\omega_s} = [0 \ 0], \quad (\mathbf{D}_{Nf,0})_{\xi_s} = [0 \ 0], \quad (\mathbf{D}_{Nf,0})_{\omega_K} = [m_s^{-1} \cdot 2\omega_K \quad m_s^{-1} \cdot 2\xi_K]$$

$$(\mathbf{D}_{Nf,0})_{\xi_K} = [0 \quad m_s^{-1} \cdot 2\omega_K], \quad (\mathbf{D}_{Nf,0})_{\gamma_t} = [0 \ 0]$$

# Appendix B-Tabulated results

## Deterministic results for different frequency ratio

In this section of the appendix are reported the values assumed by the objective function for variable frequency ratio and number of dampers. The values are reported only for fixed damping ratio for the reasons stated in the correspondent section.

Deterministic  $OF_{displ}$  (-) values for different frequency ratio  $\psi$  (-) and number of dampers

$\psi$	<b>1</b>	<b>2</b>	<b>3</b>	<b>4</b>	<b>5</b>	<b>6</b>	<b>7</b>	<b>8</b>	<b>9</b>	<b>10</b>
0.20	0.95	1.48	1.99	2.62	3.32	4.08	5.01	5.54	6.30	7.03
0.40	0.67	0.76	0.96	1.84	2.42	3.06	2.00	2.29	4.94	4.72
0.60	0.64	0.69	0.75	0.85	0.97	1.12	1.27	1.45	1.61	1.78
0.80	0.61	0.66	0.69	0.74	0.80	0.88	0.97	1.08	1.18	1.29
1.00	0.63	0.68	0.71	0.74	0.79	0.85	0.92	0.99	1.07	1.16
1.20	0.69	0.75	0.79	0.83	0.88	0.93	1.00	1.08	1.16	1.25
1.40	0.77	0.84	0.88	0.93	0.99	1.06	1.14	1.22	1.31	1.41
1.60	0.84	0.91	0.96	1.02	1.09	1.18	1.26	1.38	1.47	1.59

Deterministic  $OF_{acc}$  (-) values for different frequency ratio  $\psi$  (-) and number of dampers

$\psi(-)$	<b>1</b>	<b>2</b>	<b>3</b>	<b>4</b>	<b>5</b>	<b>6</b>	<b>7</b>	<b>8</b>	<b>9</b>	<b>10</b>
0.20	0.66	1.21	1.98	2.84	2.85	3.77	4.44	5.00	7.39	6.73
0.40	0.44	0.37	0.33	0.33	0.39	0.51	0.63	0.80	1.02	1.14
0.60	0.42	0.35	0.30	0.28	0.26	0.24	0.23	0.22	0.23	0.24
0.80	0.41	0.33	0.29	0.26	0.24	0.22	0.28	0.20	0.32	0.19
1.00	0.42	0.35	0.30	0.27	0.25	0.23	0.22	0.21	0.20	0.20
1.20	0.47	0.40	0.35	0.32	0.30	0.28	0.26	0.25	0.24	0.23
1.40	0.54	0.47	0.42	0.39	0.36	0.34	0.32	0.31	0.30	0.29
1.60	0.59	0.54	0.49	0.46	0.43	0.49	0.39	0.37	0.35	0.35

## Deterministic optimization

In this section are reported the deterministic optimization values for variable number of dampers. Being the results similar to the case of free parameters and being not convenient to adopt a fixed tuning ratio, the values are reported only for the fixed damping ratio case.

$OF_{displ}$  results for fixed damping ratio  $\xi_t$  (-) and varying tuning ratio  $\rho_t$  (-)

TMD	$\xi_t$	$\rho_{t,1}$	$\rho_{t,2}$	$\rho_{t,3}$	$\rho_{t,4}$	$\rho_{t,5}$	$\rho_{t,6}$	$\rho_{t,7}$	$\rho_{t,8}$	$\rho_{t,9}$	$\rho_{t,10}$	$\mu_{OF,displ}$
<b>1</b>	0.14	0.60	-	-	-	-	-	-	-	-	-	0.62
<b>2</b>	0.10	0.58	0.31	-	-	-	-	-	-	-	-	0.66
<b>3</b>	0.10	0.32	0.57	0.14	-	-	-	-	-	-	-	0.69
<b>4</b>	0.09	0.56	0.33	0.20	0.14	-	-	-	-	-	-	0.73
<b>5</b>	0.08	0.17	0.23	0.54	0.34	0.14	-	-	-	-	-	0.77
<b>6</b>	0.08	0.14	0.53	0.34	0.24	0.19	0.14	-	-	-	-	0.82
<b>7</b>	0.08	0.26	0.51	0.35	0.20	0.14	0.17	0.14	-	-	-	0.88
<b>8</b>	0.07	0.14	0.50	0.19	0.16	0.27	0.35	0.14	0.22	-	-	0.94
<b>9</b>	0.07	0.24	0.36	0.18	0.20	0.16	0.14	0.14	0.49	0.28	-	1.01
<b>10</b>	0.07	0.18	0.48	0.29	0.14	0.17	0.36	0.24	0.14	0.14	0.21	1.09

$OF_{acc}$  results for fixed damping ratio  $\xi_t$  (-) and varying tuning ratio  $\rho_t$  (-)

TMD	$\xi_t$	$\rho_{t,1}$	$\rho_{t,2}$	$\rho_{t,3}$	$\rho_{t,4}$	$\rho_{t,5}$	$\rho_{t,6}$	$\rho_{t,7}$	$\rho_{t,8}$	$\rho_{t,9}$	$\rho_{t,10}$	$\mu_{OF,displ}$
<b>1</b>	0.07	0.68	-	-	-	-	-	-	-	-	-	0.41
<b>2</b>	0.05	0.61	0.49	-	-	-	-	-	-	-	-	0.33
<b>3</b>	0.03	0.41	0.47	0.56	-	-	-	-	-	-	-	0.29
<b>4</b>	0.03	0.35	0.52	0.45	0.40	-	-	-	-	-	-	0.26
<b>5</b>	0.03	0.43	0.38	0.50	0.31	0.34	-	-	-	-	-	0.25
<b>6</b>	0.02	0.37	0.41	0.34	0.47	0.28	0.31	-	-	-	-	0.23
<b>7</b>	0.02	0.26	0.33	0.30	0.36	0.28	0.44	0.39	-	-	-	0.21
<b>8</b>	0.02	0.43	0.32	0.24	0.38	0.28	0.26	0.35	0.30	-	-	0.20
<b>9</b>	0.02	0.41	0.27	0.23	0.29	0.24	0.26	0.37	0.31	0.34	-	0.20
<b>10</b>	0.02	0.24	0.21	0.27	0.33	0.31	0.23	0.40	0.25	0.36	0.29	0.19

## Robust optimization

In this section of the appendix are reported the tabular data obtained from the robust optimization procedure. Being the system not effective for displacements control over a number of 3 dampers, the results are reported only for them. Every table reports for comparison also the results obtained from an uncertain analysis for the optimal parameters given by a deterministic optimization.

Displacements robust optimization results for fixed damping ratio  $\xi_t$  (-) and varying tuning ratio  $\rho_t$  (-) (1 TMD). The row "det." corresponds to the optimal deterministic parameters.

Points	$\rho_t(-)$	$\xi_t(-)$	$\mu_{OF,displ}(-)$	$\sigma_{OF,displ}(-)$
(s)	0.55	0.20	0.73	0.04
(v)	0.14	0.14	0.96	0.01
(o)	0.44	0.31	0.82	0.03
(p)	0.14	0.10	0.97	0.01
(*)	0.48	0.29	0.80	0.03
(+)	0.55	0.21	0.73	0.04
(x)	0.49	0.27	0.79	0.03
<b>det.</b>	0.60	0.14	0.60	0.05

Displacements robust optimization results for fixed damping ratio  $\xi_t$  (-) and varying tuning ratio  $\rho_t$  (-) (2 TMDs). The row "det." corresponds to the optimal deterministic parameters.

Points	$\xi_t(-)$	$\rho_{t,1}(-)$	$\rho_{t,2}(-)$	$\mu_{OF,displ}(-)$	$\sigma_{OF,displ}(-)$
(s)	0.24	0.46	0.16	0.84	0.03
(v)	0.27	0.30	0.15	0.91	0.02
(o)	0.10	0.14	0.14	0.97	0.01
(p)	0.13	0.58	0.16	0.71	0.04
(*)	0.25	0.15	0.45	0.85	0.03
(+)	0.15	0.57	0.15	0.73	0.03
(x)	0.19	0.54	0.14	0.79	0.03
<b>det.</b>	0.10	0.58	0.31	0.66	0.05

Displacements robust optimization results for fixed damping ratio  $\xi_t$  (-) and varying tuning ratio  $\rho_t$  (-) (3 TMDs). The row "det." corresponds to the optimal deterministic parameters.

Points	$\xi_t$	$\rho_{t,1}(-)$	$\rho_{t,2}(-)$	$\rho_{t,3}(-)$	$\mu_{OF,displ}(-)$	$\sigma_{OF,displ}(-)$
(s)	0.09	0.57	0.14	0.33	0.03	0.71
(v)	0.21	0.15	0.22	0.15	0.02	0.94
(o)	0.13	0.24	0.14	0.55	0.01	0.75
(p)	0.21	0.15	0.15	0.27	0.04	0.93
(*)	0.21	0.14	0.14	0.42	0.03	0.88
(+)	0.20	0.14	0.15	0.47	0.03	0.85
(x)	0.19	0.14	0.21	0.15	0.03	0.95
<b>det.</b>	0.10	0.32	0.57	0.14	0.69	0.06

Acceleration robust optimization results for fixed damping ratio  $\xi_t$  (-) and varying tuning ratio  $\rho_t$  (-) (1 TMD). The row "det." corresponds to the optimal deterministic parameters.

Points	$\xi_t(-)$	$\rho_t(-)$	$\mu_{OF,acc}(-)$	$\sigma_{OF,acc}(-)$
(s)	0.14	0.17	0.95	0.01
(v)	0.15	0.12	0.96	0.01
(o)	0.67	0.09	0.45	0.02
(p)	0.19	0.40	0.91	0.02
(*)	0.67	0.06	0.43	0.03
(+)	0.14	0.22	0.94	0.01
(x)	0.67	0.07	0.43	0.02
<b>det.</b>	0.68	0.07	0.41	0.03

Acceleration robust optimization results for fixed damping ratio  $\xi_t$  (-) and varying tuning ratio  $\rho_t$  (-) (2 TMD). The row "det." corresponds to the optimal deterministic parameters.

Points	$\xi_t(-)$	$\rho_{t,1}(-)$	$\rho_{t,2}(-)$	$\mu_{OF,acc}(-)$	$\sigma_{OF,acc}(-)$
(s)	0.05	0.60	0.50	0.34	0.02
(v)	0.08	0.60	0.48	0.39	0.01
(o)	0.10	0.47	0.59	0.46	0.01
(p)	0.09	0.61	0.43	0.44	0.01
(*)	0.09	0.61	0.43	0.43	0.01
(+)	0.06	0.61	0.48	0.35	0.02
(x)	0.05	0.61	0.48	0.35	0.02
<b>det.</b>	0.05	0.61	0.49	0.34	0.03

Acceleration robust optimization results for fixed damping ratio  $\xi_t$  (-) and varying tuning ratio  $\rho_t$  (-) (3 TMD). The row "det." corresponds to the optimal deterministic parameters.

Points	$\xi_t(-)$	$\rho_{t,1}(-)$	$\rho_{t,2}(-)$	$\rho_{t,3}(-)$	$\mu_{OF,acc}(-)$	$\sigma_{OF,acc}(-)$
(s)	0.06	0.40	0.55	0.46	0.33	0.01
(v)	0.06	0.46	0.57	0.35	0.35	0.01
(o)	0.07	0.45	0.57	0.37	0.37	0.01
(p)	0.05	0.40	0.56	0.46	0.31	0.02
(*)	0.04	0.41	0.55	0.47	0.29	0.02
(+)	0.08	0.40	0.55	0.43	0.41	0.01
(x)	0.06	0.46	0.57	0.35	0.35	0.01
<b>det.</b>	0.03	0.41	0.47	0.56	0.29	0.03

# Bibliography

- [1] “Monte Carlo Methods and Importance Sampling”. In: ed. by E. C. Anderson. Lecture notes for Stat 587C. 1999.
- [2] T. Andreucci and G. Muscolino. “Time frequency varying response functions of non classically damped linear structures under fully non stationary stochastic excitations”. In: *Probabilistic Engineering Mechanics* 54 (2018).
- [3] G. Barone et al. “Closed-form stochastic response of linear building structures to spectrum-consistent seismic excitations”. In: *Soil Dynamics and Earthquake Engineering* 125 (2019).
- [4] R. Bibibana B. and F. M. Leticia F., eds. *Optimization of parameters of tuned mass dampers for use in tall buildings subjected to wind action*. Proceedings of the XL Ibero-Latin-American Congress on Computational Methods in Engineering, ABMEC. Natal/RN, Brazil, 2019.
- [5] R.E.D. Bishop and D. B. Welbourn. “The problem of the dynamic vibration absorber”. In: *Engineering* (1952).
- [6] Ali Bozer and Saban S. Ozsariyildiz. “Free Parameter Search of Multiple Tuned Mass Dampers by Using Artificial Bee Colony Algorithm.” In: *Structural Control and Health Monitoring* 25 (2018).
- [7] John E. Brock. “A note on the damped vibration absorber”. In: *Journal of Applied Mechanics* 95 (1946).
- [8] H. Buchholdt. *Structural dynamics for engineering*. London: Thomas Telford, 1997.
- [9] S. Caddemi and G. Muscolino. “Pre-Envelope Covariance Differential Equations For White and Nonwhite Input Processes”. In: *Meccanica* 33.1 (1998).
- [10] Robert Campbell. “A true tall tale about the Hancock”. In: *Boston Globe* (1995).
- [11] A. Chateauneuf. *Principles of reliability based design optimization*. Web: Taylor and Francis, 2008.
- [12] M.-H. Chey and J.-U. Kim. “Optimum parameters of multiple tuned mass dampers for base-excited damped systems”. In: *Journal of Sound and Vibration* 202(5) (1997).
- [13] R. Clough and Penzien J. *Dynamics of structures*. New York: McGraw-Hill, 1993.
- [14] J. L. Cohon. *Multi-objective Programming and Planning*. New York: Academic Press, 1978.
- [15] S. H. Crandall and W.D. Mark. *Random Vibration in Mechanical Systems*. London: Academic Press inc, 1963.
- [16] P. Dallard et al., eds. *The London Millennium Footbridge*. Based on an invited paper presented and discussed at a meeting of the Institution of Structural Engineers, held at the Institution of Civil Engineers, 1 Great George Street, London SW1, on 26 April 2001 at 6pm. London, 2001.

- [17] J. P. Den Hartog. *The theory of the dynamic vibration absorber*. New York: McGraw-Hill, 1956.
- [18] E. Dheghan-Niri, M. S. Zharai, and A. Mohtat. “Effectiveness-robustness objectives in MTMD system design: An evolutionary optimal design methodology”. In: *Structural Control Health Monitoring* 17 (2008).
- [19] A. Florian. “An efficient sampling scheme: Updated Latin Hypercube Sampling”. In: *Probabilist. Eng. Mech* 7 (1992).
- [20] H. Frahm. *Device for damping vibrations of bodies*. US Patent 989958. 1909.
- [21] P. E. Gill, W. Murray, and M. H. Wright. *Practical Optimization*. Web: Academic Press, 1981.
- [22] D. E. Goldberg. *Genetic algorithms in search, optimization and machine learning*. Boston, Massachusetts.: Addison-Wesley Longman Publishing Co., 1998.
- [23] R. Greco and G. C. Marano. “Optimum Design of Tuned Mass Dampers by Displacement and Energy Perspectives”. In: *Soil Dynamics and Earthquake Engineering* 49 (2013).
- [24] Y. Y. Haimes and W. A. Hall. “Multi objectives in water resource systems analysis: the surrogate worth trade off method”. In: *Water Resour. Res* 10 (1974).
- [25] N. Hoang and P. Warnitchai. “Design of multiple tuned mass dampers by using a numerical optimizer”. In: *Earthquake Engineering Structural Dynamic* 34 (2005).
- [26] M. Hohenbichler and R. Rackwitz. “Improvement of Second-Order Reliability Estimates by Importance Sampling”. In: *J. Engrg. Mech* 114 (1988).
- [27] J. Horn. *Handbook of Evolutionary Computation*. Oxford Univ. Press: T. Back et al., 1997.
- [28] R. L. Husid. “Analysis de terremotos-Analisis general”. In: *Revista del IDEM* 8 (1969).
- [29] “Optimum design of dual tuned mass dampers and their effectiveness”. In: ed. by K. Iwanami and K. Seto. Proceedings of the JSME (C)(in Japanese). 1984.
- [30] A. S. Joshi and R.S. Jangid. “Parametric control of structural responses using an optimal passive tuned mass damper under stationary Gaussian white noise excitations”. In: *Frontiers of Structural and Civil Engineering* 6 (2012).
- [31] D. Kalyanmoy. *Multi-Objective Optimization using Evolutionary Algorithms*. Chichester, England: John Wiley & Sons, 2001.
- [32] M. Khatibinia, H. Gholami, and R. Kamgar. “Optimal design of tuned mass dampers subjected to continuous stationary critical excitation”. In: *International Journal of Dynamics and Control* 6 (2017).
- [33] C.-L. Lee, Y.-T. Chen, and L.-L. nad Wang Y.-P. Chung. “Optimal design theories and applications of tuned mass dampers”. In: *Engineering Structures* 28 (2006).
- [34] R. Lewandowski and J. Grzymisławska. “Dynamic analysis of structures with Multiple Tuned Mass Dampers”. In: *Journal of Civil Engineering and Management* 15 (2009).
- [35] C. Li. “Optimum multiple tuned mass dampers for structures under the ground acceleration based on DDMF and ADMF”. In: *Earthquake Engineering and Structural Dynamics* 31 (2002).
- [36] C. Li and Q. Wu. “Optimum properties of multiple tuned mass dampers for reduction of translational and torsional response of structures subject to ground acceleration”. In: *Engineering Structures* 28 (2006).
- [37] C. Li and B. Zhu. “Estimating double tuned mass dampers for structures under ground acceleration using a novel optimum criterion”. In: *Journal of Sound and Vibration* (2006).

- [38] Y.K. Lin. *Probabilistic Theory of Structural Dynamics*. Malabar: Krieger, 1976.
- [39] Rene W. Luft. "Optimal Tuned Mass Dampers for Buildings". In: *Journal of the Structural Division* 105 (1979).
- [40] Loren D. Lutes and Shahram Sarkani. *Random Vibrations: Analysis of Structural and Mechanical Systems*. Web: Elsevier Science, 2003.
- [41] G. C. Marano and R. Greco, eds. *Stochastic Optimum Design of Linear Tuned Mass Dampers For Seismic Protection of High Towers*. The 14th World Conference on Earthquake. Beijing, China, 2008.
- [42] G. C. Marano et al. "Robust Optimum Design of Tuned Mass Dampers Devices in Random Vibrations Mitigation". In: *Journal of Sound and Vibration* 313 (2008).
- [43] R. T. Marler and J. S. Arora. "Survey of multi-objective optimization methods for engineering". In: *Struct. Multidisc. Optim* 26 (2004).
- [44] M. Mohebbi et al. "Designing optimal multiple tuned mass dampers using genetic algorithms (GAs) for mitigating the seismic response of structures". In: *Journal of Vibration and Control* 0 (2012).
- [45] M. M. Murudi and S. M. Mane, eds. *Seismic effectiveness of tuned mass damper (TMD) for different ground motion parameters*. 13th World Conference on Earthquake Engineering. Vancouver, Canada, 2004.
- [46] G. Muscolino. *Dinamica delle strutture*. Milan: McGraw-Hill, 2002.
- [47] K. Nakahara et al., eds. *Earthquake response of ancient five-story pagoda structure of Horyu-Ji temple in Japan*. Proceedings of the WCEE. 2000.
- [48] N.C Nigam. "Structural optimization in random vibration environment". In: *American Institute of Aeronautics and Astronautics Journal* 551-553 (1972).
- [49] J. Ormondroyd and J. P. Den Hartog. "The theory of the dynamic vibration absorber". In: *ASME Journal of Applied Mechanics* (1928).
- [50] T.L Paez. "The history of random vibrations through 1958". In: *Sandia National Laboratories, Albuquerque* 20 (2006).
- [51] S.S. Patil, S.B. Javheri, and C.G. Konapure. "Effectiveness of MTMD". In: *International Journal of Engineering and Innovative Technology* I-6 (2012).
- [52] V. Patil and R.S. Jangid. "Optimal Multiple Tuned Mass Dampers for the Wind Excited Benchmark Building". In: *Journal of Civil Engineering and Management* 17(4) (2011).
- [53] Fredy Picauly et al. "Tuned Mass Damper on Reinforced Concrete Slab with Additional "X-Shaped Metal" Absorber". In: *Procedia Engineering* 95 (2014).
- [54] D. Poon et al., eds. *Structural Design of Taipei 101, the World's Tallest Building*. CTBUH conference. Seoul, 2004.
- [55] R. Rodriguez and J. C. Montero. *New Paradigms in Subsurface Prediction*. Heidelberg: Springer, 2003.
- [56] E. Saliby. "Descriptive Sampling: A Better Approach to Monte Carlo Simulation". In: *Journal of the Operational Research Society* 42 (1990).
- [57] H.B Seed, C. Ugas., and J. Lysmer. *Site Dependent Spectra for Earthquake Resistent Design*. REPORT N EERC 74-12. University of California, 1974.
- [58] T.T. Soong and Mircea Grigoriu. *Random Vibration of Mechanical and Structural Systems*. Englewood Cliffs: Prentice Hall, 1993.

- [59] “A statistical method of determining the maximum response of a building structure during an earthquake”. In: ed. by H. Tajimi. 2nd International conference earthquake engineering. Tokyo and Kyoto, 1960.
- [60] Plevris Vagelis. “Innovative Computational Techniques for the Optimum Structural Design Considering Uncertainties”. Phd dissertation. Web: National Technical University of Athens(NTUA), 2009.
- [61] J. Whu and C. Ghenda, eds. *Optimization of Multiple Tuned Mass Dampers for Seismic Response Reduction*. Proceedings of the American Control Conference. Chicago, Illinois, 2000.
- [62] D. H. Wolpert and W. G. Macready. “No Free Lunch Theorems for Optimization”. In: *Evol. Comput.* 1 (1997).
- [63] K. XU and T. Igusa. “Dynamic characteristics of multiple substructures with closely spaced frequencies”. In: *Earthquake Engineering and Structural Dynamics* 21 (1992).
- [64] F. Yang and E. Esmailzadeh. “Optimal design of distributed tuned mass dampers for passive vibration control of structures”. In: *Structural Control Health Monitoring* 22 (2015).
- [65] M. Zeleny. *Multiple Criteria Decision Making*. New York: McGraw-Hill, 1982.
- [66] F. Zhang. *The Schur Complement and its Applications*. web: Springer, 2005.
- [67] L. Zuo and S. A. Nayef, eds. *Optimization of the Individual Stiffness and Damping Parameters in Multiple-Tuned-Mass-Damper Systems*. Event: Smart Structures and Materials. San Diego, California, 2003.

# Index

- active systems, 120
- amplitude  $\{A(t)\}$ , 47
- auto-correlation  $\Phi_{XX}(t_1, t_2)$ , 29
- auto-covariance  $K_{XX}(t_1, t_2)$ , 29
  
- bandwidth  $q_X$ , 35
- bidimensional covariance  $\mathbf{K}_{X,Y}$ , 26
- bidimensional mean square  $\Phi_{XY}$ , 26
  
- classical damping, 60
- capacity  $R = R(\vec{X})$ , 88
- central frequency of the process  $\omega_{1,X}$ , 35
- complex conjugate  $w^*$ , 31
- conditioned event, 24
- consistent spectrum, 79
- convex function, 97
- convex set, 97
- convolution, 18
- criterion space  $V_F$ , 96
- cross-correlation  $\Phi_{XY}(t_1, t_2)$ , 29
- cross-covariance  $K_{XY}(t_1, t_2)$ , 29
- cross-power spectral density  $S_{XY}$ , 31
- crossover, 103
- Cumulative Density Function  $F(X)$ , 23
  
- demand  $S = S(\vec{X})$ , 88
- design elastic spectrum, 78
- design vector, 96
- deviation coefficient  $\eta = \sigma_X/\mu_X$ , 26
- Duhamel convolution integral, 18
  
- energy of a function, 32
- energy spectrum, 33
- ergodicity, 21
- exponential distribution, 28
- extreme value process  $\{Y(t)\}$ , 43
  
- failure, 87
- fatigue collapse, 40
  
- fatigue limit states, 87
- feasible set  $\vec{F}$ , 96
- filter, 74
- first passage collapse, 40
- first time of up-crossing  $T_X(u)$ , 43
- FORM, 91
- Fourier's spectrum, 76
- Fourier's transform, 30
- frequency mean value  $\bar{\mu}_X(\omega)$ , 31
- frequency ratio,  $\psi$ , 154
  
- Gaussian distribution, 27
- geometric spectral moments, 35
- global minimizer  $\vec{x}^*$ , 96
- global minimum  $f(\vec{x}^*)$ , 96
  
- harmonic transfer function  $H(\omega)$ , 54
- hazard function  $\eta_X(u, t)$ , 44
- Hilbert transform, 71
  
- impulse response function  $h_x(t)$ , 18
- independent events, 25
- index of vibration protection effectiveness, 143
  
- limit state, 87
- limit state function  $G = G(\vec{X})$ , 88
- limit state surface  $G(\vec{X}) = 0$ , 88
- linear correlation coefficient  $\rho_{XY}$ , 26
- local minimizer  $\vec{x}'$ , 96
- local minimum  $f(\vec{x}')$ , 96
- Lyapunov equation, 69
  
- magnification factor  $D$ , 15
- mass ratio  $\gamma_t$ , 122
- mean square  $\mu^2$ , 25
- mean value  $\mu$ , 25
- minimax optimization, 112
- modal amplitude, 60

- modal coordinate, 60
- modal matrix, 60
- mode shape, 60
- moment of a distribution  $m_k$ , 25
- monocorrelated filter, 75
- mono variate filter, 75
- Monte Carlo simulation, 92
- multi correlated filter, 75
- multi variate filter, 75
- mutation, 103
  
- narrow band envelope, 37
- nodal coordinate, 60
- non-geometric spectral moments, 69
  
- objective function OF, 96
- operator mean  $E[\bullet]$ , 26
  
- Pareto front, 109
- Pareto set, 109
- passive systems, 120
- peak factor  $\zeta((T, p)$ , 50
- penalty function  $\Phi(g(x), r)$ , 106
- performance based design, 114
- phase angle  $\varphi_p$ , 15
- phase opposition, 16
- Poisson distribution, 28
- power spectral density (PSD)  $S_{XX}$ , 31
- power spectrum, 33
- Probability Density Function  $p_X(x)$ , 22
- probability mass function  $P(X^{(j)})$ , 22
- probability of survival  $L(u, t)$ , 43
  
- random variable, 20
- rate of up-crossing, 40
- reliability index  $\beta = \mu_G/\sigma_G$ , 89
- response spectrum, 77
  
- response surface, 92
- reverse Fourier's transform, 30
  
- second order central moment  $\omega_{2,X}$ , 35
- semi-active systems, 120
- sensitivity coefficient  $\beta_i$ , 138
- serviceability limit states, 87
- SORM, 91
- spectral moment of  $j^{th}$  order  $\lambda_{j,X}$ , 34
- standard deviation  $\sigma$ , 26
- state space, 64
- state variables, 64
- state vector, 64
- stationariness, 21
- stationary correlation,  $R_{XX}(\tau = t_2 - t_1)$ , 30
- stationary covariance,  $C_{XX}(\tau = t_2 - t_1)$ , 30
- stationary mean  $\mu_X = cost.$ , 30
- stochastic (or random) process, 20
- strong motion phase, 81
- system matrix  $D$ , 65
  
- Tajimi-Kanai's spectral power density, 83
- time average, 29
- Time series, 20
- transition matrix  $\Theta(t)$ , 65
- tuning ratio  $\rho_t$ , 122
  
- ultimate limit states, 87
- unbounded optimization problem, 98
- uncertain, 87
- unilateral power spectral density  $G_{XX}$ , 32
- unit pulse function  $\delta(\bullet)$ , 17
- unit step function  $U(\bullet)$ , 17
  
- variance  $\sigma^2$ , 25
- vibrations, 11

Analytic index